SOUTH EAST EUROPE FLASH FLOOD GUIDANCE SYSTEM (SEEFFGS)

FORECASTER GUIDE

Prepared by

Petra Mutic

World Meteorological Organization

pmutic@wmo.int

Toni Jurlina

Meteorological and Hydrological Service, Croatia

Milica Djordjevic

Republic Hydrometeorological Service of Republic of Srpska, Bosnia and Herzegovina

Andrej Golob

Slovenian Environment Agency, Slovenia

Reviewed by

Celine Novenario, WMO

Ayhan Sayin, WMO

Theresa M. Modrick, HRC

Eylon Shamir, HRC

Contents

1. INTRODUCTION

While there are several types of floods, a flash flood is one of the most dangerous. They have enough power to change the course of rivers, bury houses in mud, and sweep away or destroy whatever is on their path (NOAA, 2010). Flash floods are also among the world's deadliest natural disasters with more than 5,000 lives lost annually and result in significant social, economic and environmental impacts. Accounting for approximately 85% of the flooding cases, flash floods also have the highest mortality rate (defined as the number of deaths per number of people affected) among different classes of flooding (e.g, riverine, coastal) (WMO).

The weather in South East Europe (SEE) is influenced by three major climates: Mediterranean, Continental and Alpine. The Eastern part of the Alps and the Dinaric range stretch along the Adriatic coast, creating the conditions for one of the areas with the highest annual precipitation in Europe. Montenegro's mountainous regions receive some of the highest amounts of rainfall in Europe. For example, the average annual precipitation at Crkvice was 4,927 mm from 1931-1960, and 4,631 mm from 1961 to 1990. Moreover, short-duration extreme rainfall and flash floods are major natural hazards in the small catchments (Bryndal et al., 2016) of the Carpathian mountains located in the western part of the region.

Flash floods and floods are the most dangerous hydrometeorological hazards affecting South East Europe, often followed by windstorms and hail. This is due not only to high flooding frequency, but also to the vulnerability created by various human activities. Indeed, flash floods and floods are frequent enough to be considered a component of the local climate. During the last few years, flash floods and floods in South East Europe affected more than 2 million people, and resulted in over one hundred casualties. In May 2014 alone, severe and widespread rain events triggered over 3,000 landslides in Bosnia and Herzegovina and Serbia, which damaged or destroyed around a hundred thousand houses, and caused extensive damage to livelihoods, health, water and sanitation facilities.

This was the catalyst for the development of the South East Europe Flash Flood Guidance System (SEEFFGS) as one of the Flash Flood Guidance Systems (FFGS) implemented around the world by the Hydrologic Research Center (HRC) in collaboration with the World Meteorological Organization (WMO), the US Agency for International Development Office of Foreign Disaster Assistance (USAID/OFDA), and the US National Oceanic and Atmospheric Administration (NOAA). FFGS products provide up-to-date information to National Meteorological and Hydrological Services (NMHSs) for their use in rapid assessment of current flash flood risk and to enable NMHSs to issue timely and location specific flash flood alerts, watches or warnings.

This User Guide presents FFGS products for the SEEFFGS and its models. Itand also discusses flash flood case studies, hydrological and meteorological ingredients for flash flooding, descriptions of how to prepare flash flood alerts and warnings, and geographic information system (GIS) support for spatial decisions with examples from numerous literature. As WMO Flash Flood Guidance Programme Trainers, we wanted to create User Guide that will be helpful for forecasters and those who want to learn about FFGS, flash flood forecasting, and most importantly, how to contribute to saving lives and property.

2. BACKGROUND

Flash floods are hydrometeorological phenomena requiring an integration of meteorology and hydrology in real time with an infusion of local information and expertise to deliver reliable flash flood warnings. The FFGS design aims to facilitate this.

The primary purpose of the FFGS is to provide real-time guidance products pertaining to the threat of potential flash floods in relatively small basins. The system provides the necessary products to support the development of warnings for flash floods from rainfall events through the use of remote sensing-based rainfall estimates. The system products are made available to forecasters as a diagnostic tool to analyse weather-related events that can initiate flash floods (e.g. heavy rainfall, rainfall on saturated soils) and then to make a rapid evaluation for a flash flood occurrence at a location. To assess the threat of a local flash flood, the FFGS is designed to allow product adjustments based on the forecaster's experience with local conditions, incorporation of other information (e.g. Numerical Weather Prediction output) and last minute local observations (e.g. non-traditional rain gauge data), or local observer report.

In 2001 HRC, a non-profit public benefit corporation located in San Diego, in collaboration with the U.S. National Weather Service, began the development of a regional system to support flash flood warnings for seven countries in Central America. This effort was in response to the devastating impacts of Hurricane Mitch (1998), which caused wide spreading flooding, flash flooding, landslides, thousands of deaths, and billions of dollars in damages.

The regional system incorporated remotely-sensed precipitation with the local but relatively sparse surface observation network, and semi-distributed hydrologic modelling with high spatial resolution to produce guidance products pertaining to the threat of small scale flash flooding. Evaluations of the threat of flash flooding are done over hourly to six-hourly time scales for basins from 100-300 km^2 in size. Satellite precipitation estimates are used together with available regional in-situ precipitation gauge data to obtain bias-corrected estimates of current rainfall volume over the region. These precipitation data are also used as input to hydrologic models that update soil moisture conditions. The Central America Flash Flood Guidance (CAFFG) system became the first operational, regional flash flood guidance system with its deployment in 2004. The system was designed for use by trained operational forecasters from NMHSs.

Some important technical elements of the FFGS are the development and use of a bias-corrected satellite precipitation estimate, and the use of physically-based hydrologic modelling to determine flash flood guidance and flash flood threat. These system elements can now be applied anywhere in the world, with real-time estimates of high-resolution precipitation data from satellite routinely available globally. Global digital terrain elevation databases and GIS may be used to define small (flash-flood prone) basins and their stream network topology worldwide. In addition, there are global soils and land cover spatial databases to support the development of physically based soil moisture accounting models. With these global data and information, the modelling approach of the CAFFG system can be implemented anywhere (WMO, 2007).

Recognizing a lack of capacity at NMHSs and an expressed need for flash flood warnings worldwide, a Memorandum of Understanding (MOU) was signed by WMO, USAID/OFDA, NOAA and HRC in February 2009 for a cooperative initiative to implement flash flood guidance systems on regional basis throughout the world (Modrick et al., 2014). The SEEFFGS is one of the 11 regional systems developed and implemented so far under this agreement.

2. BACKGROUND

Under the initiative, a number of regional FFGS projects have been or are being established worldwide, such as the South East Europe FFGS, Black Sea and Middle East FFGS, Central America FFGS, Haiti-Dominican Republic FFGS, Southern Africa Region FFGS, Mekong River Commission FFGS, Myanmar FFGS, Southern Asia FFGS, Southeastern Asia-Oceania FFGS, and Central Asia Region FFGS. Currently more than sixty countries are covered (Figure 1) and serve more than two billion people worldwide.

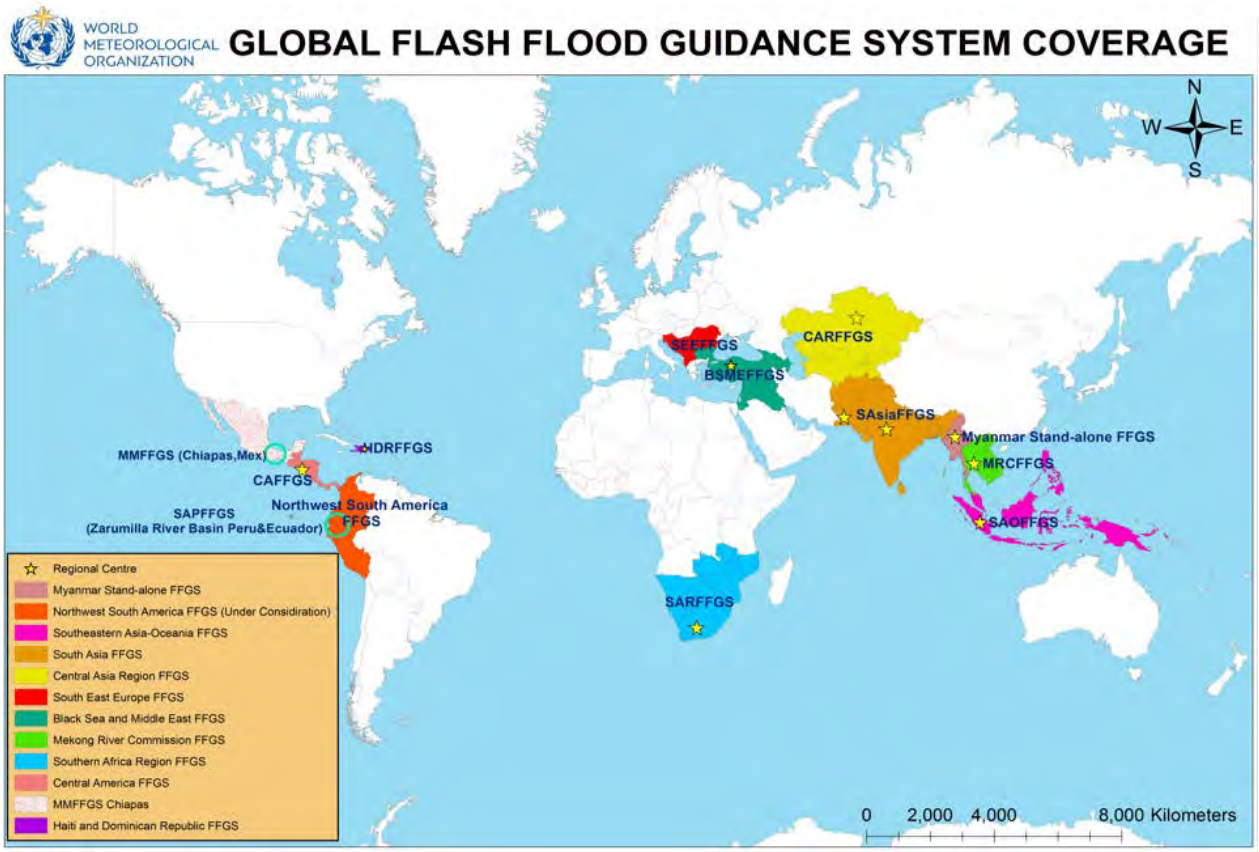

Figure 1. Global coverage of regional Flash Flood Guidance Systems

The objective of the system is to provide information so that NMHSs forecasts can make rapid assessments of the potential of flash floods, allowing for rapid mobilization of response agencies. Regional technology, training, capacity building, protocols and procedures will be developed to address the issues of mitigating the impacts of flash floods and the application of a system allowing the provision of critical and timely information by the NMHSs of the participating countries.

FFG System implementation and computations are done at a Regional Center within the region that can offer 24/7 operation and maintenance. The FFGS computations are performed at the Regional Center, and FFGS products are provided through secure internet web sites to support NMHSs. Forecasters at NHMSs access the FFGS products, can make adjustments based on local information, and produce flash flood watches and warnings within their region (country). These warnings are transmitted through the in-country warning dissemination system to disaster management agencies and the public, as appropriate. Some of the local data from the country

may also be transmitted in real time to the Regional Centre to improve the products of the computational component there. This feedback is represented in Figure 2, below, showing the Global FFG program concept. Beyond the computational role, the Regional Centers aim to ensure collaboration among the NMHSs and facilitate use of the FFGS products. Close collaboration among participating countries as well as among the respective national services of each member country are essential to get most benefits from the system. Because flash floods are truly hydro-meteorological phenomena, FFGS promotes close collaboration between hydrologists and meteorologists in real time for the development of reliable warnings.

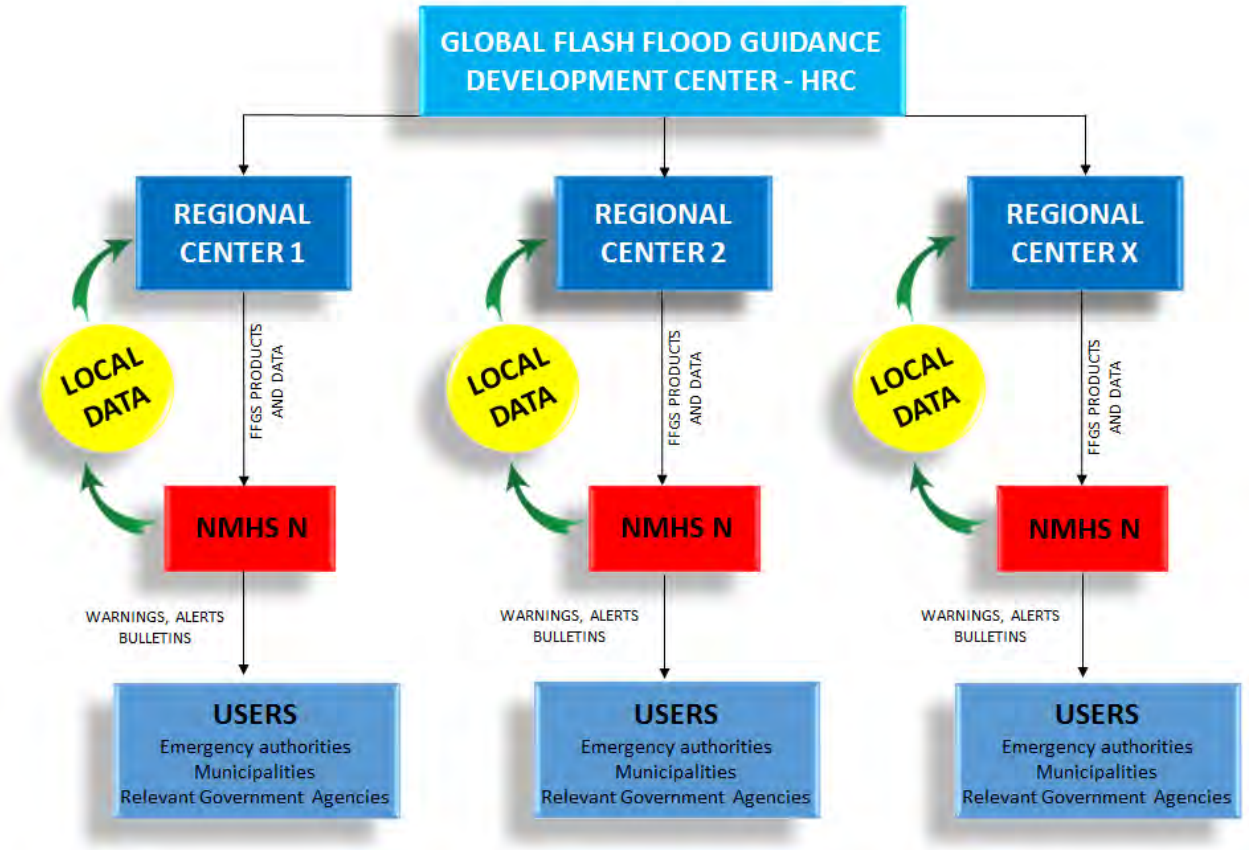

Figure 2. Global Flash Flood Guidance program concept

The South East Europe Flash Flood Guidance System covers the countries of Albania, Bosnia and Herzegovina, Croatia, Moldova, Montenegro, Romania, Serbia, Slovenia and The former Yugoslav Republic of Macedonia. The regional covered by the System is shown in Figure 3. In January 2013, it was agreed to establish the Regional Center of the SEEFFGS at the Turkish State Meteorological Service (TSMS) in Ankara

2. BACKGROUND

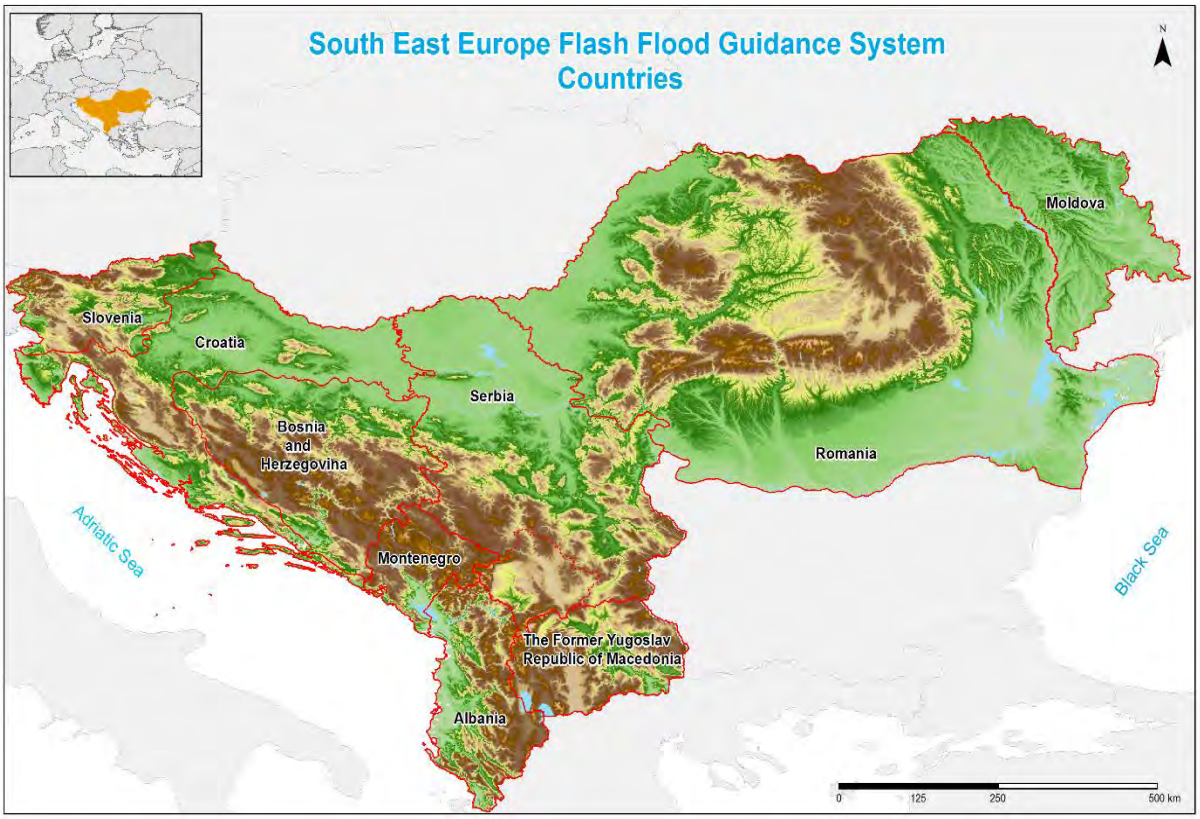

Figure 3. South East Europe Flash Flood Guidance System countries

The implementation of the SEEFFG system can be divided into four phases. First, spatial data such as digital elevation model, soil, vegetation cover, river network, lakes, reservoirs and hydrometeorological data are processed using GIS software to a priori estimate the parameters of the FFGS snow and soil models. If required data are not provided by the participating countries, datasets with global coverage from international organizations are used.

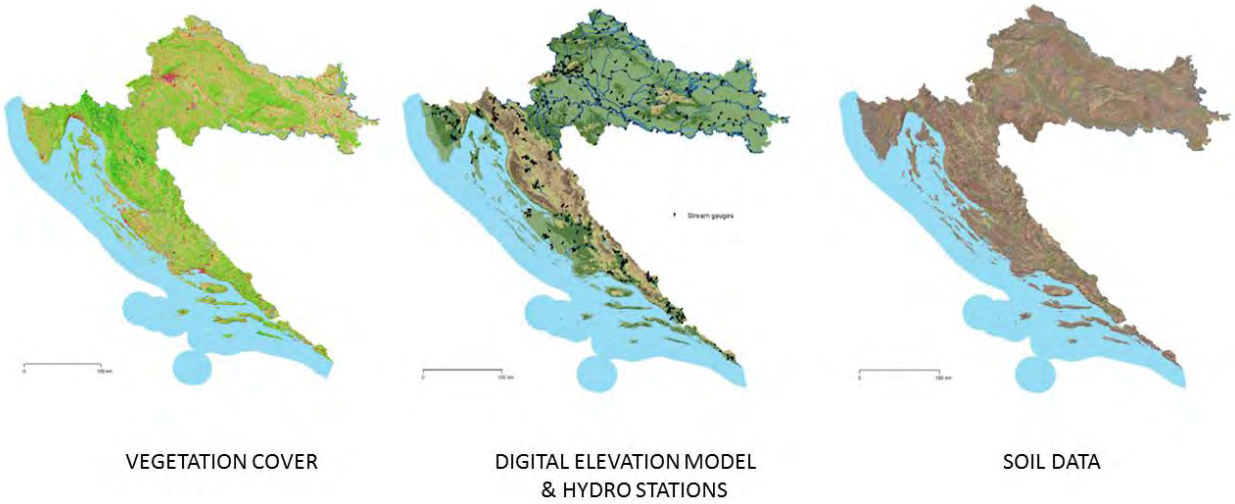

Figure 4. Example of Croatian spatial data

2. BACKGROUND

In the second phase, data from selected co-located meteorological and hydrological stations are used to calibrate the model. In the third phase, the model was implemented for a testing and development period at HRC, while the fourth phase the system is deployed at the Regional Centre in TSMS, and products are disseminated on the servers. During system operations, verification of issued warnings and alerts is done.

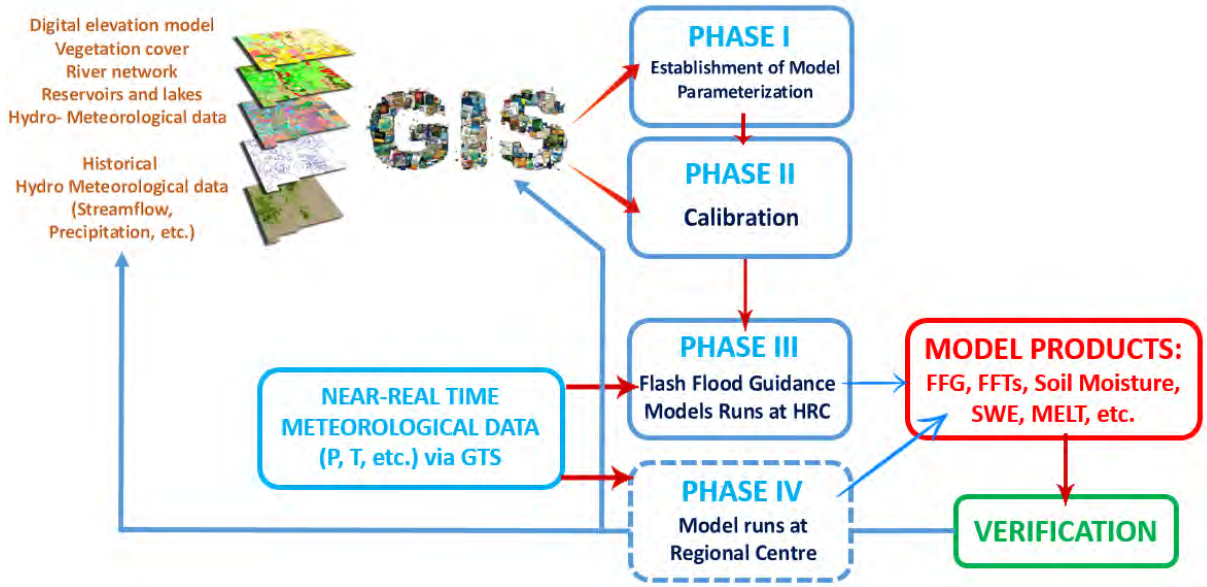

Figure 5. South East Europe Flash Flood Guidance System Implementation phases

FFGS is considered a semi-distributed hydrologic model with the model components configured and the parameters estimated for on a sub-basin basis. Figure 6. shows sub-basins in the SEEFFGS region. There are about 3500 sub-basins with an average local drainage area of 185 km^2.

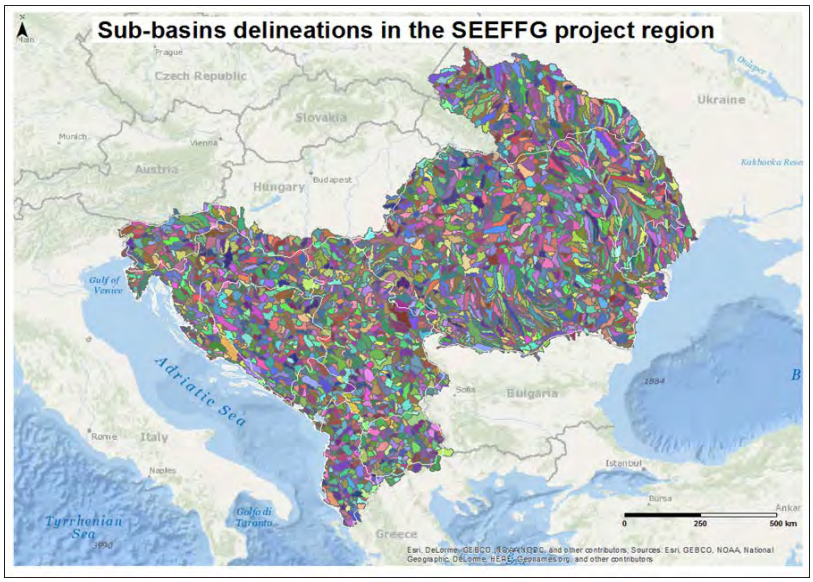

Figure 6. Sub-basins delineation in the South East Europe Project region

3. FLASH FLOOD GUIDANCE MODEL

Flash floods represent forecast and detection challenges because they are not always caused simply by meteorological phenomena. Flash floods occur when both specific meteorological and hydrological conditions exist together. Although heavy rainfall is usually a factor, a given amount and duration of rainfall may or may not result in a flash flood, depending on the hydrologic characteristics on the catchment where the rain is occurring.

WMO defines a flash flood as “a flood of short duration with a relatively high peak discharge”; while the American Meteorological Society defines it as “flood that rises and falls quite rapidly with little or no advance warning, usually as the result of intense rainfall over a relatively small area.” A more complete definition is given by the U.S. National Weather Service as “a rapid and extreme flow of high water into geomorphic low-lying areas - washes, rivers, dry lakes and basins, or a rapid water level rise in a stream or creek above a predetermined flood level”. Flash floods occur in less than six hours from the time of the causative event. A flash flood is a local hydrometeorological phenomenon that requires both hydrologic and meteorological expertise for real time forecasting and warning. It is necessary to have local, up-to-the-hour information for effective warnings including 24/7 operations to maintain vigilance. A flash flood may be caused by heavy rain associated with a storm, hurricane, or tropical storm or melt water from ice or snow flowing over ice sheets or snowfields. It is important to note that flash floods may occur under lower or moderate (or heavy) rainfall when soils are saturated, as the rainfall will runoff quickly to the stream channel.

The differences in predicting the occurrence of flash floods compared to large river floods reveal the requirement of a specialized system that enables improved diagnostic and forecasting of the natural processes leading to these dangerous phenomena. Distinctly, short lead times for forecast (usually less than 6 hours), warning and response make operational flash flood prediction challenging. Their potential occurrence with a high level of spatial and temporal uncertainty also necessitates attentive operations for flash flood forecasting and warning.

The flash flood guidance approach for issuing flash flood warnings rests on the near real-time comparison of observed or forecast rainfall amounts of a given duration and over a given catchment to an amount of actual precipitation known as Flash Flood Guidance (FFG) for that duration and catchment that generates bankfull flow conditions at the catchment outlet. If the observed or forecast rainfall volume is greater than the FFG, then flooding in the catchment is likely. In this case, the surplus of the rainfall is defined as Flash Flood Threat (FFT). The FFG for a particular catchment and duration depends on the catchment and drainage network characteristics, and the soil water deficit determined by antecedent rainfall, evapotranspiration and groundwater loss. The FFGS is based on the concepts of FFG and FFT:

Flash Flood Guidance (FFG) is the amount of rainfall of a given duration over a small drainage area needed to cause minor flooding (bankfull) condition at the outlet of the stream which drains that basin. Flash Flood Guidance is an index of how much rainfall is needed to overcome soil and channel storage capacities and to cause minorflooding.

Flash Flood Threat (FFT) is the amount of rainfall of a given duration in excess of the corresponding Flash Flood Guidance value. The flash flood threat, when used with observed rainfall, is an indicator of areas where flooding is imminent and where immediate action may be needed.

3. FLASH FLOOD GUIDANCE MODEL

The scientific components of the FFGS utilize the available real-time data from in-situ gauging stations and from remote sensing platforms, suitably adjusted to reduce bias, together with physically based soil water accounting models to produce flash flood guidance estimates of various durations over small flash flood prone catchments.

First, under soil saturated conditions the rainfall of a given duration that causes the surface runoff peak from the basin to produce bankfull flow at the catchment outlet is estimated. Then, the soil water deficit is computed at the current time from available data, and the assessment of the rainfall required to produce bankfull flow at the stream outlet under un-saturated soil conditions to that needed for the current soil water deficit (i.e., the flash flood guidance) is made. The estimation of soil water deficit requires quality precipitation input data. With radar and satellite data, an adaptive state estimator is employed to reduce bias of the input remotely sensed precipitation using data from real time reporting rain gauges. The FFGS technical components are depicted in Figure 7. The key model components consist of the Threshold Runoff Model (drainage network characteristics), which is computed once for each sub-basin. Estimated precipitation from several sources like satellites, radar as available, and gauges as available are input into a snow model (Snow-17) which estimates snow water equivalent (SWE) and MELT that are input into soil moisture accounting model (SAC-SMA) to estimate upper level soil moisture (soil water deficit). Then, the Flash Flood Guidance model is used to estimate the amount of rainfall in a given duration (e.g., one, three and six hours) that is required to cause bankfull flow at the outlet of each sub-basin considering current soil moisture conditions. The Flash Flood Threat is the amount of rainfall of a given duration that is greater than the Flash Flood Guidance value for a basin; meaning that it is the difference between the Flash Flood Guidance value for a given duration and over a basin and the corresponding estimated or forecast precipitation for the same duration and basin.

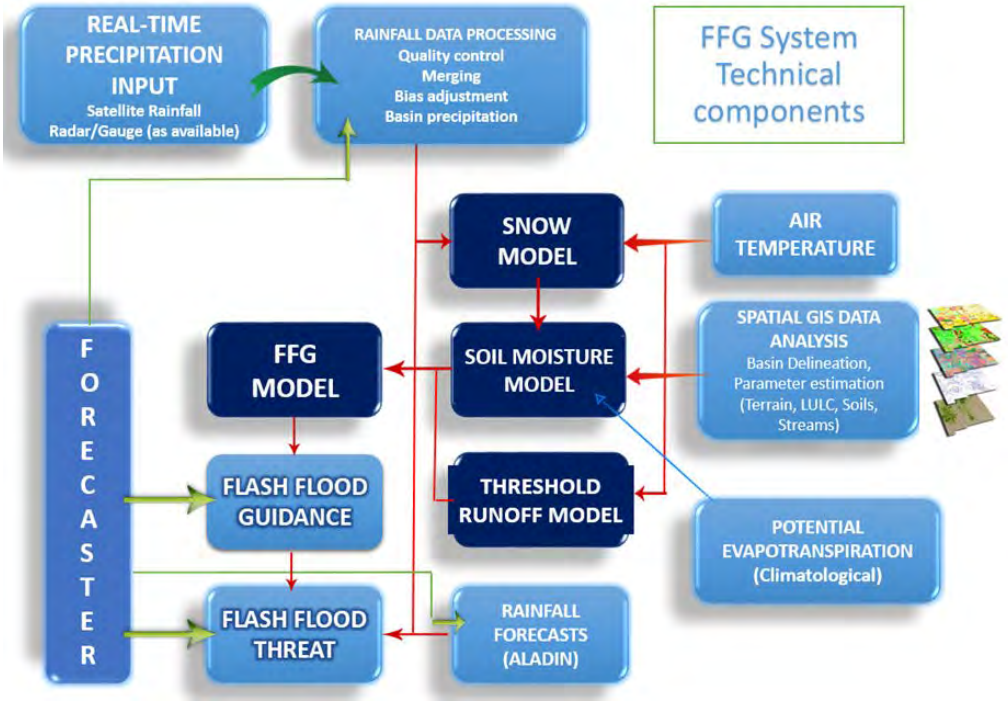

Figure 7. Flash flood guidance system technical components

3. FLASH FLOOD GUIDANCE MODEL

Forecasters should note that Flash Flood Threat itself is not a flash flood warning product but a guide to forecasters using Flash Flood Guidance System products. Hydrometeorological analysis and assessment of the guidance products is necessary to make decision on whether to issue watches or warnings. Therefore, a forecaster's input is essential for the success of the warning process.

The system is designed to allow forecasters to add their experience with local conditions and incorporate other data and information such as numerical weather prediction products and any last minute local observations from stations to assess the threat of a flash flood.

4. SEEFFG USER INTERFACE

The SEEFFG system is primarily composed of regional computational and dissemination servers that are accessed by authorized users of NMHSs. The regional user interface is accessible through a password protected website and is composed of two main parts: the Product Console and the Dashboard. The primary page for hydrologists and meteorologists on duty is the Product Console. The Product Console presents the complete system products in overview features access links to detailed output which forecasters are trained to use. The Dashboard is designed primarily for system administrators and provides a summary of system processes. The Dashboard also helps forecasters to get a brief inspection of the system status.

The Product Console serves as the primary interface for interactive review of the SEEFFGS products and for user access to system data products, which can be divided into real-time data and static resources. The Product Console provides a complete overview of the images produced by the SEEFFG system, a real-time data report of gauge information, and links to composite data tables that can be downloaded for application with GIS tools or use in other systems for data processing or visualization at local NMHS. The features of the console are listed below and displayed in Figure 8. The products are presented on thumbnails (click on thumbnails to see a larger image of the product).

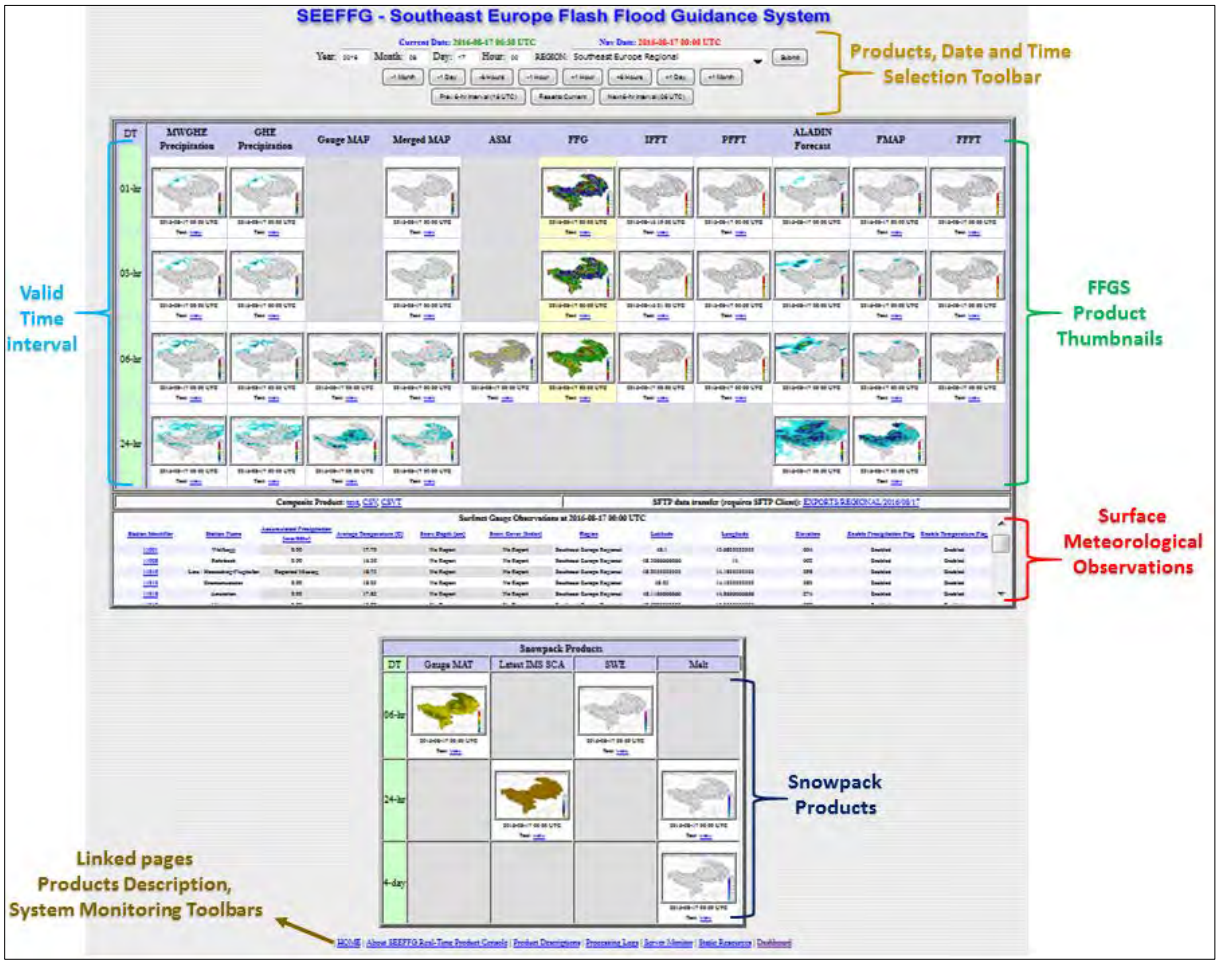

Figure 8. SEEFFG main Product Console

4. SEEFFG USER INTERFACE

The navigation controls are positioned at the top of the page and are used to review the products at various calculation times and from a regional or individual country domain. One can view a single product by selecting a thumbnail image from the main page. The controls for selecting a different product and corresponding interval of accumulation are also available.

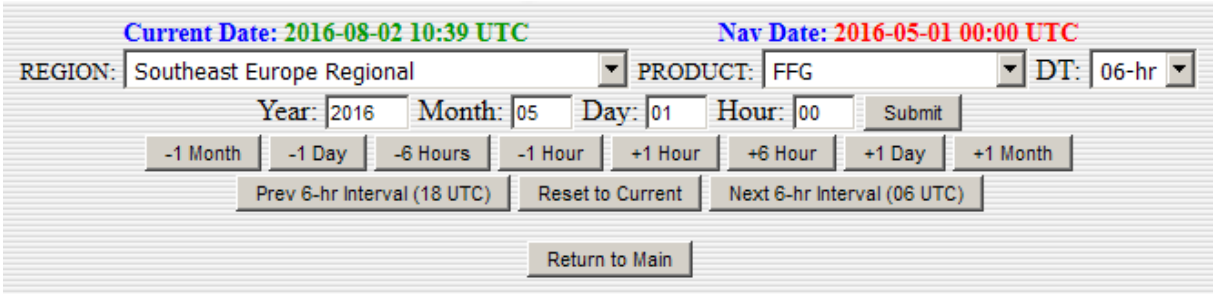

Figure 9. Product console navigation panel in the single product view
Enables fast manoeuvring between different dates, time, domains and products

The term “Navigation Hour” (Nav Date) refers to every hour at the top of the hour, while the term “Model Processing Hour” refers to the 6-hour updates of the hydrologic models matching the rainfall gauge accumulation reports (e.g. 00, 06, 12, 18).

In the products panel, images of the main products are arranged from top down according to 1, 3, 6 and 24 hour time intervals. From left to right side, the products are as follows: MWGHE (MicroWave Adjusted Global Hydro Estimator) precipitation, GHE (Global Hydro Estimator) precipitation, Gauge MAP (Mean Areal Precipitation), Merged MAP, ASM (Average Soil Moisture), FFG (Flash Flood Guidance), IFFT (Imminent Flash Flood Threat), PFFT (Persistent Flash Flood Threat), ALADIN forecast, FMAP (Forecast Mean Areal Precipitation) and FFFT (Forecasted Flash Flood Threat). These products are described in subsequent sections.

Surface meteorological observations from the synoptic stations disseminated through the WMO GTS (Global Telecommunication System) are displayed below the main products. By selecting a specific Station identifier, the station’s metadata and measured timeseries for the past 30 days are listed.

4. SEEFFG USER INTERFACE

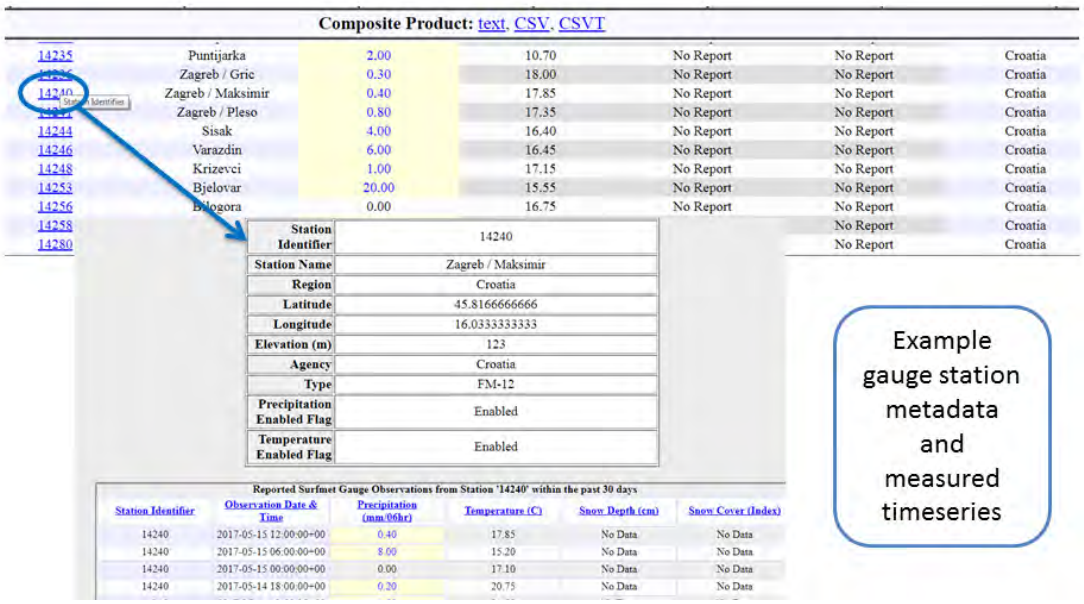

Figure 10. Example gauge station metadata and measured timeseries

Snow products include Gauge MAT (Mean Areal Temperature), Latest IMS SCA (Snow Coverage Area), SWE (Snow Water Equivalent) and MELT (Snow Melt).

At the bottom part of the page there are several links that provide access to a list of product descriptions; detailed processing logs for investigating or confirming various status indicators and processing results; and a page of static resource downloads including basin shapefiles and various software applications (e.g. free QGIS software to assist the forecaster with real time data modification and visualization).

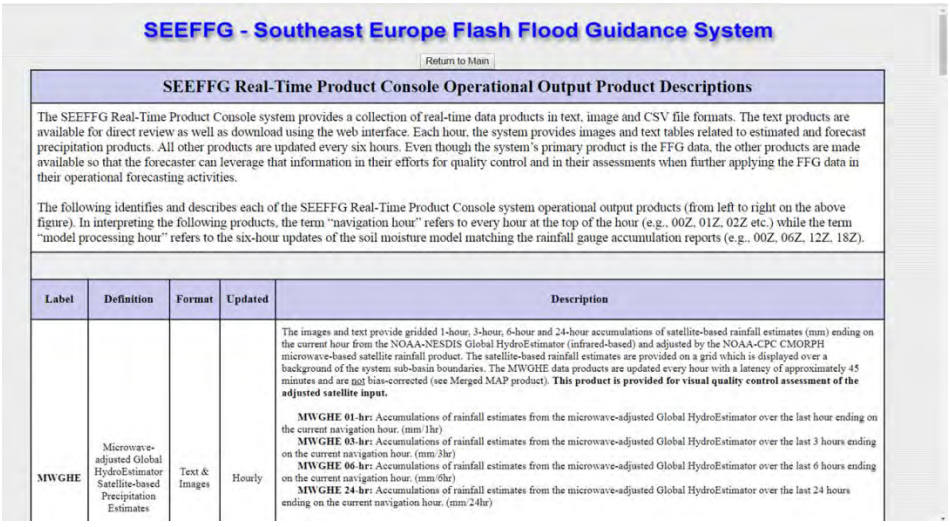

Figure 11. SEEFFG Product description page, providing detailed information about the system products

Monitoring the server processes is enabled through the four main toolbars positioned in the centre of the Dashboard: Real time data download and inventory status, Real time data processing status, Computational server status, and Dissemination server status. Dashboard has four windows of four different products displayed on the top of the console including: Global

4. SEEFFG USER INTERFACE

Hydro Estimator (GHE), Station data status, Average Soil Moisture (ASM), and Flash Flood Guidance (FFG). A user can animate these products except Station data status. At the bottom, there is a link for the Product Console. By clicking on this link, the user will access the Product Console

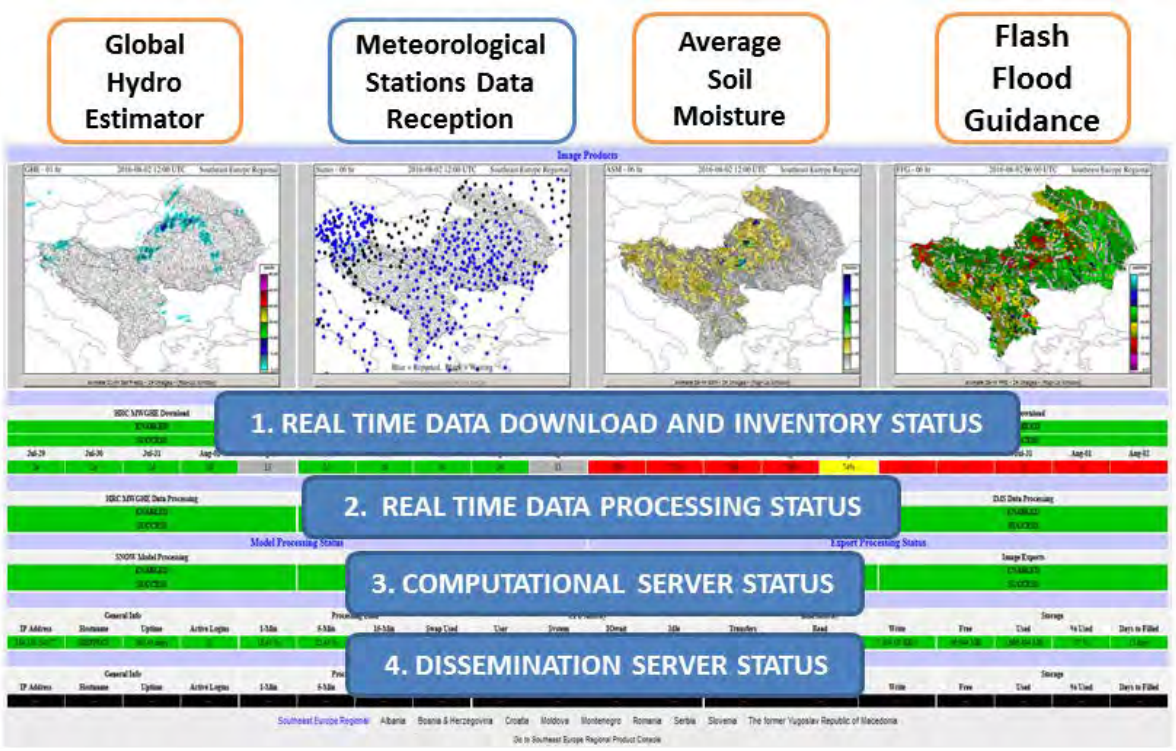

Figure 12. SEEFFG Dashboard Console

5. SATELLITE PRECIPITATION ESTIMATES

Precipitation is a vital element of the global hydrological cycle; it is discontinuous and highly variable in both space and time. Comprehensive coverage of the entire surface of the Earth can only be obtained with observations from meteorological satellites. The relatively high spatial and temporal resolution is critical since heavy rain often covers a relatively small area and can change very quickly. For the FFGS a satellite based precipitation product with short latency, data can be made available to the forecasters with delay of less than half an hour, is essential.

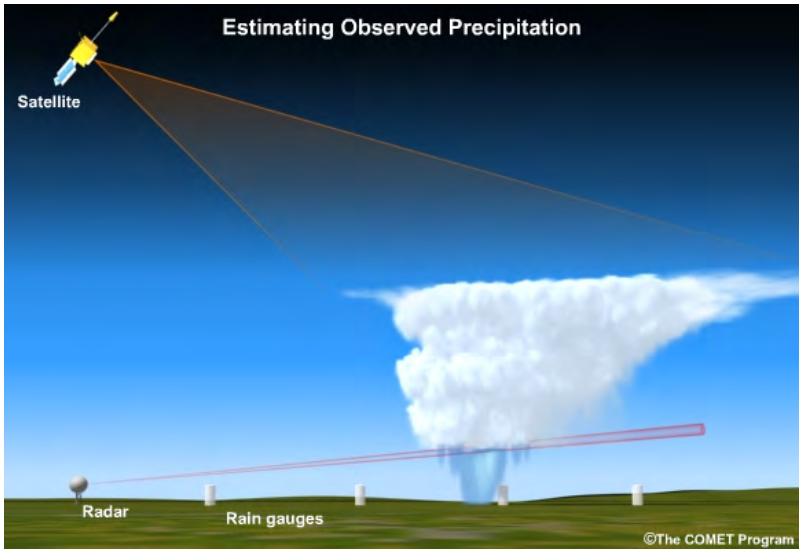

Figure 13. Conceptualized image of three main precipitation estimation technologies: a satellite, radar and a network of ground-based rain gauges

The precipitation estimates used in SEEFFGS are products of geostationary and polar orbiter satellites. Geostationary orbit is a circular orbit positioned about 35,800 km above the Earth's equator and having a period of the same duration and direction as the Earth's rotation. Because they stay above a fixed spot on the surface, they provide a constant vigil for the atmospheric "triggers" for severe weather conditions such as tornadoes, active convection), hailstorms, and hurricanes. Their precipitation estimates are based on infrared (IR) measurements, which permit a high sampling frequency, but their relationship to precipitation is indirect. Polar satellite orbit (the more correct term would be near polar) is an orbit in which the satellite passes over the North and South poles on each orbit, and eventually passes over all points on the Earth. The angle of inclination between the equator and a polar orbit is 90 degrees. The polar orbiters monitor the entire Earth, tracking atmospheric variables and providing atmospheric data and cloud images. Their precipitation estimates are based on microwave (MW) measurements, which afford a more direct inference of precipitation, although they suffer from poor temporal sampling. In the SEEFFGS a space-based precipitation product that combines the geostationary IR precipitation estimate with the orbital MW estimate is provided.

5. SATELLITE PRECIPITATION ESTIMATES

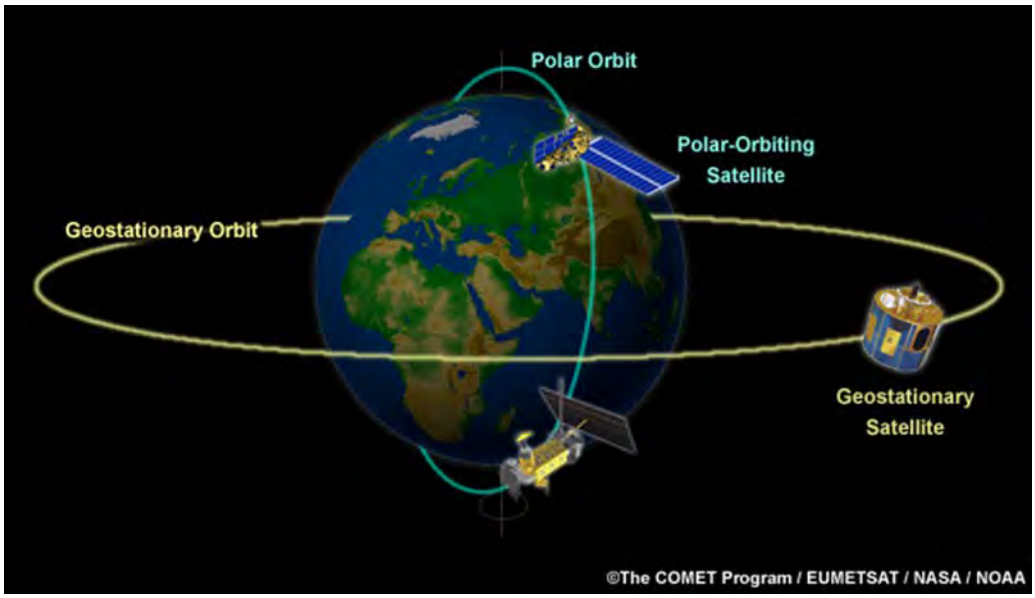

Figure 14. Polar-Orbiting and Geostationary Satellites

Forecasters should be aware that satellite can over- or under-estimate precipitation depending on the time of year and type of weather system (e.g., convective or stratiform), so they must carefully analyse satellite precipitation estimate distribution in their particular regions. Satellite products and images can provide a lot of information to forecasters on storm developments and synoptic and mesoscale features.

5.1. MWGHE SATELLITE PRECIPITATION (MicroWave adjusted Global Hydro Estimator)

Microwave satellite sensors like Advanced Microwave Sounding Unit (AMSU) have fundamentally changed how we discern cloud properties and measure precipitation particles from satellites because they directly detect precipitation in clouds - an advantage over IR-techniques, which have difficulty distinguishing between precipitating and non-precipitating clouds. Microwave detection of precipitation uses several channels, which are usually described by their frequency in gigahertz (GHz). Some channels are located in window regions where the atmospheric gases absorb very little radiation (Figure 15.). These windows allow the satellite sensors to "see" the surface of, even though, the clouds. Both the window and high absorption regions are used to derive various products for identifying surface and cloud properties.

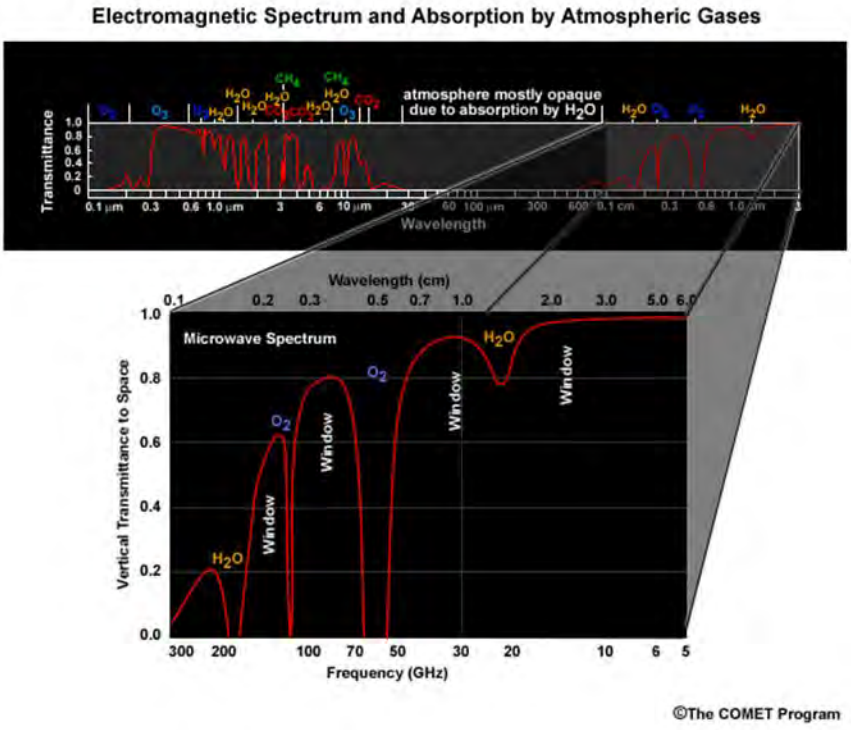

Figure 15. The microwave portion of the EM spectrum and its relative location on the EM spectrum

The AMSU passive MW instrument has been flying on the NOAA and European Metop polar-orbiting satellite series as part of a cooperative agreement between NOAA and European Organisation for the Exploitation of Meteorological Satellites (EUMETSAT). AMSU is composed of two separate instruments, the AMSU-A and –B; each instrument is equipped with channels that sense at frequencies between 23 and 190 GHz. Different channels of MW instrument measure either the scattering of high-frequency radiation by hydrometeors or the absorption of low frequency radiation by raindrops.

Present technology only allows MW instruments on board low-orbit satellites, which poses difficulties for their use in real time hydrologic forecasting, as they are not adequate for detecting the rapidly changing rainfall patterns at a single location (sampling problem). Also, MW measurements have a relatively large footprint (from 5 to more than 50 km), which in convective conditions may cause an incomplete beam-filling errors.

5.1. MWGHE SATELLITE PRECIPITATION (MicroWave adjusted Global Hydro Estimator)

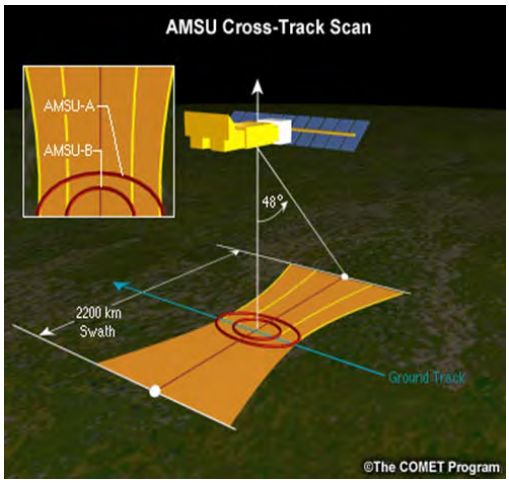

Figure 16. Illustration of AMSU cross-track scan geometry

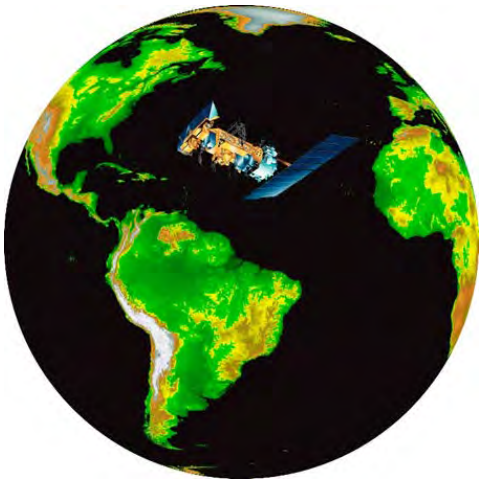

Figure 17. NOAA polar satellite orbiting the Earth

CMORPH, short for the Climate Prediction Center (CPC) morphing method, does not use IR precipitation estimates; rather it uses IR-based cloud top temperature (to be explained in the next section) to derive propagation vectors for cloud tops to interpolate the MW-based precipitation estimates and to produce half hourly 8 km resolution precipitation estimates. The CMORPH technique holds great promise for small-scale applications. Current public availability of the CMORPH precipitation estimates from the NOAA CPC has approximately 18-hour latency.

Half-hourly analysis of CMORPH at a grid resolution of 8 km (at equator) have been produced since 22 November 2002. Some modifications have been made since the processing became operational, most importantly the implementation of an improved snow-screening process (Joyce et al., 2004).

A major caveat with the CMORPH for operational application that aims to develop warnings for flash flood events is the long latency of the half-hourly 8 km rainfall estimates. However, it is anticipated that for times when both HE and CMORPH estimates are available and at spatial scale of CMORPH, valid hourly estimates of CMORPH may be used to adjust those of HE, and to develop adjustments that may also be used during times when CMORPH is not available because of latency. With this premise, the following strategy was applied to potentially improve the HE estimates of rainfall (Figure 18.).

5.1. MWGHE SATELLITE PRECIPITATION (MicroWave adjusted Global Hydro Estimator)

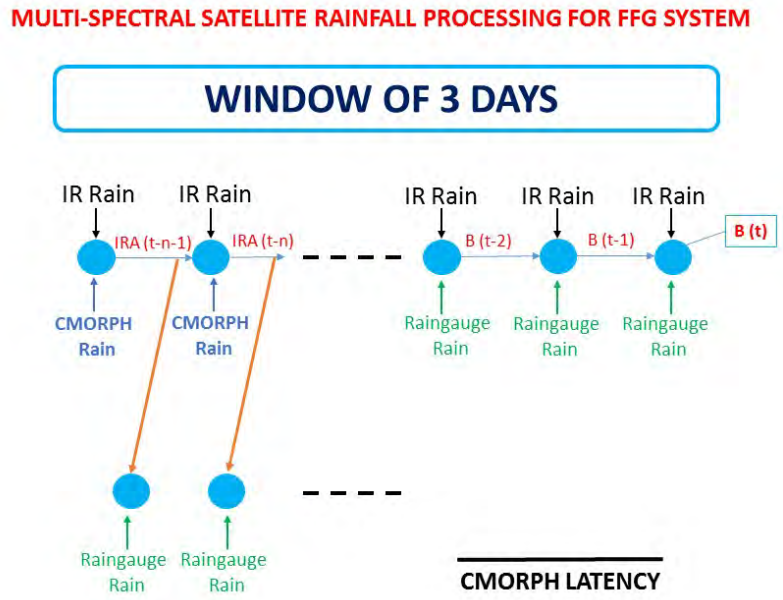

Figure 18. Procedure for processing CMORPH data and rain gauge data to adjust HE rainfall estimates

Starting from the current time t, a processing window extending back to three days from present time is defined. During part of that window, both HE and CMORPH estimates are available for processing while during the rest of the time until present, only HE is available due to the period of CMORPH latency. During the time when both estimates are available, the HE estimates are adjusted to match those of the CMORPH at the scale of 8 km throughout the domain of the FFGS. This results in adjusted HE estimates. During this period adjustment factors are computed for HE, which are then applied to the HE estimates during the rest of the time until present when no CMORPH data is available. In that way, the HE estimates are adjusted for the biasin the estimates relative to the CMORPH data up to the present time .

The Microwave-adjusted Global Hydro Estimator (MWGHE) Satellite-based precipitation product provides Global Hydro Estimator (GHE) satellite-based accumulated precipitation estimate (IR-based) adjusted by available MW-based satellite precipitation estimates to improve GHE accuracy. It is important to note that in some conditions the MW based CMORPH precipitation estimate may underperform compared to the HE. For example, the CMORPH precipitation estimate is masked in areas with snow cover. In addition, large uncertainties in the CMORPH precipitation estimate has been reported in coastal regions and during small scale local convective precipitation events.

The images and text in the SEEFFGS provide gridded 1-hour, 3-hour, 6-hour and 24-hour accumulations of satellite-based rainfall estimates (mm) ending on the current hour from this MWGHE product (NOAA-NESDIS Global HydroEstimator (IR-based) and adjusted by the NOAA-CPC CMORPH MW-based satellite rainfall product).

5.1. MWGHE SATELLITE PRECIPITATION (MicroWave adjusted Global Hydro Estimator)

The satellite-based rainfall estimates are provided on a grid which is displayed over a background of the system sub-basin boundaries. The MWGHE data products are updated every hour with a latency of approximately 45 minutes and no adjustment for bias is precipitation bias is made for the gridded products. A bias correction is applied during the computation of mean areal precipitation (MAP) as will be described in a subsequent section.

Each of the 3-, 6- and 24-hour MWGHE accumulations are produced from the 1-hour MWGHE rainfall input products summed over the corresponding interval, ending on the navigation hour.

Each of these accumulations requires the availability of at least 50% of the 1-hour MWGHE products over the corresponding interval. If more than 50% of the 1-hour products are missing or unavailable over any accumulation interval, a grey image is shown to indicate insufficient 1-hour satellite input data were available.

Examples of 6-hour GHE precipitation accumulations for the SEE without and with (MWGHE) CMORPH adjustment are shown below (figure 19).

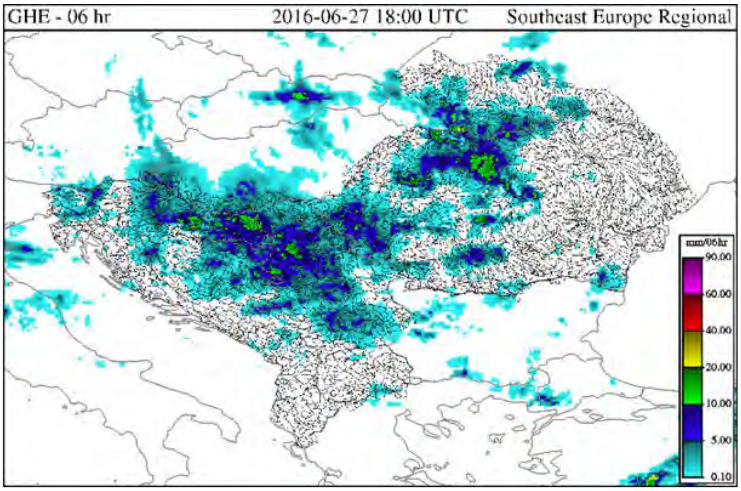

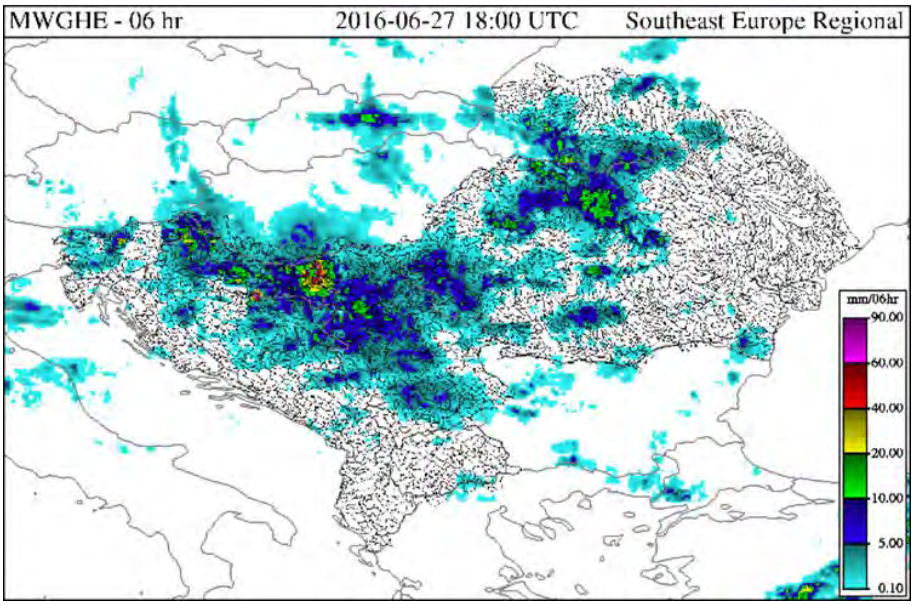

5.1. MWGHE SATELLITE PRECIPITATION (MicroWave adjusted Global Hydro Estimator)

Figure 19. SEEFFG GHE precipitation accumulations without (GHE) and with (MWGHE) CMORPH adjustment

In the example shown, there are significant changes evident in the 6-hour GHE and MWGHE products. The MWGHE showed much heavier rainfall, especially near Croatian-Serbian border. This is the result of additive correction performed by the adjustment procedure.

5.2. GHE (GLOBAL HYDRO ESTIMATOR) SATELLITE-BASED PRECIPITATION ESTIMATES

The Global Hydro Estimator (GHE) is a satellite based precipitation product from NOAA NESDIS (National Environmental Satellite, Data, and Information Service). GHE provides hourly accumulations (mm) of precipitation with latency of a few minutes (up to 20 minutes globally) and with resolution of approximately 4 km by 4 km at the equator. The Hydro-Estimator has been an operational precipitation algorithm since 2002 to produce precipitation estimates for the entire globe using five different geostationary satellites.

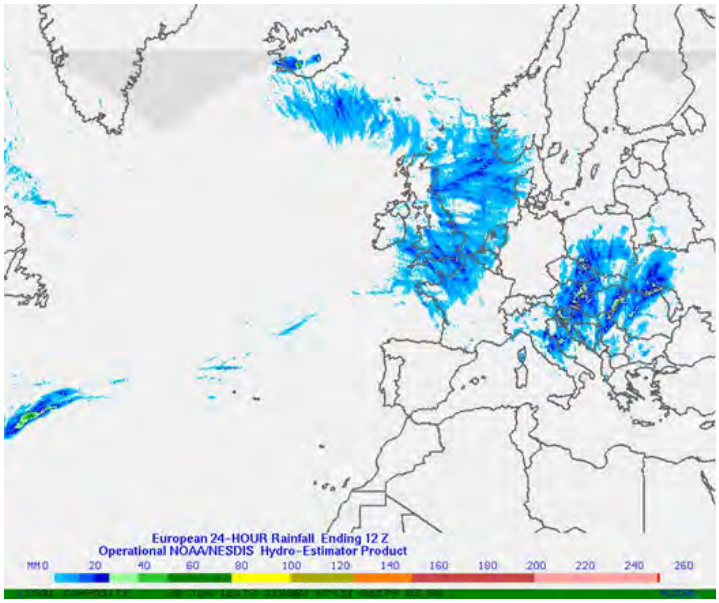

Figure 20. NOAA/NESDIS 24-hour rain accumulations 20 June 2016

The presently available HE precipitation estimates are based on procedures that evolved from the earlier auto-estimator formulations and include enhancements for atmospheric moisture effects, orography, convective equilibrium levels for warm-top convection, local pixel brightness temperature difference with surroundings, and distinguishing between convective core and no-core regions. Several of these enhancements use information from operational numerical weather prediction (NWP) models.

Like other infrared-based algorithms, the GHE uses the brightness temperature (Tb) or cloud top temperature in the infrared (IR) window channel (10.8 μm) to determine raining areas and rain rates. Three basic assumptions are used for estimating rainfall using infrared data from satellites:

- → Cloud-top brightness temperature is inversely related to cloud-top height: colder clouds have higher tops and warmer clouds have lower tops.
- → Cloud-top height is related to the strength of the convective updraft (higher-topped clouds have stronger updrafts).
- → Clouds with stronger updrafts are transporting moisture upward more rapidly and thus producing heavier rain than clouds with weaker updrafts.

5.2. GHE (GLOBAL HYDRO ESTIMATOR) SATELLITE-BASED PRECIPITATION ESTIMATES

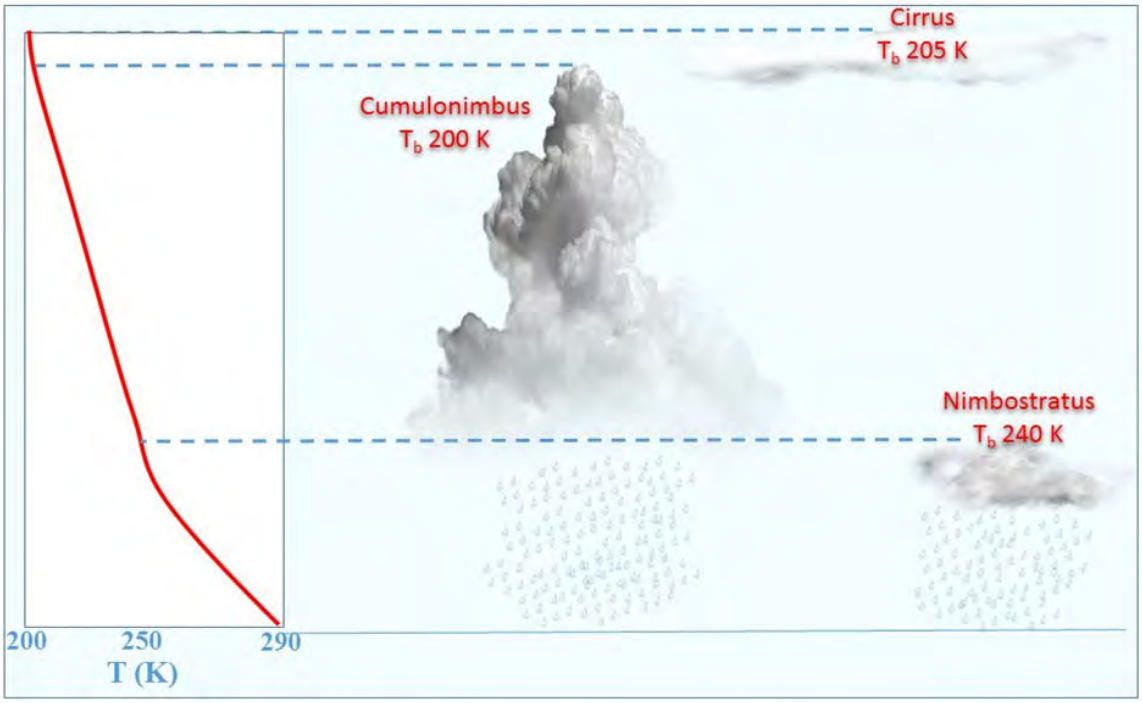

Figure 21. Infrared signal and rain rate relationship

The assumption regarding the relationship between cloud-top temperature and rainfall rate is reasonable for convective clouds (i.e., warm season showers, thunderstorms), but incorrect identification of cold cirrus clouds as raining is a significant problem. This results in the overestimation of the extent of heavy rainfall in many IR-based algorithms. Second, stratiform clouds usually do not have very cold tops in IR imagery but can produce significant rainfall that will be underestimated (or even not detected) by IR algorithms.

The GHE also uses relative temperature to determine the rain rate. It assumes that the pixels closest to coldest pixels are at the centre of the convective core and have the highest rain rates, whereas pixels farther away have a lower rain rate for a given brightness temperature. The plots on the bottom compare the rainfall rates, which are on the y-axis, with brightness temperature, which is on the x-axis. The rain rates get higher as the clouds get colder, but for the “core” pixels, the rain rates for a given brightness temperature are higher than for the “non-core” pixels.

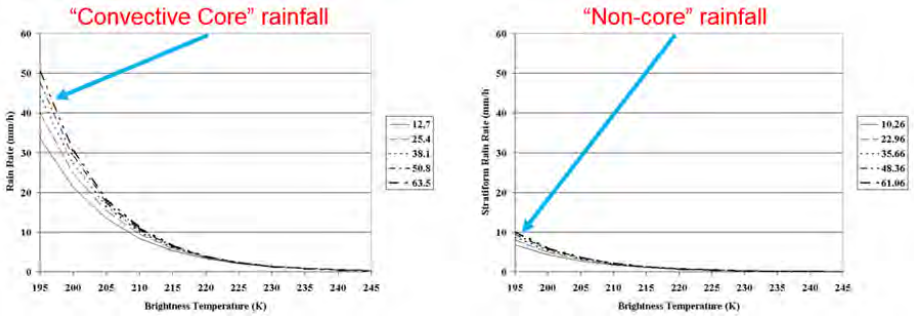

Figure 22. Relationship between rain rates, brightness temperature and convective (non-)core rainfall

5.2. GHE (GLOBAL HYDRO ESTIMATOR) SATELLITE-BASED PRECIPITATION ESTIMATES

Convective equilibrium level temperature is used to identify regions where strong updrafts and heavy rain can occur even if the thermodynamic profile does not support very cold clouds.
The HE algorithm accounts for orographic effects by using digital elevation model and upper-level winds (850 hPa) to derive the vertical component of wind, which is then scaled into a multiplicative adjustment to the rainfall rate. The HE identifies regions where the terrain will cause the air to flow upward or downward, and adjusts the rain rates to moisten the areas with upward motion and to dry out areas with downward motion.

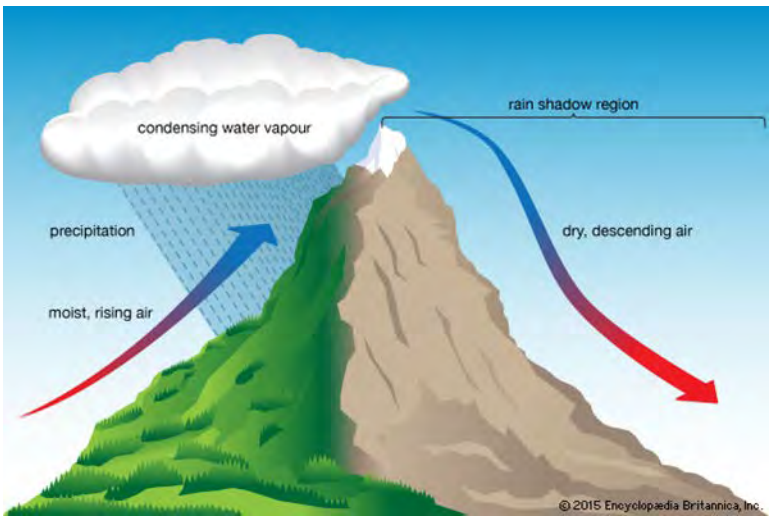

Figure 23. Illustration of orography effect

Details on the algorithm, which also uses data from numerical weather prediction models to correct for evaporation of raindrops, topographic influence on rainfall, and other factors, can be found at the Technique Description link and in Scofield and Kuligowski (2003).

The NOAA/NESDIS provides a 1-hour precipitation accumulation that is then used in the SEEFFGS to determine 1-hour, 3-hour, 6-hour and 24-hour accumulations of satellite-based rainfall estimates (mm) ending on the current hour from the HE. The satellite-based rainfall estimates are provided on a grid which is displayed over a background of system sub-basin boundaries. The data products are updated every hour with a latency of approximately 25 minutes (it is the only global product that is available with such a short delay) and the gridded products are not bias-corrected.

The image below shows the GHE-24-hour product, which was current between 06:00 UTC of 10th of October 2015 and 06:00 UTC of 11th of October 2015 for the SEE region domain.

5.2. GHE (GLOBAL HYDRO ESTIMATOR) SATELLITE-BASED PRECIPITATION ESTIMATES

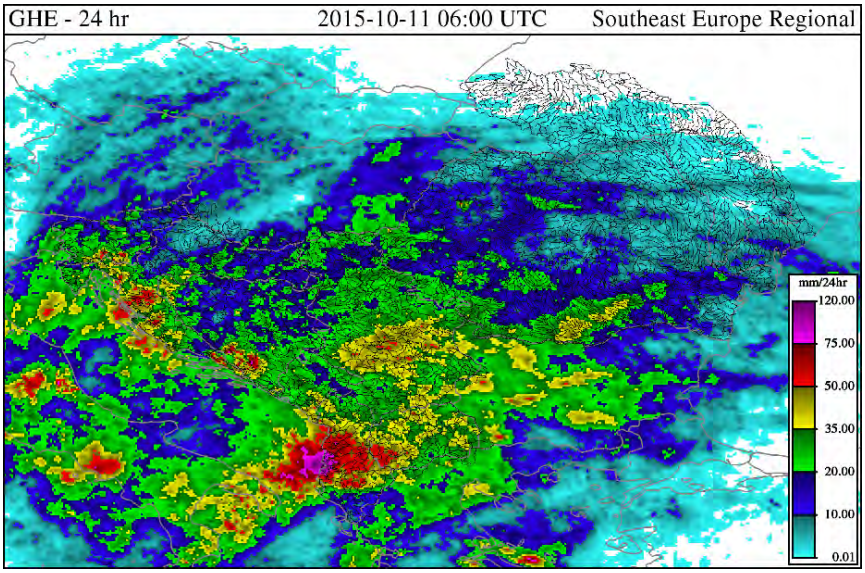

Figure 24. Accumulations of rainfall estimates from the GHE over the last 24 hours ending on the current navigation hour

Each of the 3-, 6- and 24-hour GHE accumulations are produced from the 1-hour GHE rainfall input products summed over the corresponding interval, ending on the navigation hour. Each of these accumulations requires the availability of at least 50% of the 1-hour GHE observations over the corresponding interval. If more than 50% of the 1-hour GHE observations are missing or unavailable over any accumulation interval, a grey image is shown to indicate insufficient 1-hour satellite input data were available.

If the 1-hour GHE input product is unavailable or missing, the sub-basin boundaries are displayed in red.

GHE precipitation estimates are used in the SEEFFGS as backup to the MWGHE for model forcing and flash flood treat analysis. Because the satellites provide spatially uniform coverage and low data latency for rainfall rate estimation, they are critical features for supporting FFGS.

6. GAUGE MAP (Mean Areal Precipitation)

Gauge MAP (Mean Areal Precipitation) is generated using synoptic observations that are disseminated through the WMO GTS and FTP. The GTS distributes a wide range of earth data observations with standardized data formats and content. The more data submitted via GTS by member countries, the more accurate the Gauge MAP product produced.

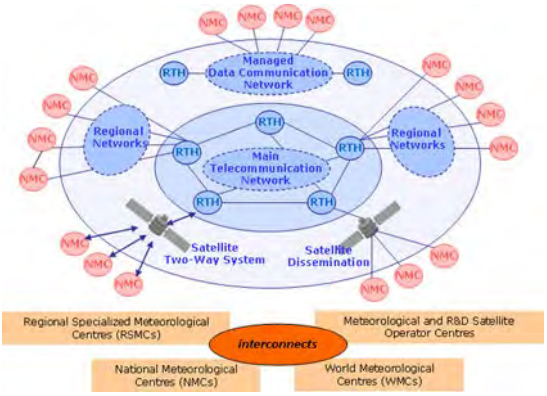

Figure 25. WMO GTS structure

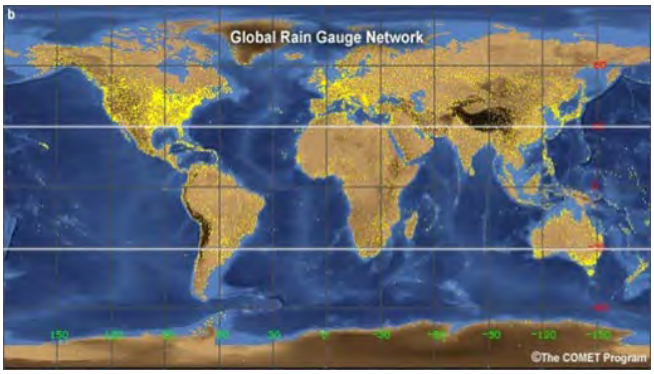

Figure 26. Global Rain Gauge Network

Because surface meteorological measurements are point data and basin areal precipitation is used in hydrologic studies, gauge mean areal precipitation is estimated for each basin. From the practical point of view forecasters, the gauge MAP is less than the maximum point measurement in the sub-basins. Forecasters should note that GTS does not have quality control. If the forecaster has information that a particular gauge has wrong measurements, it should contact the Regional Centre.

To generate the Gauge MAP, real time reporting synoptic stations are used: 7 from Albania, 9 from Bosnia and Herzegovina, 39 from Croatia, 4 from Moldova, 36 from Montenegro, 139 from Romania, 36 from Serbia, 19 from Slovenia, and 17 from The former Yugoslav Republic of Macedonia (as of July 2016). Reporting station status are displayed in the SEEFFG system Dashboard (Figure 27) and individual station data can be displayed in the “Product console” (Forecaster Interface) by clicking on the Station Identifier in the Surface Meteorological Gauge Observations area. (Figure 28).

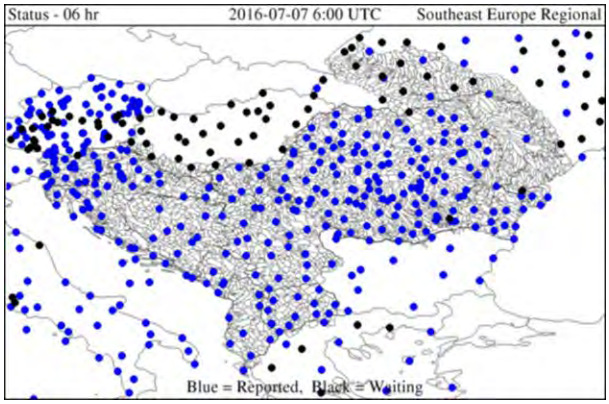

Figure 27. An example of the gauge reporting status for the date of 2016-07-07 at 06:00 UTC

6. GAUGE MAP (Mean Areal Precipitation)

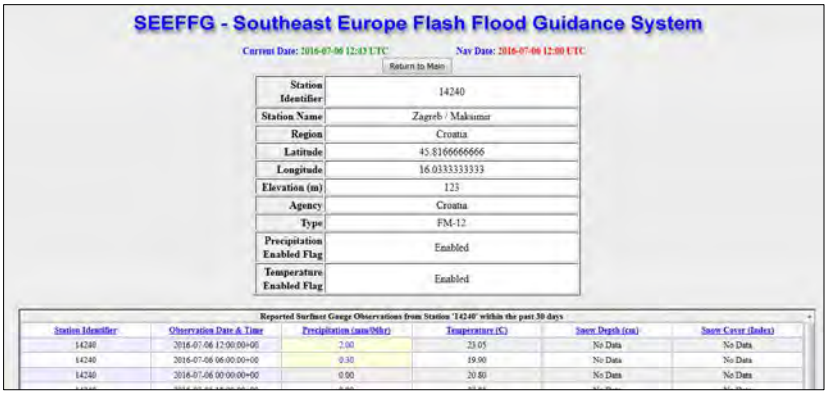

Figure 28. Example gauge station time series report from the SEEFFGS

In the SEEFFGS, the images and text provide 6-hour and 24-hour accumulations of mean areal precipitation (mm) estimates for each sub-basin produced from interpolation of precipitation gauge data. The Gauge MAP data products are updated every six hours and reflect accumulations of basin-average precipitation for a given duration ending on the current navigation hour. The interpolation of the gauge precipitation is performed on the observations made by a predefined list of "Active" stations. Only observations from these stations are incorporated into the gauge precipitation interpolation. Zero precipitation is assigned to active stations that did not report an observation. The Gauge MAP product is then derived for all sub-basins from the interpolated 6-hourly station observations. The Gauge MAP is used for the bias adjustments of MWGHE and GHE precipitation products.

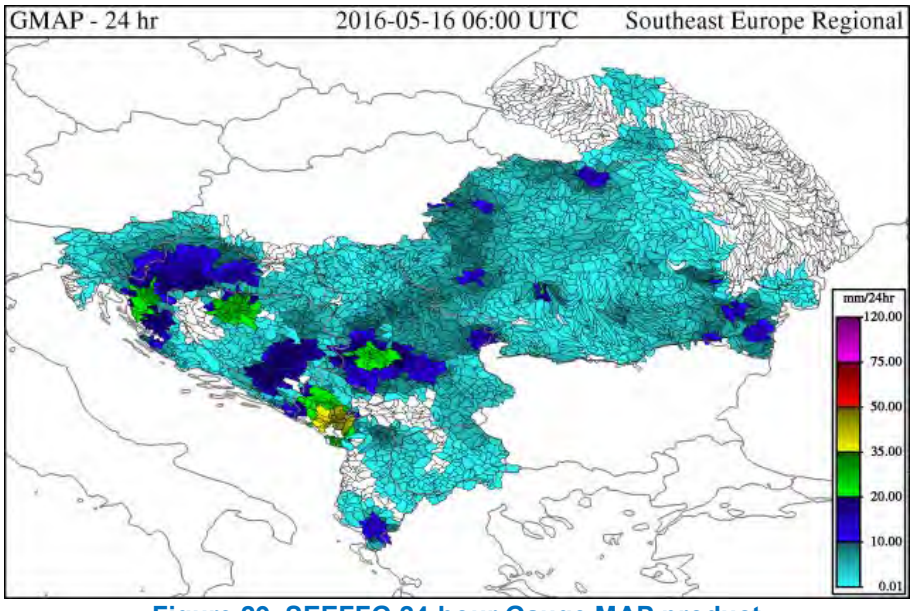

Figure 29. SEEFFG 24-hour Gauge MAP product

7. BIAS ADJUSTMENTS

As mentioned previously, the satellite estimates of precipitation used in the FFGS are indirect measures of precipitation at the ground surface, and bias may exist in these estimates relative to the in-situ measurements. Therefore, FFGS allows for climatological bias corrections and real-time bias corrections to remotely sensed data (satellite or radar precipitation). Both corrections are based on the estimation of regional bias factor (B) computed from rain gauge rainfall reports and corresponding satellite rainfall grids:

$$B = \frac{\sum_{i=1}^{N_G} R_{G_i}}{\sum_{j=1}^{N_G} R_{S_j}}$$

In equation (1), R_{G_i} and R_{S_j} represent the i^{th} rain gauge and j^{th} satellite pixel value corresponding to a rain gauge location, and N_G denotes the number of rain gauge-satellite pairs used in a region (Figure 30). To simplify the notation, it is assumed that there is only one rain gauge contained in each satellite pixel. If more are included, the arithmetic average of the values is used as the rain gauge value for that pixel. Note that the product of the regional bias and the satellite rainfall values produces regional averages that are equal to the corresponding regional rain gauge averages.

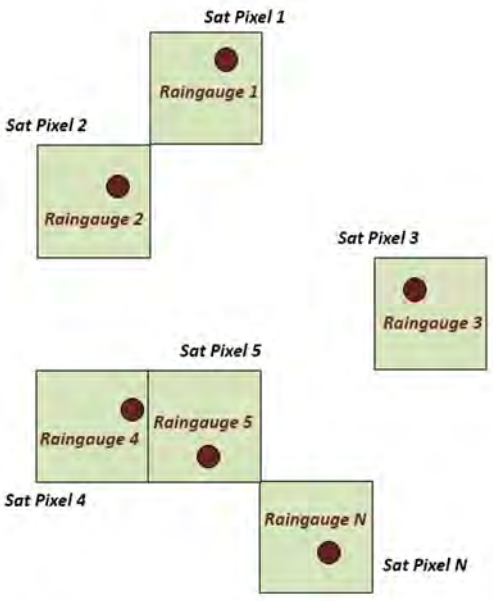

Figure 30. Example of raingauge-satellite pairs within a bias-correction region.

Climatological Bias Factor Estimation

In this case, historical information is collected from global data sources (for satellite precipitation estimates) and from each country (in-situ gauge precipitation measurement) to form the requisite database to develop estimates of climatological bias. Consistent satellite precipitation estimates from the Hydroestimator (HE) algorithm are available since approximately 2012and, thus, bias factor analysis may be done for the period 2008 to present in most regions of the world. The climatological bias represents the ”long-term“ average ratio between observed precipitation

available from historical records of rain gauge stations and the Hydroestimator (HE) precipitation product. It is intended to identify consistent biases that may vary monthly or seasonally (due to seasonal differences in the type of weather systems), or may vary across hydroclimatological sub-regions within a regional FFGS. The climatological bias estimation involves the following general steps: *(a)* the region of the flash flood guidance system application is divided into sub-regions of similar precipitation climate and topography, and with consideration for data adequacy for bias analysis; *(b)* bias factors are computed for each month of the year and for each sub-region based on the data collected for each region (e.g., daily data or hourly data) and for a variety of thresholds of minimum precipitation, number of gauge-satellite pairs, and duration of precipitation; (c) a decision as to the monthly bias factor value to adopt is made based on the stability of the climatological values computed for the various combinations of parameters. Often, the climatological bias analysis can utilize historical data from additional rain gauges than those available in real-time to get a better representation of long-term bias in the satellite precipitation estimates.

Climatological bias factors are derived and are parametric input to the FFGS to serve as a baseline adjustment to the satellite precipitation input in situations where the real-time bias adjustment is not implemented, or as initial conditions for the real-time bias adjustment and where conditions for calculation of the real-time adjustment are not met. Climatological bias factors are determined independently for the GHE and MWGHE precipitation estimates, and applied prior to the computation of merged MAP.

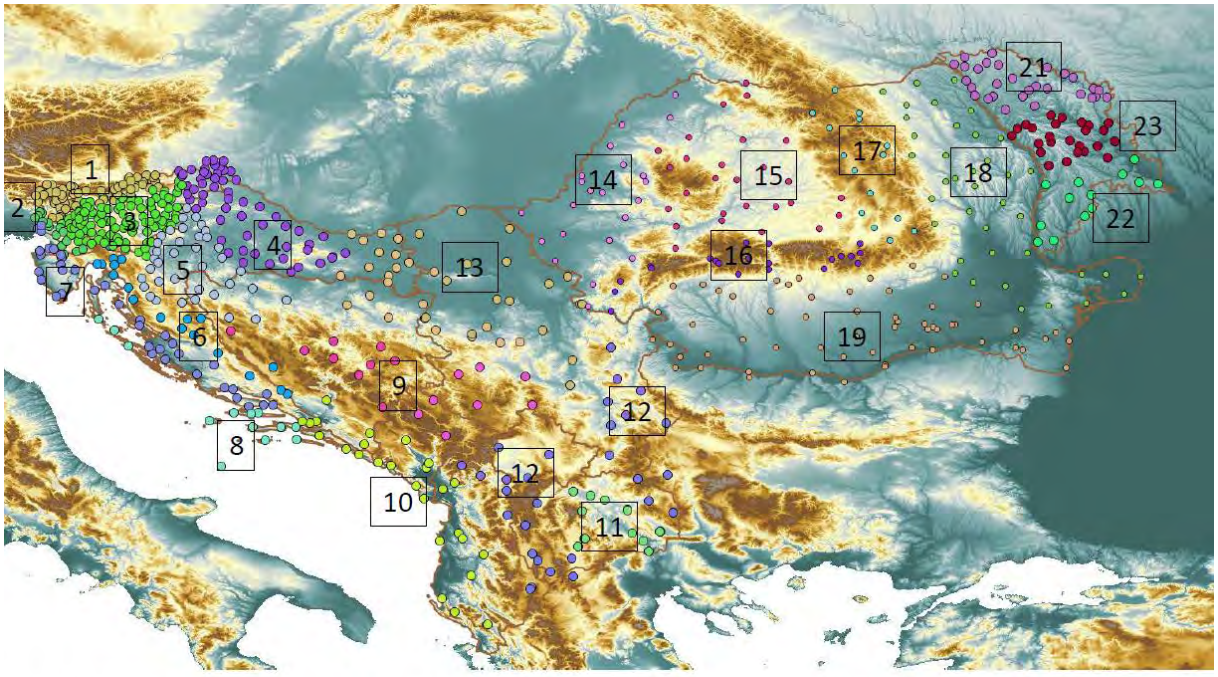

1: Slovenia, north
2: Slovenia, low
3: Slovenia, pre-alpine, central
4: Slovenia & Croatia, low land
5: Croatia & Bosnia-H., inland
6: Croatia, coastal mtn
7: Croatia & Slovenia, coastal
8: Croatia, coastal islands
9: Bosnia-H. & Serbia, contin.
10: BiH, Monte, Alb - coastal
11: Macedonia, low elev
12: Albania, Macedonia, mtns
13: Croatia-Serbia, low elev
14-19: Romania
21-23: Moldova

7. BIAS ADJUSTMENTS

Figure 31. SEEFFG Sub-regions of similar precipitation climate and topography

The climatological bias adjustment factors for the South East Europe region were developed based on daily precipitation records available from within country agencies and global databases. The periods of overlap for these stations and satellite precipitation data were the historical years 2012 through 2014. The available stations were subset to provide a relatively uniform coverage of stations by selecting stations with the greatest number of non-missing precipitation records. Figure 31 presents sub-regions and location of the gauges selected for the climatological bias analysis.

As examples of the bias in regional average precipitation based on satellite estimates versus gauges, Figure 32 shows the cumulative distribution function (CDF) for gauge vs MWGHE for Region 7 and Region 18. In Region 7, satellite product underestimates gauge rainfall slightly more than in Region 18.

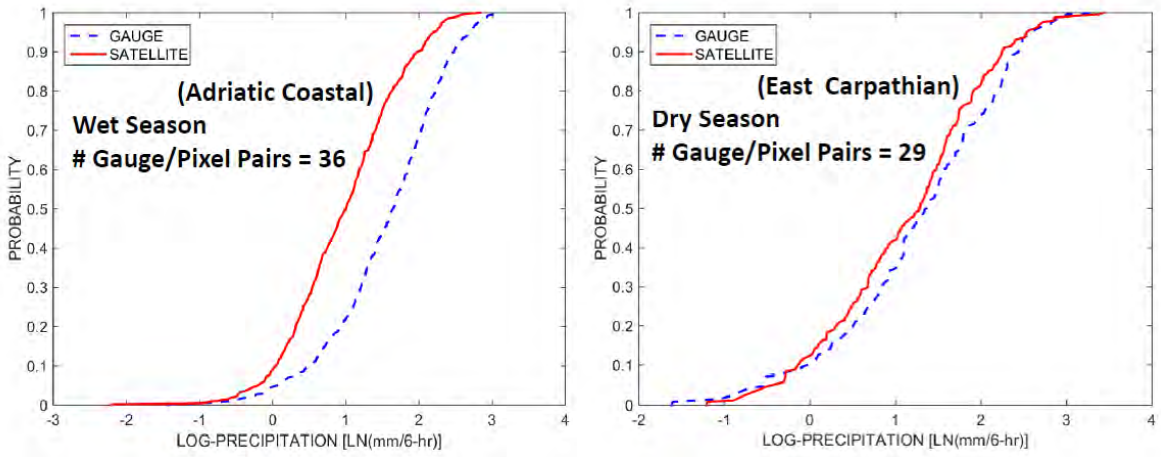

Figure 32. Cumulative distribution function for gauge vs MWGHE; Regions 7 & 18

Climatological precipitation bias adjustment should be reviewed and updated on a regular basis (every 2-3 years) by operational personnel. Updates could include additional stations (i.e., not in real-time archive) with consistent resolution. Figure 33 shows a bias adjustment scheme overview.

7. BIAS ADJUSTMENTS

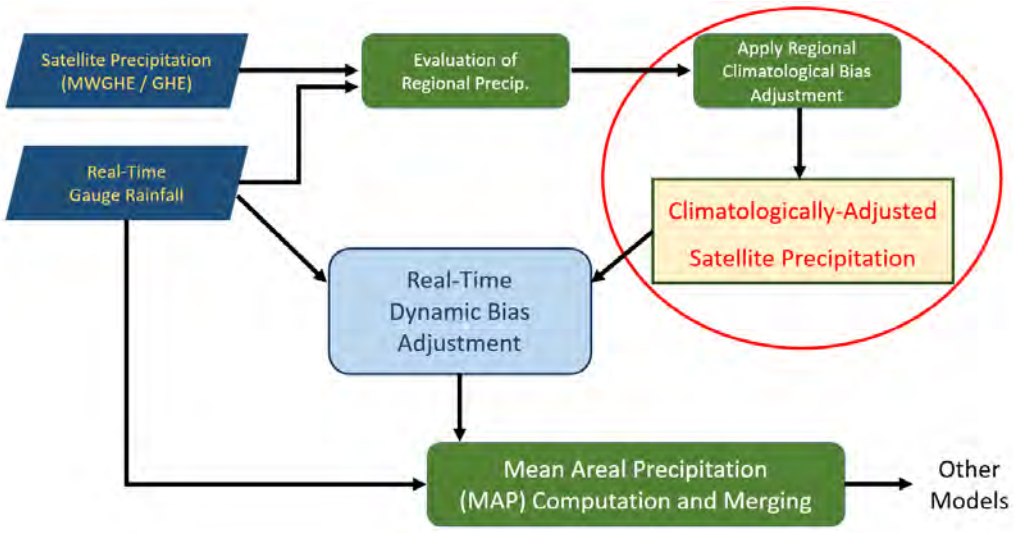

Figure 33. Bias adjustment scheme overview

In addition to the climatological bias adjustment, an algorithm that compares near real time satellite and gauge precipitation estimates is implemented in the operational SEEFFG system for near real time dynamic bias adjustment. The dynamic bias adjustment is based on the Kalman Filter approach, and considers the number of reporting real-time gauges within each sub-region, as well as the gauge data quality to track differences in the satellite versus gauge precipitation estimates as events occur in real-time. The dynamic bias adjustment is applied after the climatological adjustment to account for event-based and time-varying differences in the satellite precipitation. There are a set of criteria for the dynamic bias adjustment to be applied which includes the number of gauge/satellite pixel pairs reporting precipitation and precipitation over given thresholds. If these criteria are not met, no dynamic adjustment is applied for the specific time and sub-region.

8. MERGED MAP (Mean Areal Precipitation)

Due to the complexity of the problem, the design of on-site networks has received considerable attention, both in the operational hydrologic environment (WMO 1994) and in the hydrologic research environment (Bras 1990). Hydrologists have developed several methods for estimating MAP over watersheds from rain gauge data. In most cases, the MAP estimation is based on a weighted average method, and because of the lack of ‘‘ground truth’’ data in most cases, the reliable estimation of precipitation estimate errors is an important issue studied using synthetic data generation (Tsintikidis et al., 2002).

Merged MAP in SEEFFG System provides bias-corrected, best estimates of 1-, 3-, 6- and 24-hour precipitation accumulations over each of FFG system basins. This product is derived by selecting the best-available 1-hour precipitation input product for each basin from the bias-adjusted MWGHE or bias-adjusted GHE or the gauge-interpolations, with preference for selection in that order. The Merged MAP data products are updated every hour and reflect accumulations of basin-average precipitation of a given duration ending on the current navigation hour. Figure 34 shows the 24-hour accumulated MAP product. This is the accumulations of mean areal precipitation estimates for the sub-basins over the last 24 hours ending on the navigation hour. This example product is valid for precipitation accumulation starting 18:00 UTC on 24 May 2016 and ending 18:00 UTC on 25 May 2016.

The Merged MAP 6-hour accumulation product is applied during model processing as the precipitation input to the Snow-17 Model, the Sacramento Soil Moisture Accounting Model and flash flood threat model.

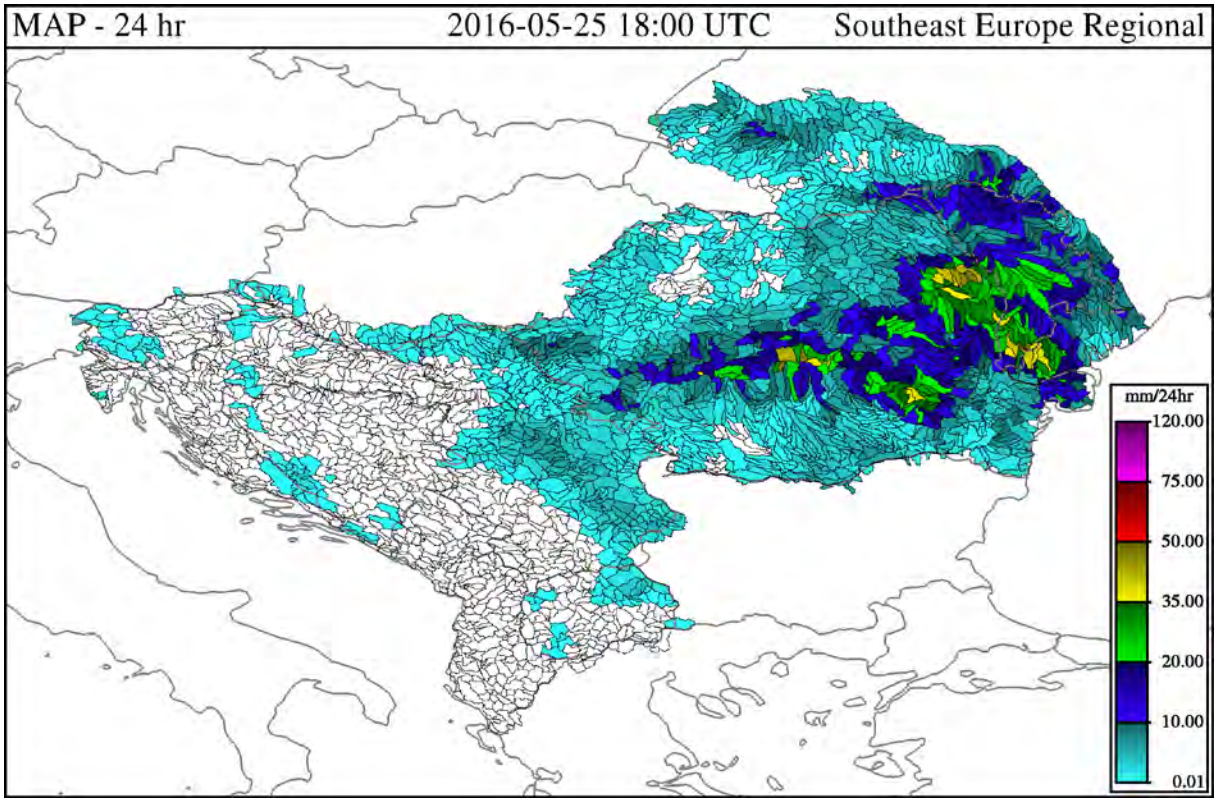

Figure 34. SEEFFGS 24-hour Merged MAP product

9. ASM (Average Soil Moisture)

Soil moisture content indicates the volume of water present in the soil pores and is typically measured in m^3/m^3 (volume of water per total volume). For hydrologic applications, depth-integrated soil moisture is also used, expressed in mm of water over the depth of soil. Soil moisture varies temporally and spatially and is an important component of the FFG model. It provides the available storage for buffering part of rainfall, reducing the runoff and potential to flash flooding.

The Average Soil Moisture (ASM) product shows soil water saturation fraction (dimensionless ratio of contents over capacity) for the upper zone water contents (20-30 cm depth) of the Sacramento Soil Moisture Accounting Model (SAC-SMA) for each of the sub-basins. Saturation of the upper zone is important for flash floods because if rainfall continues, most of the rainfall will become surface runoff. The forecaster must pay attention to spatial and temporal distribution of ASM. Temporal variation is quite rapid, depending on precipitation intensity and duration and soil type. If the upper soil moisture saturation fraction is high and meteorological models show continuation of rainfall in those regions, flash flood occurrence can be a concern depending on rainfall amounts/duration and the FFG values, i.e., these sub-basins should be monitored by the forecasters to assess if the rainfall will likely trigger flash flooding.

Within the SEEFFGS, the ASM products are updated every 6 hours at the model-processing hour at 00, 06, 12 and 18 UTC.

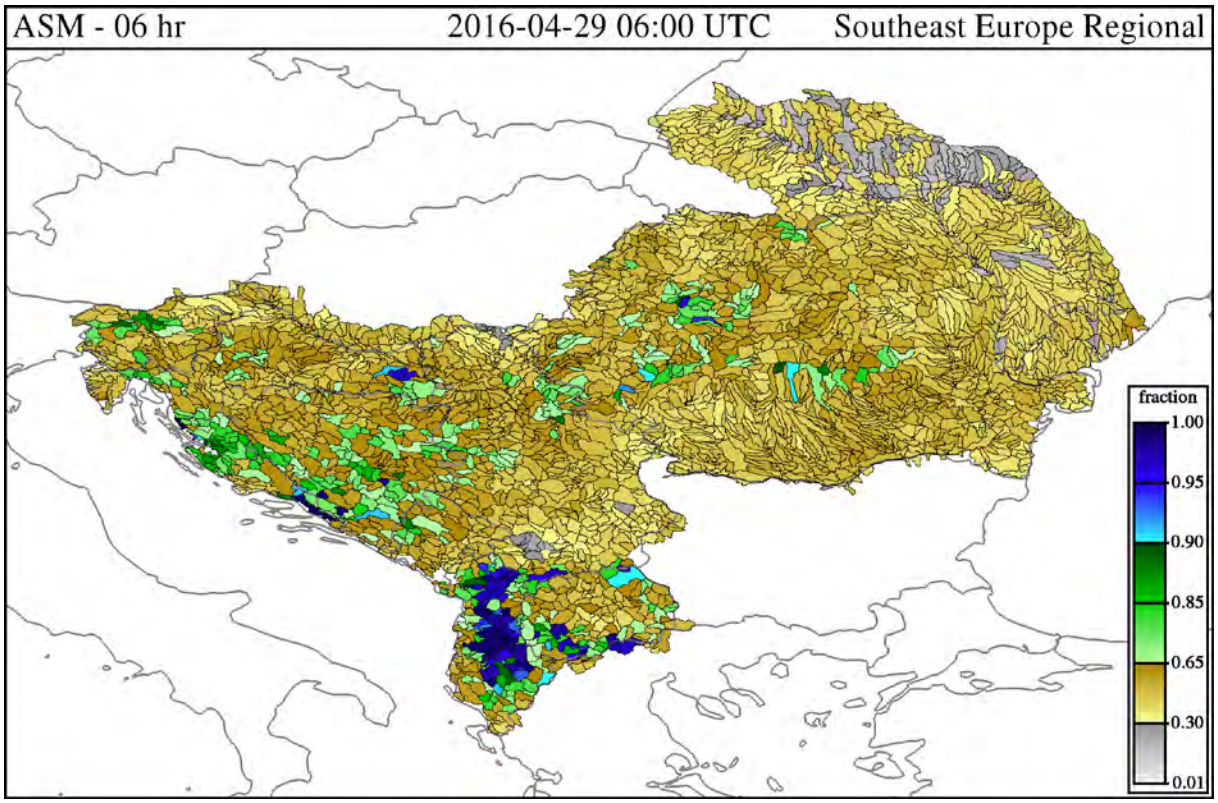

Figure 35. SEEFFG 6-hour Average Soil Moisture (ASM) product

9. ASM (Average Soil Moisture)

The image above shows ASM product for the SEE region for 29 April 2016 at 06 UTC. The scale indicates the fraction of soil moisture for a given sub-basin, with 1.00 meaning fully saturated. In this example, most sub-basins in Albania (and some in southern part of Croatia and Bosnia and Herzegovina) have approached complete saturation (dark blue) which makes this area vulnerable to the occurrence of flash floods if rainfall occurs at a level that may bring the stream channel to bankfull.

ASM provides information on the hydrologic state of the land surface and the land surface's capability to accept more rainfall input prior to generating fast runoff. The soil saturation in the upper zone is most relevant for flash flooding as this provides indication of the fast-response runoff generation. This is a key product for assessment of flash flood potential. Forecasters should be attentive to rapid changes in soil saturation.

Also, during the summer and when soil is dry, soil crusts can be formed. These can significantly reduce soil infiltration rate and subsequently the utilization of water resources, and increase surface runoff, especially during intense summer convective rainfall.

9.1. SAC-SMA (SACRAMENTO SOIL MOISTURE ACCOUNTING) MODEL

The Sacramento Soil Moisture Accounting Model (SAC-SMA) is a conceptual, continuous, area-lumped model that describes the wetting and drying process in the soil. In the following we provide a concise description of the model while a detailed SAC-SMA description and formulation is presented in Burnash et al. (1973) and Georgakakos (1986) for the discrete-time and continuous-time forms, respectively. The SAC-SMA simulates soil column response to tension and gravity forces to determine the water content of various soil layers at a given time, the evapotranspiration flux and surface and subsurface flow components (percolation to the deeper soil layers, interflow and baseflow).

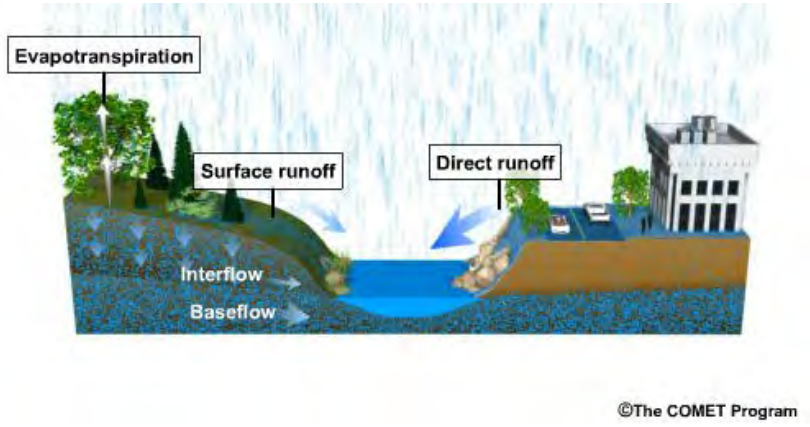

Figure 36. The SAC-SMA Model Elements

Real time input variables for the model in the SEEFFGS are 6-hour mean areal precipitation, Soil, terrain and land cover and snow melt data are, used to a priori estimate the model's time invariable parameters.

9. ASM (Average Soil Moisture)

The SAC-SMA model is comprised of a two-layer structure of a relatively thin upper layer that represents the top soil regime and interception storage and a commonly thicker lower layer that supplies moisture to meet the evapotranspiration demand and channel baseflow (flow that is not direct response to a rainfall rate). Each layer tracks water content changes to estimate soil moisture states through conceptual tension and free gravitational water storage components.

Surface runoff that contributes significantly to flash flooding is the result of filled upper soil water tension and free water reservoirs and the relationship between rainfall rates and percolation rates to the deeper soil layers.

Direct runoff contributes to flooding from permanently impervious areas and variable impervious-area surface runoff allows for flooding contribution by the increase and decrease of the saturated soil area near the stream.

9.1. SAC-SMA (SACRAMENTO SOIL MOISTURE ACCOUNTING) MODEL

Tension water refers to the portion of the soil moisture system, which can be separated from the soil and returned to the atmosphere through processes of evapotranspiration. Normally, tension water is held in position against the force of gravity by the molecular attraction between soil particles and water molecules. The potential volume of tension water within the soil is generally determined by interrelationship between the area's climate, the catchment's soil types and the characteristics of those plant forms that exist in the catchment.

Free water is water in the liquid state, which is free to travel through or across the soil. Such water will percolate through the soil, resupplying any soil moisture deficiencies it encounters. When rainfall occurs at a rate that is greater than the rate at which the surface can transfer water to its depths, the excess rain will reach the stream channel as surface runoff. The relative components of tension and free water, which can be held within the soil, vary with soil types. For a given quantity of soil, the small particle sizes associated with clay soils will generally accommodate the highest proportion of tension water. The large particle sizes associated with sandy soils provide more storage space between soil grains, and such soils will generally accommodate the highest proportion of free water.

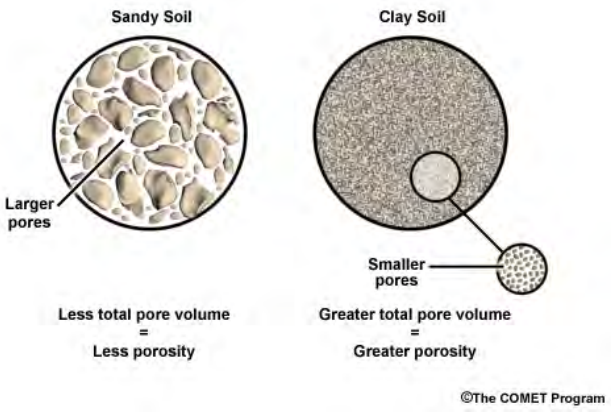

Figure 37. Pore space in sandy soil vs. clay soil

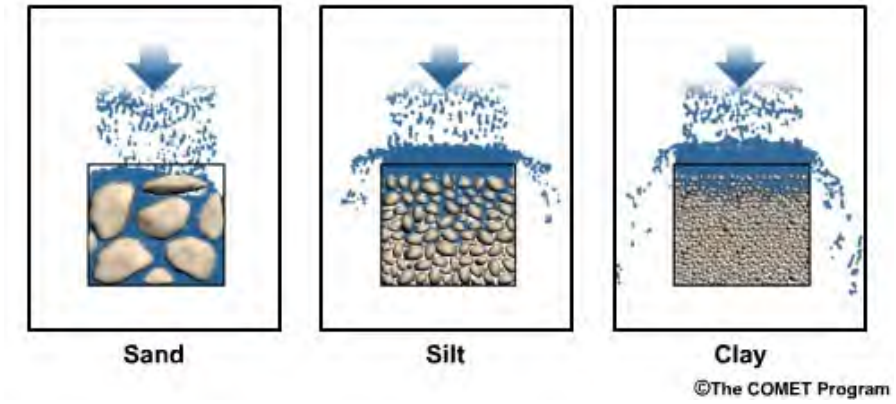

Figure 38. Infiltration variations by soil texture

In temperate regions (like in SEE) with deciduous vegetation, the catchment interception has a seasonal variation of little more than a millimetre in depth. The SAC-SMA, as a simplified

representation of catchment processes, includes intercepted precipitation as a portion of upper soil's tension water volume.

Despite the physical conceptualization embedded in the model structure, the model parameters (Table 1) cannot be directly measured from in-situ field observations. When streamflow, rainfall and soil moisture data are available for a specific basin, the parameter values are often estimated with an interactive calibration methodology that explicitly recognizes the function of the physical/conceptual components of the models (e.g. NWS 1999; Koren et al. 2000; Shamir et al. 2005; Georgakakos et al. 2013; Shamir and Georgakakos 2014).

Table 1. SAC-SMA Model Parameters

PARAMETER	DESCRIPTION	A PRIORI ESTIMATE
UZTWM	Upper zone tension maximum water capacity (mm)	Dup (FCup – WPup)
UZFWM	Upper zone free maximum water capacity (mm)	Dup (POup – FCup)
LZTWM	Lower zone tension maximum water capacity (mm)	Dlw (FClw – WPlw)
LZFPM	Lower zone primary free water capacity (mm)	0.83Dlw (POlw – FClw)
LZFSM	Lower zone supplemental free water capacity (mm)	0.17Dlw (POlw – FClw)
UZK	Upper zone drainage depletion coefficient (1/day)	1 – (FCup/POup) $^{1.6}$
LZPK	Lower zone primary drainage depletion coefficient (1/day)	(Evaluated from hydrographs)
LZSK	Lower zone supplementary drainage depletion coefficient (1/day)	UZK/[1+2(1-WPlw)]
ZPERC	Percolation equation coefficient	Carpenter et al., 2004
REXP	Percolation equation exponent	Carpenter et al., 2004
PFREE	Percentage of percolated water to Lower Zone Free Water	(WPlw/POlw) $^{1.6}$
SIDE	The ratio of non-channel sub-surface outflow to channel baseflow	Assumed 0
ADIMP	Percent of additional impervious area	Derived from Land cover land use data
PCTIM	Percent of permanently impervious area	

*where D is depth, WP is wilting point, FC is field capacity, PO is porosity for the upper and lower layers

The coarseness or porosity (PO) of the soil determines two other important factors – field capacity (FC) and wilting point (WP). If the pore spaces are filled with soil water and this water can drain freely from the soil as "gravity water," then the soil is called saturated. As the water drains from the soil, some pores will become filled with air and water vapour. When the pores no longer drain by gravity force, the capillary tension of the soil holds the water in place. Some of the larger pores will have drained but most still contain water. At this point the soil is said to be at field capacity. FC is also defined as the soil moisture level at or above which vegetation transpires at the maximum possible rate.

As water continues to be removed from the soil through evapotranspiration, more of the pore space will empty of water. As this process continues, only the tightly held water to the soil particles remains. There is a point where the tension of the water to the soil particle becomes so

tight that the water cannot be used by plant roots. This is called the "wilting point." WP which is also defined as the soil moisture level at or below which vegetation will not be able to transpire.

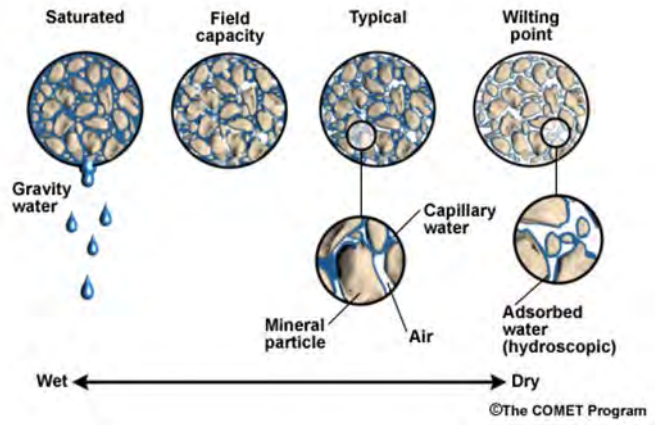

Figure 39. Generalized soil moisture conditions

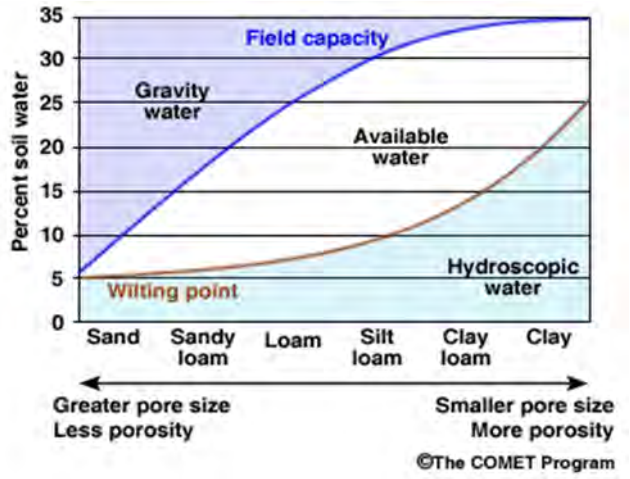

Figure 40. Soil moisture conditions for various soil textures

The link of the SAC-SMA parameters to soil and land cover characteristics was developed by Koren et. al (2000) – it is based on empirical association between soil-texture classes and soil hydraulic indices (such as saturated hydraulic conductivity and volumetric water content that is associated with wilting point, field capacity and saturated retention conditions). This method of parameter estimation requires spatial information that includes soil texture, soil depth and land cover. For the land cover data, Land cover USGS AVHRR (Advanced Very High Resolution Radiometer; 1 km resolution) was used.

The SAC-SMA parameters for the SEE region were derived from the European Soil Database (vector data) except Slovenia that provide high resolution soil data, developed in collaboration with the European Soil Bureau Network, which holds a joint copyright to the data with the

9.1. SAC-SMA (SACRAMENTO SOIL MOISTURE ACCOUNTING) MODEL

European Commission. Figure 41 shows a map of soil texture categories while Figure 42 shows a priori estimates of key SAC-SMA parameters for SEE region.

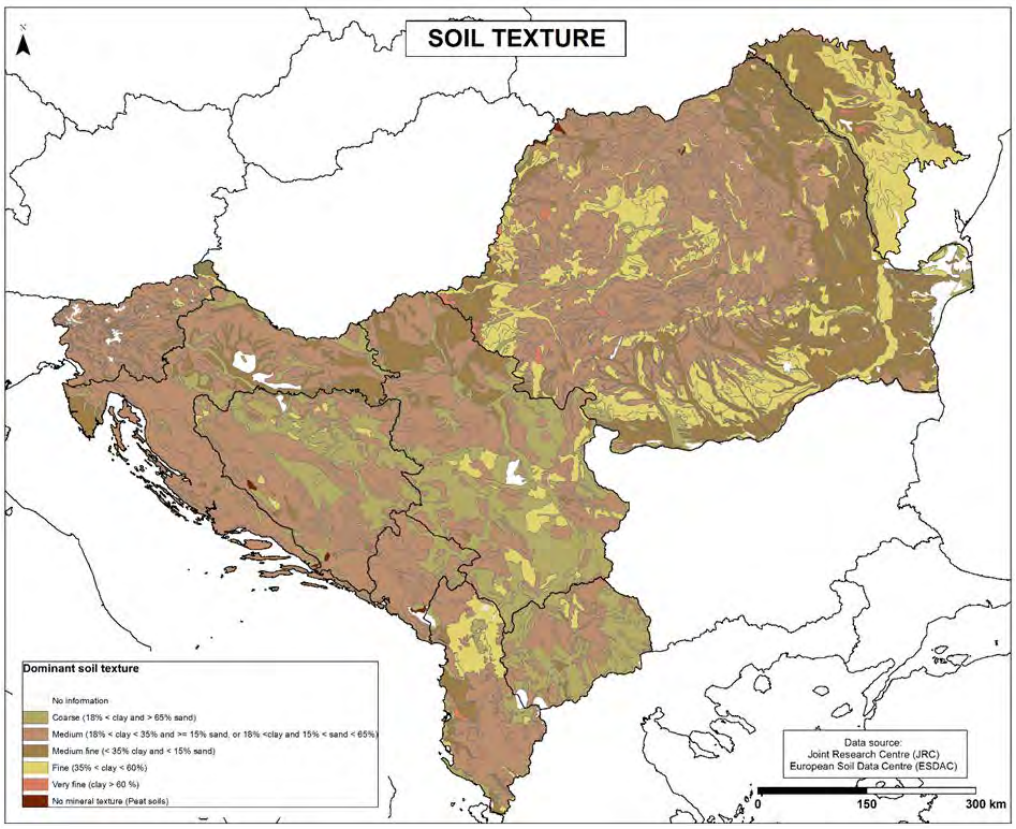

Figure 41. Soil texture for SEE region

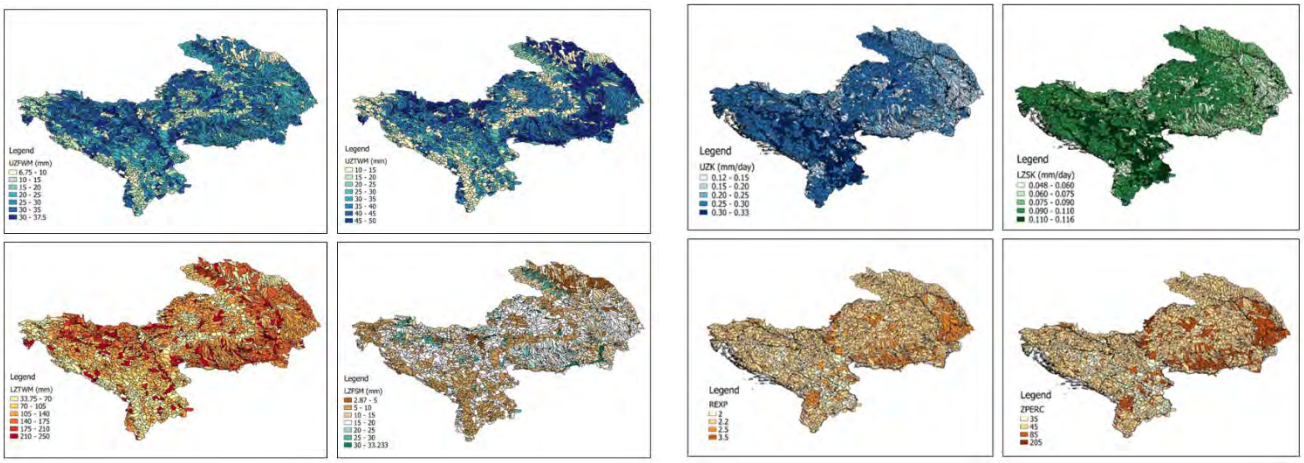

Figure 42. SAC-SMA basin parameters for SEE region

The SAC-SMA utilizes a set of storage of determinable capacities that are linked by process which allow the system to approximate many soil moisture conditions that control the production of streamflow. The algorithm computes runoff in five basic forms: 1) Direct runoff from

9.1. SAC-SMA (SACRAMENTO SOIL MOISTURE ACCOUNTING) MODEL

permanent and temporary impervious areas; 2) surface runoff due to precipitation occurring at a rate faster than percolation and interflow can take place when both upper zone storages are full; 3) interflow resulting from the lateral drainage of a temporary free water storage; 4) supplemental baseflow;, and 5) primary baseflow.

According to the Burnash (1995), the images below visualize the SAC-SMA model storages and typical seasonal response of soil moisture and discharge. The sequence shown in these figures traces the transition from a very dry condition, through a seasonal wetting cycle, and the return to dry weather.

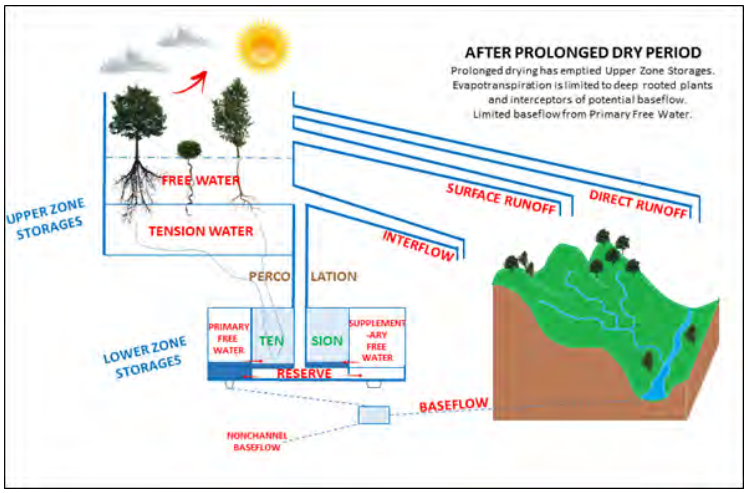

Figure 43. The SAC-SMA after prolonged dry period

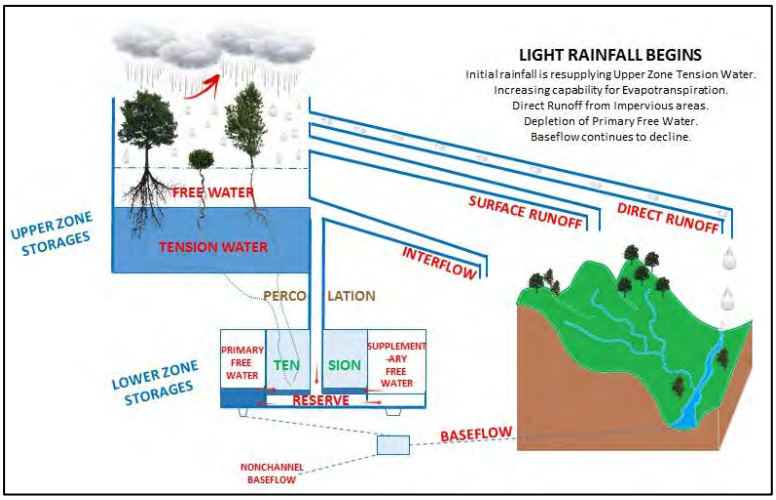

Figure 44. The SAC-SMA after light rainfall begins

9.1. SAC-SMA (SACRAMENTO SOIL MOISTURE ACCOUNTING) MODEL

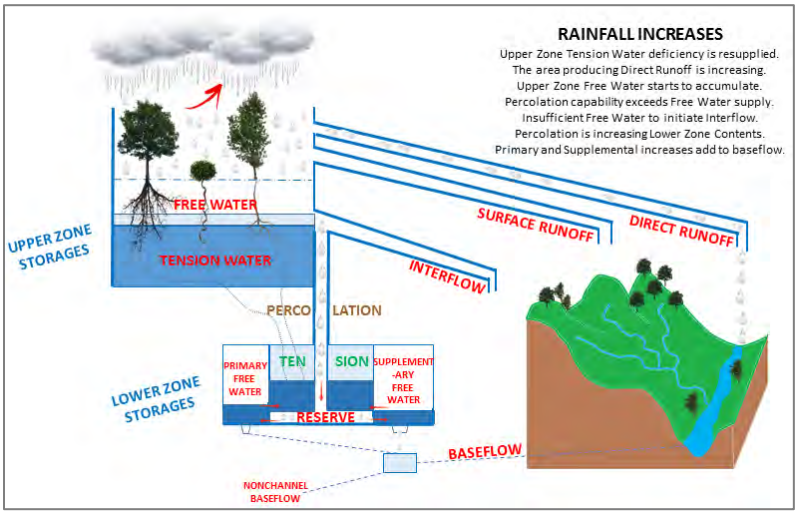

Figure 45. The SAC-SMA after rainfall increases

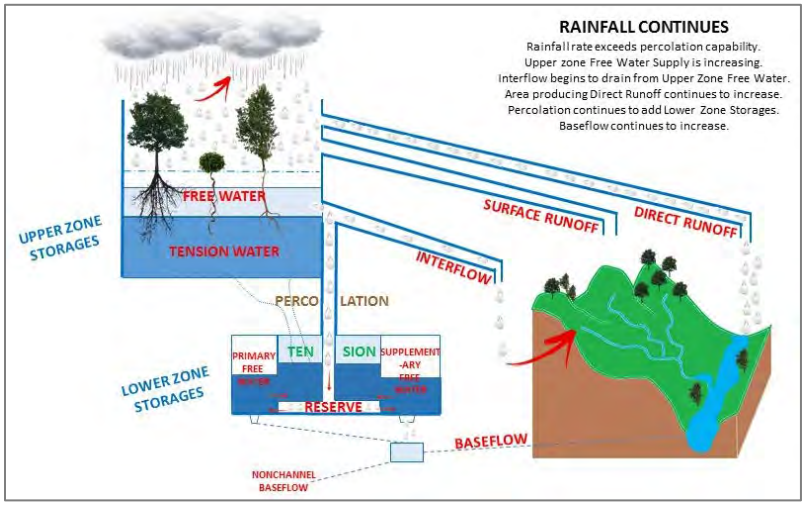

Figure 46. The SAC-SMA rainfall continues

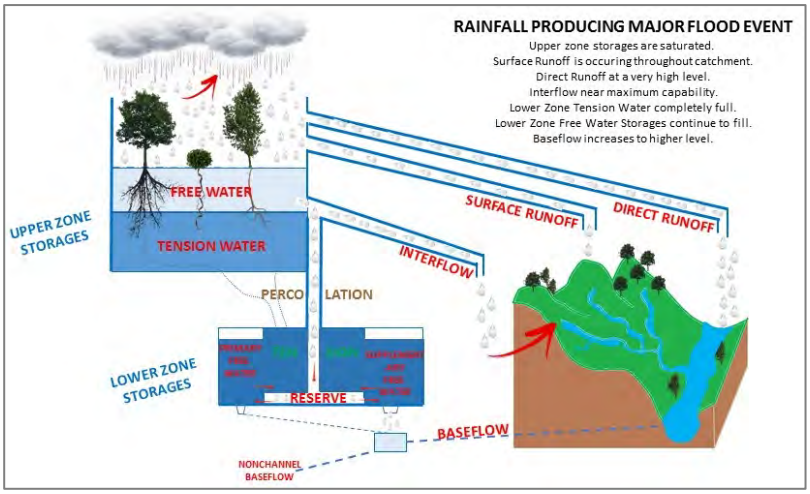

Figure 47. The SAC-SMA rainfall producing major flood event

9.1. SAC-SMA (SACRAMENTO SOIL MOISTURE ACCOUNTING) MODEL

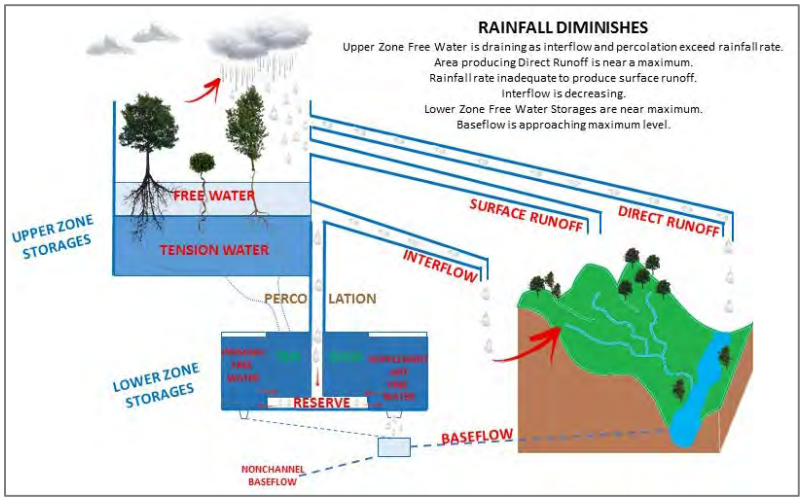

Figure 48. The SAC-SMA rainfall diminishes

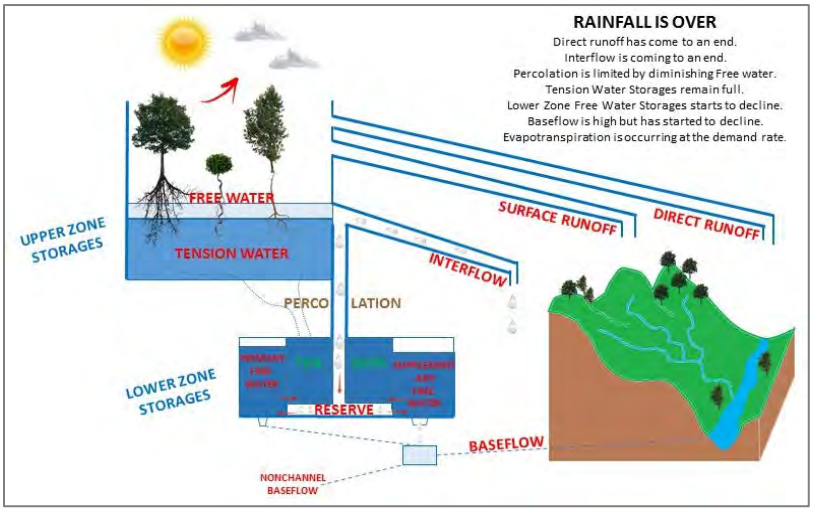

Figure 49. The SAC-SMA rainfall is over

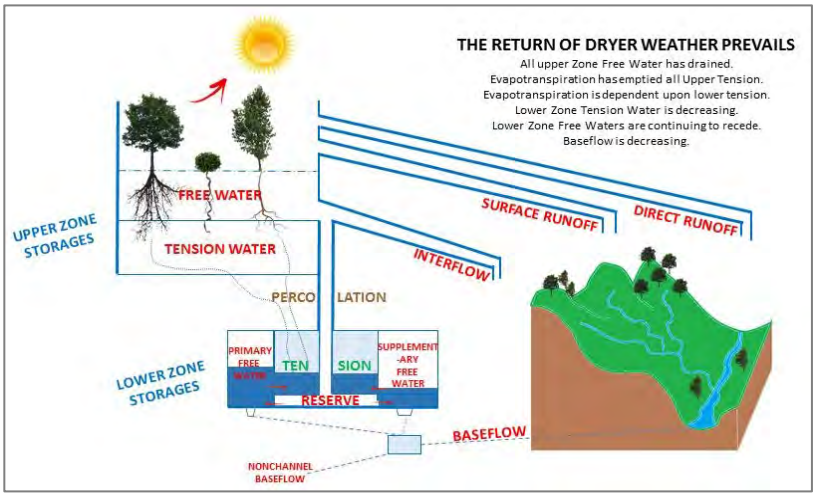

Figure 50. The SAC-SMA – the return of dry weather prevail

10. FFG (Flash Flood Guidance)

The term “flash flood guidance” refers to the volume of rainfall of a given duration distributed uniformly over a small catchment that is just enough to cause minor flooding at the outlet of the draining stream. Flash flood guidance values determined statistically or based on geomorphological principles have been used in an operational environment for quickly assessing localized flash flood threats within a large area by comparing to same-duration observed or forecast rainfall accumulations (e.g., Mogil et al. 1978; Sweeney et al. 1992). The details of the formulation of the elements of geomorphologically-based flash flood guidance systems are given in Carpenter et al. (1999) and Georgakakos (2006). Ntelekos et al. (2005) examine in detail the uncertainty in models and input data (Georgakakos, 2005).

The FFG is the key product in the determination of flash flood potential when using FFGS. The FFG is defined as the amount of actual rainfall (the total volume of rainfall) of a given duration (e.g. 1, 3 or 6 hours) that is just enough to cause bankfull flow at the outlet of the catchment. Flash Flood Guidance then is an index that indicates how much rainfall is needed to overcome soil and channel storage capacities and to cause minimal flooding at the outlet of a given small basin. The FFG is calculated and updated at every six hours at the model processing hour of 00, 06, 12 and 18 UTC and is valid for the next 1, 3 and 6 hours. If this FFG amount is known, one may compare it to the forecast or nowcast rainfall of the same duration and for the same period (and other local information) to determine whether there is a risk of flash flooding in the sub-basins. If the observed or forecast rainfall volume exceeds the FFG value of the same duration (MAP – FFG), this excess is termed the Flash Flood Threat (FFT) and indicates that flooding at or near the catchment outlet can be possible.

Values of FFG (1, 3, and 6-hour) are greyed not displayed in the graphical products (they are greyed) or provided in the data text files for basins with areas of 40% or greater snow cover or basins with an accumulated drainage area greater than 2,000 km^2.

Forecasters are advised to pay attention to the inverse relationship between the possibility of flash flood occurrence and FFG values. The lower the FFG, the higher possibility of flash flood occurrence.

The images below present example 6-hour FFG products – i.e., the required rainfall over the next 6 hours to cause bankfull flow following the most recent (current) model processing hour (mm/6hr). The images show how the FFG values changed over time and what their magnitudes were. The presented time period, 13-15 May 2014, were during the worst flood events in the SEE region in over a hundred years.

10. FFG (Flash Flood Guidance)

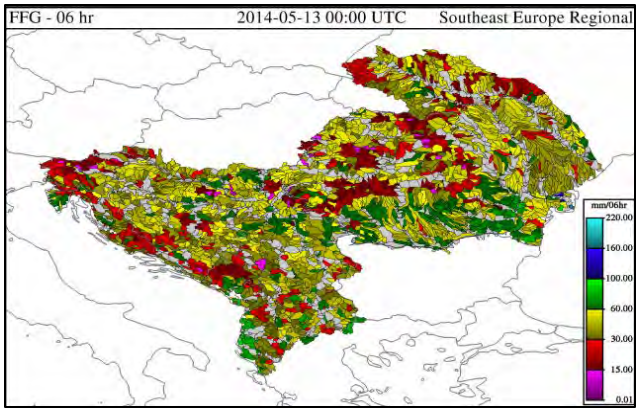

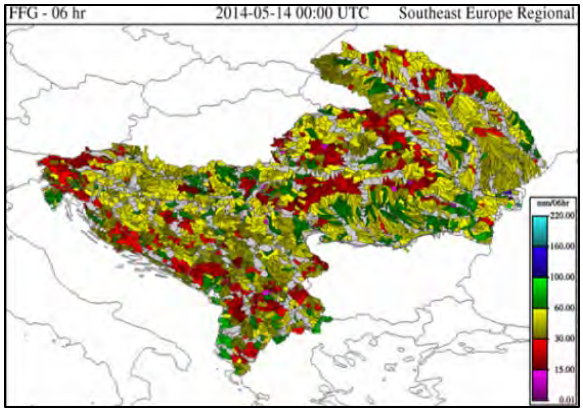

Figure 51. 6-hr FFG on 13 May 2014, 00 UTC Figure 52. 6-hr FFG on 14 May 2014, 00 UTC

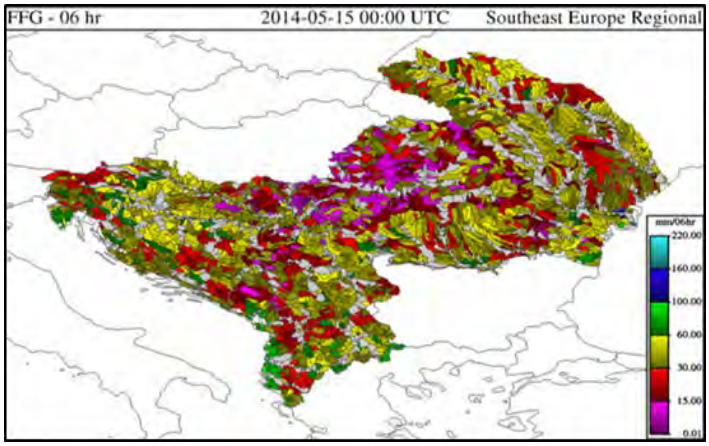

Figure 53. 6-hr FFG on 15 May 2014 at 00 UTC

The 6-hr FFG products showed that FFG values significantly decreased from 13 May 2014 at 00 UTC to 15 May 2014 at 00 UTC from predominantly 30-60 mm (yellow sub-basins) to 0-15 mm (pink). Reduction of FFG values over time and space is very good indication for the forecasters to pay attention to these sub-basins for possible flash flood occurrences.

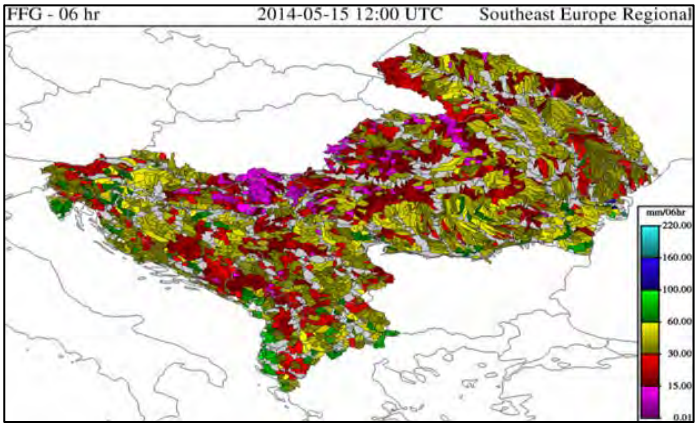

Figure 54. 6-hr FFG on 15 May 2014 at 12 UTC

10. FFG (Flash Flood Guidance)

On 15 May 2014 at 12 UTC, 6-hour FFG values reached their minimums during this event, with values of 0-15 mm (pink) over northern Serbia, Bosnia and Herzegovina, eastern Croatia, and western Romania.

Subsequently on 16 May 2014 at 12 UTC, the 6-hour FFG values had increased significantly. This provides an indication that the precipitation had reduced considerably or stopped, and that the soil moisture was draining. FFG values increased reflecting the capacity of the soils to accept additional rainfall.

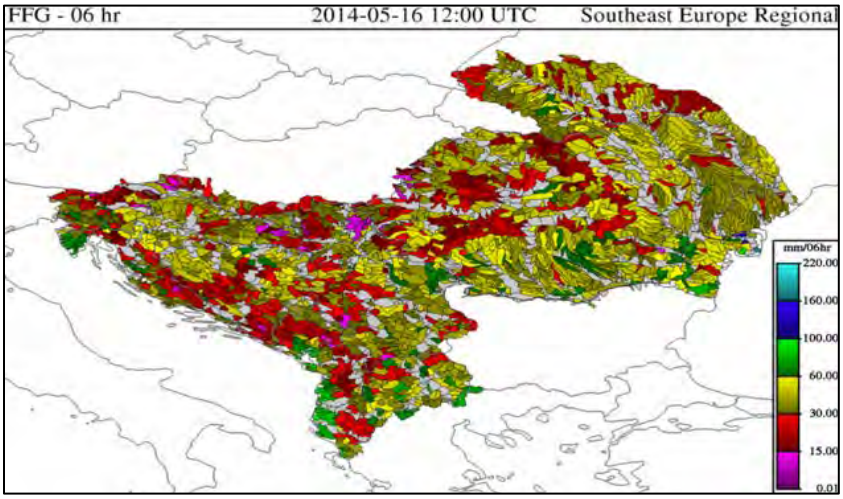

Figure 55. 6-hr FFG on 16 May 2014 at 12 UTC

11. IFFT (Imminent Flash Flood Threat)

Imminent Flash Flood Threat (IFFT) is one of the three flash flood threat products. The values indicate the difference of the Merged MAP of a given duration and the corresponding past model processing hour FFG of the same duration for a given sub-basin. That is, the IFFT value is considered a current “observation”. IFFT indicates that a flash flood is happening now or is imminent. IFFT provides the forecaster with an idea of likely regions of imminent flash flood threats. Each IFFT product is updated every six hours. Outputs are provided graphically for each of the FFG system basins and as text. It should be noted that this product concerns the past rainfall and should be evaluated before using for warnings. IFFT is offered as a baseline product that must be carefully evaluated by the forecaster in real-time. Descriptions of the products can be accessed by clicking on the “Product Description“ button at the bottom of the SEEFFGS Products Console.

Values of IFFT (1-, 3-, and 6-hour) are not displayed in the graphical products or provided in the data text files for basins with areas of 40% or greater snow cover or basins with an accumulated drainage area greater than 2,000 km^2. Basins meeting either of these criteria are shown in grey coloured shading in the SEEFFGS products and as -999.00 in the text files.

11.1. 1-Hour Imminent Flash Flood Threat (1hr-IFFT)

IFFT 01-hr: Difference of 01-hr FFG from a previous model processing hour and 01-hr MAP observed over the following 1 hour (mm/1hr). The 1-hour IFFT is valid at (01, 07, 13, and 19 UTC) as shown in Figure 56.

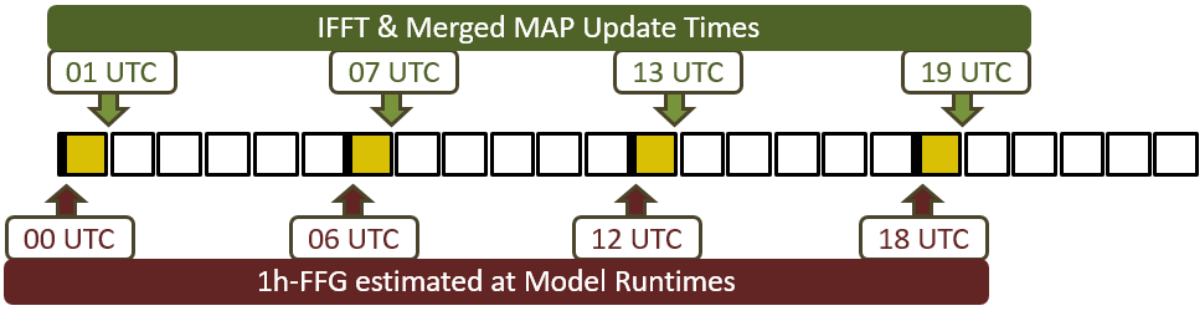

Figure 56. 1-hr IFFT estimation scheme

$$1h\ IFFT_t = 1h\ merged\ MAP_t - 1h\ FFG_{t\text{-}1h},\ where\ t = 01, 07, 13\ and\ 19\ UTC$$

The 01-hr IFFT at 01:00 UTC = the difference between the 01-hr Merged MAP from 01:00 UTC and the 01-hr FFG from 00:00 UTC (valid for 01 UTC). The 01-hr IFFT at 07:00 UTC = the difference between the 01-hr Merged MAP from 07:00 UTC and the 01-hr FFG from 06:00 UTC (valid for 07 UTC). The 01-hr IFFT at 13:00 UTC = the difference between the 01-hr Merged MAP from 13:00 UTC and the 01-hr FFG from 12:00 UTC (valid for 13 UTC). The 01-hr IFFT at 19:00 UTC = the difference between the 01-hr Merged MAP from 19:00 UTC and the 01-hr FFG from 18:00 UTC (valid for 19 UTC).

11. IFFT (Imminent Flash Flood Threat)

11.2. 3-Hour Imminent Flash Flood Threat (3hr-IFFT)

IFFT 03-hr: Difference of 03-hr FFG from a previous model processing hour and 03-hr MAP observed over the following 3 hours (mm/3hr). The 3-hour IFFT is valid at (03, 09, 15, and 21 UTC) as shown in Figure 57.

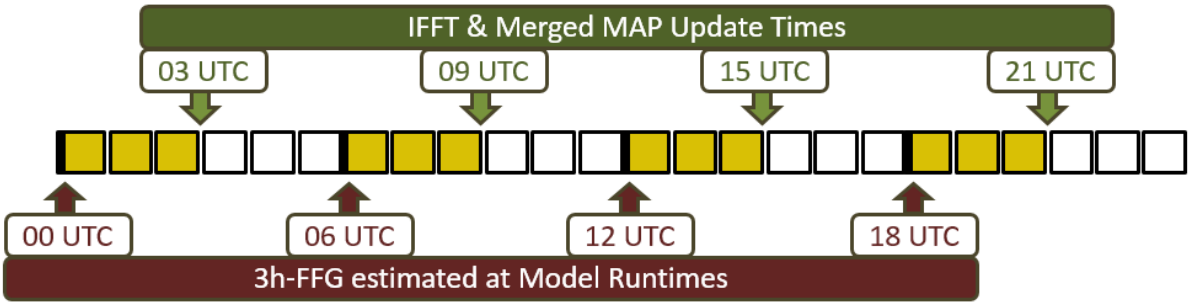

Figure 57. 3-hr IFFT estimation scheme

$$3h\ IFFT_t = 3h\ merged\ MAP_t - 3h\ FFG_{t-3h},\ where\ t = 03, 09, 15\ and\ 21\ UTC$$

The 03-hr IFFT at 03:00 UTC = the difference between the 03-hr Merged MAP from 03:00 UTC and the 03-hr FFG from 00:00 UTC (valid for 03 UTC). The 03-hr IFFT at 09:00 UTC = the difference between the 03-hr Merged MAP from 09:00 UTC and the 03-hr FFG from 06:00 UTC (valid for 09 UTC). The 03-hr IFFT at 15:00 UTC = the difference between the 03-hr Merged MAP from 15:00 UTC and the 03-hr FFG from 12:00 UTC (valid for 15 UTC). The 03-hr IFFT at 21:00 UTC = the difference between the 03-hr Merged MAP from 21:00 UTC and the 03-hr FFG from 18:00 UTC (valid for 21 UTC).

In our example, the 03-Hour IFFT at 09 UTC, 11 October 2015 is shown on Figure 58. IFFT values are displayed for sub-basins located on the north coastal region of Croatia and southern region of Bosnia and Herzegovina. The IFFT values are 0-10 mm/3h in yellow, 10-40 mm/3h in orange and 40-100mm/3h in red. Catchments of orange or red colour have highest probability that flash flood has already occurred or is going to occur very soon. FFT products are not intended to be the forecast; rather, these are indicators of regions of potential concern that the forecaster should review.

11. IFFT (Imminent Flash Flood Threat)

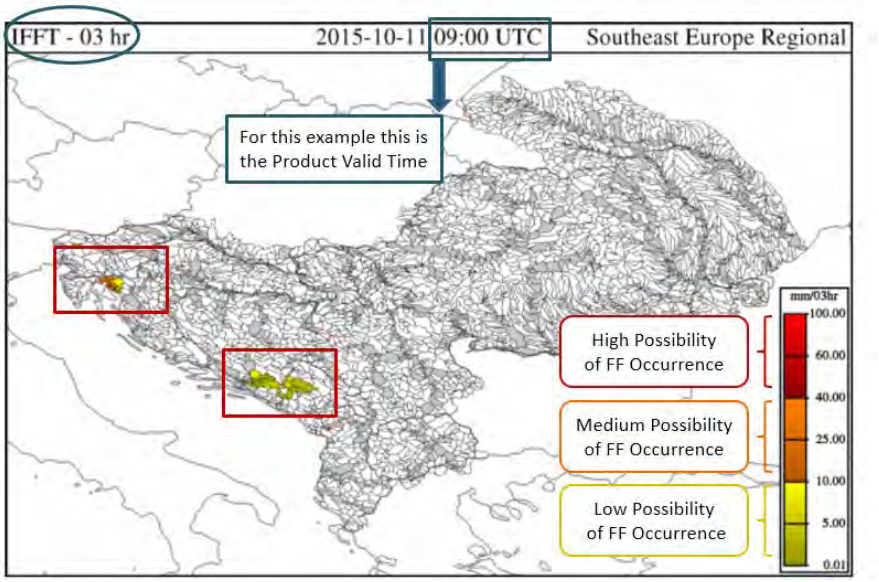

Figure 58. 03-hr IFFT at 09 UTC, 11 October 2015

11.3. 6-Hour Imminent Flash Flood Threat (6 hr-IFFT)

IFFT 06-hr: Difference of 06-hr FFG from a previous model processing hour and 06-hr MAP observed over the following 6 hours (mm/6hr). The 6-hour IFFT is valid at (00, 06, 12, and 18 UTC) as shown on Figure 59.

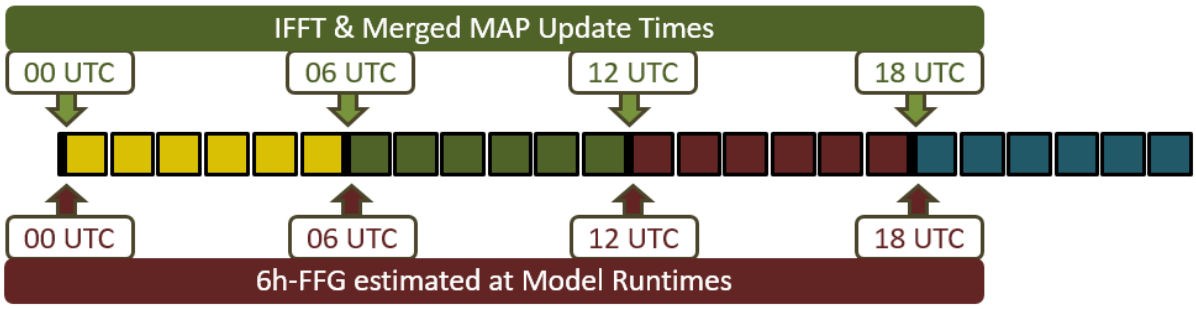

Figure 59. 6-hr IFFT estimation scheme

$$6h\ IFFT_t = 6h\ merged\ MAP_t - 6h\ FFG_{t\text{-}6h},\ where\ t = 00, 06, 12\ and\ 18\ UTC$$

The 06-hr IFFT at 00:00 UTC = the difference between the 06-hr Merged MAP from 00:00 UTC and the previous 06-hr FFG from 18:00 UTC (valid for 00 UTC). The 06-hr IFFT at 06:00 UTC = the difference between the 06-hr Merged MAP from 06:00 UTC and the previous 06-hr FFG from 00:00 UTC (valid for 06 UTC). The 06-hr IFFT at 12:00 UTC = the difference between the 06-hr

11. IFFT (Imminent Flash Flood Threat)

Merged MAP from 12:00 UTC and the previous 06-hr FFG from 06:00 UTC (valid for 12 UTC). The 06-hr IFFT at 18:00 UTC = the difference between the 06-hr Merged MAP from 18:00 UTC and the previous 06-hr FFG from 12:00 UTC (valid for 18 UTC).

12. PFFT (Persistence Flash Flood Threat)

Persistence Flash Flood Threat (PFFT) is the second flash flood threat product. Persistence is the simplest method of forecasting the weather and relies upon the current moment's conditions to forecast conditions for the next. The concept of PFFT is that previous precipitation of a given duration will persist for the same duration into the future. Therefore, the PFFT is considered a forecast flash flood threat using persistence for the rainfall forecast. Note that this set of products uses a crude rainfall forecast and contains large uncertainties and because of that, forecasters should be very careful with this product.

PFFT is the difference between the merged MAP estimated and updated at the FFG model runtime and the corresponding FFG value. 1-hour, 3-hour and 6-hour Persistence Flash Flood Threat products are estimated and updated at 00 UTC, 06 UTC, 12 UTC and 18 UTC. Descriptions of the products can be accessed by clicking on the “Product Description“ button at the bottom of the SEEFFGS Products Console.

12.1. 1-Hour Persistence Flash Flood Threat (1hr-PFFT)

PFFT 01-hr: Difference of 01-hr FFG for current model processing hour and current 01-hr MAP persisted for the next 1 hour (mm/1hr) as shown on Figure 60.

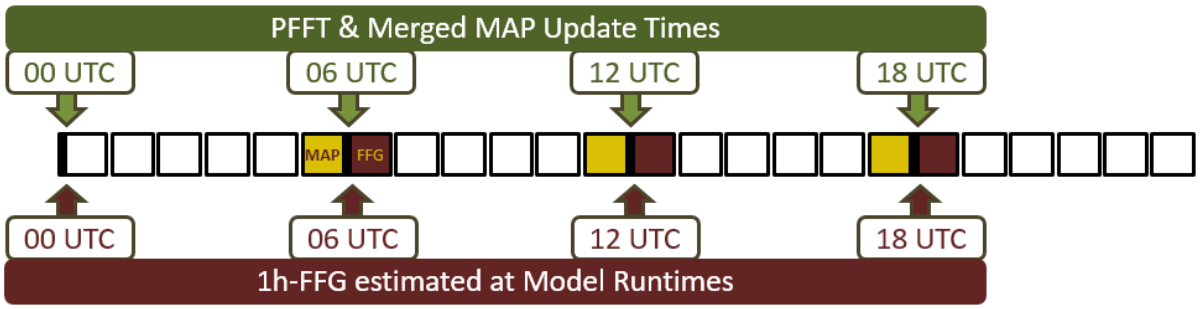

Figure 60. 1-hr PFFT estimation scheme

$$1h\ PFFT_t = 1h\ merged\ MAP_t - 1h\ FFG_t, \text{ where } t = 00, 06, 12 \text{ and } 18\ UTC$$

The 01-hr PFFT at 00:00 UTC = the difference between the 01-hr Merged MAP from 00:00 UTC and the 01-hr FFG from 00:00 UTC, considered valid at 01:00 UTC. The 01-hr PFFT at 06:00 UTC = the difference between the 01-hr Merged MAP from 06:00 UTC and the 01-hr FFG from 06:00 UTC, considered valid at 07:00 UTC. The 01-hr PFFT at 12:00 UTC = the difference between the 01-hr Merged MAP from 12:00 UTC and the 01-hr FFG from 12:00 UTC, considered valid at 13:00 UTC. The 01-hr PFFT at 18:00 UTC = the difference between the 01-hr Merged MAP from 18:00 UTC and the 01-hr FFG from 18:00 UTC, considered valid at 19:00 UTC.

12. PFFT (Persistence Flash Flood Threat)

12.2. 3-Hour Persistence Flash Flood Threat (3hr-PFFT)

PFFT 03-hr: Difference of 03-hr FFG for current model processing hour and current 03-hr MAP persisted for the next 3 hours (mm/3hr) as shown on Figure 61.

The 03-hr PFFT at 00:00 UTC = the difference between the 03-hr Merged MAP from 00:00 UTC and the 03-hr FFG from 00:00 UTC, valid at 03:00 UTC. The 03-hr PFFT at 06:00 UTC = the difference between the 03-hr Merged MAP from 06:00 UTC and the 03-hr FFG from 06:00 UTC, considered valid at 09:00 UTC. The 03-hr PFFT at 12:00 UTC = the difference between the 03-hr Merged MAP from 12:00 UTC and the 03-hr FFG from 12:00 UTC, considered valid at 15:00 UTC. The 03-hr PFFT at 18:00 UTC = the difference between the 03-hr Merged MAP from 18:00 UTC and the 03-hr FFG from 18:00 UTC, considered valid at 21:00 UTC.

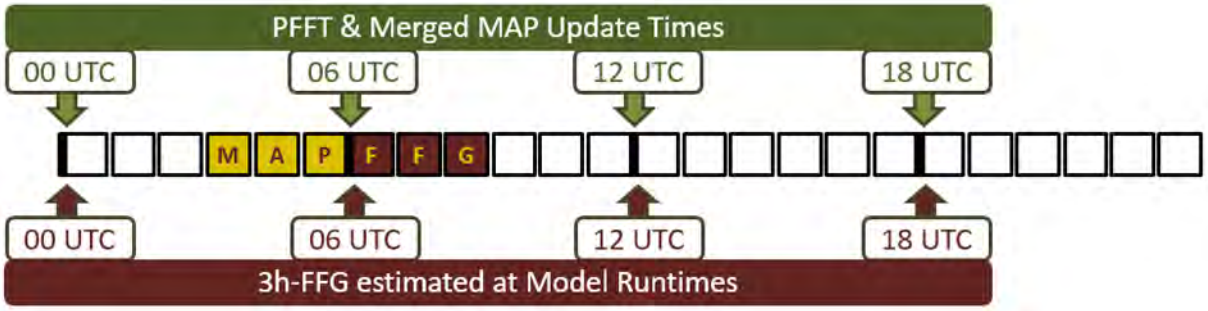

Figure 61. 3-hr PFFT estimation scheme

3h $PFFT_t$ = 3h merged MAP_t – 3h FFG_t, where t = 00, 06, 12 and 18 UTC

In our example, the 03-hr PFFT at 00 UTC, 11 October 2015 is shown on Figure 62. PFFT values are displayed for sub-basins located on the north coastal region of Croatia, western Slovenia, Albania, and The former Yugoslav Republic of Macedonia. The scale is an approximate measure of uncertainty of PFFT estimates and is indicated by colours. The PFFT values are 0-10 mm/3-hr in yellow, 10-40 mm/3-hr in orange and 40-100mm/3-hr in red. Catchments of orange or red colour have highest probability that flash flood occurrence is most likely if rainfall conditions persist.

12. PFFT (Persistence Flash Flood Threat)

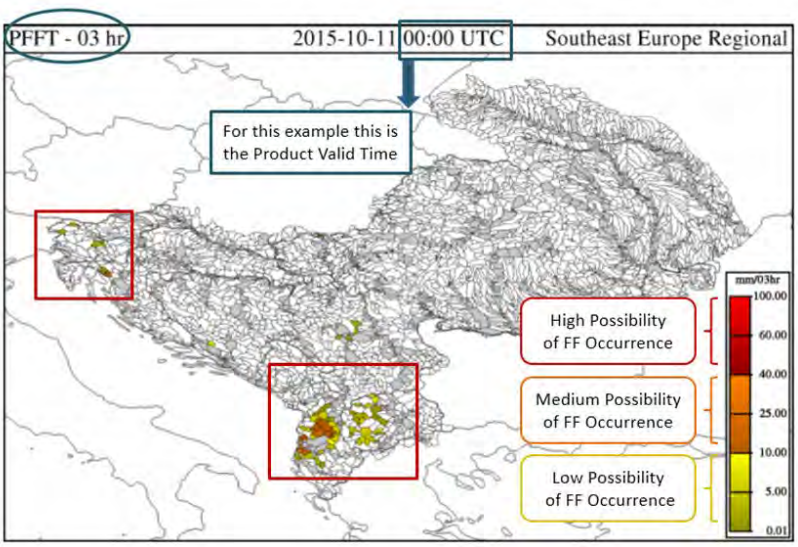

Figure 62. 03-hr PFFT at 00 UTC, 11 October 2015

12. PFFT (Persistence Flash Flood Threat)

12.3. 6-Hour Persistence Flash Flood Threat (6hr-PFFT)

PFFT 06-hr: Difference of 06-hr FFG for current model processing hour and current 06-hr MAP persisted for the next 6 hours (mm/6-hr) as shown on Figure 63.

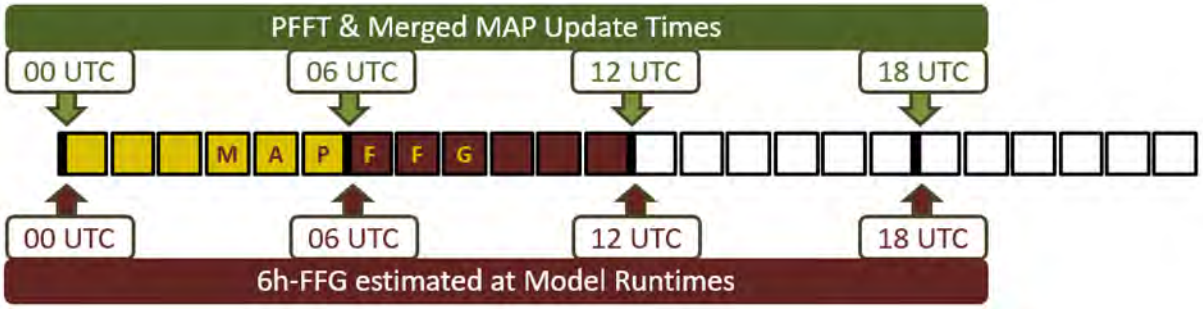

Figure 63. 6-hr PFFT estimation scheme

$$6h\ PFFT_t = 6h\ merged\ MAP_t - 6h\ FFG_t,\ where\ t = 00, 06, 12\ and\ 18\ UTC$$

The 06-hr PFFT at 00:00 UTC = the difference between the 06-hr Merged MAP from 00:00 UTC and the 06-hr FFG from 00:00 UTC, considered valid at 06:00 UTC. The 06-hr PFFT at 06:00 UTC = the difference between the 06-hr Merged MAP from 06:00 UTC and the 06-hr FFG from 06:00 UTC, considered valid at 12:00 UTC. The 06-hr PFFT at 12:00 UTC = the difference between the 06-hr Merged MAP from 12:00 UTC and the 06-hr FFG from 12:00 UTC, considered valid at 18:00 UTC. The 06-hr PFFT at 18:00 UTC = the difference between the 06-hr Merged MAP from 18:00 UTC and the 06-hr FFG from 18:00 UTC, considered valid at 00:00 UTC.

The 06-hr PFFT at 00 UTC, 11 October 2015 is shown in Figure 64. The PFFT values are 0-10 mm/3-hr in yellow, 10-40 mm/3-hr in orange and 40-100mm/3-hr in red. Catchment of orange or red colour have highest probability that flash flood occurrence is most likely if rainfall conditions persist. Figure 64 shows two main regions with numerous sub-basins that have PFFT values - north-west and south of the SEEFFG domain.

12. PFFT (Persistence Flash Flood Threat)

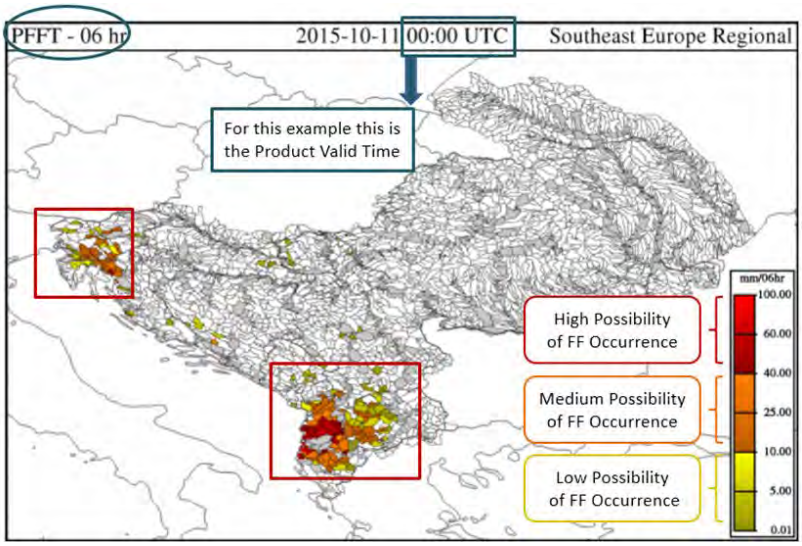

Figure 64. 06-hr PFFT at 00 UTC, 11 October 2015

13. ALADIN PRECIPITATION

Numerical weather prediction (NWP) models are one of the tools used for the complex process of providing an accurate weather forecast (Tudor et al, 2013). Global NWP models forecast weather over the entire Earth more than seven days in advance. These large scale global models do not provide high-resolution, which are important for the weather in a particular location. These details are often provided by limited area models (LAMs) that cover a particular area of interest. A high-resolution LAM is intended to predict the sub-synoptic weather features forced by topography or other local characteristics that can be absent in the main synoptic pattern (Tudor et al, 2013). The Croatian Meteorological and Hydrological Service (DHMZ uses ALADIN (Aire Limitée Adaptation Dynamique développement InterNational, ALADIN International Team, 1997) limited area model for the operational weather forecast (Tudor et al, 2013). ALADIN has been developed by a group of scientists from 16 countries (Figure 65).

The operational forecast suite in DHMZ uses the initial lateral boundary conditions from the ARPEGE (Action de Recherche Petite Echelle Grande Echelle) global NWP model run operationally at Meteo-France. Another set of initial and boundary conditions available in DHMZ is from the Integrated Forecast System (IFS) of the European Centre for Medium-Range Weather Forecast (ECMWF). The files received from Meteo-France and ECMWF do not contain the global model fields covering the whole Earth on the native ARPEGE or IFS grid and model levels (Tudor et al, 2013). To optimize the data transfer, the model data is interpolated to a limited-area Lambert projection grid in a resolution like the one of the global model in that area and it is covering a wider geographical area than the local LAM that uses it.

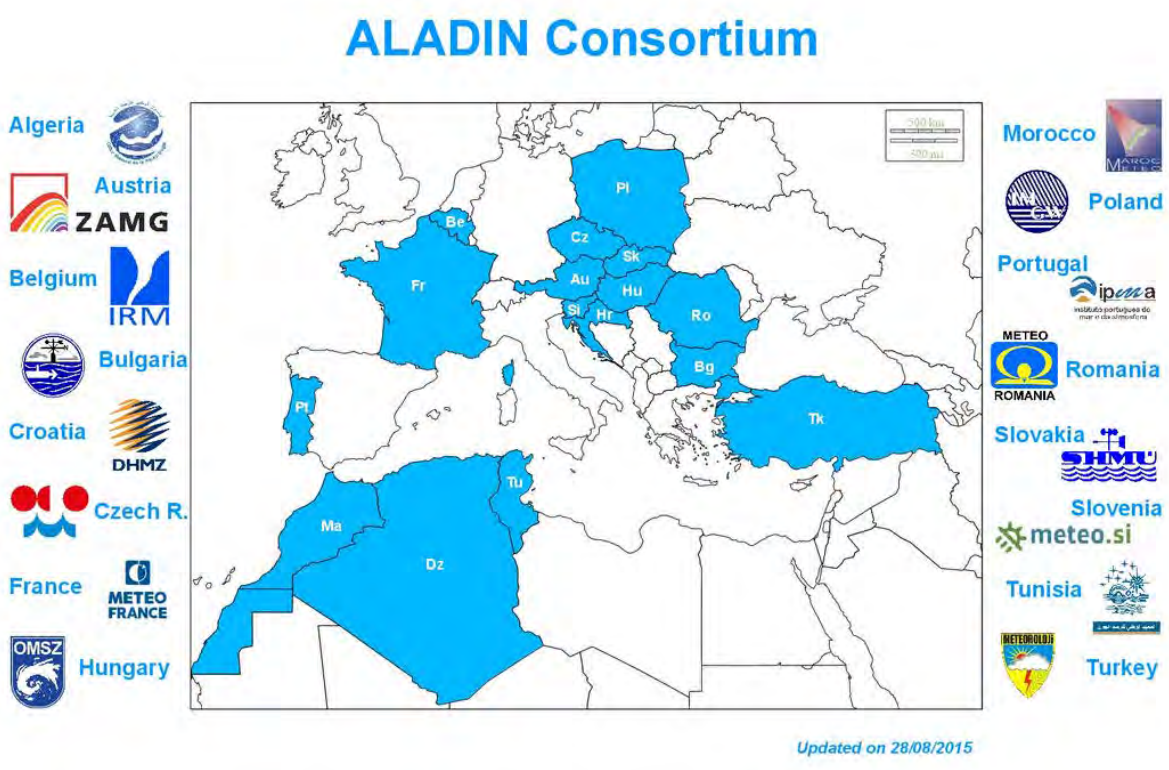

Figure 65. Member countries of ALADIN Consortium

13. ALADIN PRECIPITATION

The SEEFFGS is using a forecast precipitation product from the merging of two different ALADIN forecast model, produced by the Croatian and Turkish Meteorological services (DHMZ and TSMS, respectively) (Figure 66).However, the northern part of Moldova remains uncovered by an NWP (Figure 67).

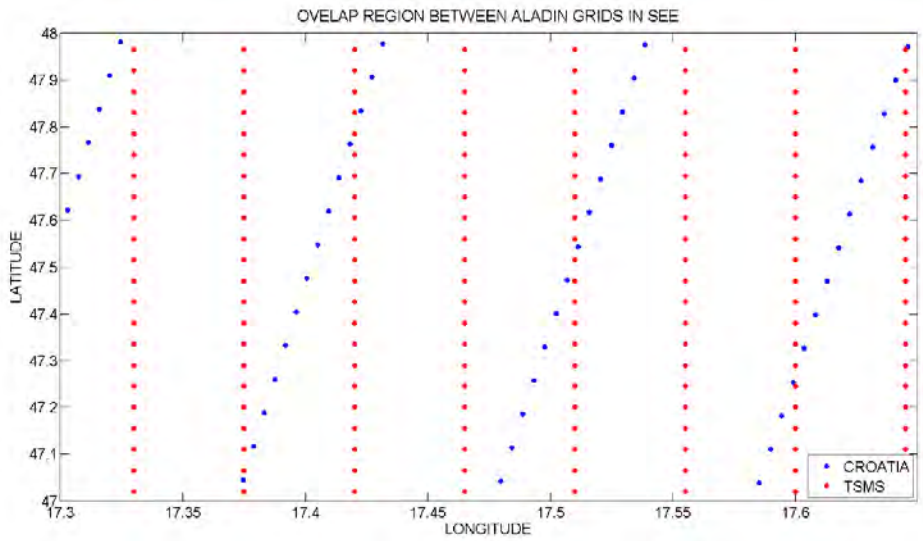

Figure 66. Intersection of the grid points of ALADIN Croatia and ALADIN Turkey

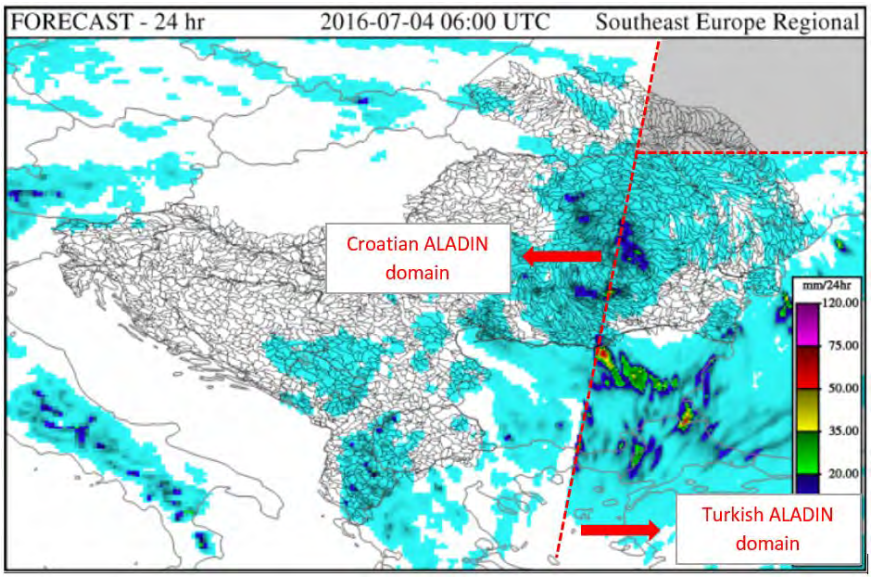

Figure 67. SEEFFG region with Croatian ALADIN domain and Turkish ALADIN domain

Currently, the Croatian Meteorological and Hydrological Service is running a hydrostatic version of ALADIN with 4 km horizontal resolution (HR44). It runs four times a day at 00 UTC, 06 UTC, 12 UTC and 18 UTC. Turkish State Meteorological Service is running a non-hydrostatic version

13. ALADIN PRECIPITATION

of ALADIN with 4.5 km horizontal resolution. It also runs four times a day at 00 UTC, 06 UTC, 12 UTC and 18 UTC producing precipitation forecasts out to 72 hours.

1-hour, 3-hour, 6-hour and 24-hour ALADIN precipitation products are generated and updated every hour and displayed in the SEEFFGS Main Products console. A robust precipitation forecast is the key for the estimation of Forecast Flash Flood Threat (FFFT) and is a useful tool for forecasters to issue flash flood watches and warnings taking into consideration existing and forecasted weather conditions. Soon, the plan is to implement a few more NWP models for full coverage of the SEE region. Also, there is a possibility for implementation of NWP models with finer resolutions, probabilistic NWP models, and an option for the forecaster to choose whichever NWP model in his/her opinion is the best for the current time and place.

14. FMAP (Forecast Mean Areal Precipitation)

Forecast Mean Areal Precipitation (FMAP) products are generated from the NWP precipitation forecasts for each catchment for 1-hour, 3-hours, 6-hours and 24-hours. Forecasters should analyse the catchments where intense precipitation has occurred and is forecast to occur for a given period and watch these regions during the forecast period.

An example in Figure 68 is showing 6-hour FMAP for 11 October 2015. The highest amount of precipitation was expected to occur in southern sub-catchments, near The former Yugoslav Republic of Macedonian-Albanian border. ALADIN predicted that precipitation amounts are going to be even greater over 24-hour period as it is shown in Figure 69. In the same image, the abrupt discontinuation of FMAP between sub-catchments in northern part of Moldova, where there is no NWP coverage, and surrounding sub-catchments may be seen.

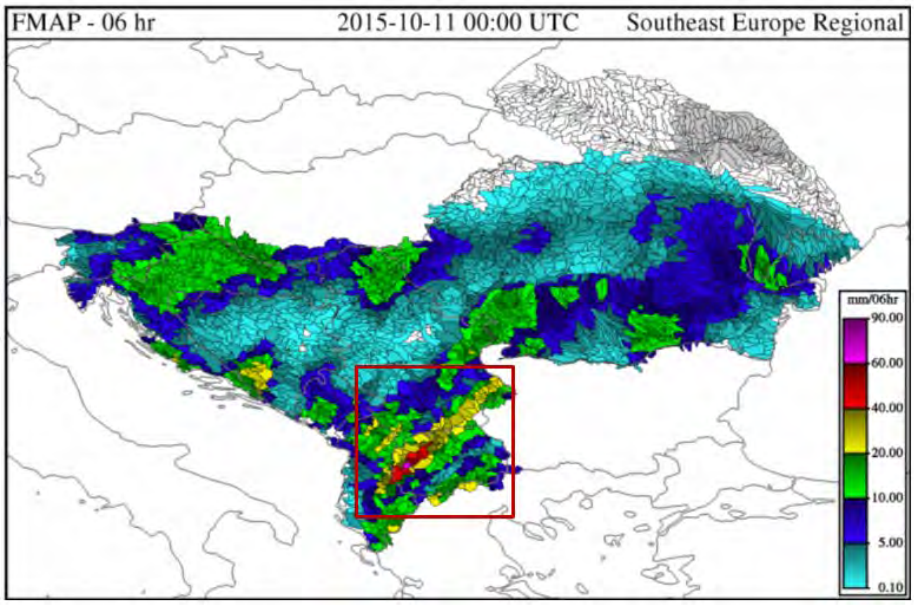

Figure 68. 6-hour accumulated Forecast Mean Areal Precipitation

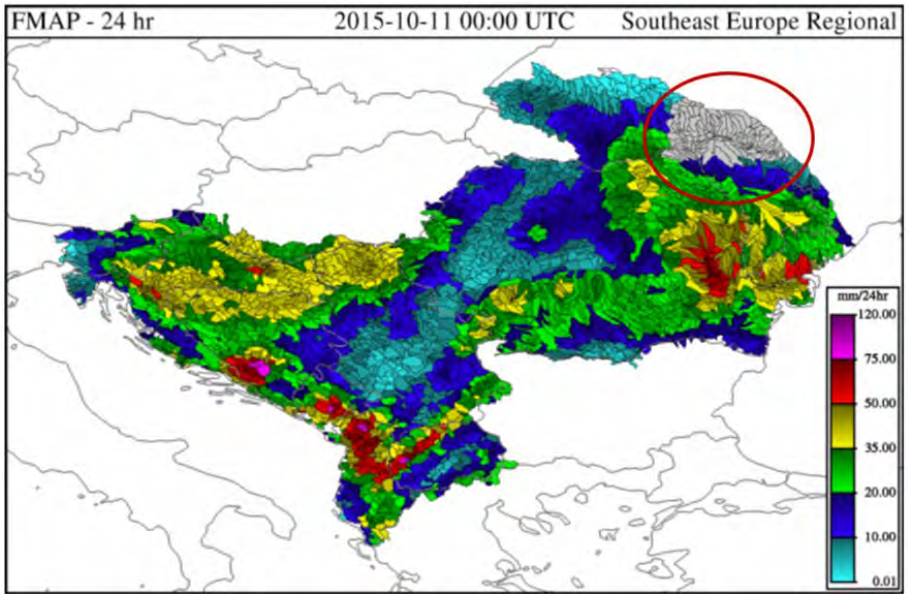

Figure 69. 24-hour accumulated Forecast Mean Areal Precipitation

15. FFFT (Forecast Flash Flood Threat)

Forecasters should note that unlike IFFT and PFFT that use merged Mean Areal Precipitation generated from bias adjusted satellite (or radar) measurements (Merged MAP) or gauge surface measurements (Gauge MAP), Forecast Flash Flood Threat (FFFT) estimation uses forecasts mean areal precipitation generated from ALADIN (FMAP). These two quite different kinds of source of quantitative precipitation. Therefore, forecasters must analyse both types of products carefully.

FFFT provides the forecaster with an idea of regions forecasted to be of concern for flash flooding based on the difference of FMAP forecasters of mean areal rainfall and the corresponding current FFG. In the computation of FFFT products, the 1-, 3-, and 6-hour FMAP products are all considered with current corresponding FFG products. These products are updated at 00-hr, 06-hr, 12-hr and 18-hr UTC.

15.1. 1-Hour Forecast Flash Flood Threat (1 hr-FFFT)

As it shown in figure 70, 1-Hour FFFT is estimated and updated at 00 UTC, 06 UTC, 12 UTC and 18 UTC. FFFT 01-hr: Difference of 01-hr FMAP for current model processing hour and current 01-hr FFG (mm/hr).

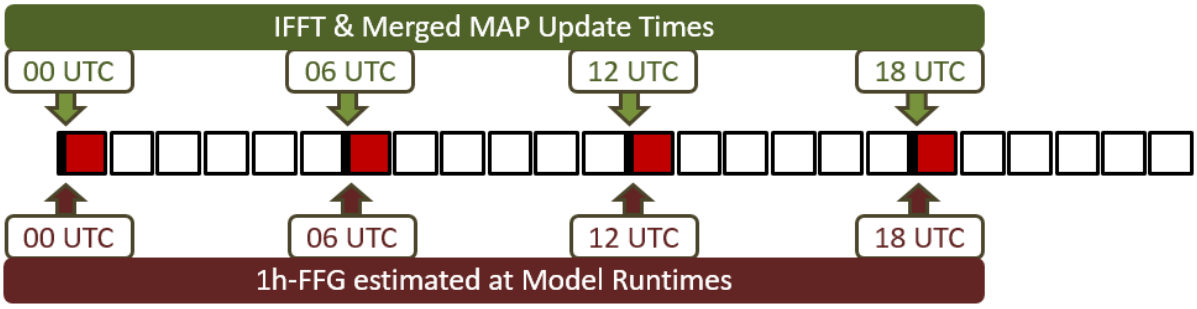

Figure 70. 1-hr FFFT estimation scheme

$$1h\ FFFT_t = 1h\ FMAP_t - 1h\ FFG_t, \text{ where } t = 00, 06, 12 \text{ and } 18\ UTC$$

The 01-hr FFFT at 00:00 UTC = the difference between the 01-hr Forecasted MAP from 00:00 UTC and the 01-hr FFG from 00:00 UTC, valid at 01:00 UTC. The 01-hr FFFT at 06:00 UTC = the difference between the 01-hr Forecasted MAP from 06:00 UTC and the 01-hr FFG from 06:00 UTC, valid at 07:00 UTC. The 01-hr FFFT at 12:00 UTC = the difference between the 01-hr Forecasted MAP from 12:00 UTC and the 01-hr FFG from 12:00 UTC, valid at 13:00 UTC. The 01-hr FFFT at 18:00 UTC = the difference between the 01-hr Forecasted MAP from 18:00 UTC and the 01-hr FFG from 18:00 UTC, valid at 19:00 UTC.

15. FFFT (Forecast Flash Flood Threat)

15.2. 3-Hour Forecast Flash Flood Threat (3 hr-FFFT)

As it is shown in Figure 71, 3-Hour FFFT is estimated and updated at 00 UTC, 06 UTC, 12 UTC and 18 UTC. FFFT 03-hr: Difference of 03-hr FMAP for current model processing hour and current 03-hr FFG (mm/3hr).

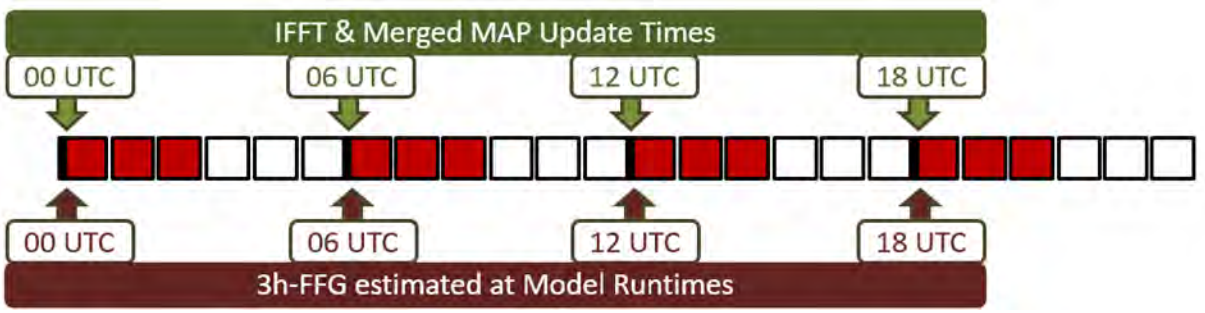

Figure 71. 3-hr FFFT estimation scheme

$3h\ FFFT_t = 3h\ FMAP_t - 3h\ FFG_t$, where t = 00, 06, 12 and 18 UTC

The 03-hr FFFT at 00:00 UTC = the difference between the 03-hr Forecasted MAP from 00:00 UTC and the 03-hr FFG from 00:00 UTC, valid at 03:00 UTC. The 03-hr FFFT at 06:00 UTC = the difference between the 03-hr Forecasted MAP from 06:00 UTC and the 03-hr FFG from 06:00 UTC, valid at 09:00 UTC. The 03-hr FFFT at 12:00 UTC = the difference between the 03-hr Forecasted MAP from 12:00 UTC and the 03-hr FFG from 12:00 UTC, valid at 15:00 UTC. The 03-hr FFFT at 18:00 UTC = the difference between the 03-hr Forecasted MAP from 18:00 UTC and the 03-hr FFG from 18:00 UTC, valid at 21:00 UTC.

15.3. 6-Hour Forecast Flash Flood Threat (6 hr-FFFT)

As it is shown in Figure 72, 6-Hour FFFT is estimated and updated at 00 UTC, 06 UTC, 12 UTC and 18 UTC. FFFT 06-hr: Difference of 06-hr FMAP for current model processing hour and current 06-hr FFG (mm/6hr).

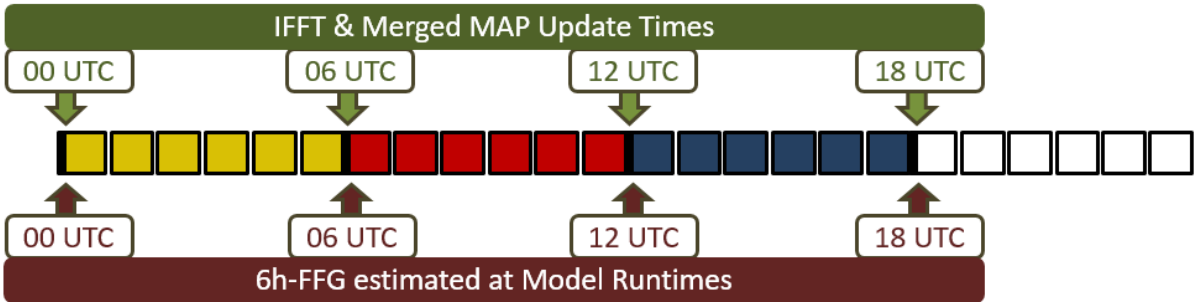

Figure 72. 6-hr FFFT estimation scheme

$6h\ FFFT_t = 6h\ FMAP_t - 6h\ FFG_t$, where t = 00, 06, 12 and 18 UTC

15. FFFT (Forecast Flash Flood Threat)

The 06-hr FFFT at 00:00 UTC = the difference between the 06-hr Forecasted MAP from 00:00 UTC and the 06-hr FFG from 00:00 UTC, valid at 06:00 UTC. The 06-hr FFFT at 06:00 UTC = the difference between the 06-hr Forecasted MAP from 06:00 UTC and the 06-hr FFG from 06:00 UTC, valid at 12:00 UTC. The 06-hr FFFT at 12:00 UTC = the difference between the 06-hr Forecasted MAP from 12:00 UTC and the 06-hr FFG from 12:00 UTC, valid at 18:00 UTC. The 06-hr FFFT at 18:00 UTC = the difference between the 06-hr Forecasted MAP from 18:00 UTC and the 06-hr FFG from 18:00 UTC, valid at 00:00 UTC.

Figure 73. is showing 06-h FFFT on 10 October 2015 at 18 UTC. Low, medium and high values of FFFT occurred in highlighted region.

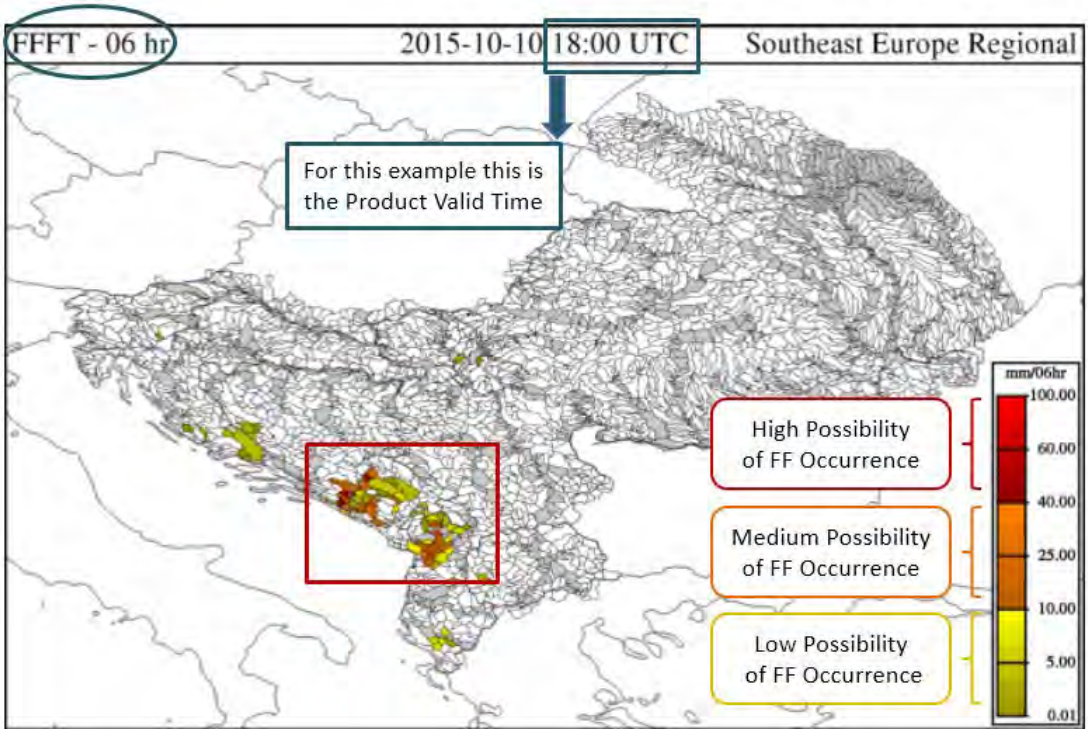

Figure 73. 06-hr FFFT at 18 UTC, 10 October 2015

16. SNOW-17

The SNOW-17 snow accumulation and ablation model was first described by Anderson (1973) as a component of the National Weather Service River Forecast System (NWSRFS). SNOW-17 is a conceptual model.

SNOW-17 is an index model using air temperature as an index to determine the energy exchange across the snow-air interface (Anderson, 2006). In addition to temperature, the only other input variable needed to run the model is precipitation. Air temperature is also used as an indicator to estimate snowmelt. Air temperature is a commonly measured and operationally available variable. The estimation of the spatial variation of air temperature in most cases is associated with other meteorological variables that affect the snow energy balance. Elevation differences is a dominant factor that explains the temperature variability over an area. The ability to reasonably extrapolate air temperature data to higher elevations is critically important for snow modelling since in many mountainous regions, most of the snow runoff comes from areas that are higher than any measurement site (Anderson, 2006).

SNOW-17 was primarily designed for use in river forecasting (Anderson, 2006). This means that the model needs to use both historical data for calibration and real-time data for operational applications. SNOW-17 is typically applied on an areal basis to estimate the contribution of melt from the snow pack to a rainfall/runoff model, as well as the amount of snow water equivalent. In flat terrain, SNOW-17 is typically applied to a headwater drainage or local area though in some cases large drainages may be divided into several sub-areas. In mountainous regions, due to the significant variation in the amount of snow and the timing of melt with elevation, watersheds are typically divided into 2 or 3 elevation zones when using SNOW-17.

While some guidelines have been developed relating SNOW-17 model parameters to physiographic factors, the model needs to be calibrated to produce quality simulation results (Anderson, 2006). Recommendations for determining initial parameter values and for calibrating the SNOW-17 model are included in a comprehensive guide for historical data analysis and model calibration for river forecasting applications (Anderson, 2002). In order to optimize the SNOW-17 simulations for river forecasting applications, three things must occur:

1. The model must be properly calibrated;
2. The input data (precipitation and temperature) used operationally must be unbiased compared to that used for calibration; and
3. Well devised, ideally objective, updating schemes must be used to remove bias and to minimize random errors to the maximum extent possible.

The approach used when developing SNOW-17 was to first try to represent the physical processes that occur in a column of snow. Then, features were added so that the model could be applied to an area. This is a similar approach to that later used when the Sacramento Soil Moisture model was developed. The main processes included in the model for a column of snow are:

- → Form of precipitation,
- → Accumulation of the snow pack,
- → Energy exchange at the snow-air interface,
- → Internal state of the snow pack,

→ Transmission of water through the snow pack, and
→ Heat transfer at the soil-snow interface.

In order to apply the model to an area, the areal extent of the snow pack is computed and used to determine the fraction of the area from which melt and outflow from the snow cover can occur. When the model is applied at a point location, the algorithm used to compute the areal extent of the snow cover is not used. When applied to an area, SNOW-17 keeps track of mean areal values of variables such as water equivalent. In order to get the average over the snow-covered area, one must divide these mean areal values by the areal extent of the snow cover (Anderson, 2006). In the SEEFFGS because of relatively small basin areas, whenever the simulated SWE is above 2 mm the snow model is applied over the entire drainage area of the basin. Figure 74 shows a basic flowchart of the SNOW-17 model.

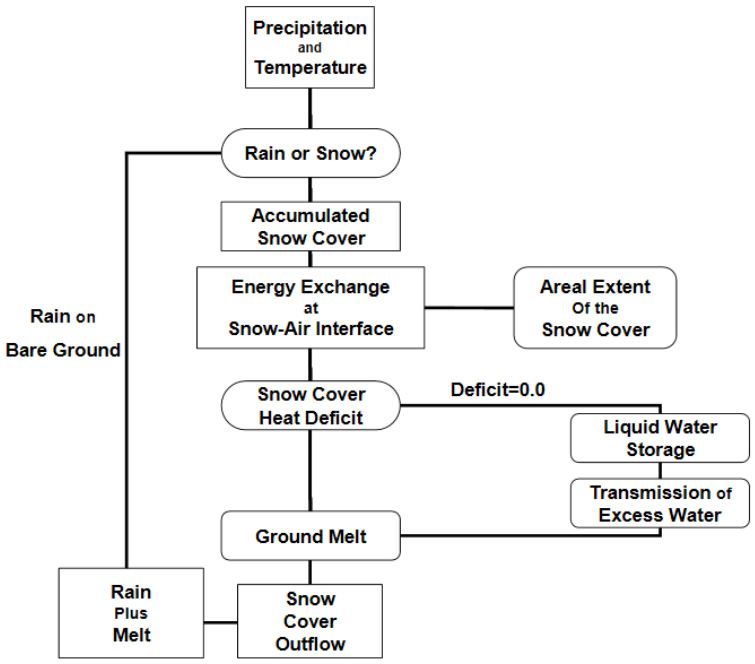

Figure 74. SNOW-17 algorithm flowchart (Anderson, 2006)

The computational time interval, i.e. the minimum period for which the model can be run, is the time interval associated with the temperature data. An appropriate time interval for the snow model should represent the diurnal cycle of temperature. For river forecasting, the model has most frequently been applied at a 6-hour interval. Many of the model parameters are defined for that period and are then adjusted if computations are done at a different interval.

The input data for SNOW-17 is precipitation and temperature. The precipitation is the total over a specified time interval. When doing areal computations, the precipitation is normally the mean amount over the area though the code does include a multiplying factor, PXADJ, that can be applied to all precipitation values entering the model (PXADJ is usually equal to 1.0).

16. SNOW-17

16.1. Snow Model Parameters and State Variables

Ground level temperature is a good, but not perfect, indicator as to whether precipitation is falling as rain or snow. The form of precipitation can vary with surface level temperature. The variation of the form of the precipitation at a given location is based on data from the Snow Investigations (Snow Hydrology, 1956). It shows that rain can occur at temperatures below 1℃ and snow can occur when the air temperature is 4℃. From that study, the typical temperature separating rain from snow is around 1.5℃.

The temperature of precipitation, whether rain or snow, can probably best be approximated by the wet bulb temperature. When precipitation is occurring, the relative humidity is generally quite high and thus under these conditions the wet bulb temperature is close to the air temperature. When snow falls at temperatures below freezing, it must eventually be warmed to 0℃ before melting.

The SNOW-17 model has 12 parameters. This counts the areal depletion curve as one parameter though it is input as a series of nine values used to define the shape of a curve. Some of the parameters have more influence on the simulation results than others. The most sensitive parameters are those that typically should be determined through calibration even though some guidelines are available to obtain initial estimates (Anderson, 2002). The others less sensitive parameters typically can be assigned values based on the climatological conditions at the location being modelled.

16. SNOW-17

The major parameters for the SNOW-17 model are:

1. SCF – The multiplying factor which adjusts precipitation that is determined to be in the form of snow. SCF primarily accounts for gauge catch deficiencies, but also implicitly includes the net effect of vapour transfer (sublimation and condensation, including from intercepted and blowing snow) and transfers across areal divides.
2. MFMAX – Maximum melt factor during non-rain periods ($mm \cdot °C^{-1} \cdot 6\ hr^{-1}$).
3. MFMIN – Minimum melt factor during non-rain ($mm \cdot °C^{-1} \cdot 6\ hr^{-1}$).
4. UADJ – The average wind function during rain-on-snow periods ($mm \cdot mb^{-1}$). UADJ is only a major parameter when there are frequent rain-on-snow events with relatively warm temperatures.
5. SI – The mean areal water equivalent above which there is always 100 percent areal snow cover (mm). SI is not a major parameter when the model is applied at a point location or when significant bare ground appears soon after melt begins, no matter the magnitude of the snow cover.
6. PXTEMP – The temperature that separates rain from snow (°C). If the air temperature is less than or equal to PXTEMP, the precipitation is assumed to be in the form of snow. The PXTEMP parameter, as defined for SNOW-17, is not used if a rain-snow elevation time series is used to determine the form of precipitation.
7. MBASE – Base temperature for snowmelt computations during non-rain periods (°C). Typically, a value of 0 °C is used.

The minor parameters for the SNOW-17 model are:

1. NMF – Maximum negative melt factor ($mm \cdot °C^{-1} \cdot 6\ hr^{-1}$). The negative melt factor has the same seasonal variation as the non-rain melt factor.
2. TIPM – Antecedent temperature index parameter (real – range is 0.01 to 1.0). Controls how much weight is put on temperatures from previous time intervals when computing ATI. The smaller the value of TIPM, the more previous time intervals are weighted.
3. PLWHC – Percent liquid water holding capacity (decimal fraction). Indicates the maximum amount of liquid water, as a fraction of the ice portion of the snow, that can be held against gravity drainage (maximum allowed value is 0.4)
4. DAYGM – Constant daily amount of melt which takes place at the snow-soil interface whenever there is a snow cover ($mm \cdot day^{-1}$)

The SNOW-17 model has 14 state variables. These are as follows:

1. Water equivalent of the ice portion of the snow cover (mm),
2. Heat deficit (mm),
3. Antecedent temperature index (°C),
4. Liquid water held by the snow (mm),
5. The maximum amount of water equivalent that existed during an accumulation period (mm),
6. The water equivalent when new snowfall first occurs on a partly bare area, i.e. the water equivalent at the point where the areal cover leaves the depletion curve (mm),

17. GMAT Gauge Mean Areal Temperature

Gauge Mean Areal Temperature (GMAT) is generated by using synoptic observations that are disseminated through the WMO GTS. Accuracy of the mean areal temperature product depends on amount of data submitted via GTS by member countries. Areal temperature is needed for each sub-basin for use in the SNOW-17 model. The areal temperature is generated from the point data from the GTS through interpolation.

The interpolation of the gauge observations to mean areal temperature uses the analysis and short lead time forecast of the 2-meter temperature fields from the 0.5 degrees Global Forecast System (GFS) from NOAA.

GMAT is estimated four times a day over the last 6 hours ending at 00 UTC, 06 UTC, 12 UTC, and 18 UTC. On Figure 75, it is represented 06-Hour GMAT ending at 06 UTC on 3 April 2016.

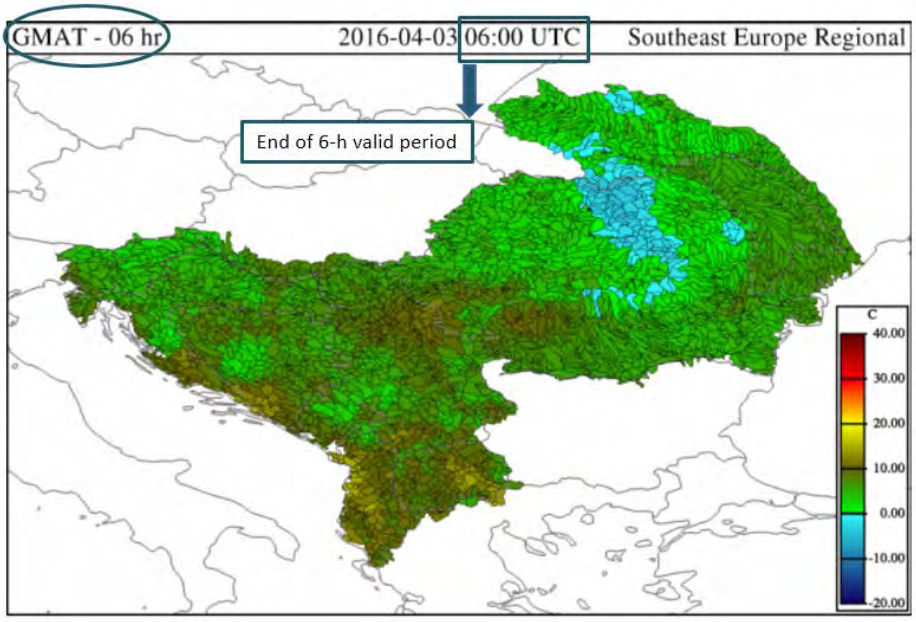

Figure 75. 06-hr gauge Mean Areal Temperature (GMAT)

18. Latest IMS SCA (SNOW COVERAGE AREA)

Accurate monitoring of global snow and ice cover is a key component in the study of climate and global change as well as daily weather forecasting.

The Interactive Multi-sensor Snow and Ice Mapping System (IMS) product was primarily created to improve the quality and timeliness of Northern Hemisphere snow and ice maps for National Centers for Environmental Prediction (NCEP) numerical forecasting. The IMS is produced daily using GIS technology. While there are potentially many uses, the primary function of the product is to provide cryospheric input for environmental modelling. Snow plays an important role in model input and can lead to substantial error in forecast results based on incorrect representations of snow distributions, age, depth, snow water equivalent (SWE), and snow density. The advanced resolution product begun in February 2004 allows for greater details of snow and ice information to be conveyed to the user community.

For the SEEFFG system, snow cover is retrieved daily from the IMS, made available as a Northern Hemisphere product from the National Snow and Ice Data Center, NOAA. The product is made available daily around 23:00 GMT and it provides snow cover information at 4km x 4km resolution that is based on summary of multiple sensors on-board of various satellites. These include geostationary and polar orbiters with sensors such as MODIS, AVHRR, and passive microwave sensors. The product, which has been operationally available since 2006, is developed in conjunction with modelling, climatological maps, and personnel expertise. Description of the IMS snow cover product is available at Helfrich et al. (2007).

Outputs are provided graphically for each FFG basin and as text. Figure 76 shows 24-hr SCA on 3 April 2016 at 00 UTC, indicating that still there are some sub-catchments of SEEFFGS's region covered by snow, and some of those sub-catchments are fully covered by snow. Snow accumulation and melting have significant importance for the region because of the flash flood occurrence due to rapid melting during the spring.

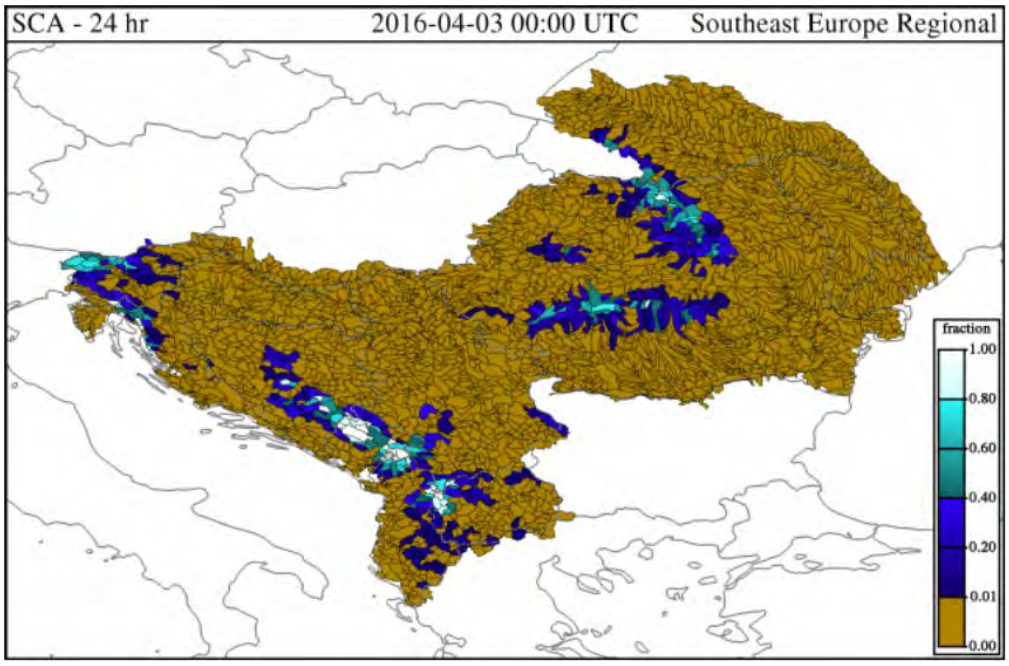

Figure 76. 24-hr Snow Coverage Area

19. SWE (Snow Water Equivalent)

Snowmelt provides significant volumes of water to river systems. The depth of water produced if a snow cover is completely melted on a horizontal surface is known as the snow water equivalent.

The Snow Water Equivalent (SWE) product is a direct output of SNOW-17 accumulation and ablation model in the SEEFFGS and is estimated at 00 UTC, 06 UTC, 12 UTC and 18 UTC (Figure 77).

The model is forced by 6-hourly mean areal precipitation and surface air temperature. Surface air-temperature threshold parameters are used to distinguish between rainfall and snowfall events. Parameters of the model depend on terrain, land cover and its use, and the regional climate. The SNOW-17 model has two input variables, namely MAT and merged MAP, and simulates several products including SWE and MELT (described in the next Section) by using equations that solve for energy and mass balance.

Water produced by snowmelt is an important part of the annual water cycle in many parts of the world, in some cases contributing high fractions of the annual runoff in a watershed. In the SEE region, snow accumulation takes place during the winter season, especially in mountainous areas. SWE is a very important product to show available water content in each sub-basin for flash flooding.

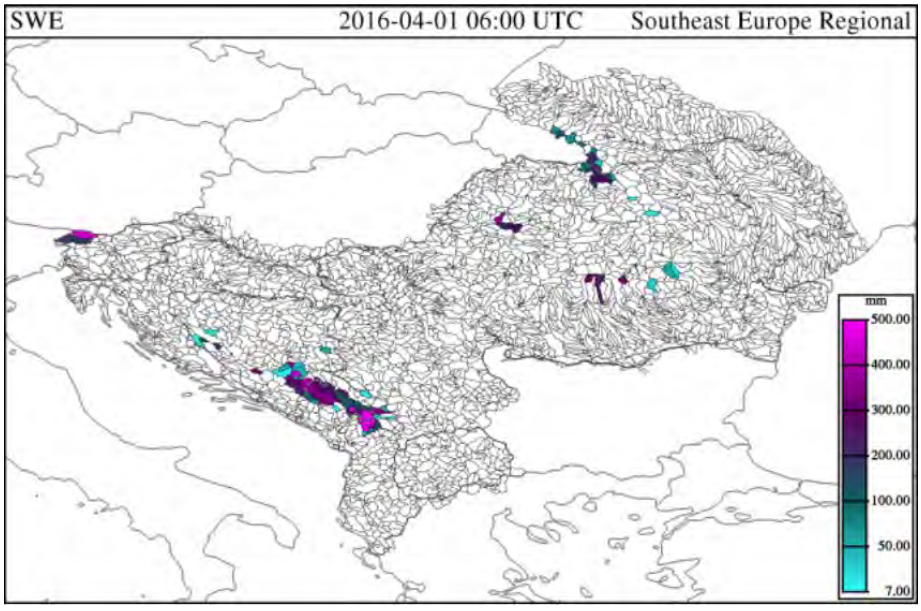

Figure 77. SEEFFG Snow Water Equivalent (SWE) product

20. MELT

MELT is the estimate of ablation due to melt processes and is the direct output of the SNOW-17 model. MELT is estimated every six hours at the model runtimes of 00 UTC, 06 UTC, 12 UTC and 18 UTC. The product provides six-hour cumulative melt over periods of 24 and 96 hours (Figure 78).

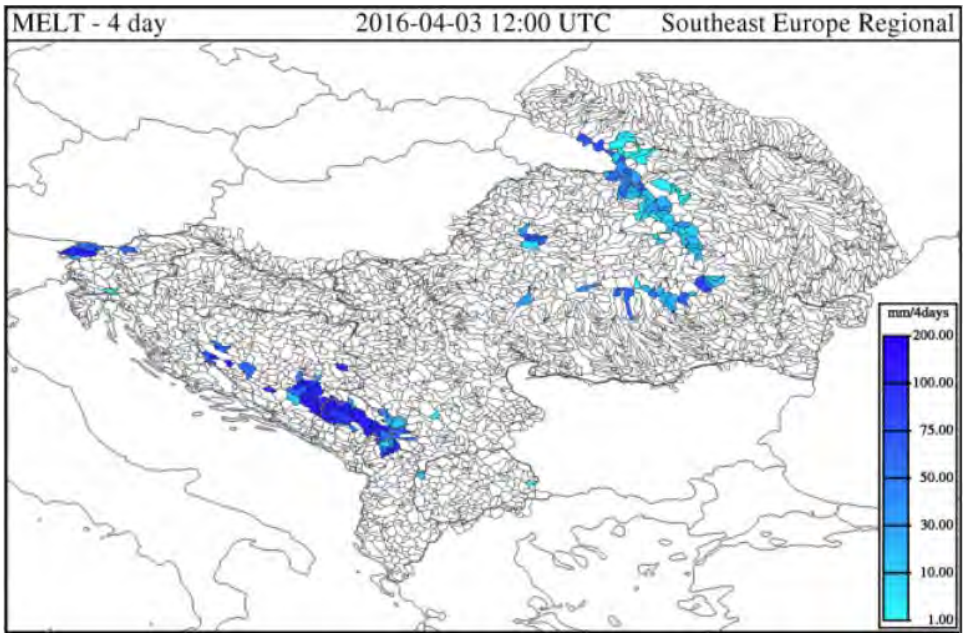

Figure 78. 96-hr MELT product

21. POST-PROCESSING OF PRODUCTS WITH GIS

GIS is designed to support spatial decision-making, which is also very important for issuing flash flood warnings. The SEE forecaster product console displays products for each sub-basin but does not provide any geographical (spatial) information like topography, cities, roads, rivers, lakes, administrative boundaries, etc. Because flash floods often occur in small areas, forecasters would like to see not only the SEEFFG products but also additional layers that are displayed with the products so that precise location can be determined. Forecasters can easily download the shapefiles of sub-basins from the SEEFFGS Static resources and tab-delimited hourly FFGS output data from the Product console. Using GIS software and SEEFFGS products, forecasters can produce maps for flash flood bulletins, hydrologic studies, etc. Based on his/her experience, the in-country forecaster can use GIS to make adjustments to various FFGS products for various sub-basins and at various time durations for the country. Using the adjusted products, the forecaster then assesses the situation and makes the decision to issue (or not) alerts and warnings for specific areas and times.

The Regional Centre – TSMS uses ArcGIS Server to provide 2D and 3D displays of products with additional GIS layers.

Free, open-source GIS raster and/or vector data can be found at Natural Earth, Global Map, Diva GIS Country Data, ASTER GDEM, SRTM, EU DEM Copernicus, European soil database, Euro Global Map, Corine Land Cover Land Use, etc.

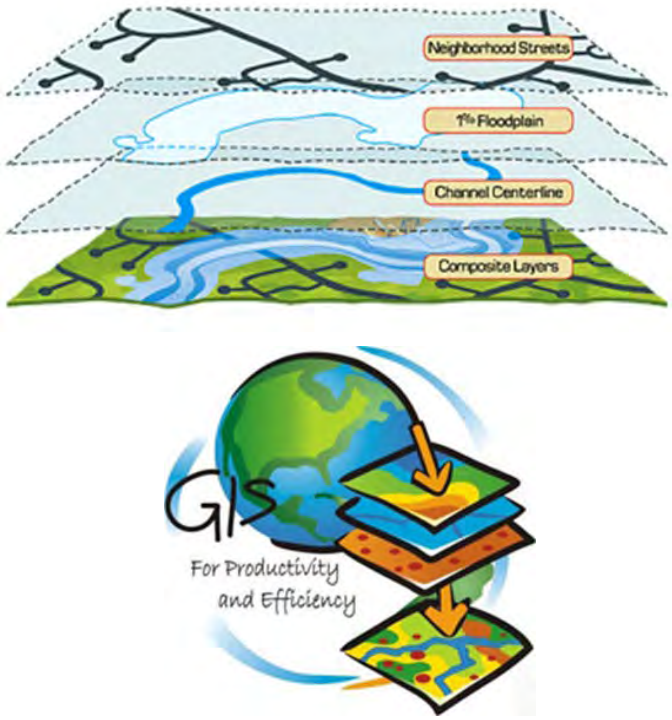

Figure 79. Illustration of GIS Spatial Data Layers

22. METEOROLOGY

1. Introduction

What are the ingredients needed for flash flood-producing storms? Heavy precipitation is the result of sustained high rainfall rates. In turn, high rainfall rates involve the rapid ascent of air containing substantial water vapour and also depend on precipitation efficiency. The duration of an event is associated with its speed of movement and the size of the system causing the event along the direction of system movement (Doswell et al, 1996).

This leads to a consideration of the meteorological processes by which these basic ingredients are brought together. A description of those processes and of the types of heavy precipitation-producing storms suggest some of the ways in which heavy precipitation occurs. Since the right mixture of these ingredients can be found in a wide variety of synoptic and mesoscale situations, it is necessary to know which of the ingredients is critical in any given case. By knowing which of the ingredients is most important in any given case, forecasters can concentrate on recognizing the development of heavy precipitation potential as meteorological processes operate (Doswell et al, 1996).

2. Ingredients for flash floods

a) Ingredients for heavy precipitation

The heaviest precipitation occurs where the rainfall rate is the highest for the longest time. The total precipitation produced, *P*, is $P = \overline{R}D$, where $\overline{R}$ is the average rainfall rate and *D* is the duration of the rainfall.

Precipitation is produced by lifting moist air to condensation. Rising air should have a substantial water vapour content and a rapid ascent rate for a significant precipitation rate to develop. The vertical moisture flux can be related to the condensation rate, which in turn is the ultimate source for precipitation. But not all the water vapour flowing into a cloud falls out as precipitation. The precipitation efficiency, *E*, is the coefficient of proportionality relating rainfall rate to input water flux, so that $R = Ewq$, where *w* is the ascent rate and *q* is the mixing ratio of the rising air (Doswell et al, 1996). Precipitation efficiency is defined as the ratio of the mass of water falling as precipitation, m_p, to the influx of water vapour mass into the cloud, m_i, such that $E = m_p/m_i$. Figure 80 illustrates this process schematically to show that precipitation efficiency is most logically understood as a time average over the history of a precipitation-producing weather system. The smallest unit for which it makes sense to calculate precipitation efficiency is a convective cell. But calculation of a single cell's precipitation efficiency is of minor significance; what matters is being able to anticipate the efficiency in a general sense (Doswell et al, 1996).

Forecasters need to wonder how likely it is that the potential flood-producing storm is going to have high precipitation efficiency. Of the input water vapour in a convective storm, virtually all of it will condense, since a convective updraft is typically tall enough that the saturation mixing ratio at the storm top is on the order of 0.1 g kg^{-1} (Doswell et al, 1996). This value is about 1% of a typical input mixing ratio, implying that 99% of the input water vapour condenses. Of the water vapour that does condense, some evaporates, some falls as precipitation, and some is carried

away by the clouds. In forecasting the precipitation efficiency, it is important to assess how much moisture will be available, and consider what percentage of the moisture entering the cloud will fall as rain. A key observable factor related to evaporation is environmental relative humidity. As the relative humidity decreases, the evaporation rate increases and the precipitation efficiency falls. There can be other environmental factors, such as wind shear, that alter precipitation efficiency (Doswell et al, 1996).

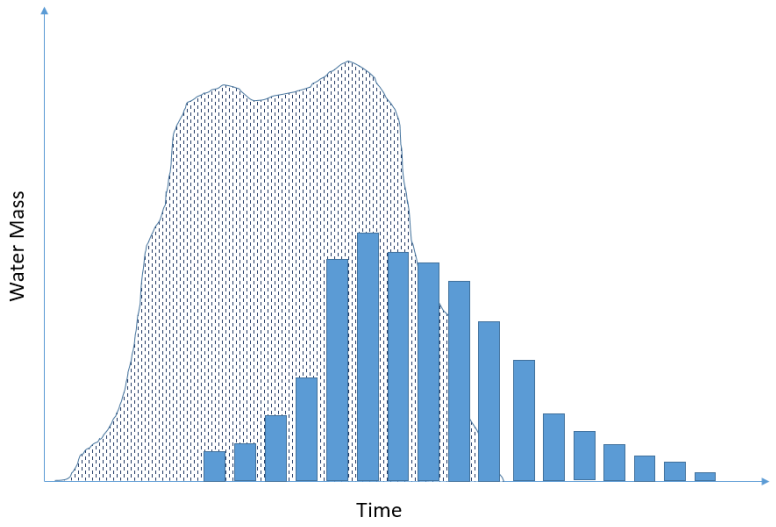

Figure 80. Schematic illustration of the time variation of water vapour input (cross-hatched area) and the precipitation output (vertical bars) over the lifetime of a precipitation system, Source: *Doswell et al, 1996*

b) Ingredients for deep, moist convection

Deep, moist convection normally occurs during the warm season when high moisture content is possible and buoyant instability promotes strong upward vertical motions (Doswell et al, 1996). Thus, the rainfall rates associated with convection tend to be higher than with other rain-producing weather systems. Deep moist convection is associated with buoyancy. In order to produce buoyancy and deep convection, 1) the environmental lapse rate must be conditionally unstable, 2) there must be sufficient moisture that some rising parcel's associated moist adiabat has a level of free convection (LFC), and 3) there must be some process by which a parcel is lifted to its LFC.

c) The character of flash flood-producing storms

The most important flash floods are produced by quasi-stationary convective systems, wherein many convective cells reach maturity and produce their heaviest rainfall over the same area. By this means, a convective event achieves a relatively long duration, since individual convective cells have lifetimes that are almost always too short to produce heavy rainfall even though the individual convective cell rainfall rates can be high. For a convective system made up of a number of convective cells, the duration of the high precipitation rate in any location is related to:

1) system movement speed, 2) system size, and 3) within-system variations in rainfall intensity. As a general rule, flash floods are associated with slow-moving precipitation systems. System movement, denoted by the system motion vector $\boldsymbol{C}_s$, can affect the duration, but an Eulerian view requires knowledge of the system size along $\boldsymbol{C}_s$; denote this length by L_s. the idea is illustrated in Figure 81.; the rainfall total from the system is $\overline{R}D$, where *D* can be expanded to $D = \mathbf{L}s(\mathbf{C}s)^{-1}$. Long duration is associated with systems that have a) slow movement, b) a large area of high rainfall rates along their motion vector, or c) both.

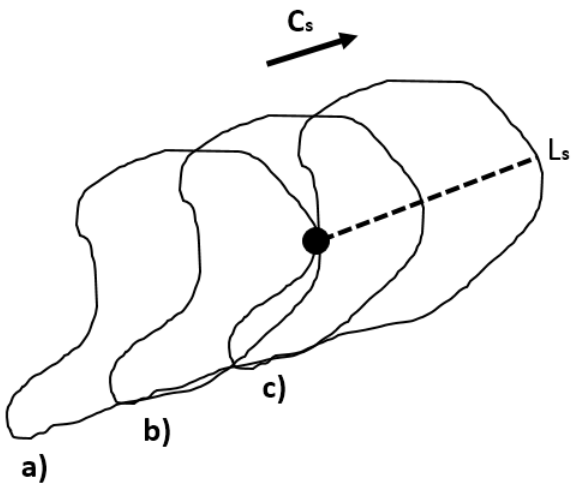

Figure 81. Schematic illustrating the concept of the length of a system, L_s, as it passes a point. The system motion vector is denoted by C_s, Source: *Doswell et al, 1996*

A squall line with a large motion *normal* to the line will not produce long-lasting precipitation at any point (Figure 82 a), whereas the same line with most of its motion parallel to the line will take a longer time to pass a point (Figure 82 b)), resulting in more rainfall. Mesoscale convective systems with a large region of ”stratiform“ precipitation trailing a leading convective line may end up with a long duration of moderate-to-heavy rain showers following a relatively brief intense rainfall associated with the leading convective line, exacerbating the effect of the heavy rainfall (Figure 82 c). The case where many intense convective cells pass in succession over the same spot, the so-called train effect, is the situation producing the highest rainfall totals (Figure 82 d)).

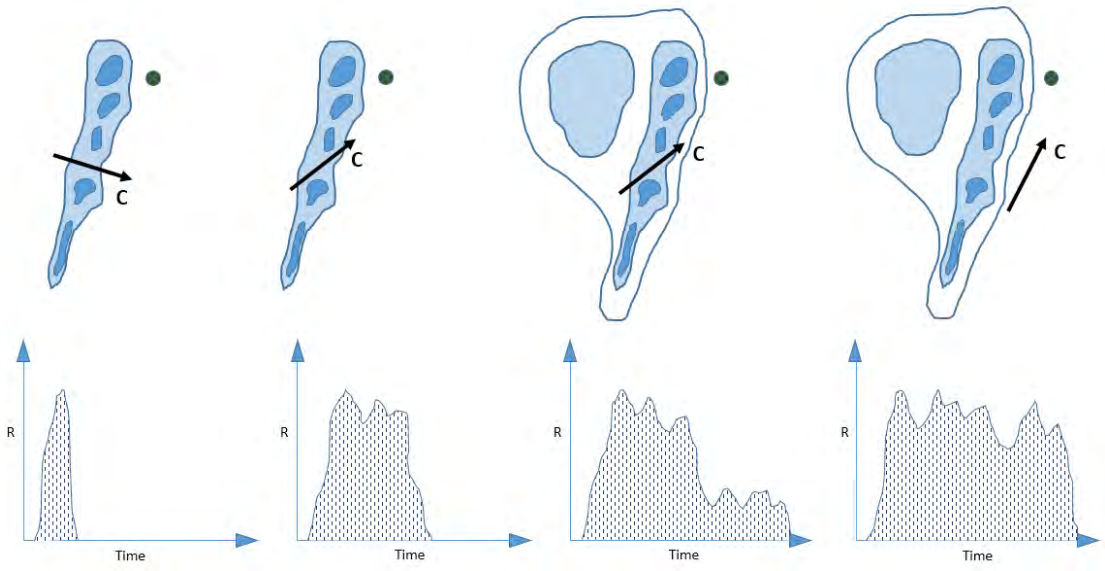

Figure 82. Schematic showing how different types of convective systems with different motions affect the rainfall rate (R) at a point (indicated by a dot) as a function of time; contours and shading indicate radar reflectivity, Source: *Doswell et al, 1996*

Chappell (1986) indicates that convective cell movement, $\boldsymbol{C}_c$, is related to $\boldsymbol{V}_m$, the mean wind through some deep tropospheric layer (in which the cloud is embedded). Thus, slow system movement could be associated with weak winds. However, having strong winds within the troposphere by no means excludes the potential for convective precipitation to have long duration as tome given location. Convective system movement, $\boldsymbol{C}_s$, is the vector sum of the contributions from $\boldsymbol{C}_c$ and the so-called propagation effect, denoted by $\boldsymbol{P}_s$. In the context of convective storms, “propagation“ is the contribution to system movement from the development and dissipation of individual convective cells. Convective systems are processes made up of a number of sub-processes (convective cells), through which air parcels are flowing (Doswell et al, 1996). It is a near cancellation of the cell movement via propagation effects that results in slow system movement (Figure 83).

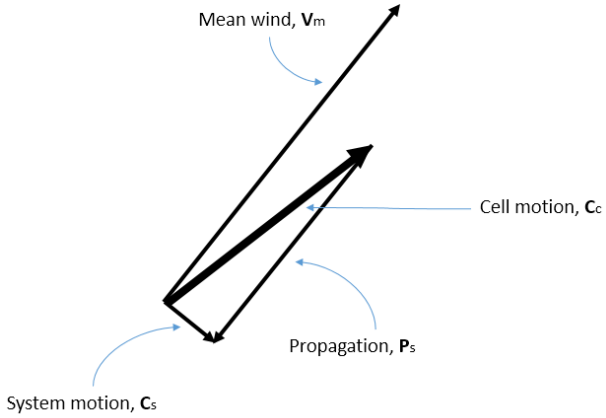

Figure 83. Schematic showing the near cancellation between cell motion, C_c, and propagation, P_s, Source: *Doswell et al, 1996*

Anticipating cell movement is relatively simple, since cells generally move more or less with $\boldsymbol{V}_m$. that is, simple advection dominates cell movement in most cases. Forecasting the contribution from propagation is much more difficult, because the convection can interact with its movement to develop new convection in preferred locations relative to the existing cells. New convective development can be influenced heavily by the outflow boundary produced from the existing (and previous) cells. Rapid boundary movement is virtually never associated with long-duration rainfall at a point.

Propagation can be affected by processes external to the convective storm itself. That is, features that have an independent existence prior to the development of the convection (such as fronts, old outflow boundaries, sea-breeze fronts, etc.) can also influence the development of new convective cells. These ”external“ factors need to be considered in anticipating system movement. There are some synoptic/mesoscale patterns typically associated with flash floods, and it is clear that these patterns favour slow system movement.

d) Flash flood-producing storm types

Anticipating flash flood potential apparently requires one to know what storm types are likely to be involved. Johns and Doswell (1992) have offered an ingredients-based approach to forecasting severe weather-producing convection; their methodology is predicated mostly on the importance of supercell storms in severe weather. Heavy precipitation can be associated with a wide variety of storm types. In developing this classification, it is important to recognize that the process is *sensor dependent*. The storm structure seen from the perspective of a geostationary satellite can be quite different from that seen by a radar.

1) MULTICELL CONVECTION

Convection can be classified into single-cell, multicell, supercell, and squall line structures. This is primarily a radar-based perception. A single cell consists of a single ”bubble“ of buoyant parcels, and the typical deep, moist convective storm is made up of a number of such bubbles,

even though its radar echo can give the appearance of a single entity. The vast majority of isolated radar echoes that persist for many lifetimes of a single cell (~20 min) are multicell events.”Multicell“ classification offers little or no value simply because most convection is multicellular, even supercells and squall lines. Most flash flood-producing convection, therefore, is multicellular, but this knowledge is not helpful if virtually all convection is also multicellular. Convective organization is a complex topic involving the interaction among updrafts, downdrafts, and the environmental conditions.

The life cycle of a single cell can be separated into three stages: Developing stage, mature stage and dissipating stage (Figure 84). The developing stage lasts 5 to 10 minutes, a distinct single updraft is prevailing, the diameter of the cell is between 2 and 8 km (*http://www.eumetrain.org/satmanu*). Entrainment at the cloud edges causes the reduction of water vapour content, resulting in the evaporation of water droplets. This causes cooling and consequently reduction of buoyant energy. A supply of humidity from lower levels supports further growth of the developing cell. At the end of this stage, lightning is most intense. The mature stage lasts 25 to 30 minutes, downdrafts develop and are accelerated because of cooling by the evaporation of cloud droplets. Hail stones are no longer kept aloft by the updraft and fall. The updraft starts to weaken because the warm humid air below the cell is replaced by cool air from the downbursts. The downdraft initiates successive developments of new cells which can be observed as gust fronts. Rain and hail are most intense; hail with a diameter over 5 cm develops in the updrafts of the order 30-40 m/s. In the dissipating stage, downdrafts kill the updraft and the Cb dissipates.

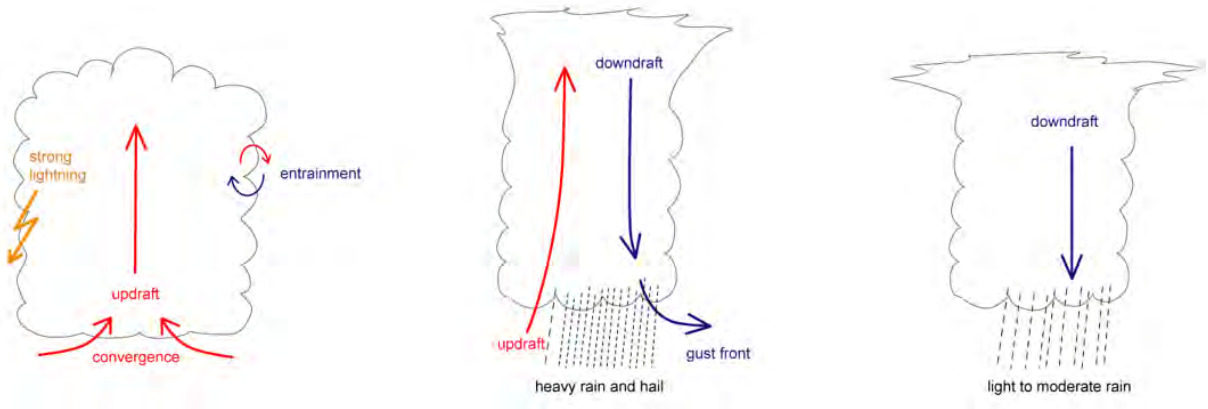

Figure 84. Life of a convective cell, Source: *http://www.eumetrain.org/satmanu*

The life time and intensity of a Cb and MCS depend upon the vertical wind shear:

- → The shear perpendicular to the convective line supports updraft
- → Most important is the shear in the lowest layer reaching from the surface up to 2-3 km
- → Cells developing within strong vertical shear have long lifetime and severe weather
- → Most intense thunderstorms develop when there is change both in speed and direction of the wind

Multi-cell storms develop from a single cell:

- → The single cell produces a gust front around it; the gust front lifts the air to the level of free convection (LFC), and new cells (daughter cells) form
- → New cell growth is favoured on the downwind side of the moving single cell where the lift is the greatest
- → Daughter cells develop mostly in the right leading side of the mother cell (so called "right movers"), but they can also develop in the left side (so called "left mover"). They can be distinguished from the structure of the vertical wind shear
- → Left movers move faster than mean low level flow, whereas right movers move slower than it
- → Tornadoes are uncommon in left movers
- → The diameter of the daughter cells is 3-5 km, and the distance to the centre of the thunderstorm is approximately 30 km.
- → The mother cell and daughter cells form together a Multi-Cell Storm. New cells develop ahead of the leading edge of the storm while older cells dissolve in the rear parts
- → Daughter cells develop more rapidly than the mother cell because entrainment is not slowing the process on the rear side. If the sequence of successive cells is short enough, the Multi-Cell Storm can turn into a Super Cell Storm.

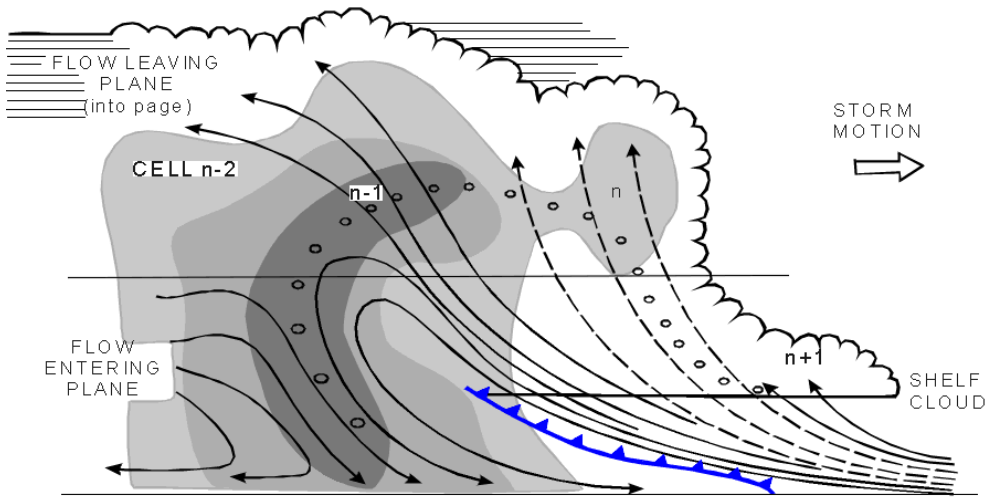

Figure 85. A typical cross section through a Multi-Cell Storm, Source: *Browning et al. 1976.*

The diagram above (adapted from Browning et al., 1976; grey shades represent radar reflectivity of 35, 45 and 50 dBz) shows a typical cross section through a Multi-Cell Storm. There are four successive cells in different stages of development, each of which takes about 15 minutes:

- → Cell *n-2* is already in dissipating stage
- → Cell *n-1* is in mature stage and forms the centre of the storm
- → Cell *n* (a daughter cell) is in developing stage
- → A shelf cloud *n+1* with a crisp, flat base indicating an active updraft forms ahead of cell

During the warm season, MCS triggering peaks at around 2 pm (local solar time) due to the heating in the lower levels of the atmosphere. However, in Europe, where MCS last in average 5.5 hours, 20% of MCS triggering happens during the night (between 10 pm and 9 am), when other lifting mechanisms are expected to play a key role, as low-level convergence, mid-level cold pools or out-flows of pre-existing MCSs.

2) SUPERCELL CONVECTION

What is important about supercells in the context of flash floods is their tendency to have strong updrafts. By virtue of their interaction with the environment, such storms can have a substantial contribution to their updraft from dynamic (non-buoyant) vertical accelerations. Supercells also tend to have significant low-level moisture associated with their environment, so the combination of intense updrafts and substantial low-level moisture suggest some potential for heavy rainfall rates. Typical supercell environments have two general characteristics that mitigate against heavy rainfalls: dry lower mid-troposphere, suggesting a significant reduction in precipitation efficiency due to evaporation, and high wind speeds aloft, resulting in significant supercell motion (Doswell et al, 1996).

3) SQUALL LINES (RADAR)

As the low-level outflow from convection spreads out in a pool of precipitation-cooled air, it tends to be the locus for the development of new updrafts. The general tendency for convection to form in lines is almost certainly associated with this characteristic. Outflow boundaries enhance any existing lifting processes (such as fronts, drylines or orography) that might cause the initial convection to be organized in lines. Moreover, the outflows from neighbouring convective cells can merge to form an extensive pool of outflow along which new convection develops. If convection exhibits any organization at all, it frequently is a linear structure, so many flash flood producing convective events exhibit this characteristic. The train effect (as described above) where cells form and pass repeatedly, in succession, over the same location, results from a linear organization. What matters, of course, is the movement of organized convective lines on many occasions. When the linear structure is associated with synoptic-scale processes, such as fronts, the speed of movement of those processes tents to be closely matched to the speed of movement of convection (Doswell et al, 1996).

4) MESOSCALE CONVECTIVE SYSTEMS

In developing the early studies of those systems, Maddox (1980) proposed a set of criteria to define what he called “mesoscale convective complexes“ (MCCs). MCCs are only the largest, most persistent, most nearly circular cold cloud shield members of a spectrum of convective systems. This categorization of convection is based only on satellite-observable characteristics. Since persistent convection is inevitably multicellular in character, almost any persistent convective system will develop substantial anvil, thus making it appear as an MCS on satellite, with the anvil size depending on updraft strength and the number of convective cells. Systems meeting MCS criteria have their convection arranged in a more or less linear fashion as seen on radar. To the extent that MCCs and MCSs contribute to flash flood events (Fritsch et al. 1986), this implies that a radar depiction of those events would probably show a linear organization in many cases. Such MCSs have a trailing “stratiform“ precipitation region that can contribute to the storm precipitation totals and exacerbate the flash flood threat by a prolonged period of

moderate rainfall that follows the initial, shorter duration period of the most intense precipitation (Doswell et al, 1996).

5) SQUALL LINES (SATELLITE)

Whereas MCSs with more nearly circular cold cloud tops may have a linear structure on radar, what appear as “squall lines“ on satellite may or may not have a predominantly linear structure on radar. Individual convective systems within such an extensive line can include relatively isolated storms as well as radar-observed squall lines. It is typical for satellite-observed linear structures to be associated with synoptic scale boundaries (e.g. fronts). Although there is no a priori reason to assume that such structures move relatively rapidly, it appears to be uncommon for satellite-observed squall line-type MCSs to produce flash floods (Doswell et al, 1996).

6) NONCONVECTIVE PRECIPITATION SYSTEMS

Although most flash flood events are produced by deep, moist convection, there are situations where one can develop the proper ingredients in a nonconvective situation. That is, the strong updrafts leading to heavy precipitation are forced rather than freely buoyant. Probably the most common way in which this occurs is for the vertical motion to be forced by orography. There is no difference if upward motion is free or forced as far as the atmosphere is concerned; moist air ascending condenses and produces precipitation in essentially the same way. Often, forced uplift does not attain the heights associated with free convection, so the precipitation-producing cloud tops may not be very cold. Low-topped precipitation systems clearly will affect the satellite depiction of an event and can be a factor in the capability of radar to detect the event as well, notably at long ranges from the radar.

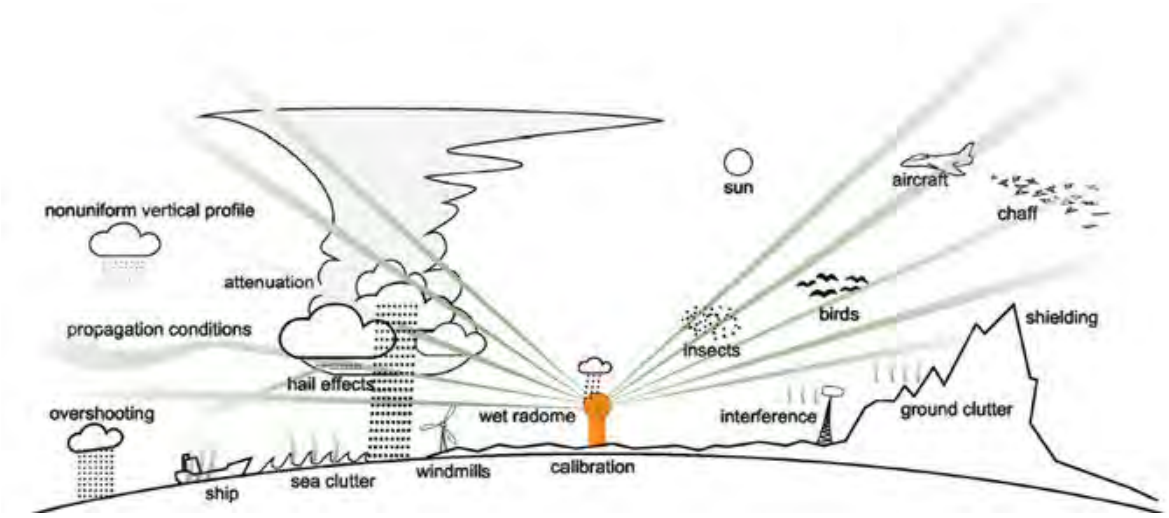

Figure 86. Illustration of radar beams

Ignoring the challenge to radar in situations involving complex terrain, the interpretation of radar in terms of precipitation amounts typically has been through a Z-R relationships, where Z is the observed radar reflectivity and R is the rainfall rate. In general, Z-R relationships vary in space and time, even during a single event and certainly can change from case to case. Although radar is a potentially powerful tool in depicting precipitation, it has some limitations and may not

always give a reliable quantitative estimate of precipitation (Figure 86.). What is important is to recognize the potential in the meteorological analysis of the situation, so that when precipitation commences, detection of an important rainfall event does not depend only on a literal acceptance of the quantitative precipitation estimates from the radar (Doswell et al, 1996).

3. Meteorological processes concatenating ingredients

Large-scale processes

Although large-scale vertical motions typically do not provide the lifting necessary to initiate convection, there is an unmistakable connection between synoptic-scale weather systems (i.e., short-wave troughs) and deep, moist convection. Approaching systems have more or less predictable basis structures, based on their evolution up to the point of the forecast, and the numerical weather prediction (NWP) models may have a reasonably accurate diagnosis and prognosis of those systems. Further, many flash flood events arise in what are superficially benign synoptic conditions. The important aspects of flash flood cases can be subtle and may escape attention if forecaster vigilance has been decreased by days of relatively inactive weather. Maddox et al. (1979) note that many flash flood events occur near a synoptic-scale 500-mb ridge axis, a region not always identified as a locus for important weather events. This apparently anomalous activity may be a direct consequence of the suppressing effect of the anticyclone. That is, the synoptic-scale subsidence occurring with the ridge aloft tends to suppress deep convection and enhances diabatic heating processes that can contribute substantially to increasing the lapse rate. This suppression of convection also allows the return of moisture al low levels; deep, moist convection can consume moisture at a rate far greater than can be supplied by synoptic-scale processes (Doswell et al, 1996).

The initiation of convection in association with a synoptic-scale anticyclone or ridge typically occurs on the margins of the suppressed area, where sharp thermal boundaries often exist. This leads to the so-called ring-of-fire effect, in which active convection surrounds the zone of most intense synoptic-scale suppression (Doswell et al, 1996).

a) Mesoscale processes

A major role for mesoscale processes is to provide the lifting needed for convective initiation. Although the needed lift may be related to processes on scales even below that normally considered “mesoscale“, one typically must begin the search for candidate mechanisms on the mesoscale. The role of mesoscale terrain, an important lifting mechanism when the flow is upslope, also must be considered. Mesoscale processes associated with MCSs can be responsible for heavy precipitation events in a number of ways. They can influence system propagation, and their typical organizational structure involves both a deep convective part and stratiform part, such that MCSs often produce large pools of outflow that persist for many hours after the rain-producing convection itself has dissipated (Doswell et al, 1996).

b) Storm-scale processes

Once deep convection is under way, the evolution of the convective event can be modified significantly by the convection itself. A major contributor to how the convection behaves is the outflow created by convective downdrafts. If the storm evapourates a great deal of condensate,

this produces a significant chilling of the air that, in turn, creates negative buoyancy. Strong downdrafts are associated with this process, and so the likelihood that a convective storm will develop a cold outflow is associated with the “evaporation potential“ of its environment. High evaporation rates are associated with low precipitation efficiency. As already noted, individual convective updrafts tend to move with a speed and direction roughly comparable to the mean wind in the tropospheric layer containing the updraft; cells simply are propagated along (more or less) in the mean wind flow. Interaction with opposite directions between advection and propagation is how quasi-stationary storms arise.

Numerical parameters for small scale convective cloud systems

1. CAPE

An air parcel must have sufficient potential energy for convection. The indicator for this energy is CAPE - the Convective Available Potential Energy. Hence, a key to the possibility for the growing of convective storms is the presence of CAPE, not the environmental lapse rates alone. Not all situations with conditional instability are characterised by air parcels with CAPE. Thus, the moisture content of the air is important for knowing whether conditional instability actually contains the potential for parcels to become buoyant. In that case, an external source of energy must be supplied to the air mass to convert its potential instability into actual instability and lift the parcel through its condensation level to its Level of Free Convection (LFC) - that means, for instance, the change from potential instability to conditional instability. The amount of this supplied energy is known as the Convective Inhibition (CIN). From the LFC to the Equilibrium Level (EL), the parcel accelerates vertically, drawing the energy for this acceleration from the CAPE (*http://www.eumetrain.org/satmanu*).

All levels of sounding or pseudotemp are used for the calculation of CAPE. The unit of CAPE is J/kg; it describes the maximum amount of potential energy which the air parcel has available for convection. CAPE is calculated by integrating over height the (virtual) temperature difference of lifted air parcel and the environment. In a thermodynamic diagram, this represents the area that is between the curve of lifted air parcel and that of the environment. The integration normally starts from the level of free convection (LFC), which is the level above which the lifted parcel is warmer than environment. The upper limit for the integration is the level of neutral buoyancy (LNB) in which the parcel and environment curves meet again. CAPE values in pre-thunder conditions range from a few hundreds of J/kg up to thousands of J/kg. The greatest observed values are of the order of 5000-7000 J/kg. The definition of CAPE doesn't take into account the existence of entrainment, liquid water loading, aerodynamical effects or the vertical motions in the environment, which have a decreasing effect on the value of CAPE. CAPE can also be calculated with starting integration level not being the LFC, but instead, either a fixed level (e.g. 850 hPa), a lifted condensation level (LCL) or a convective condensation level (CCL).

2. Stability indices

Stability indices are a group of indices that have been developed to illustrate the potential for convection within an air mass based upon a radiosonde or model derived sounding. In most

cases, stability indices are derived from the temperature and humidity data of the sounding at certain fixed levels. Some stability indices even use information from all observed levels of the sounding (such as CAPE, see previous chapter). Some indices also contain a contribution of wind information. All indices, however, eventually give only one numerical value (which may be dimensionless). This value represents the potential for convection at a certain fixed location (either the radio sounding site, if the index is calculated from radio sounding data, or a numerical model grid point, if numerical data is used for calculation). The value of the stability index is compared to some statistical threshold value differentiating e.g. non-thunderstorm and thunder storm cases. For air mass classification purposes, index values are plotted and analysed on a weather map. This latter method is particularly effective for model derived stability indices, since model derived soundings can be calculated at each model grid point for each model time step. In meteorology, the use of convection indices varies from country to country, reflecting different methods. A full list of indices used would contain tens of different indices and would go beyond the scope of this manual. For this reason, only a small selection of stability indices - containing those used in this manual - is mentioned in this chapter (for more details visit *http://www.eumetrain.org/satmanu)*:

- → Showalter Index (SI)
- → Boyden Index
- → K-Index

3. Convection and instability

Large scale areas often contain synoptic conditions suitable for the development of convection, however, convective features are much smaller scale. The concept of a buoyant air parcel is best understood using hydrostatic information describing the state of the air column above. Information about the quality of an air column can be gained from radio soundings or with model derived soundings (e.g. from a LAM model like ALADIN). Consequently, for single CBs and MCSs, other parameters and their vertical distribution become more important than those commonly associated with larger scale conceptual models.

Atmospheric conditions for convection

Convection in general is mass motion within a fluid resulting in transport and turbulent mixing of the properties of that fluid by vertical movement, in matters of transport of energy (heat), water vapour and momentum. As such, it is one of the three main processes by which energy (heat) can be transported vertically: radiation, conduction, and convection. Meteorologists typically use the term convection to refer to heat transport by the vertical component of the flow associated with an updraft. Convection is best explained by the so-called lifted parcel theory. Here, the environment of the parcel is not affected by this displacement, and the upward force affecting such a rising plume (i.e. parcel) of air is buoyancy, which is defined by

$$B = -\frac{\rho_p - \rho_e}{\rho_e} g = \frac{T_V(z)_p - T_V(z)_e}{T_V(z)_e} g.$$

The difference in density (left term) or in virtual temperature (right term) between the rising parcel (*p*) and the parcel environment (*e*) causes the updraft. Consequently, a parcel with greater temperature and less density will be controlled by buoyancy and displaced vertically. The virtual temperature is conservative in association with the moisture within the parcel. Vertically integrated, the right term in the buoyancy formula gives the amount of available convective energy. It is clear that the vertical displacement and acceleration of an air parcel is directly associated to buoyancy (*http://www.eumetrain.org/satmanu)*.

2 main types of convection can be distinguished:

1. Free convection (also called gravitational or buoyant convection): motions that are predominantly vertical and driven by buoyancy forces arising from hydrostatic instability, with locally significant deviations from hydrostatic equilibrium. Free convection can mostly be related to diabatic heating through insolation (short wave radiation) on surfaces with higher heat capacity than the neighbouring environment or thermal forcing through greater diabatic heating at elevated surfaces.
2. Forced convection: motion induced by mechanical forces such as deflection by a large-scale surface irregularity, turbulent flow caused by friction at the boundary of a fluid, or motion caused by any applied pressure gradient. Furthermore, this type of convection is caused by lifting owing to dynamical convergence, lifting through orography, lifting within the lee circulation of a mountain ridge or gravity waves.

The unstable stratification of the atmosphere causes deep moist convection, whatever the reason may be for convective initiation or the type of appearance of convective cells. Therefore, the different types of instability are now considered further:

The origin of instability is heat, both latent and sensible, that is produced as a result of solar heating and evapotranspiration of water vapour (also due to solar heating) in the lower troposphere. Convection transports the excess sensible heat and water vapour from low levels into the upper troposphere, and transports cooler, dry air downward, thereby reducing the instability. Thus, the instability is initiating DMC, but convection will only continue until the instability is removed.

Hydrostatic stability is a state variable for the stratification of the atmosphere or at least of a column of air. It can be indicated by various variables like temperature, humidity or density. The change, usually a decrease of those parameters, is shown in the lapse rate. In the hydrostatic approach, the process lapse rate is distinguished from the environmental lapse rate of the lifted air parcel. For parcel theory, the term "environment" means the immediate vicinity to the parcel. This environment is not affected by the processes applied to the parcel.

The dry adiabatic lapse rate of an air parcel is the rate of decrease of temperature with height of a parcel of dry air which is lifted through the atmosphere in hydrostatic equilibrium. That means if a parcel of air is vertically displaced without saturation its temperature will change with the amount of Γ

$$\Gamma \equiv -\left(\frac{dT}{dz}\right)_{dry} = \frac{g}{c_p} = 0.98\,°C/100m.$$

During the process of lifting, an air parcel will cool and may reach the point of saturation. If it is still buoyant and continuing its ascent, its temperature will decrease moist adiabatically. The moist adiabatic lapse rate is smaller because of the release of latent heat through condensation: $\Gamma_m \approx 0.65\,°C/100m$. The process lapse rate is $\gamma = -\left(\frac{\partial T}{\partial z}\right)$. The relation between γ and Γ/Γ_m is the degree for stability.

Table 1. Conditions of stability

Unsaturated		Saturated
$\gamma > \Gamma$	**Unstable**	$\gamma > \Gamma_m$
$\gamma = \Gamma$	**Neutral**	$\gamma = \Gamma_m$
$\gamma < \Gamma$	**Stable**	$\gamma < \Gamma_m$

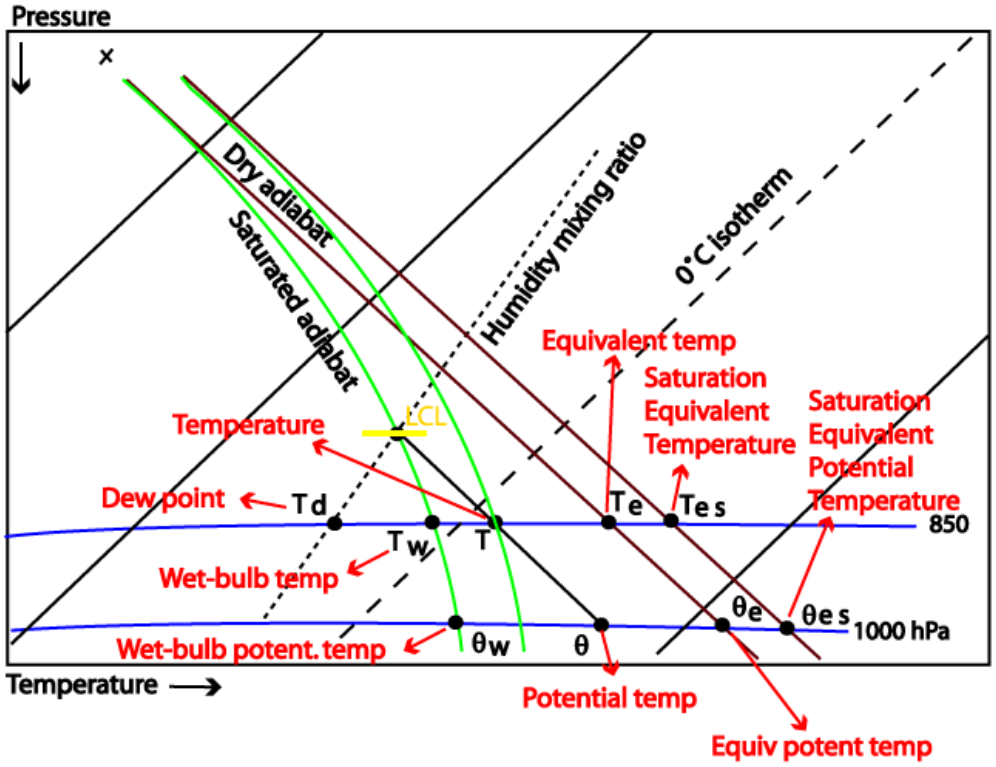

Figure 87. Tephigram (thermodynamical diagram) illustrate thermodynamic variables based on a parcel of air at 850 hPa with a given temperature, wet-bulb temperature and dew point. Formerly

used variables like potential and equivalent temperatures can be obtained from the diagram, Source: *http://www.eumetrain.org/satmanu*

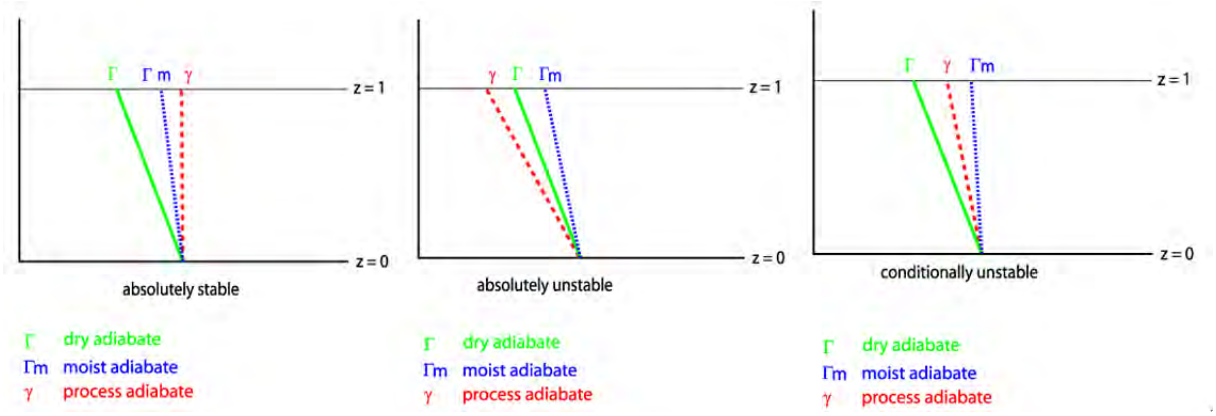

Figure 88. Illustration of conditions of stability, Source: *http://www.eumetrain.org/satmanu*

In an absolutely stable case, an air parcel has the same temperature or is colder as its environment. Therefore, there will be no lifting force on that parcel. When absolutely unstable, the state of a column of air in the atmosphere when the lapse rate of temperature is greater than the dry-adiabatic lapse rate. The temperature of the air parcel is warmer than its environment, thus the parcel will be buoyant and will rise further. An air parcel vertically displaced is accelerated in the direction of the displacement and the kinetic energy consequently grows with the increasing distance from its level of origin. The atmosphere is said to be conditionally unstable where the environmental lapse rate is greater than the pseudo-moist adiabatic lapse rate, but less than the dry - adiabatic lapse rate. The condition for instability when $\Gamma > \gamma > \Gamma_m$ is that the air parcel is saturated. When the environmental lapse rate is greater than Γ, an air parcel is unstable when it is saturated. If the environmental lapse rate is less than pseudomoist adiabatic, the atmosphere is conditionally stable. If $\gamma = \Gamma_m$ the atmosphere is neutral with respect to saturated vertical displacements. An interesting case occurs when the environmental lapse rate lies between the dry adiabatic and the saturated adiabatic, that is $\Gamma_s < \Gamma < \Gamma_d$. In such a case, a moist unsaturated air parcel can be lifted high enough to become saturated, since the decrease in its temperature due to adiabatic cooling is offset by the faster decrease in water vapour saturation pressure, and starts condensation at the LCL. Upon further lifting, the air parcel eventually gets warmer than its environment at a level termed *Level of Free Convection (LFC)* above which it will develop a positive buoyancy fuelled by the continuous release of latent heat due to condensation, as long as there is vapour to condense. This situation of *conditional instability* is most common in the atmosphere, especially in the Tropics, where a forced finite uplifting of moist air may eventually lead to spontaneous convection. On Figure 89, which is one of the meteograms discussed earlier in the chapter, pressure decreases vertically, while lines of constant temperature are tilted 45 rightward, with temperature decreasing going up and to the left. The thick solid line represents the environment temperature profile. A moist air parcel initially at rest at point *A* is lifted and cools at the adiabatic lapse rate Γ_d along the thin solid line

until it eventually gets saturated at the Lifting Condensation Level at point *D*. During this lifting, it gets colder than the environment. Upon further lifting, it cools at a slower rate at the pseudoadiabatic lapse rate Γ_s along the thin dashed line until it reaches the LFC at point C, where it attains the temperature of the environment. If it goes beyond that point, it will be warmer, hence lighter than the environment and will experience a positive buoyancy force. This buoyancy will sustain the ascent of the air parcel until all vapour condenses or until its temperature crosses again the profile of environmental temperature at the *Level of Neutral Buoyancy (LNB).* Actually, since the air parcel gets there with a positive vertical velocity, this level may be surpassed and the air parcel may overshoot into a region where it experiences negative buoyancy, to eventually get mixed there or splash back to the LNB. In practice, entrainment of environmental air into the ascending air parcel often occurs, mitigates the buoyant forces, and the parcel generally reaches below the LNB.

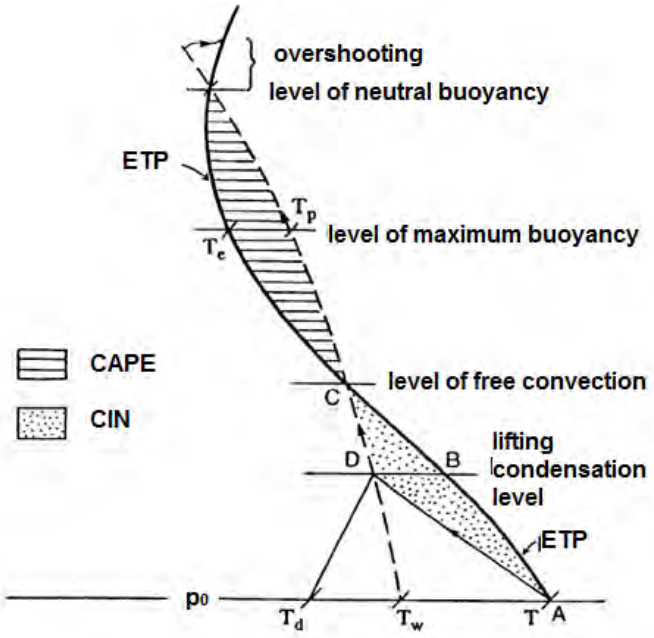

Figure 89. Thick solid line represents the environment temperature profile. Thin solid line represents the temperature of an ascending parcel initially at point A. Dotted area represent CIN, shaded area represent CAPE, Source: *Atmospheric Thermodynamics, 2011.)*

An air parcel initially in *A* is bound inside a "potential energy well" whose depth is proportional to the dotted area, and that is termed *Convective Inhibition (CIN)*. If forcedly raised to the level of free convection, it can ascend freely, with an available potential energy given by the shaded area, termed CAPE. CIN measures the amount of energy required to overcome the negatively buoyant energy the environment exerts on the air parcel, the smaller, the more unstable the atmosphere, and the easier to develop convection. So, in general, convection develops when CIN is small and CAPE is large. We want to stress that some CIN is needed to build-up enough CAPE to eventually fuel the convection, and some mechanical forcing is needed to overcome CIN. This can be provided by cold front approaching, flow over obstacles and sea breeze.

23. HYDROLOGY

Flash floods have a different character than river floods – notably, short time scale and occurring in small spatial scales – which make the forecasting of flash floods a different challenge than traditional flood forecasting approaches. Forecasters must be educated and trained to understand the unique challenges associated with flash floods. As the knowledge and experience of trained forecasters increase, so does their ability to identify areas where their local knowledge and FFG system provide applicable and realistic results, as well as gaining a sense of the meteorological and hydrologic conditions likely to lead to flash flooding for their country (Modrick et al., 2014). This chapter provides not only a short explanation of the ingredients that contribute to flash flooding, but also a simplified explanation of the models, which are used in SEEFFG System.

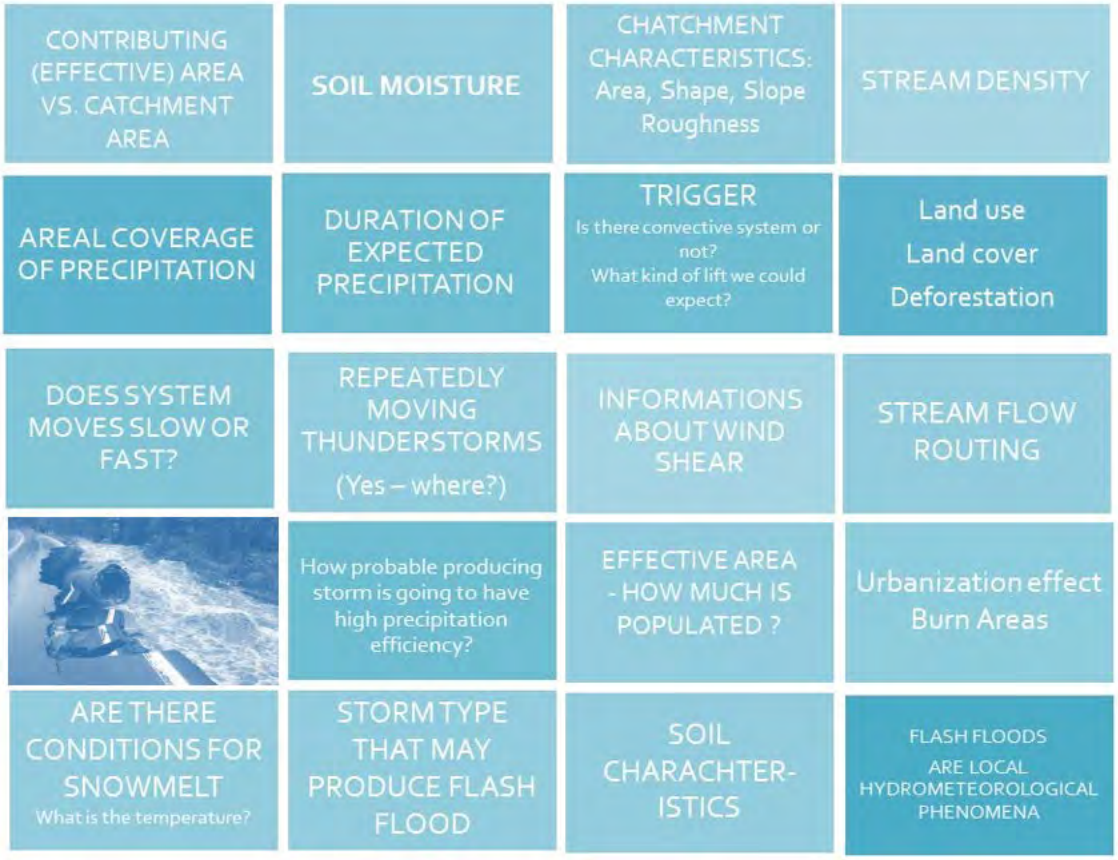

Figure 90. The facts and questions that forecaster should know when forecasting flash floods

A catchment is defined as land area from which water drains toward a common watercourse in a natural basin or an area having a common outlet for its surface runoff. The physical characteristics of a catchment and its river and stream network influence the amount and timing of a runoff and therefore the likelihood of flash flooding in the catchment's outlet. In some cases, the catchment influences are more important than the precipitation.

Catchment, watershed, basin and drainage basin are all terms used to describe the area contributing to the runoff which begins at the drainage divide that marks parameters of the catchment.

23. HYDROLOGY

Figure 91. Illustration of catchment

Runoff is the most important component of flood prediction; once we know the amount of water expected to become runoff, other tools such as the unit hydrograph can assist us with estimating the resulting discharge in the river. In flash flood forecasting, an accurate estimate of runoff from rainfall or snowmelt is one of the most important elements. Runoff is affected by meteorological factors and the physical geology and topography of the land. Soil moisture is an important factor also affecting runoff.

A number of terms are commonly used to describe the runoff process: baseflow, interflow, runoff, and surface runoff. Baseflow or base runoff is the long-term supply of water that keeps at least some water in the stream even during extended dry periods. Baseflow comes from water that percolates down into the deep storage. The term percolation is sometimes used interchangeably with infiltration. Percolation refers to the movement of water within the soil, while infiltration specifically refers just to the process of water entering a soil.

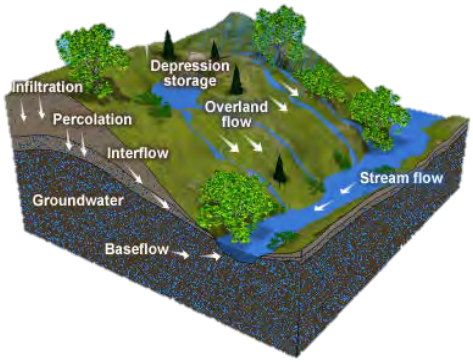

Figure 92. Illustration of runoff components

Regarding infiltration, infiltration rate and infiltration capacity have to be defined. The infiltration rate is the amount of water able to enter the soil in a specified time period. It is expressed as depth per time (e.g. 20 mm per hour), while the infiltration capacity is the upper limit of the infiltration rate. It includes surface infiltration and percolation, and is also expressed in depth per time. In the SEEFFGS the infiltration and percolation rates are dynamic and changes with the soil moisture condition. If the precipitation rate is greater than the infiltration capacity, surface runoff occurs. If the precipitation rate is equal to or less than the infiltration capacity, no surface runoff occurs. Surface runoff is the movement of water across the soil surface toward the stream channel. For stream channel flow, this definition also includes the water which makes its way to the stream channel below the surface.

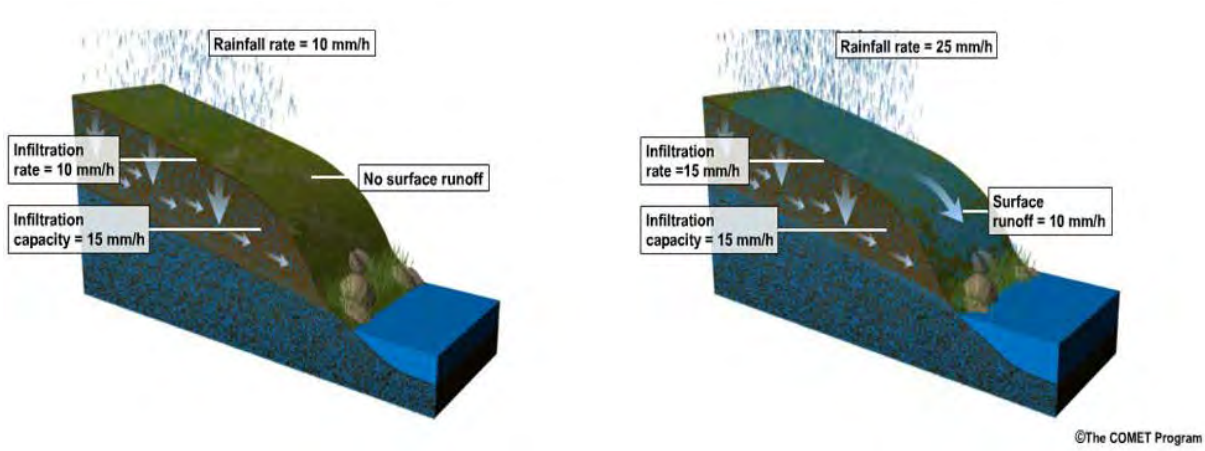

Figure 93. Conceptualized relationship between rainfall, infiltration and runoff

There are two types of surface runoff that occur during rainfall or snowmelt: infiltration excess overland flow and saturation excess overland flow. Infiltration excess overland flow occurs with soil that is not saturated. In fact, soil can be quite dry, but soil properties or land cover do not allow for infiltration to keep up with high rainfall or snowmelt rates. The water cannot infiltrate and becomes surface runoff. Infiltration excess overland flow is sometimes called Hortonian flow, and it is common with short-duration intensive rainfall. It also often occurs in areas with high clay content or where the surface has been altered by soil compaction, urbanization or fire.

Saturation excess overland flow occurs when the soil becomes saturated and there is no longer any space for water to infiltrate. It is most common with long-duration, gentle to moderate rainfall, or with successive precipitation and snowmelt events. It can occur anywhere the soil is wet, and it is common in humid climates with gently sloped or flat basins.

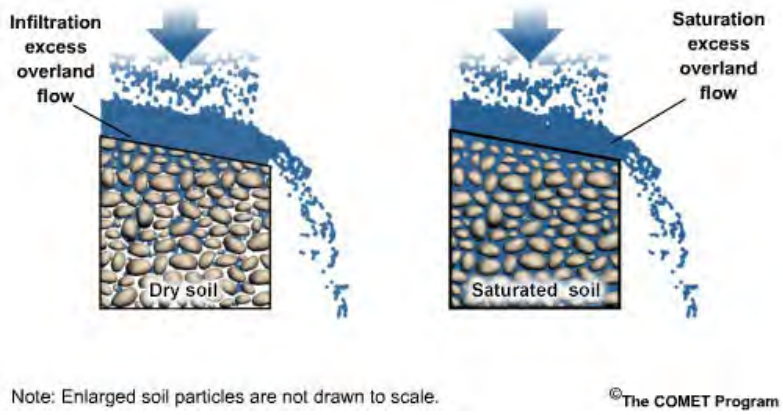

Figure 94. Types of surface runoff

Interflow or subsurface runoff is a relatively rapid flow toward the stream channel that occurs below the surface. It occurs more rapidly than baseflow, but more slowly than surface runoff. In some cases, interflow may be as surface runoff for forecasting rapid rises in the stream channel. In regions with high infiltration rates and steep terrain, interflow may be the dominant process by

which streams react quickly to rainfall or snowmelt. This process is most likely to occur in humid, deep-soil areas, but significant interflow contribution may also occur in thin-soiled regions when there is an impermeable layer such as bedrock beneath the more permeable surface soil layer.

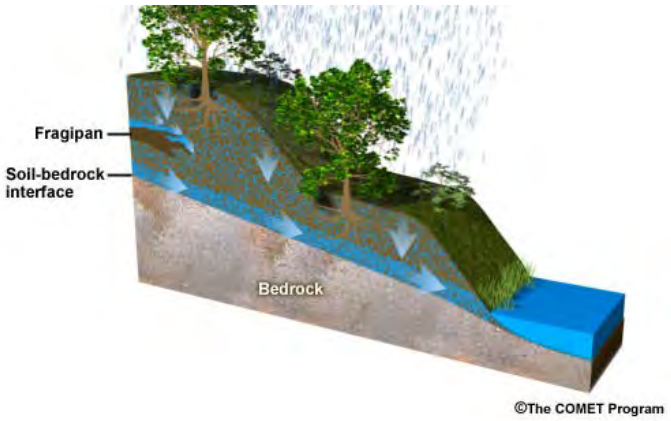

Figure 95. Interflow along soil bedrock

If a fragipan layer exists, it has low permeability, like rock or clay, and may serve to focus the lateral subsurface flow. Fragipan features can exist at relatively shallow depths and play an important role in enhancing both interflow and even surface runoff after the soil layers above the fragipan are saturated.

Some of the interflow that quickly finds its way to the stream is not necessarily from the current rainfall. In this case, there is already considerable water in the soil layers that is displaced as new water infiltrates. The water that appears in the stream immediately following a rainfall or rapid snowmelt may be from previous precipitation events, or pre-event water. In humid climates, studies have shown that pre-event water is often the greatest contributor to rapid rises in the stream channel.

Another mechanism that can contribute to runoff is groundwater ridging. It is defined as the formation of a high-pressure subsurface ridge along the stream, coupled with relatively steep hydraulic head gradients on both sides of ridge (Szilagyi, 2006).

Rainwater or snowmelt reaches the groundwater level near the stream channel more quickly than it does further up the hill away from the stream. The water table begins to rise near the stream channel more quickly, creating a groundwater ridge close to the stream. The gradient between the groundwater ridge and the stream channel results in more rapid interflow to the stream.

The physical properties of a catchment and its stream and river network influence the amount and timing of the runoff. These properties may come from natural and human factors. The physical geology and topographic characteristics influencing runoff are catchment and contributing area, shape, topography, elevation, vegetation cover, land use, river and stream network, and soil type.

If rain falls in a uniform manner over a larger and smaller catchment, of course, the larger catchment produces more runoff volume. However, many rainfall events only cover a part of a catchment, so the runoff volume will be determined by the contributing area – that part of catchment covered by rainfall, not the total size of catchment.

23. HYDROLOGY

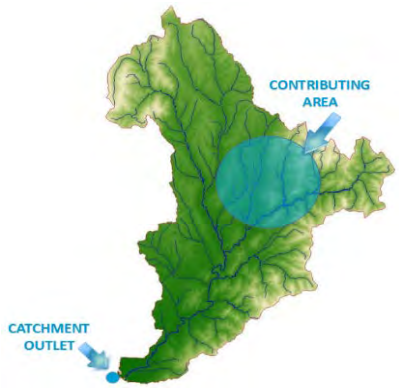

Figure 96. Contributing area

The size of the contributing area of the rainfall in a catchment has a direct impact on the total volume of runoff that drains from that catchment.

Runoff in a smaller catchment will take less time to reach outlet than in the larger catchment.

Basin shape has an influence on the magnitude and timing of the peak flow at the basin outlet. Given two basins with equal areas, a longer and narrower basin water from multiple locations is less likely to arrive at the same time than in a rounder basin, resulting in a greater peak flow.

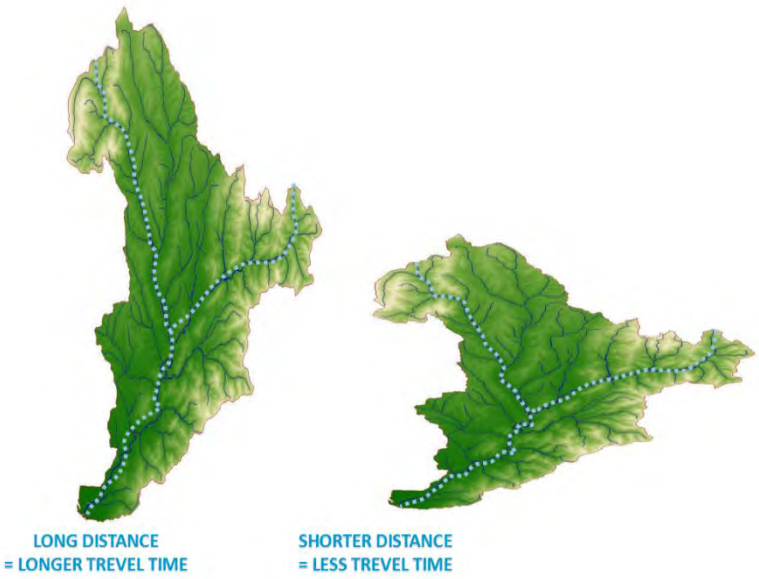

Figure 97. Influence of basin shape on runoff

The roughness of the channel has a direct impact on how quickly water will move in the channel. The roughness of a stream channel increases due to the presence of rocks, vegetation and debris. Channelization of streams in urban areas where vegetation is removed and lined with concrete decreases roughness and causes water velocity to increase. Channels with smooth

banks and bed have less friction and result in faster water velocities and greater peak flows. In contrast, large numbers of angular rocks and coarse-grained banks increase friction and result in reduced overall velocity. Manning's equation is often used in hydrology to account for the roughness factor.

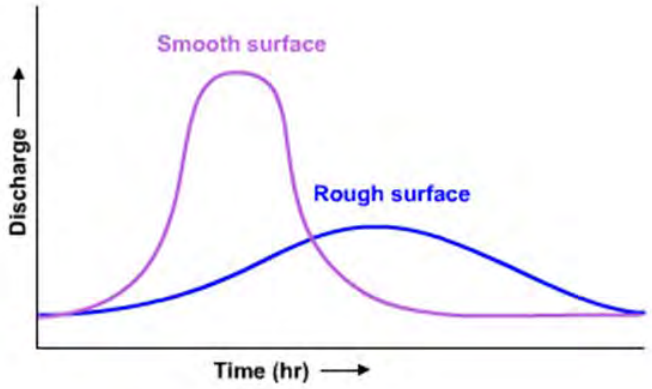

Figure 98. Hydrographs for smooth and rough surface

Urbanization can have a great effect on surface-runoff patterns. Roads and buildings have replaced most of the watershed surface and these impervious surfaces drain into sewer networks that carry flow efficiency downstream. When rainfall occurs, it cannot infiltrate the impervious surface, but will flow to the sewer network or become direct surface runoff and flow directly and discharge into the natural streams.

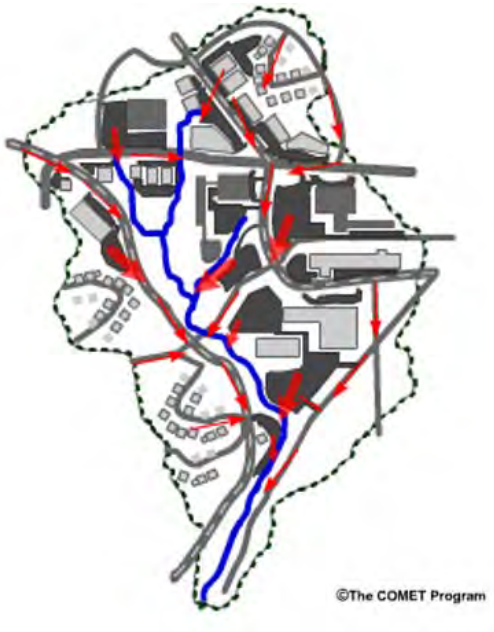

Figure 99. Effect of urban grid on runoff

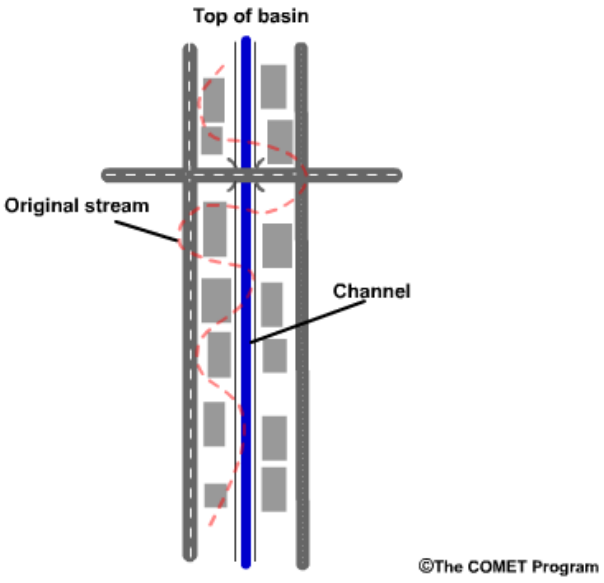

Figure 100. Urban channelization

Sometimes, as part of channelization, urban streams are straightened. This also effectively increases the slope because the stream now experiences the same elevation drop but in a shorter distance. Decreasing the distance travelled and increasing slope will cause a more rapid flood response from the runoff by having meanders removed. This decreases the distance that water travels from the top to the bottom of the drainage basin.

Urban features such as road embankments and berms can act to break down natural catchments into smaller sub-catchments. Smaller drainages react more quickly to localized rainfall than larger catchments.

The slope of the catchment affects the amount and the timing of runoff. As the terrain of the land becomes increasingly steep, water will move faster and have less time in contact with the ground surface, reducing the time during which it could infiltrate; therefore, more water will become surface runoff. In general, the steeper the land slope and the steeper the drainage channel, the quicker the response and the higher the peak discharges.

The amount of sediment carried by flowing water is also important. Erosion occurs when water removes sediment from the ground surface. Although it is dependent on soil type and ground cover, erosion generally increases with increasing slope. With higher amounts of sediment in the water, the surfaces pores in the soil, which the water might otherwise enter, can become plugged, reducing infiltration.

Another important factor is the stream or drainage density, which is defined as the total length of the all streams and rivers in a catchment divided by the total area of the catchment. It depends on the climate and physical characteristics of the catchment.

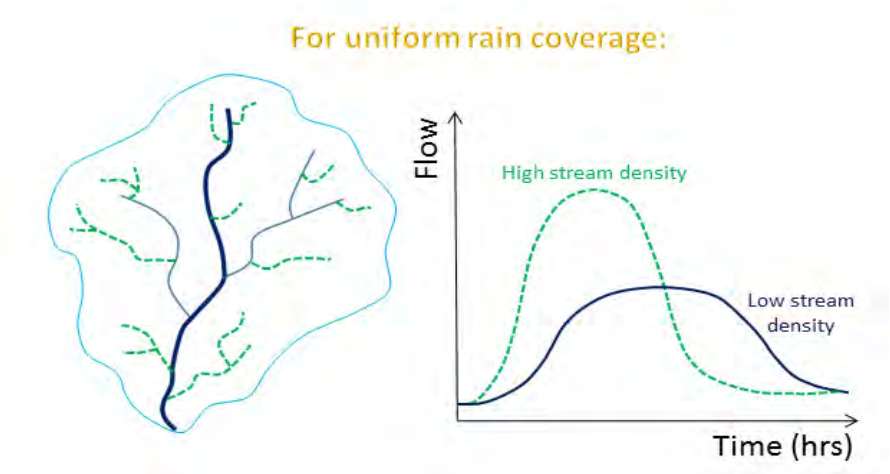

Figure 101. Comparison of high and low stream density for uniform rain coverage

A catchment with many tributaries has a higher stream density, which allows the landscape to drain more efficiently. More efficient drainage means that water moves into streams and creeks faster, causing peak storm flows to be larger and to occur sooner. Drainage density is the most important characteristic for evaluating potential runoff. A catchment with lower stream density is usually on deep, well developed soils. In this case, water is more likely to infiltrate into the soil rather than become surface runoff and enter into the channel network.

23. HYDROLOGY

Forestation along streams is particularly important in reducing both runoff amounts and runoff speed.

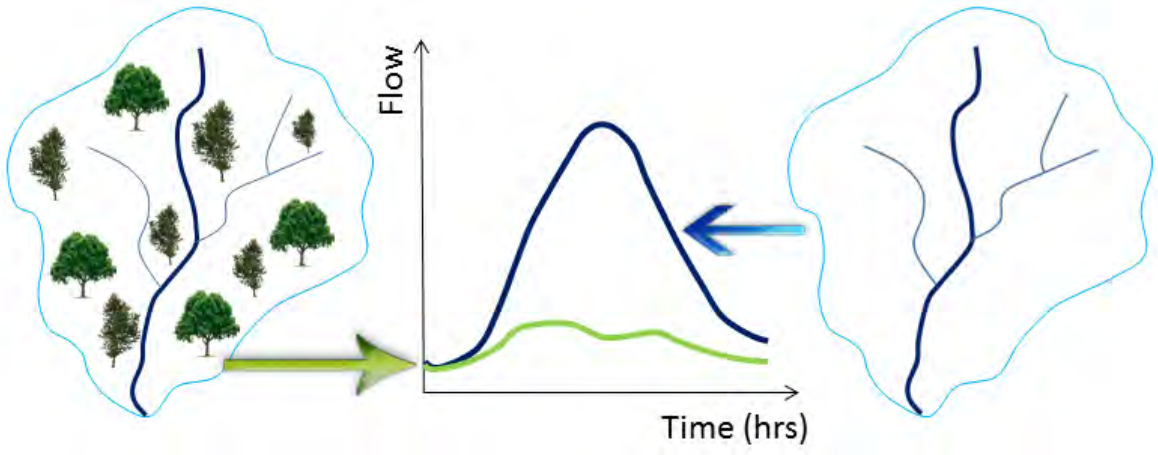

Figure 102. Hydrography for catchment with and without vegetation

Another important effect on forests is that they retain some and slow down the snow melting, in some cases, this can last almost a month, which favors infiltration in soil and reduces the size of floods.

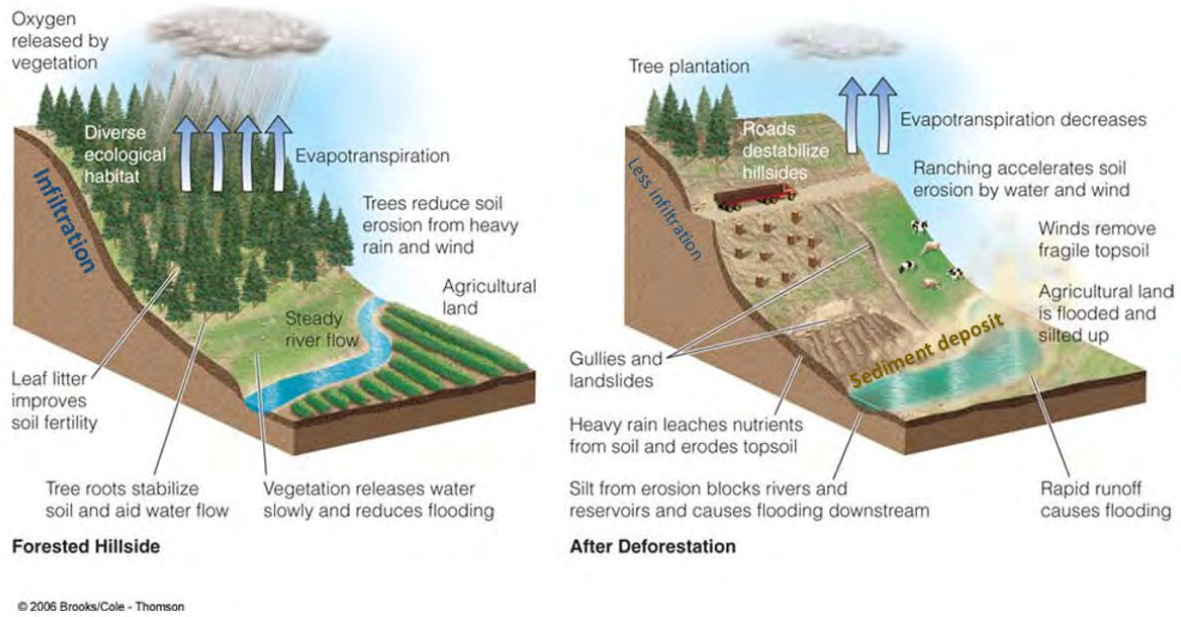

Figure 103. Before and after deforestation on the hillside

Deforestation and wildfires can also increase the flash flood risk by increasing the runoff volume and the potential for sediment transport (debris flow) within the runoff.

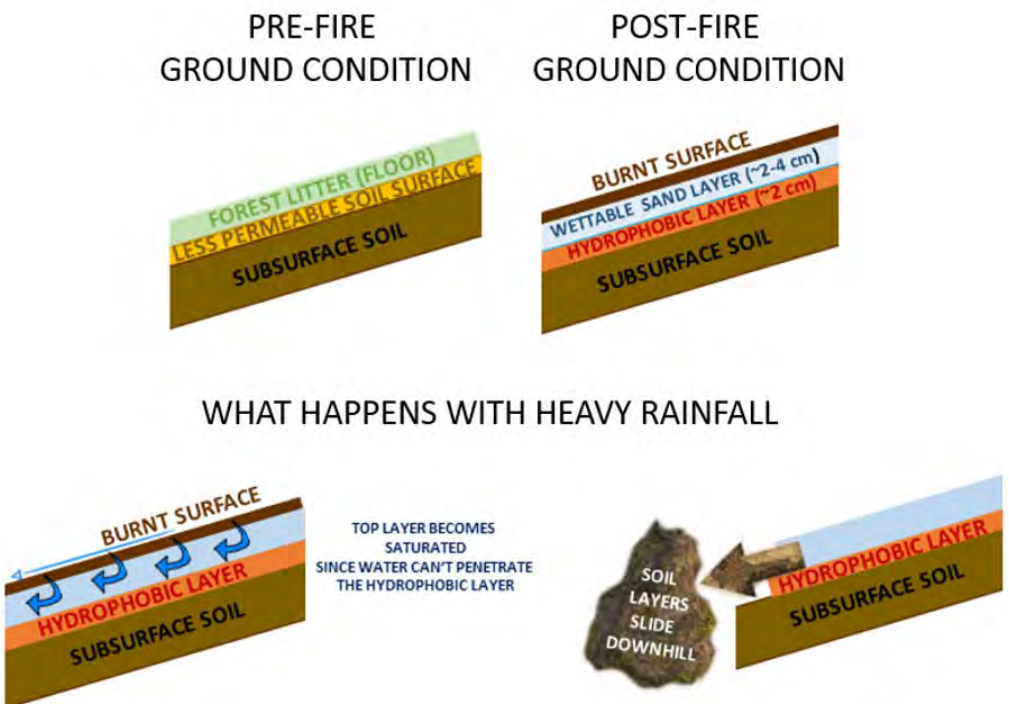

Figure 104. The impact of heavy rain on the land affected by fires

Wildfires can alter soil properties so that burn areas become hydrophobic, i.e., tending to repel and not absorb water for weeks or even years following a fire. Indeed, some of the greatest flash flood risks occur after high-intensity fires in coniferous forests. The time required for a flash flood to begin depends on how severe the fire was and how steep the terrain is, combined with the rate of precipitation. Steep terrain combined with a severe burn scar and light precipitation can result in flash flooding within minutes of precipitation beginning. Areas of less severe burn damage and flatter terrain will be able to absorb more water, leading to more time before flooding develops even in heavier precipitation.

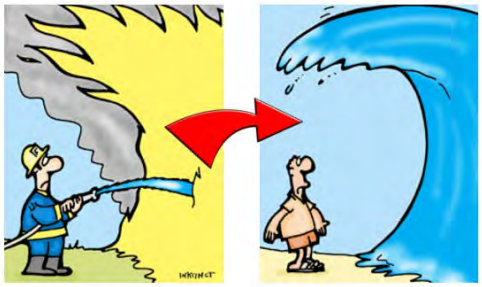

Hydrologic influences on the ground can have a major impact on timing, location, and severity of flash flooding. Although rainfall is often considered the most important factor for forecasting floods, what happens to the rain once it is on the ground can sometimes be of greater importance. In some cases, the runoff production process may be more important than rainfall characteristics (Flash Flood Early Warning System Reference Guide).

The hydrological processes in the SEEFFG system serve to estimate current flash flood guidance (FFG) at each processing time step and for each small watershed defined for SEE region. The FFG is defined as a numerical estimate of the basin average rainfall for a specified

watershed and duration required to initiate flash flooding at the outlet of a stream basin. The characteristic volume of rainfall for that watershed and duration relies on both surface and subsurface elements that lead to bankfull conditions at the stream outlet. In some situations, the runoff characteristics can be as important as the rain rate.

For forecasters who are new to flash food forecasting, the hydrologic components of soil moisture, threshold runoff, watershed delineation, stream flow, and the concept of bankfull flow are the biggest challenges (Modrick et. al, 2014). Because of that, some of them are explained in this chapter.

The computation of FFG is divided into two components: a static component, which summarizes the characteristic of the watershed, and a dynamic component, which incorporates time-varying changes in soil saturation conditions within each watershed.

The static component consists of an analysis to define a characteristic of each watershed called threshold runoff. Threshold runoff (TR) is defined as the amount of effective rainfall of a given duration which produces the volume of runoff required to cause bankfull conditions at the watershed outlet. Effective rainfall is the residual amount after accounting for all losses such as interception and soil moisture storage. Bankfull stage is depth of water in the channel at which flooding begins. Bankfull flow is a conservative measure of flooding and is not generally associated with flood damage. It may be associated with flow of given return period (typically 2-5 years).

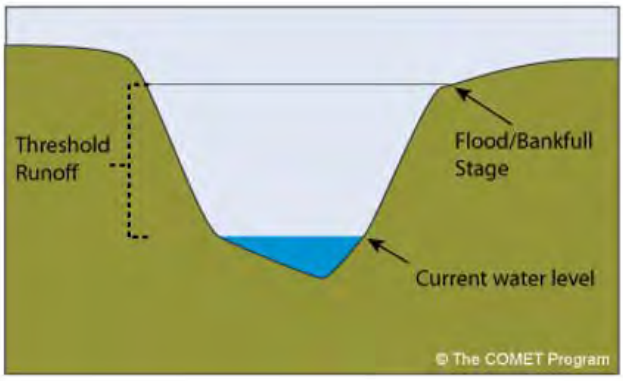

Figure 105. Illustration of bankfull

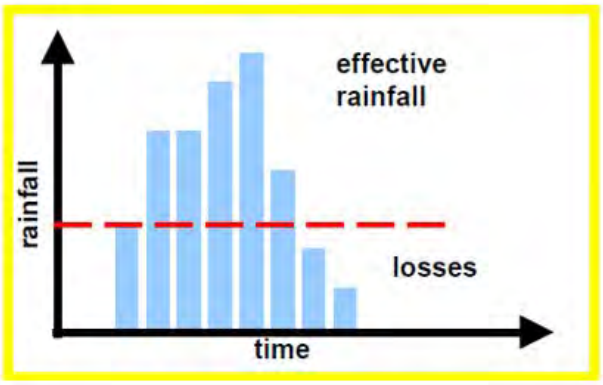

Figure 106. Effective rainfall

TR is a characteristic of the watershed; it is a static, one time calculation. TR applies at the watershed outlet and it is not computed for watersheds with drainage areas larger than 2000 km^2. It is calculated using the Geomorphologic Instantaneous Unit Hydrograph (GIUH) theory, which relates the peak response of a watershed for a unit rainfall input to catchment physical and geomorphologic characteristics (drainage area, stream length, slope), and the bankfull flow, which may be estimated by hydrologic principles based on the channel cross-sectional geometry. The GIS and its spatial analysis are used to extract watershed scale properties with the use of global digital terrain elevation (90 m SRTM DEM). Channel cross-sectional properties (channel top width at bankfull, hydraulic depth at bankfull) for the SEEFFGS are estimated from regional relationships with watershed scale properties. Typically, these relationships are derived from country-provided channel cross-sectional survey information, but because of the lack of such data to establish local relationships, relationships which were developed on cross-sectional surveys within Romania were used within the SEE region.

23. HYDROLOGY

$$R = f\ (A, L, B_b, D_b, S_c)$$

Threshold runoff (R) is a function of a drainage area (A), stream length (L), channel top width (Bb), hydraulic depth (Db) and stream slope (Sc).

According to the Carpenter et al. (1999), under the assumption that catchments respond linearly to rainfall excess, threshold runoff, R, may be found by equating the peak catchment rainfall, determined from the catchment unit hydrograph of a given duration, to the stream flow at the basin outlet associated with flooding. Mathematically, this is expressed as:

$$Q_p = q_{pR}\ R\ A$$

where Qp is flooding flow (cms), q_{Pr} peak of the unit hydrograph of duration Tr, R threshold runoff (mm), and A catchment area (km^2).

One conservative measure of a "flooding flow" is the bankfull discharge. The bankfull discharge is computed from channel geometry and roughness characteristics using Manning's steady, uniform flow resistance formula (Chow et al., 1988):

$$Q^p = Q_{bf} = B_b\ D_b^{5/3}\ S_c^{0.5} / n$$

Georgakakos et al. (1991) based on data by Jarret (1984), presents Manning's roughness coefficient (for n > 0.035) as a function of local channel slope, S_c (dimensionless) and hydraulic depth, D_b (m):

$$n = 0.43\ S_c^{0.37} / D_b^{0.15}$$

The catchment response is determined from the catchment unit hydrograph of a given duration. Rodriguez-Iturbe and Valdes (1979) developed geomorphologic instantaneous unit hydrograph based on the geomorphologic structure of basins, using Horton's geomorphologic laws (e.g see Bras, 1990, for a description of Horton's laws). They began by expressing the peak magnitude and time to peak of instantaneous unit hydrograph as a function of Horton's ratios, stream length and the catchment velocity. Rodriguez-Iturbe et al. (1982) eliminated the catchment velocity from the expressions and converted the peak magnitude and time to peak of the instantaneous unit hydrograph to the peak magnitude and time to peak of a unit hydrograph corresponding to a uniform rainfall excess of a given duration t_R.

$$qp = \frac{0.871}{\pi^{0.4}}$$

$$\frac{Sc^{0.5}}{nBb^{2/3}}$$

$$\pi = \frac{L^{2.5}}{\frac{R}{t_r} R_L \alpha^{1.5}}$$

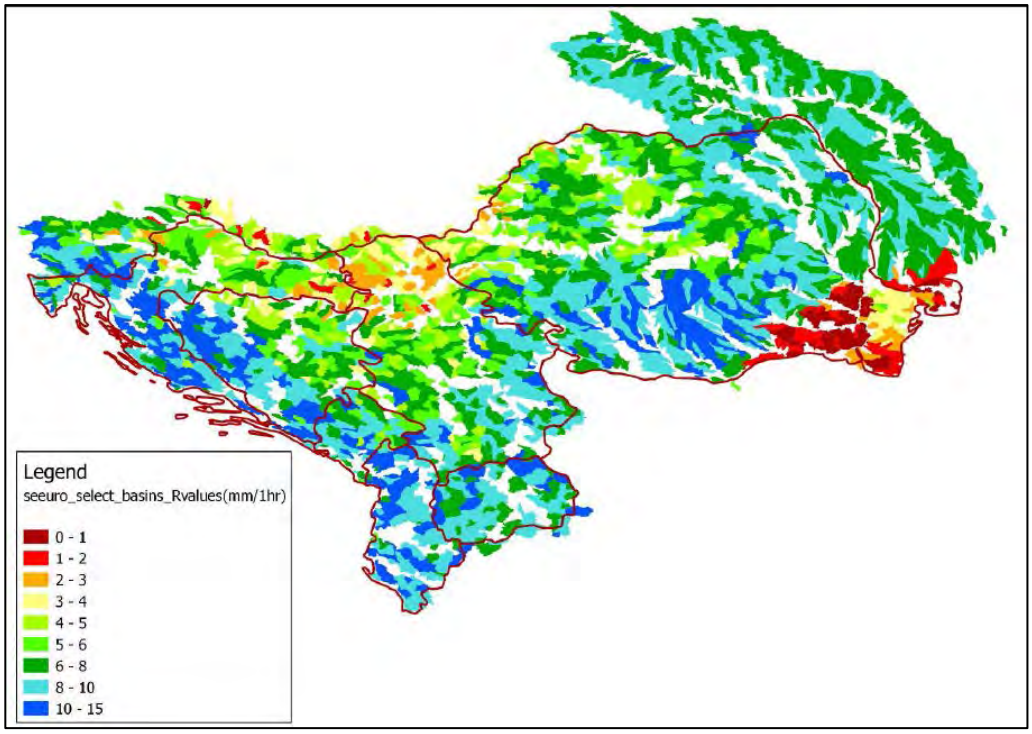

Figure 107. Threshold Runoff estimates for SEE region

The dynamic component involves time varying accounting of soil moisture and evapotranspiration for each watershed to assess the current soil saturation deficit at each processing timestep. The aim of the soil moisture accounting process is to account for the losses in transformation of rainfall to runoff (e.g. between actual and effective rainfall). The soil moisture accounting process considers the variation in oil properties and characteristics, along with land use characteristic along the SEE region. The current FFG at any timestep and for any given watershed is then computed from the threshold runoff and current soil saturation deficit (FFG = TR + all precipitation losses at the current processing time step).

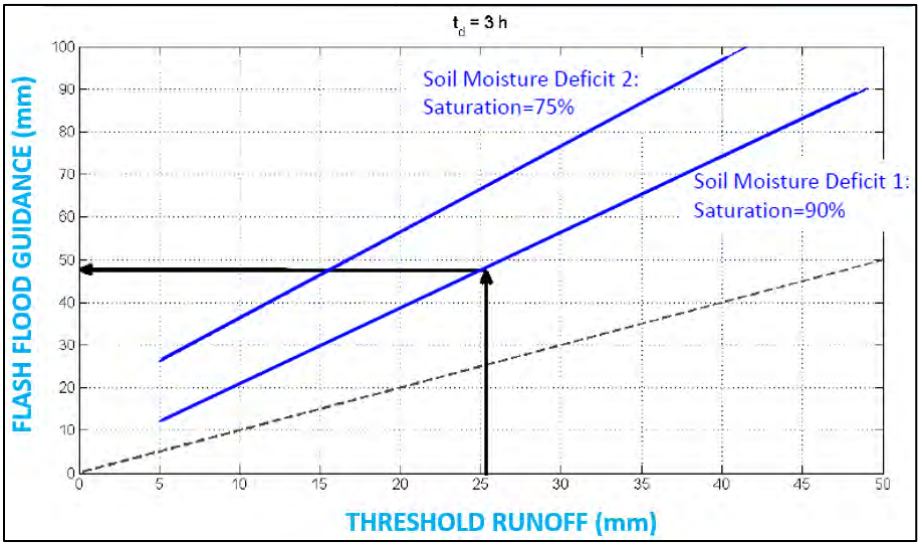

Figure 108. Relationships between Threshold runoff, Flash Flood Guidance and Soil moisture

The FFG model uses potential evapotranspiration (PET) as a measure of the ability of the atmosphere to remove water from the surface through the process of evaporation and transpiration when and where there is a sufficient water supply. The potential evapotranspiration is higher in the summer days, and on clean and windy days (this is also true for the regions closer to the equator because of higher levels of solar radiation).

In the FFG model, PET rate values are updated daily for each watershed and are based on: the areal average surface temperature, the day of the year the latitude to estimate the extra-terrestrial incoming radiation, and coefficients representing the land cover information about the plant annual cycle.

The approach commonly used with the implementation of the SAC-SMA model is to estimate evapotranspiration demand (ET_d). Lack of sensitivity for short-term predictions implies that for catchment scale hydrological models, especially in data scare regions, long term seasonal climatological estimates of evapotranspiration components may be adequate. The daily potential evapotranspiration demand values were calculated for the basins as calendric climatological values using the Jensen-Haise (J-H) procedure (Jensen and Haise, 1963) – robust and efficient when used for short term modelling objectives such as flood warning applications. The J-H equation has two parameters (scaling and threshold) and requires the estimate of climatological mean monthly temperature values and the maximum extra-terrestrial radiation, which can be calculated as a function of latitudinal location and for a given calendric day (Allen et al. 2005). Potential evaporation at given location (mm/day):

$$\mathbf{PE = [Re\ T_a\ K_2] / K_1\ (\lambda p) \quad for\ T_a > K_2}$$

where, R_E is the extra-terrestrial radiation (MJm-2day-1), T_a is is climatological mean monthly temperature, K_1(°C) is minimum temperature in which below PE=0 (~5), K_2(°C) is scale parameter (50-100), λ is latent heat flux (MJ kg^{-1}) and ϕ is density of water (kg^{-1}). The R_e values depend on latitudinal location and Julian day while T_a depend on Julian day and elevation. The K_1 and K_2 are empirical scaling and threshold parameters that have to be estimated based on regional mass balance studies, or can be calculated if ET_p values are known.

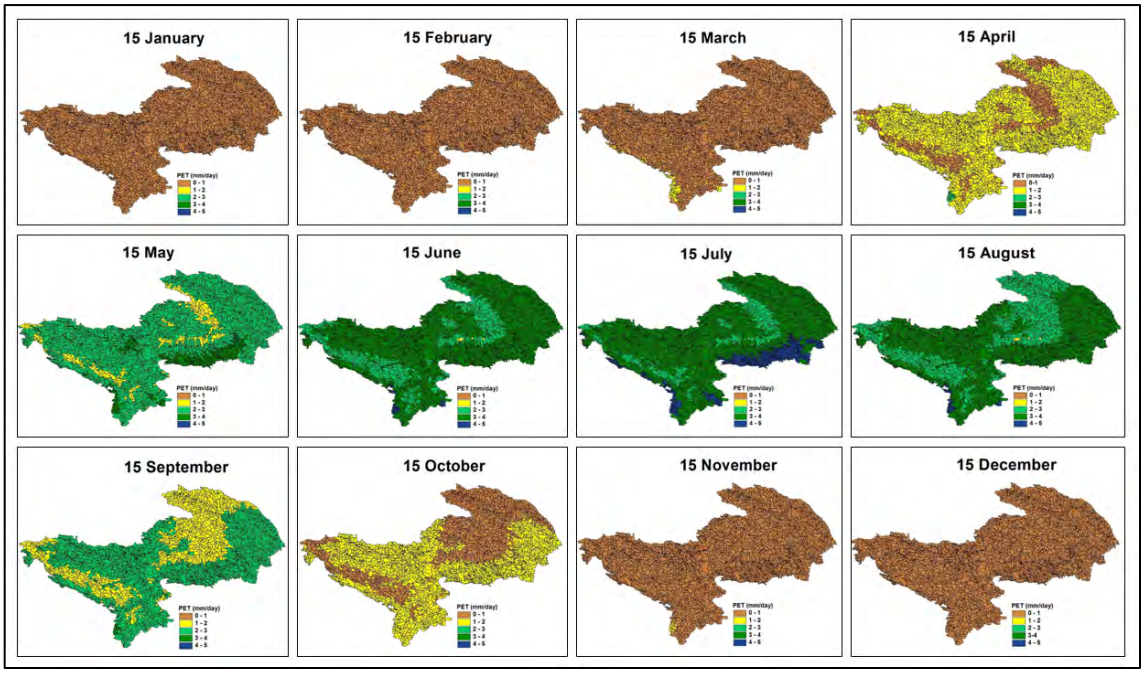

Figure 109. Daily potential evapotranspiration for the SEE

24. CASE STUDIES

In flash flood forecasting, forecasters should use all available tools to better understand the weather situation in their particular region, as well as apply local knowledge and experience and the current situation from field. As usual, forecasters should first do synoptic scale analysis, mesoscale analysis and small-scale analysis, and interpretation of FFGS products. As part of the nowcast process, forecasters should use satellite images, radar products and information from station.

It is very important to take in consideration past weather events (few days) so one can get a better picture of soil moisture and stage of rivers. Also, flash floods can cause two different types of weather: a big frontal system with heavy and steady rain and convective heavy rain with fast development.

1. Synoptic Analysis

Synoptic analysis should include past few days and forecast for few future days for the region using global models and local area models. Analysis should contain:

- Surface analysis:
  -Current weather
  -Low pressure systems and frontal systems and their movement in time
  -Winds
  -Precipitation types and amounts

- 850 hPa analysis:
  -Trough and ridges
  -Warm and cold air advection
  -Low level convergence
  -Wind
  -Humidity

- 500 hPa analysis:
  -Trough and ridges
  -Warm and cold air advection
  -Convergence and divergence areas
  -Wind
  -Vertical motions

- JET stream locations and movement in time
- Satellite images
- Various LAM models
-

2. Mesoscale analysis

Mesoscale weather analysis should be more detailed with focus on local areas. Analysis should contain:

- Detailed surface analysis
- Dry line

- Gust fronts
- Instability
- Satellite images

3. Nowcasting analysis

Nowcasting is very short forecasting with high resolution spatial features. Analysis depends of available data and tools for better tracking of precipitation, thunderstorms development and movement. In nowcast analysis, time is very important and every new information or radar/satellite scan can give us crucial information of potential dangerous weather. Analysis should contain:

- Instability analysis
- Precipitation analysis and forecast
- Ground observations
- Satellite images
- Radar images
- Lightning detections

24.1. Flash Flood in West part of SEE Region, October 2015

The analysis of the precipitation amounts for October 2015, compared to the 1961-1990 average, showed that the precipitation amounts throughout Croatia were exceeding climatological average. October 2015 was characterized as wet, very wet and, in some parts of Croatia, even extremely wet.

From 10-16 October 2015, two cyclones from the central Mediterranean brought an extreme amount of precipitation to certain parts of Croatia and Bosnia and Herzegovina causing great damage. The Croatian media and civil protection agency reported on flood and flash flood events in which approximately 100 landslides happened, infrastructure was flooded, and roads and vents were damaged. Fortunately, there were no human losses.

Synoptic Analysis

The first cyclone that affected Croatia and Bosnia and Herzegovina on 10 and 11 October moved quite quickly from the Tyrrhenian Sea over Italy into the Adriatic.

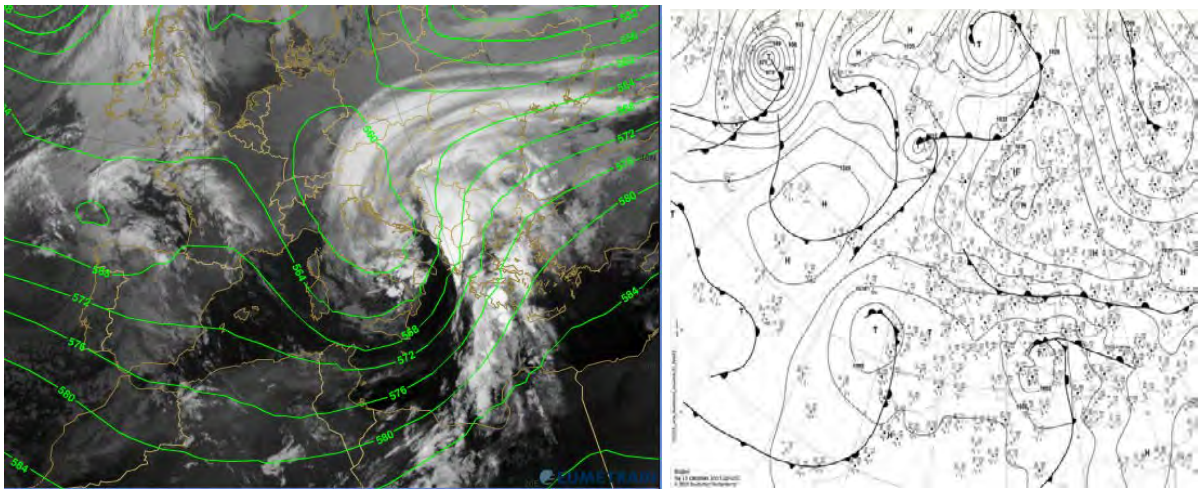

Figure 110. Meteosat IR overlayed with H500 (Eumetsat, Eumetrain, ECMWF) and DWD surface analysis, 11 October 2015 at 00 UTC

Cyclonic vortex and short-wave trough in the upper levels pushed very unstable air with large moisture content over the Adriatic, especially to its southern part. The setup of several factors, such as passage of a cold front and an occlusion, advection of very moist air in combination with very steep lapse rates in the mid-levels, enhanced by the orographic lifting, resulted in excessive rain along the eastern Adriatic coast. The inflow of very humid air continued in the following days, ahead of a deep trough stretching from Algeria to NW Germany. Within this trough, a cut-off low cantered over NW Germany. From 13 to 16 October, the cut-off low moved southwards and deepened, which contributed to surface cyclogenesis over north Italy.

24.1. Flash Flood in West part of SEE Region, October 2015

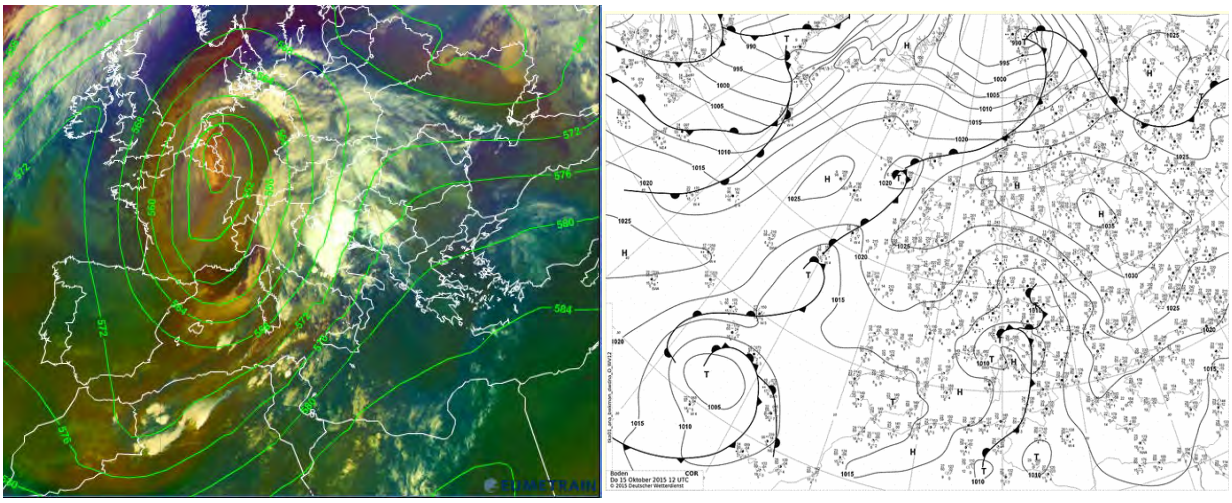

Figure 111. Meteosat Airmass RGB overlayed with H500 (Eumetsat, Eumetrain, ECMWF) and DWD surface analysis, 14 October 2015 at 18 UTC

Instability Analysis

A strong jet streak curved along the cut-off low, resulting in high values of deep layer shear (DLS), but also significant low level shear (LLS), which was present especially during the slow passage of the cold front. Similar to the previous case, ahead of the cold front in the mid-levels, air with steep lapse rates advected over moist air in the lower layers, which resulted in high amounts of CAPE. Overlapping of high CAPE, strong DLS, LLS and lift, both orographic and synoptic, resulted in organized and long lived convection. Heavy rain along the coastline caused flash floods, but excessive rain (Figure 112) in the inland also caused river floods, especially in the surroundings of town Karlovac. (Mutic et al, 2016).

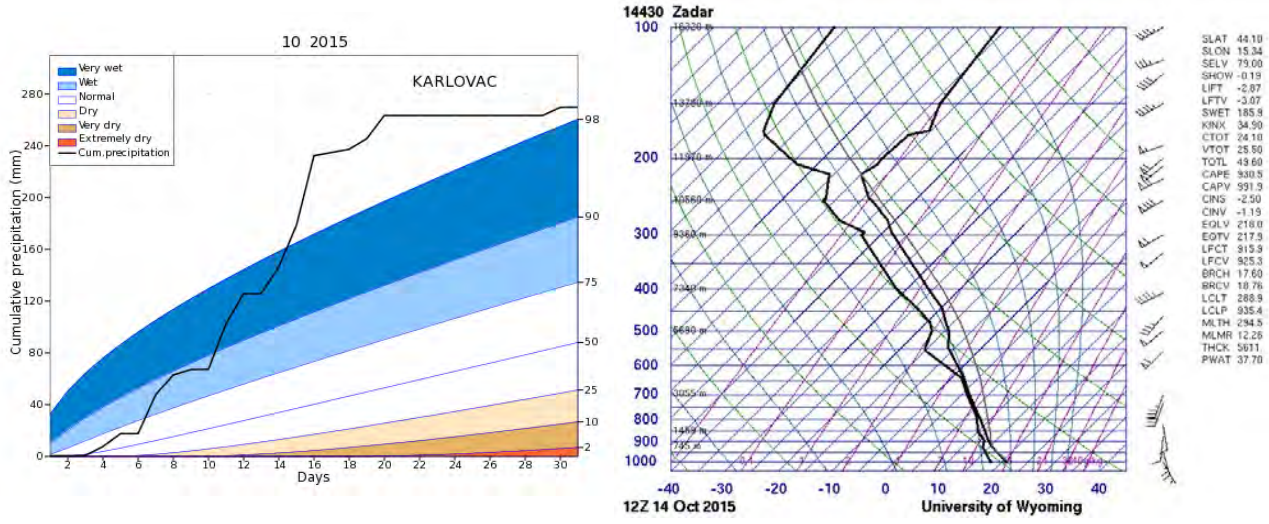

Figure 112. Cumulative precipitation amount (mm) in October 2015 and theoretical percentiles (2., 10., 25., 50., 75., 90. and 98.) curves from the period 1961-2000; Zadar upper air sounding on 14 October 2015 at 12 UTC

24.1. Flash Flood in West part of SEE Region, October 2015

Figure 113 shows CAPE for 14 and 15 October at 12 UTC. This indicates potential instability of atmosphere with moderate CAPE from 1000 J/kg values at Adriatic coast, which were high enough for thunderstorms to develop.

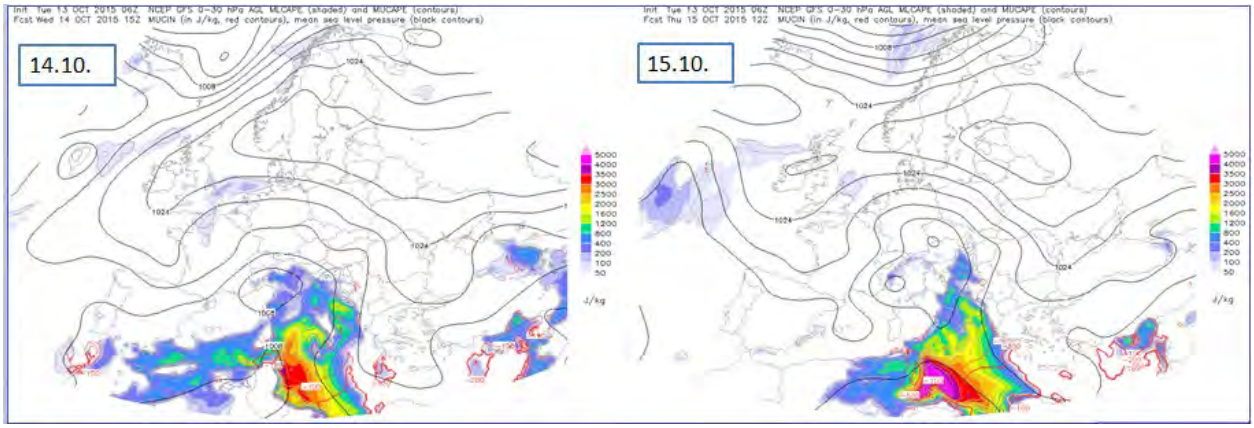

Figure 113. CAPE values on 14 and 15 October

Satellite and Radar images

EUMETSAT geostationary satellite images showed the development of cumulonimbus clouds with high cloud tops over Italy, Croatia, and Bosnia and Herzegovina which produced heavy rain along the coastline and subsequently flash floods in the region. On the IR-colour enhanced image below (Figure 114.), deep convection with strong cumulonimbus with high cloud top is presented.

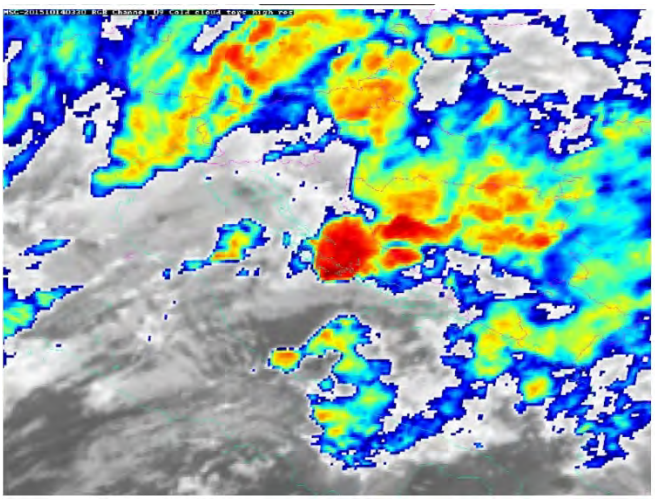

Figure 114. IR COLOUR ENHANCED on 14 October 2015 at 03:30 UTC (EUMETSAT)

Since radar provides near real time two and three-dimensional scans of the weather with finer spatial and temporal coverage, it is strongly advised to use radar products in particular vertical cross sections of a storm and its spatial and temporal development for the flash flood

24.1. Flash Flood in West part of SEE Region, October 2015

Watches/Warnings/Alerts. Radar is a very good tool to monitor convective activities that may occur in the warmer part of the year. If the radar images are available, forecasters must monitor storm development and precipitation intensity closely. Radar 1-hour rainfall accumulations are shown in Figure 115, indicating that precipitation pattern spread across the Croatia and Bosnia and Herzegovina with maximum values of 20-50 mm/1-hr at 12 UTC.

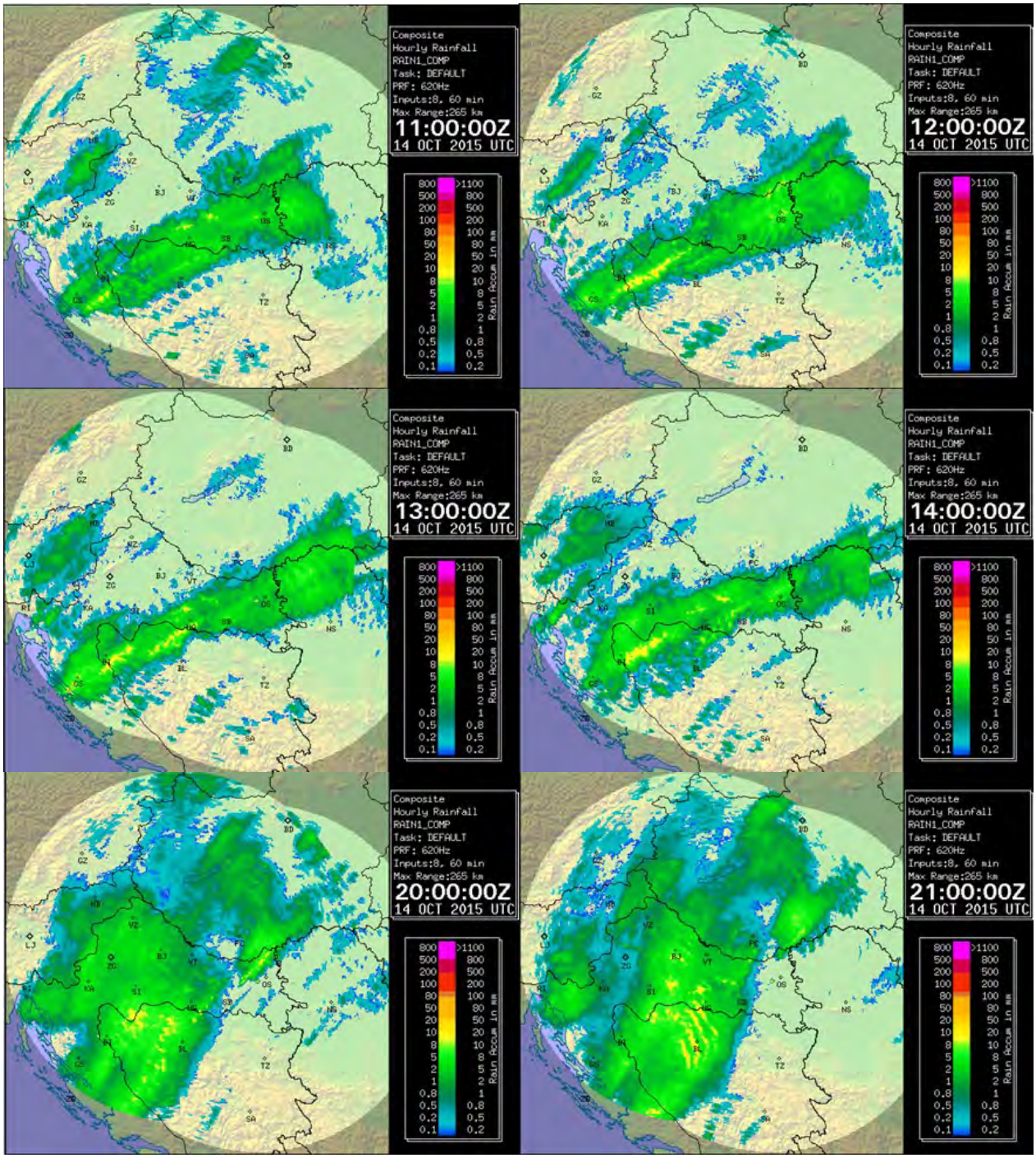

Figure 115. 1-hour radar rainfall accumulations (Meteorological and Hydrological Service of Croatia)

24.1. Flash Flood in West part of SEE Region, October 2015

It is important to note that weather Radar precipitation products, depending on the availability, could be used if they were well calibrated and bias adjusted with ground gauge data.

SEEFFG Products

Having performed weather analysis, it is now imperative to study SEEFFG products before the event occurrence. First, FFGS Diagnostic products need to be analysed to investigate the hydrological response of the catchments. The 6-hour GHE and MWGHE products on 14 October 2015 at 00 UTC showed that precipitation was low over the central parts of the Adriatic coast and on the islands (Figure 116).

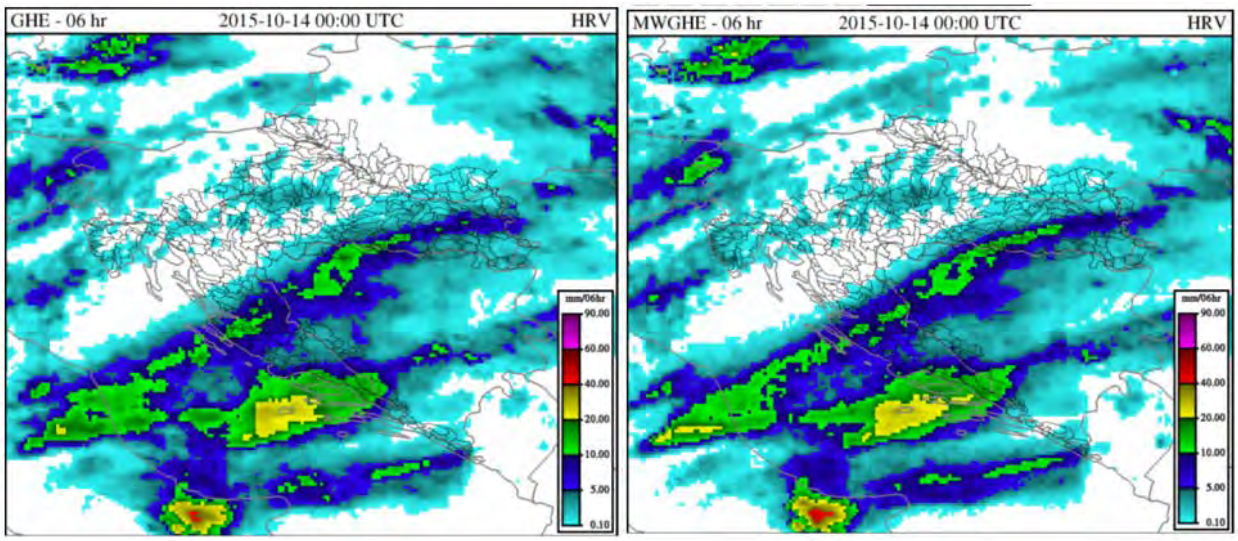

Figure 116. 6-hr Global Hydro Estimator (GHE) and 6-hr Micro Wave adjusted Global Hydro Estimator (MWGHE) on 14 October 2015 at 00 UTC

On the other hand, 6 hours later, at 06 UTC, 6-hour GHE had a maximum value of 20-40 mm along the Adriatic coast (figure 117.), while 6-hour Gauge MAP (GMAP) at 06 UTC had a maximum precipitation accumulation of 60 mm. The Merged MAP from 06 UTC had maximum value of 40 mm in the central parts of the coastal region (figure 118.).

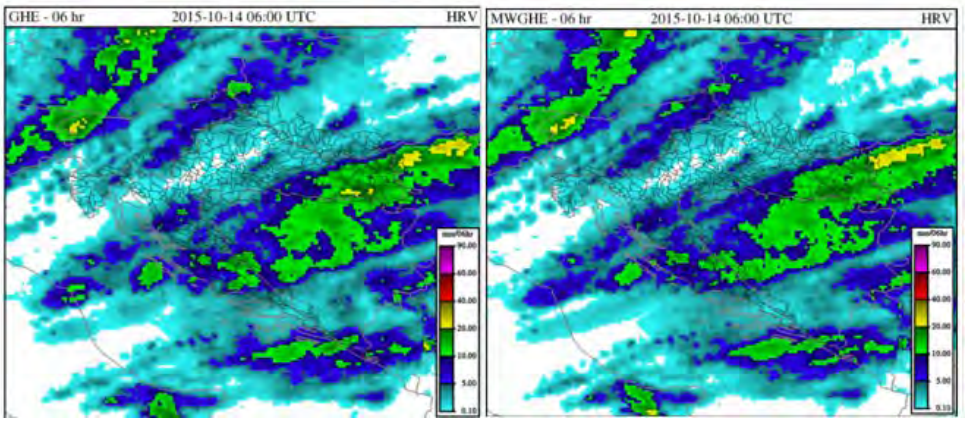

Figure 117. 6-hr Global Hydro Estimator (GHE) and 6-hr MicroWave adjusted Global Hydro Estimator (MWGHE on 14 October 2015 at 06 UTC, Croatia

24.1. Flash Flood in West part of SEE Region, October 2015

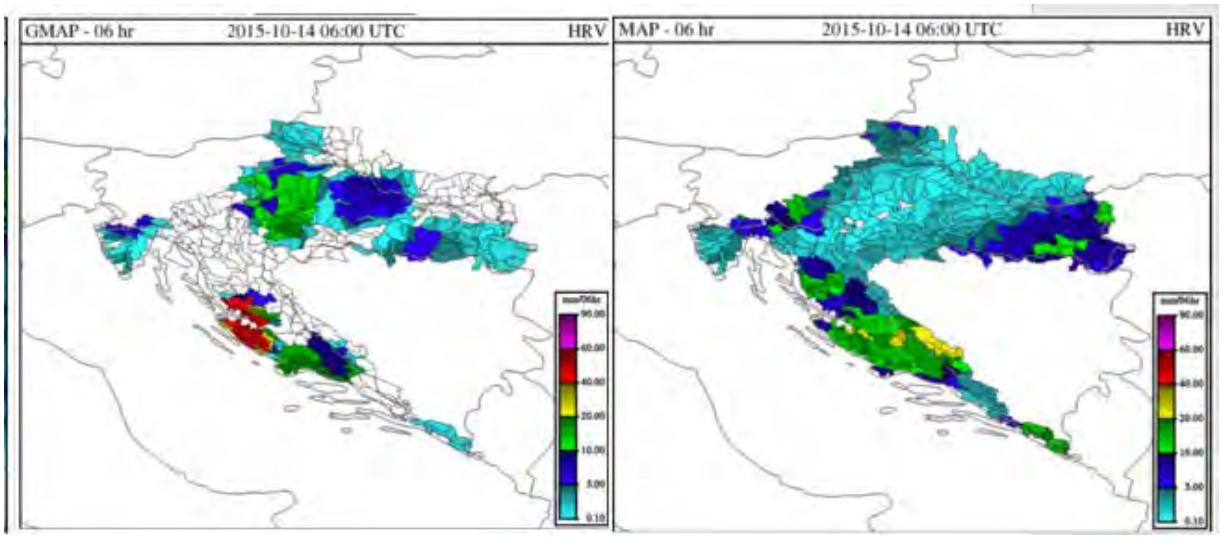

Figure 118. 6-hr Gauge MAP and 6-gr Merged MAP on 14 October 2015 at 06 UTC, Croatia

The next step was to investigate the soil moisture deficit to find out how the top soil moisture changed with precipitation variations in the sub-basins. As shown in Figure 118, the 6-hour Average Soil Moisture (ASM) product showed that upper soil in the Croatian coastal and mountainous regions in Croatia and Bosnia and Herzegovina were completely saturated.

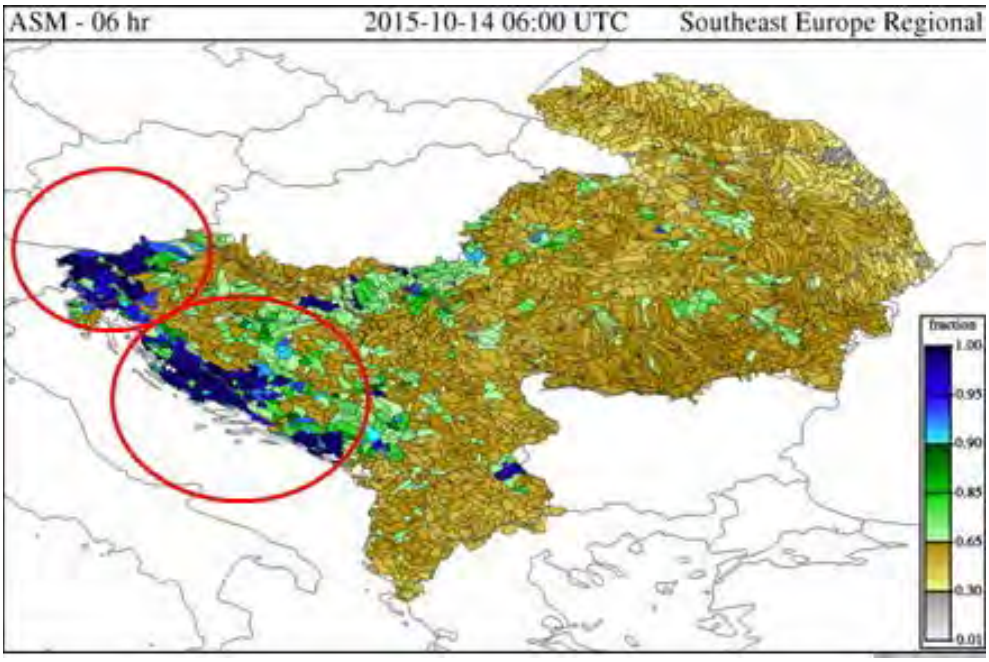

Figure 119. Average soil moisture (ASM) for SEE region on 14 October 2015 at 06 UTC

24.1. Flash Flood in West part of SEE Region, October 2015

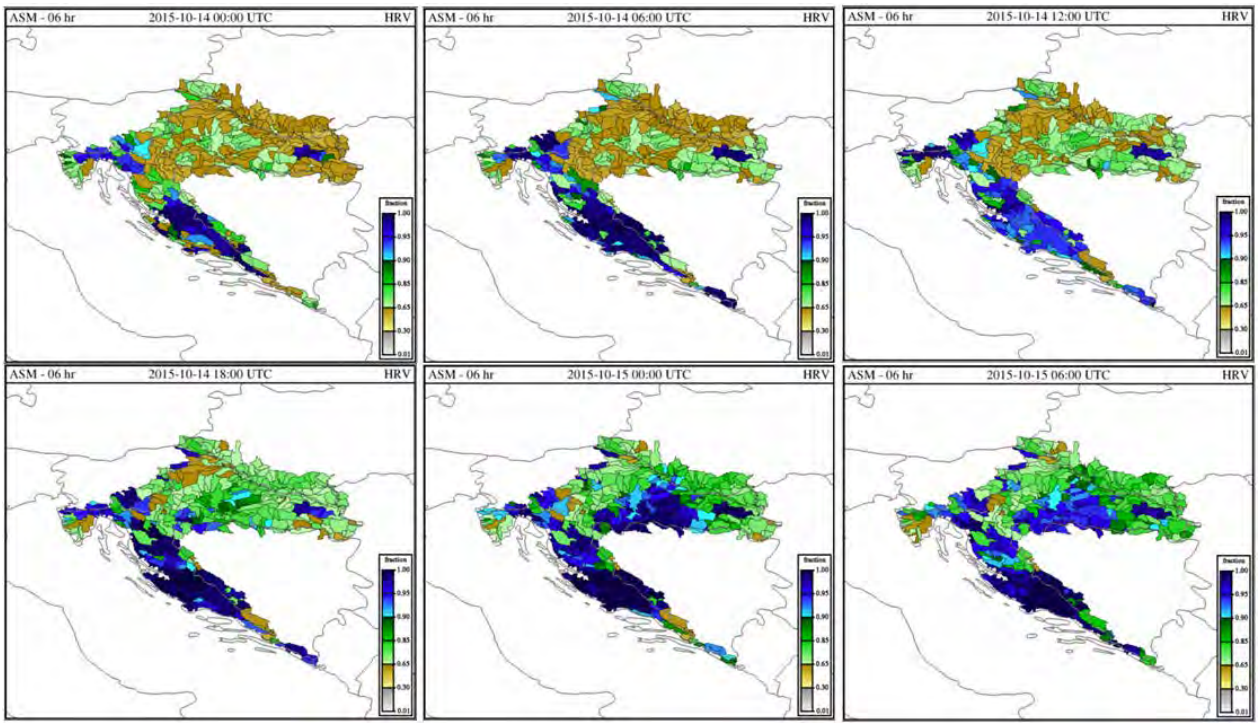

Figure 120. Temporal and spatial distribution of Average Soil Moisture (ASM), Croatia

As we recall, FFG is the actual amount of rainfall that may cause bankfull flow at the outlet of a catchment for a given duration. The lower FFG value, the higher possibility of flash flood occurrence. Figure 119 shows FFG estimates at 06:00 UTC for Croatia and at 12 UTC for SEE. In the case study region, FFG estimates were very low. Their values varied from 0.01 mm (pink) to 15 mm (dark red).

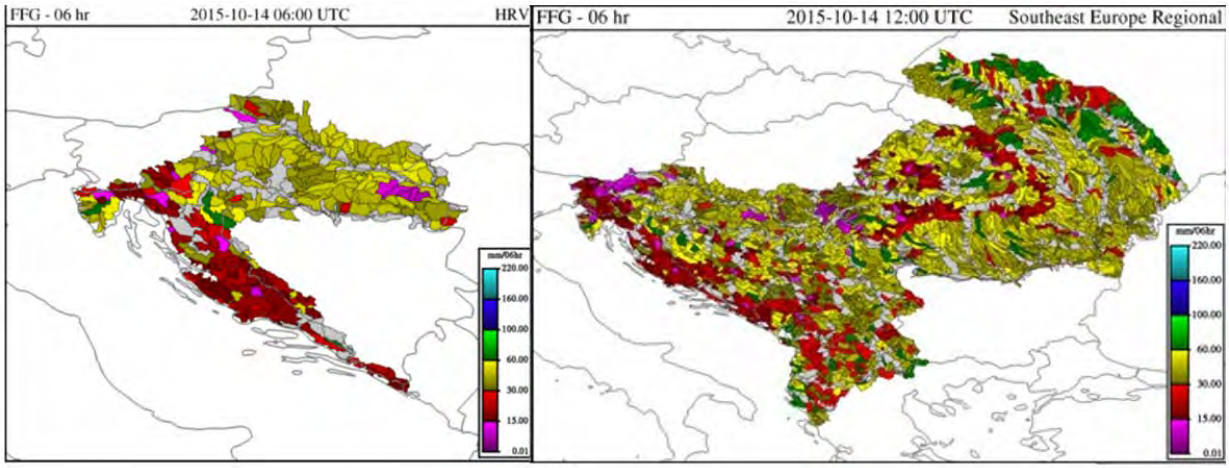

Figure 121. Flash Flood Guidance (FFG) on 14 October 2015 at 06 UTC (Croatia) and 12 UTC (South East Europe)

FFG values at 18 UTC remained very low for the same areas (figure 120.) If the accumulated rainfall amount for the 1, 3, and 6-hour duration were higher than these FFG values, the probability of the occurrences of flash floods was quite high, depending on the access amount of rainfall that determined the degree of flash floods threats.

24.1. Flash Flood in West part of SEE Region, October 2015

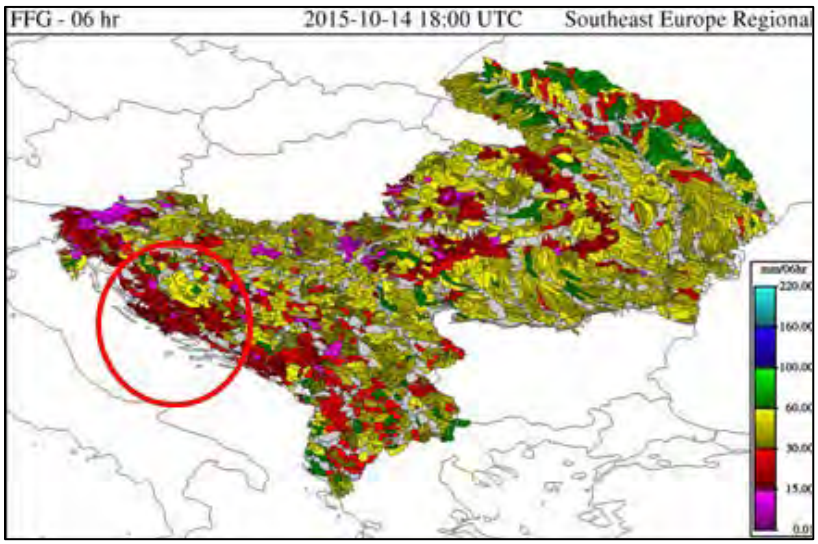

Figure 122. Flash Flood Guidance (FFG) on 14 October 2015 at 18 UTC for South East Europe

On Figure 121, 24-hour ALADIN QPF at 06 UTC and 12 UTC were presented, indicating maximum values of more than 120 mm, while 6-hour FMAP at 06 UTC and 12 UTC had maximum precipitation accumulation of 90 mm.

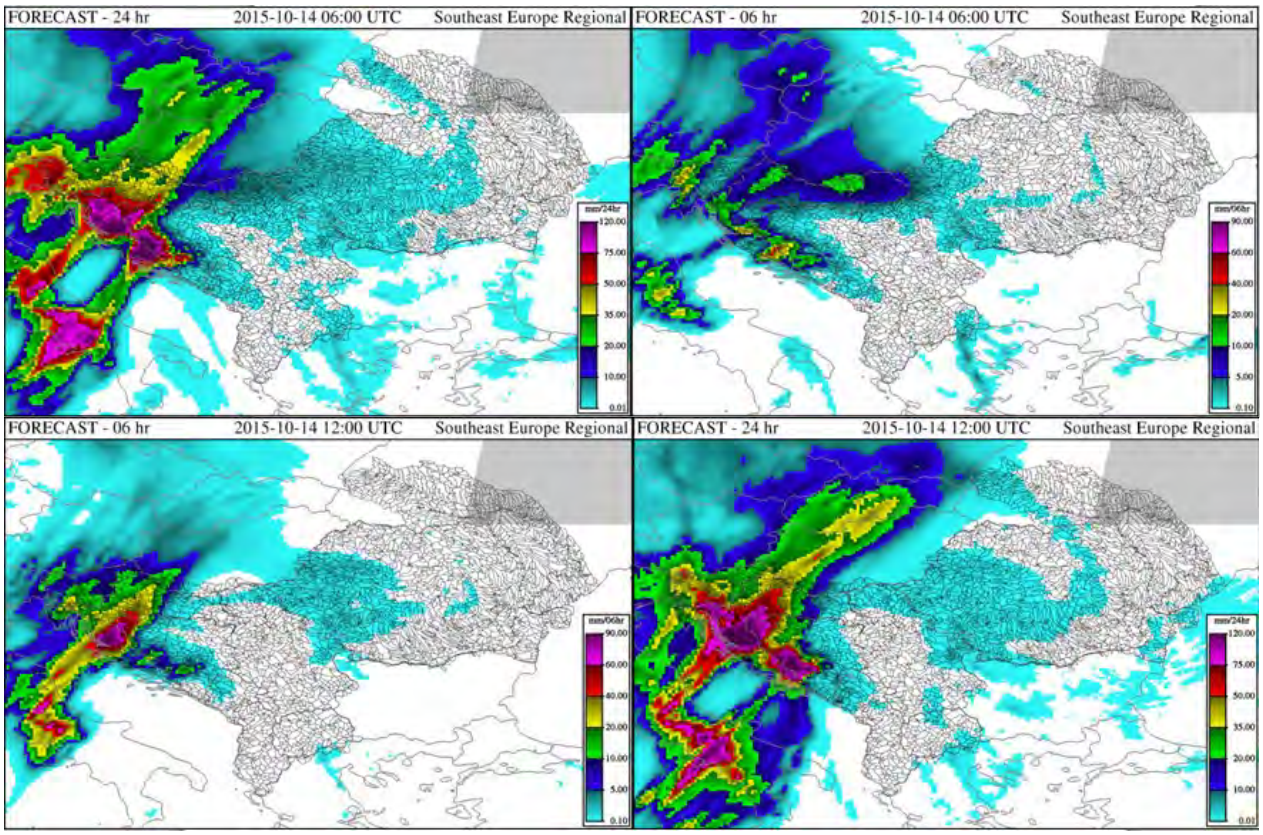

Figure 123. 6-hr and 24-hr ALADIN QPF on 14 October 2015 at 06 UTC and 12 UTC

24.1. Flash Flood in West part of SEE Region, October 2015

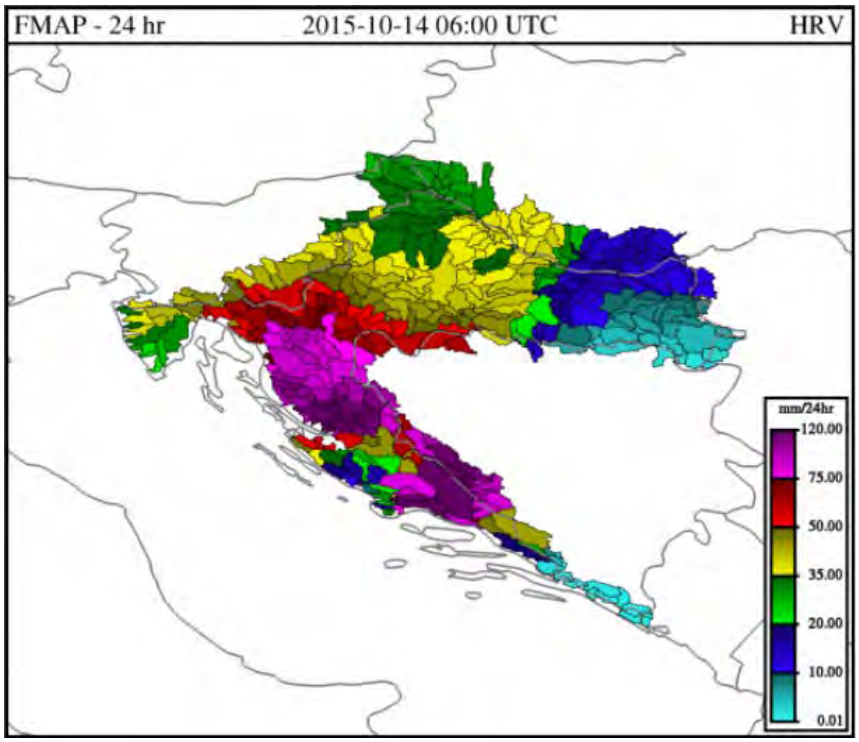

Figure 124. Forecasted Mean Areal Precipitation (FMAP) on 14 October 2015 at 06 UTC, Croatia

The 6-hour Forecasted Flash Flood Threat (FFFT) at 12 UTC and 18 UTC with high FFFT values existed over mountainous Croatia and Bosnia and Herzegovina, and coastal Croatia.

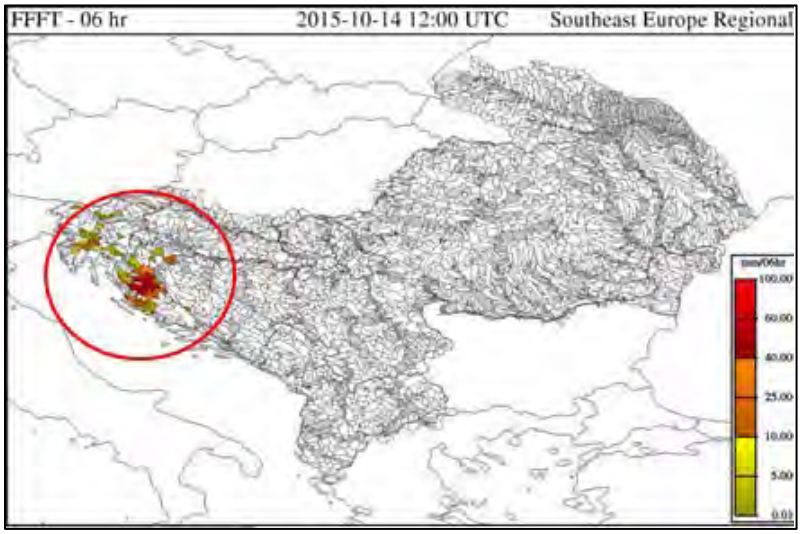

Figure 125. 6-hr Forecasted Flash Flood Threat (FFFT) on 14 October at 12 UTC, South East Europe region

24.1. Flash Flood in West part of SEE Region, October 2015

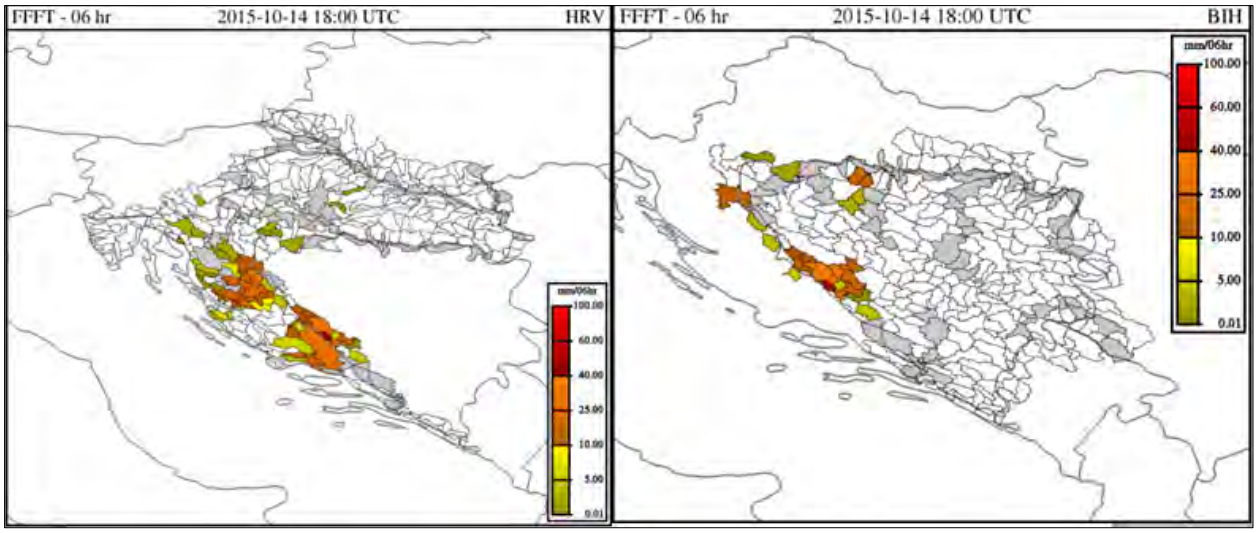

Figure 126. 6-hr Forecasted Flash Flood Threat (FFFT) on 14 October at 18 UTC for Croatia (left) and Bosnia and Herzegovina (right)

In both countries, flash flood bulletins were prepared to issue warnings for these sub-basins, where flash flood actually happened.

The Croatian Meteorological and Hydrological Service issued several flash flood warnings to the National Protection and Rescue Directorate (NPRD) and via Meteoalarm to the public and media during the event. Post-event assessment indicated a 90% probability of detection and a 10% probability of a false alarm. The affected area was Dinaric karst, and Croatian media and NPRD all reported flash flood events. In addition, during this event, approximately 100 landslides occurred, infrastructure was flooded, and roads and vents were damaged, but fortunately there were not any human losses.

Because time is the most critical factor, collaboration and involvement is necessary for an effective “end-to-end” flash flood forecasting and warning system. The SEEFFG system proved valuable for disseminating warnings in Croatia, and highlighted a great opportunity enhancing collaboration with response agencies in disaster risk reduction and raising community awareness (Mutic and Jurlina, 2016; Mutic et al., 2016).

24.1. Flash Flood in West part of SEE Region, October 2015

Figure 127. Flash floods along the coastal Croatia on 14 October 2015

In Bosnia and Herzegovina, several flash flood events occurred, but also with timely and accurate flash flood warnings.

Figure 128. Prijedor (left) and Čitluk (right), Bosnia and Herzegovina

This case study indicates accurate forecasts and warnings during this event. However, both countries need more effective action strategies. For affected countries, the SEEFFG system was very valuable supplementary tool for forecasting flash floods events.

24.2. Flash Flood and Flood Event in the SEE Region, May 2014

In mid-May 2014, Croatia, Bosnia and Herzegovina and Serbia faced severe flooding, in some places the worst in 120 years. Floods killed approximately 80 people and affected the lives of nearly three million others. The disaster followed torrential rainfall that triggered flash floods and led to large-scale flooding in major rivers. The water caused 3000 landslides in the area, but also exposed or moved many landmines left from 1990s war. The flood not only shifted mines, but also displaced warning signs. According to the U.N., 70% of flood-affected areas in Bosnia and Herzegovina may contain landmines and unexploded ordnance, and 800 km^2 of suspected contaminated areas are flooded[1]. The situation urged the Croatian Government to declare the event a catastrophe, the first since Croatia's independence. In the region, a state of emergency was declared in 18 towns and cities, including Belgrade in Serbia. The Serbian Prime Minister declared this the greatest flooding disaster ever. The floods and flash floods caused an economic loss to the region estimated at 3.3 billion euros.

Figure 129. Red sign that reads Mine Field sits on the shore of the Sava River in the village near the Bosnian town of Orasje, May 2014

The whole month of April 2014 can be characterized as a period of unstable weather, with intense cyclonic activity. Several cyclonic systems passed over the SEE region during April, bringing significant temperature drops, frequent rainfall and even snow in some mountain areas. Continuous precipitation was recorded at some meteorological stations (i.e. Banja Luka, Doboj in Bosnia and Herzegovina) from 14 April till 4 May. Recorded rainfalls were significantly above long-term average on almost all measuring stations in the middle and lower part of Sava River basin in the SEE region. Unusual and extreme heavy rainfall caused the saturation of soils in large areas of the region.

In terms of climatology, April 2014 was wet or very wet across the area of east Croatia. The analysis of precipitation amounts for April 2014, given in percentages (%) of climatological average (1961 -1990), shows that monthly precipitation quantities at most of the analysed stations were above average. In Slavonski Brod, a station next to the Sava River, close to the area affected by floods, total monthly precipitation in April 2014 reached 200% of the climatological average and rainy weather continued at the beginning of May.

[1] "Bosnia and Herzegovina – Flood Disaster Situation Report." United Nations. Last modified 27 May 2014. http://reliefweb.int/sites/reliefweb.int/files/resources/Situation%20Report%2027May2014%20.pdf

24.2. Flash Flood and Flood Event in the SEE Region, May 2014

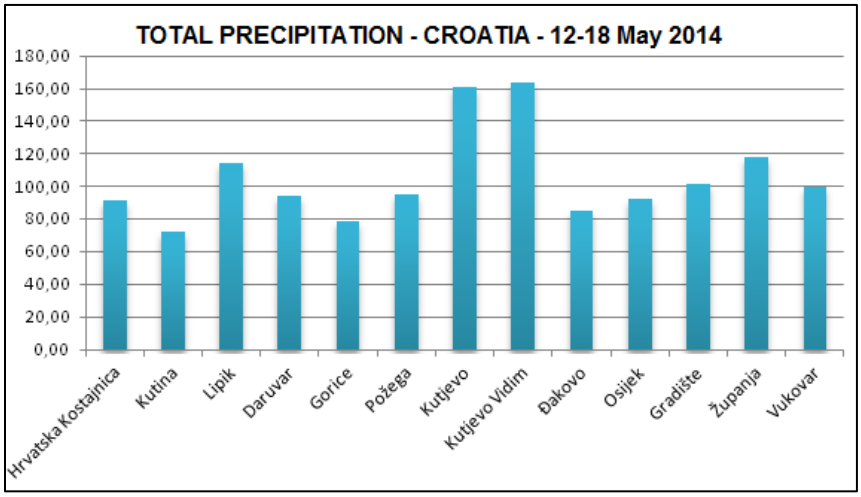

Figure 130. Total precipitation at some meteorological stations in Croatia

In Serbia, the greatest historical monthly precipitation totals were recorded during May since the beginning of the measurements on the main meteorological stations were exceeded on nine stations in the period between 1 and 31 May 2014. Precipitation totals for May on met stations Loznica, Valjevo and Belgrade are three to four time higher than the average values for May.

MMS	Precipitation amount 1 - 31.5. 2014	The highest precipitation amount for May before 2014	Year of highest amount for May
NOVI SAD	201.9	175.7	1987
LOZNICA	314.6	218.6	1938
S.MITROVICA	189.0	184.9	1939
VALJEVO	317.6	213.2	1957
BELGRADE	278.5	191.7	1900
KRAGUJEVAC	227.0	169.7	1970
S.PALANKA	238.2	164.7	1929
ZLATIBOR	195.6	172.5	1956
POZEGA	199.4	177.9	1980

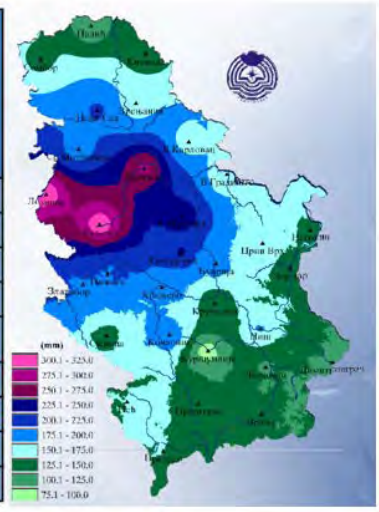

Figure 131. Total precipitation at some meteorological stations in Serbia

In Bosnia and Herzegovina, 24-hour precipitation accumulation of some stations are presented in Figure 143. In case of Tuzla station, the normal rainfall for the May is 90 mm whereas over the period 1 to 16 May, 303 mm was registered (normally, yearly rainfall is 911 mm). In many cases, meteorological stations in affected municipalities registered more than half of their annual average over a period of a few days in May 2014.

24.2. Flash Flood and Flood Event in the SEE Region, May 2014

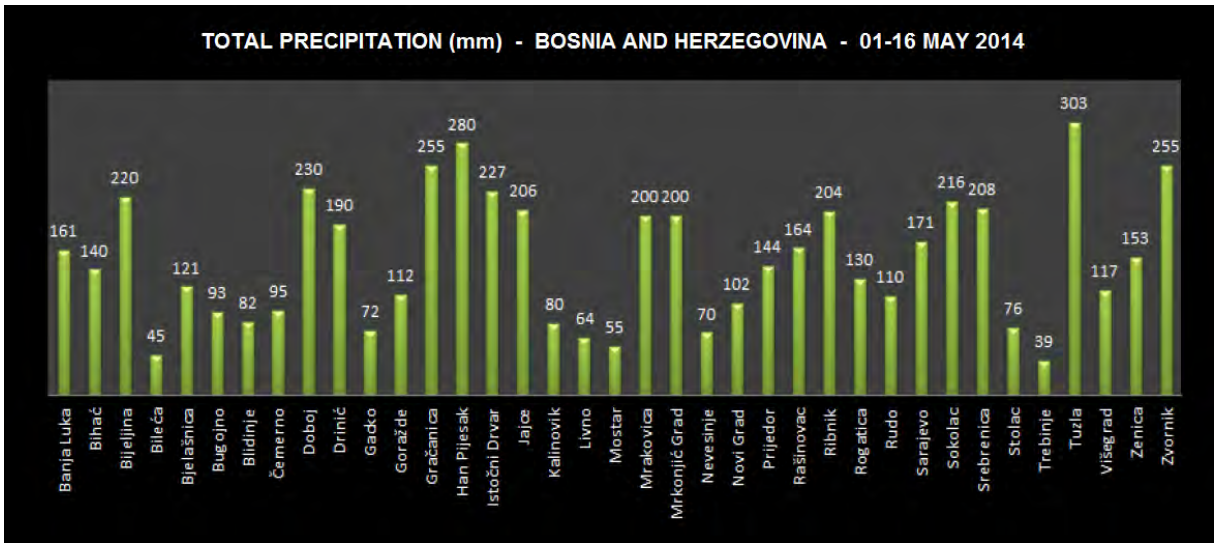

Figure 132. Total precipitation at some meteorological stations in Bosnia and Herzegovina

Synoptic Analysis

In the period between 12 and 15 May, an upper level pressure trough was moving from the west of Europe towards the southeast. The axis of the trough, and with it also the surface front, moved across central Europe and the Balkans during the night of 11 May and the morning of 12 May. After the front passed over central Europe and the Balkan Peninsula, cold air from northern Europe arrived (Figure 133) (Strelec Mahovic et al., 2015).

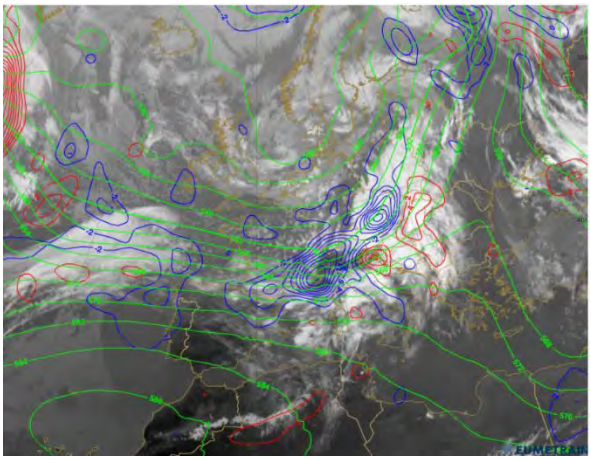

Figure 133. AT 500 (green) and temperature advection at 700hPa (red:warm, blue:cold) from the ECMWF model, overlaid on Meteosat IR 10.8 μm image on 11 May 2014, 18 00 UTC

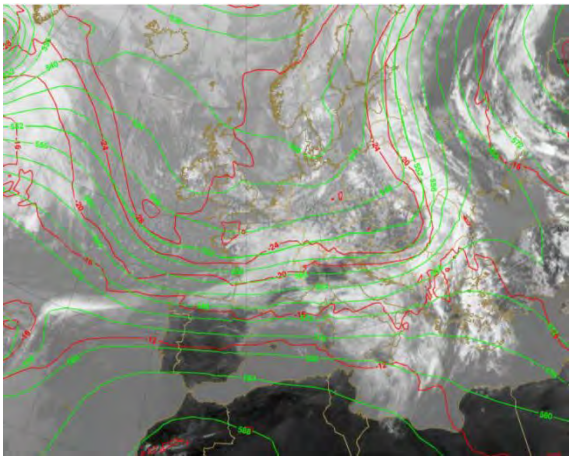

Figure 134. AT (green) and temperature at 500 hPa (ECMWF), overlaid on Meteosat 10 IR 10.8 μm image on 12 May 2014, 12 00 UTC

24.2. Flash Flood and Flood Event in the SEE Region, May 2014

At the same time, in the strong westerly flow from the Atlantic, large quantities of humid air arrived (visible in Figure 134 west of Alps). By the end of the 12 May, a new upper-level trough formed west of the Bay of Biscay (Figure 135). It moved very quickly eastwards with very strong westerly winds and was getting deeper during the 13 May (Figure 136).

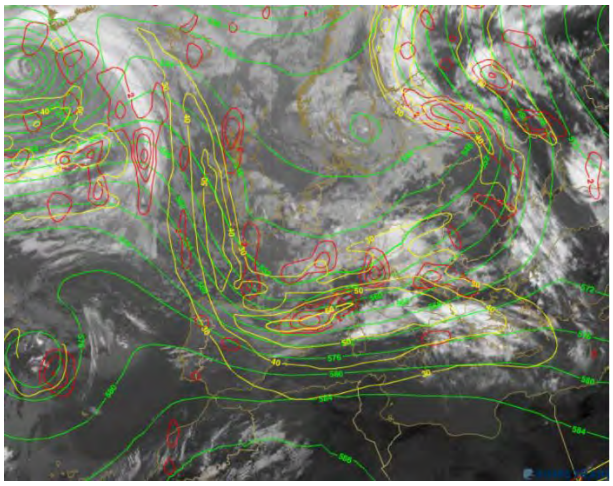

Figure 135. AT 500 (green), isotachs at 300hPa and cyclonic vorticity advection at 300 hPa (red) from ECMWF model, overlaid on Meteosat IR 10.8 μm image on 13 May 2014, 06 00 UTC

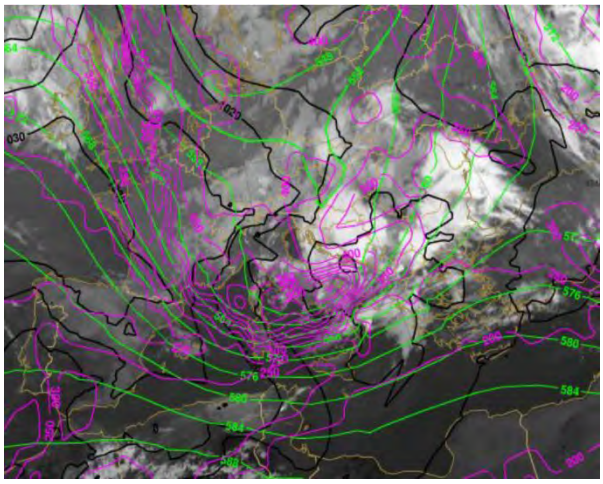

Figure 136. AT 500 (green), Mean Sea Level Pressure (MSLP) (black) and height of IPV=1.5 PVU, from ECMWF, overlaid on Meteosat IR 10.8 μm image on 14 May 2014, 00 00 UTC

The process intensified when the upper-level through crossed over the Alps. A surface low formed over northern Italy and the Adriatic on 13 May, moving slowly towards NE. On 14 May, the trough closed into a deep cyclonic vortex, stretching almost through the entire troposphere, with the cyclone axis being placed almost vertically, so that the centre of the upper-level low in the highest layers was almost exactly above the centre of the surface cyclone. This contributed to the intensity and stationary of the entire system.

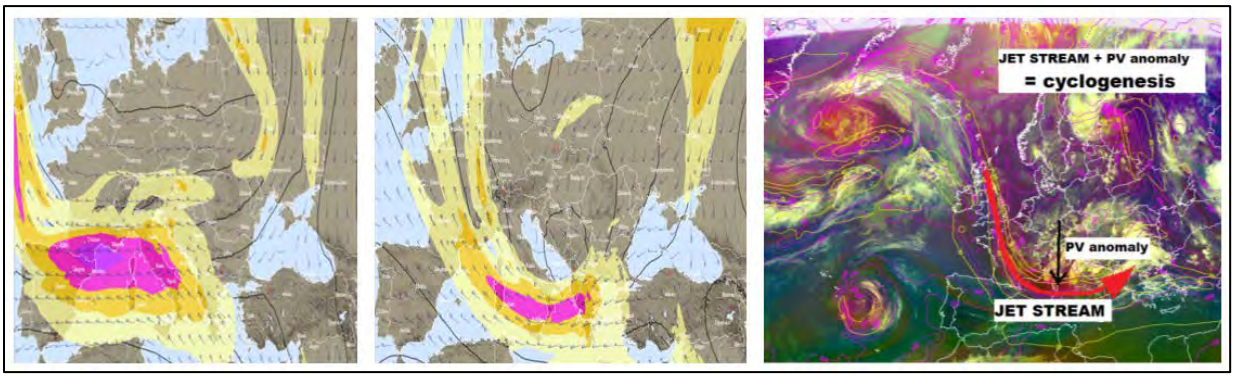

Figure 137. Jet stream analysis

Jet is associated with movement of the fronts and air masses. Curvature is important for weather developments. On 13 May at 00+3h and +24h, jet stream analysis showed that jet cores with values of 120 knots and 100 knots were located over the northern Mediterranean region and southern Italy, bringing cold polar air to the mid-latitudes.

24.2. Flash Flood and Flood Event in the SEE Region, May 2014

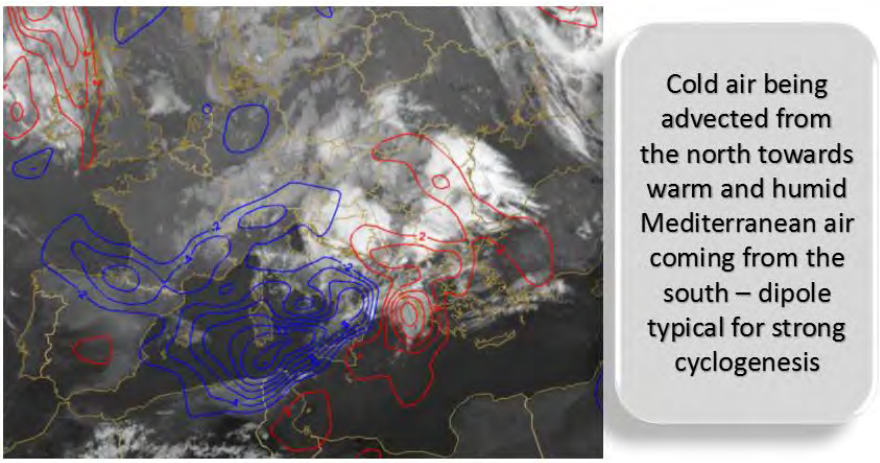

Figure 138. TA 700 from ECMWF model, overlaid on Meteosat IR 10.8 µm image on 14 May 2014, 00 UTC

Within the next 24 hours, a deep low intensified, stretching vertically throughout the whole troposphere. The axis of the low was vertical, with no tilt, making the cyclone stationary and very intense with the maximum on 15 and 16 May, while its centre shifted only slightly towards northeast (Figure 138) (Strelec Mahovic, 2014).

The system received humidity from the Mediterranean and the Black Sea, while pulling cold air from the north. On 15 May, the centre of the surface low was over the central parts of the Balkan Peninsula. The cyclone remained quasi-stationary for more than 3 days over SE Europe. Precipitation was additionally enhanced by the orography of the mountains in Bosnia with many thunderstorms embedded in the cyclonic cloud system. Because of the northeasterly flow in the upper levels, the cyclonic vortex slowly returned westwards, the cyclonic vortex slowly returned westwards, while at the same time the anticyclone ridge (Figure 139) grew stronger.

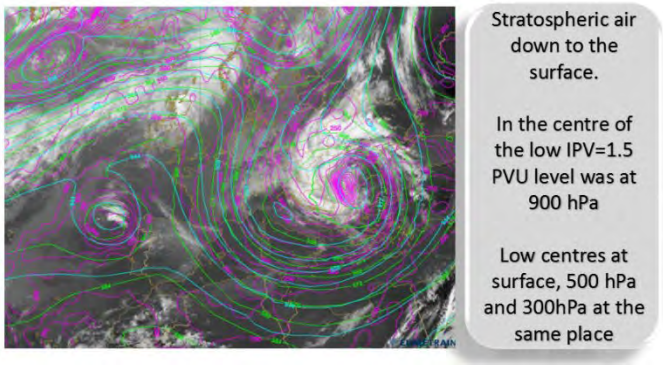

Figure 139. AT 500, AT 300 and height of IPV=1.5 PVU from ECMWF model, overlaid on Meteosat IR 10.8 µm image on 15 May 2014, 06 UTC

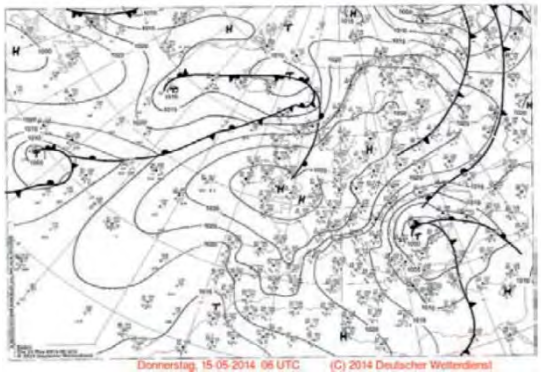

Figure 140. Surface air pressure analysis and position of frontal system on 15 May 2014 at 06 UT, *Source: DWD*

Under such circumstances, large differences in the surface air pressure developed, causing, besides heavy rainfall, very strong winds in many regions, with gusts locally reaching hurricane force. Very intense development in the cyclone led to formation of a thick cloud layer and heavy precipitation in the area of northern Croatia, but also extremely heavy and long-lasting

precipitation in most of Bosnia and Herzegovina and Serbia. This was mostly rain, but snow also formed on mountains higher than 1200 m. In some places in Bosnia and Herzegovina, the snowfall was quite heavy. During the 16 May, the centre of the upper level cyclone was located over Serbia, weakening towards the end of the day.

Precipitation forecasts

The May 2014 event was forecasted well and on time by European and local meteorological agencies. Although precipitation rates were underestimated in certain areas, numerical models provided very good indicators for warnings on extreme weather conditions. The damage and casualties caused by floods would have been even worse had the event not been forecasted on time. The ECMWF model forecasted the precipitation quantity in the period from the 14 to 17 May (Figure 141.) well, with dark violet areas denoting amounts 50-100 mm.

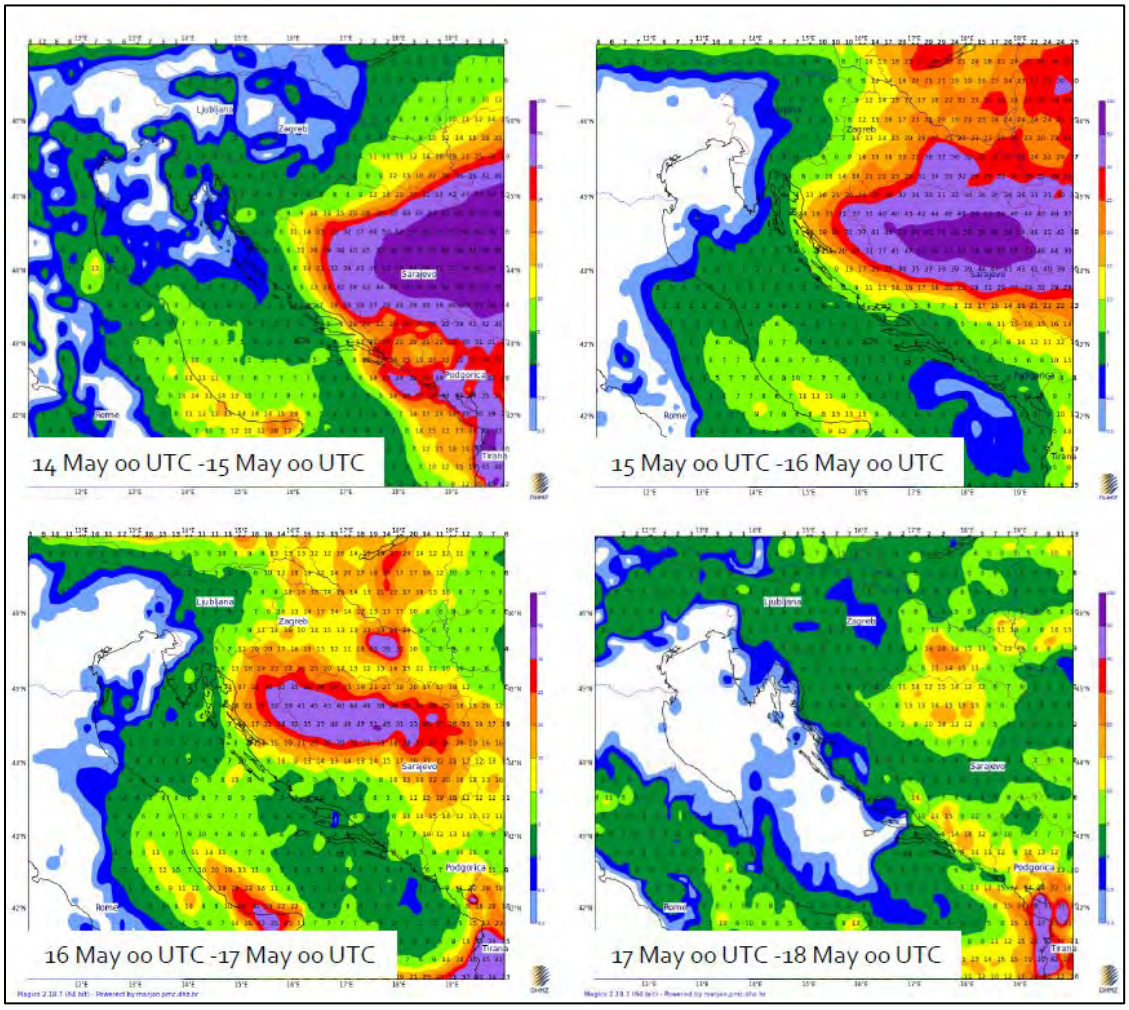

Figure 141. ECMWF 24 hours total precipitation,
Source: Meteorological and Hydrological Service of Croatia

24.2. Flash Flood and Flood Event in the SEE Region, May 2014

For the Croatian region, the ALADIN LAM run locally at DHMZ forecast 24-hour precipitation of between 20 and 100 mm for the area of east Croatia over the period from 06 00 UTC on 15 until 06 00 UTC on 16 May, which was very close to the actual precipitation measured.

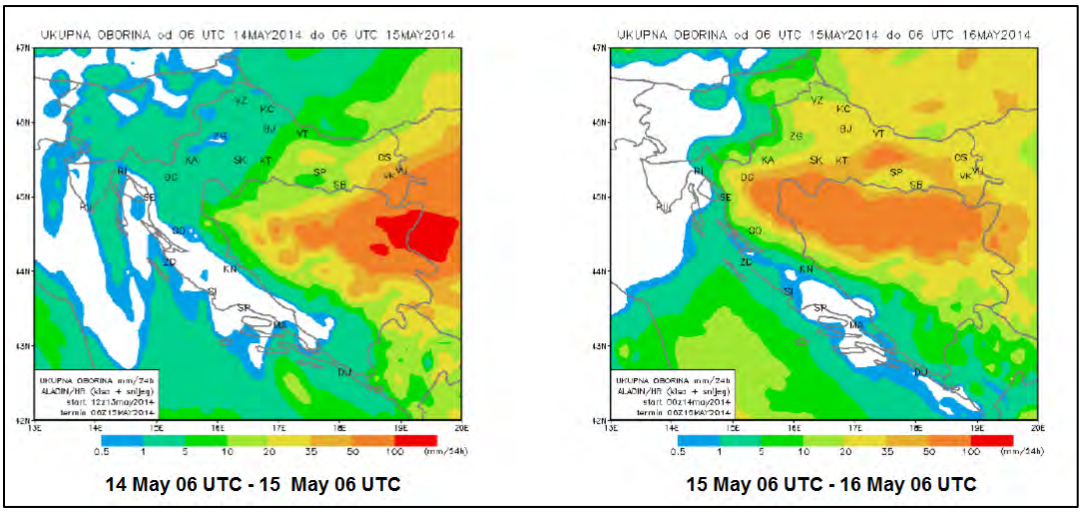

Figure 142. ALADIN 24 hours total precipitation,
Source: Meteorological and Hydrological Service of Croatia

Regional NMM39 WRF-model with horizontal resolution of 4 km and 1.33 km and input data from the ECMWF numerical model for a period of 72 hours in advance gave the value of the nearest to the observed precipitation. In Figure 143, areas with a total precipitation of 100 to 250 mm are shown. In some locations in western Serbia and areas with rainfall of over 250 mm (grey) are visible.

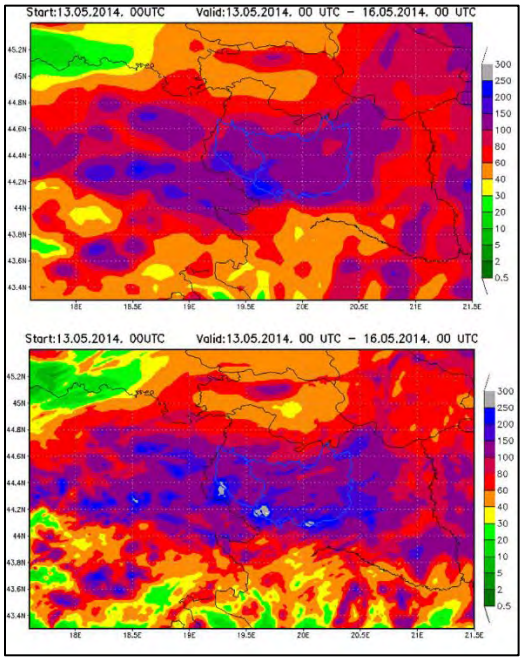

Figure 143. WRF-NMM 72 hours total precipitation,
Source: Republic Hydrometeorological Service of Serbia

24.2. Flash Flood and Flood Event in the SEE Region, May 2014

Satellite and Radar images

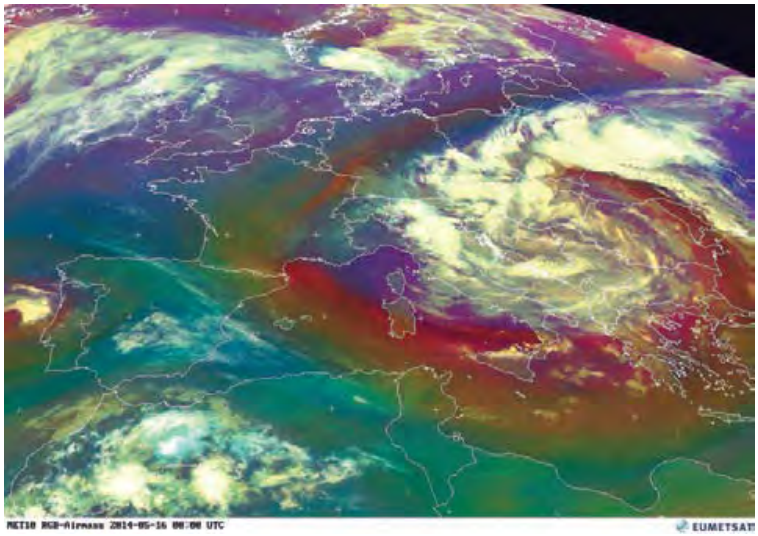

Figure 144. Meteosat 10 Airmass RGB image on 16 May 2014, 00 UTC, showing a deep low system over SE Europe

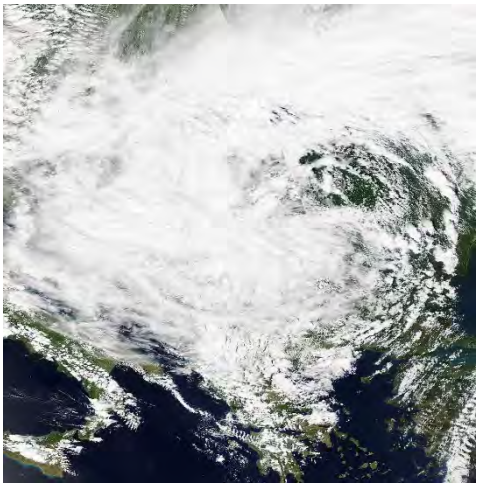

Figure 145. Cyclone over Europe (NASA)

Soil moisture analysis

The figures below show the analysis of soil moisture level 1,2,3 with 3 days apart, starting from 10 May. Here, one can see that the ground was very wet already before the rainfall.

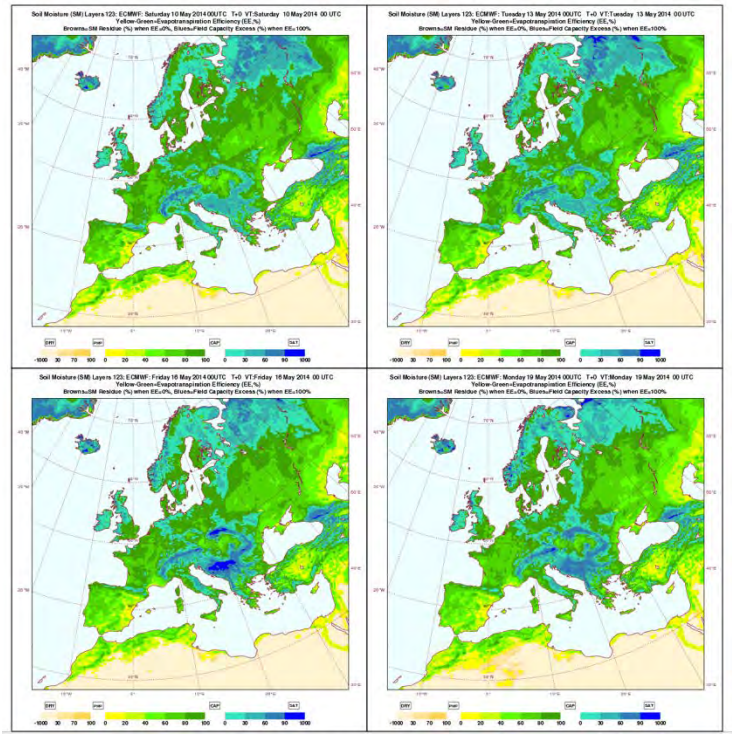

Figure 146. Soil moisture layers, 10, 13, 16 and 19 May 2014 at 00 UTC,
Source: ECMWF

24.2. Flash Flood and Flood Event in the SEE Region, May 2014

Warnings

The NMHSs of all three countries affected by the May 2014 flood are part of the Network of European Meteorological Services (EUMETNET), and hence members of Meteoalarm, a platform aimed at providing comprehensive weather warnings across Europe. The Croatian Meteorological and Hydrological Service issued a yellow alert for precipitation for the affected area in Meteoalarm on 14 May, and orange for precipitation and red for wind on 15 May. The first flood warning for the Sava River was issued on 15 May and official flood defence stages were soon proclaimed. Following Meteoalarm, the red alarm for precipitation in Bosnia and Herzegovina was issued on 12 May. The Republic Hydrometeorological Service of Serbia also issued red alerts for heavy rainfall on 13, 14 and 15 May. This information and alert on significant increase on rivers in western, southwestern and central Serbia were also dispatched in the Operational Hydrometeorological Bulletin. In all three countries, reports to the authorities were made, as well as public releases on web, radio and TV.

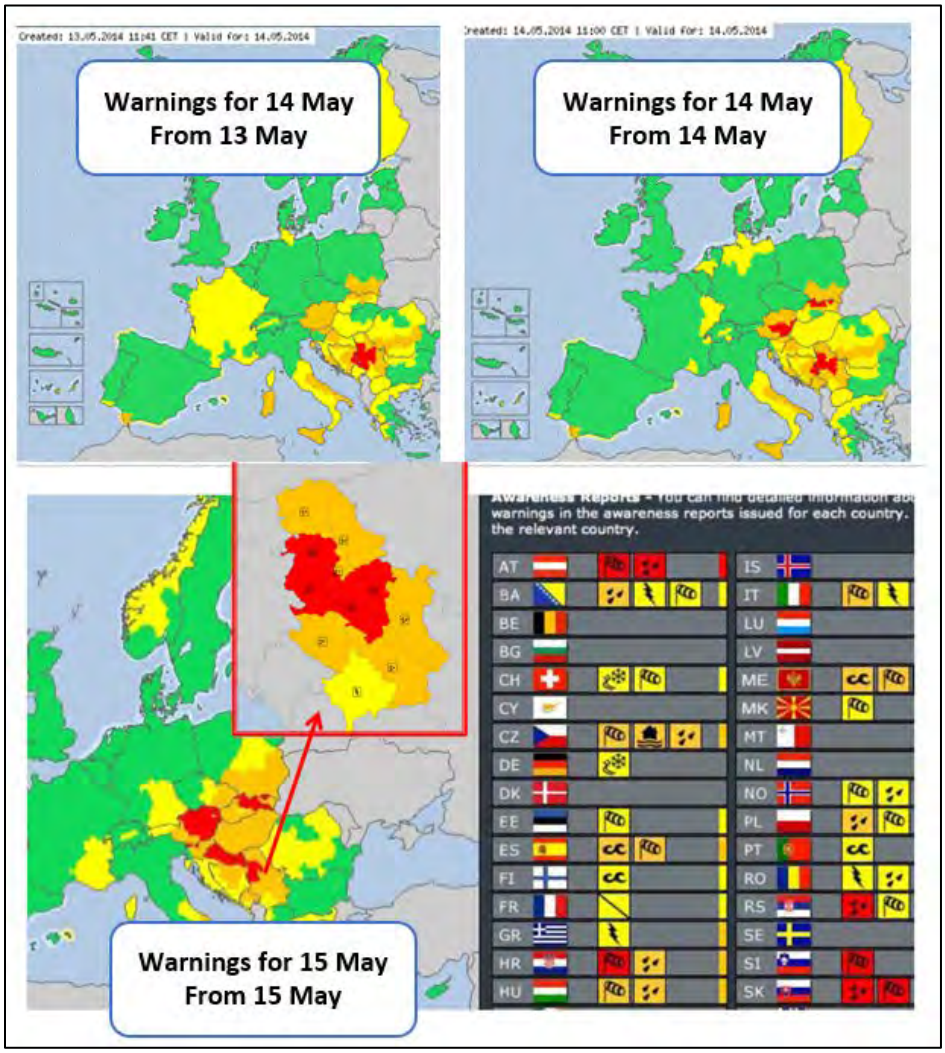

Figure 147. Warning on Meteoalarm for 14 and 15 May

24.2. Flash Flood and Flood Event in the SEE Region, May 2014

SEEFFGS Products

Having analysed the weather situation in the region, it is imperative to analyse SEEFFGS products very carefully. First, the SEEFFGS diagnostic products should be investigated to find out hydrological responses of catchments. The 6-hour microwave adjusted GHE (MWGHE), a global satellite precipitation retrievals by NESDIS, showed that on 13 May 2014 at 00 UTC, there was very little rainfall in the SEE region (Figure 148). On the other hand, on 14 May 2014 at 00 UTC, maximum precipitation accumulation was up to 10-20 mm (Figure 149) and then at 18 UTC, it was 20-40 mm (Figure 150).

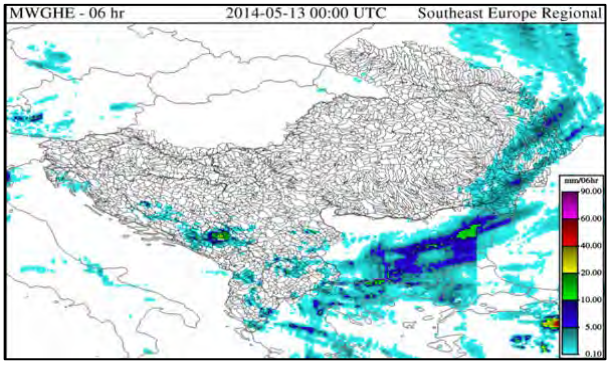

Figure 148. 6-hr MWGHE, May 13 2014 at 00 UTC

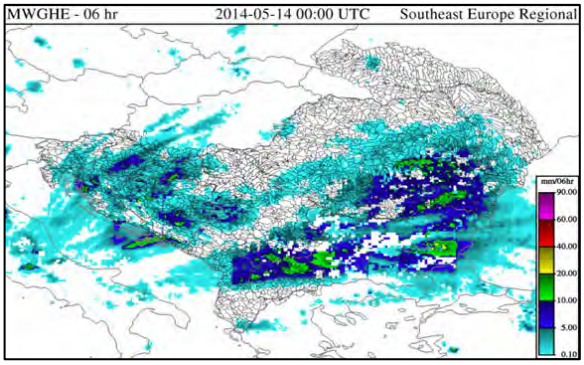

Figure 149. 6-hr MWGHE, 14 May 2014 at 00 UTC

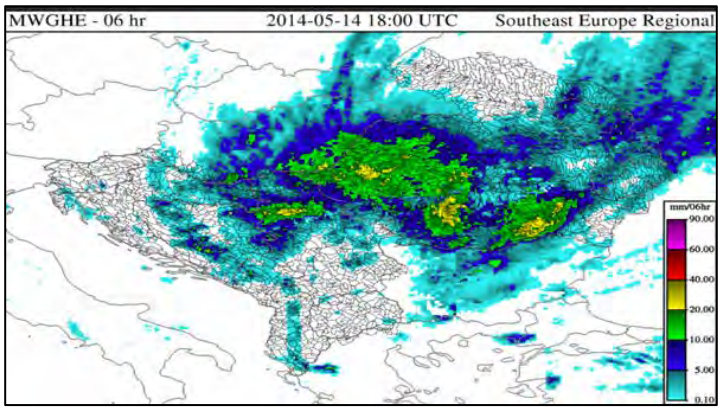

Figure 150. 6-hr MWGHE, 14 May 2014 at 18 UTC

On 15 May 2014 00 UTC (Figure 151), precipitation area extended to the northeast with maximum values of 40-60 mm over Bosnia and Herzegovina and Serbia (red). At 06 UTC (Figure 152), 6-hour precipitation intensity reduced over last six hours but rainfall continued in a patchy way over Bosnia and Herzegovina and Serbia with maximum values of 40-60 mm.

24.2. Flash Flood and Flood Event in the SEE Region, May 2014

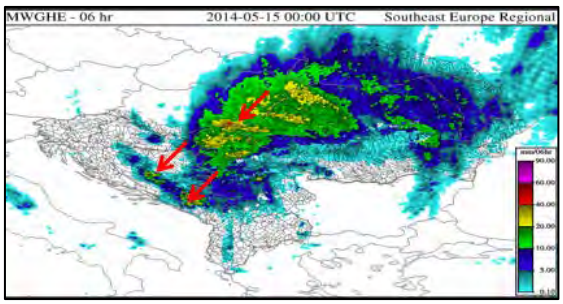

Figure 151. 6-hr MWGHE, 14 May 2014, 18 UTC

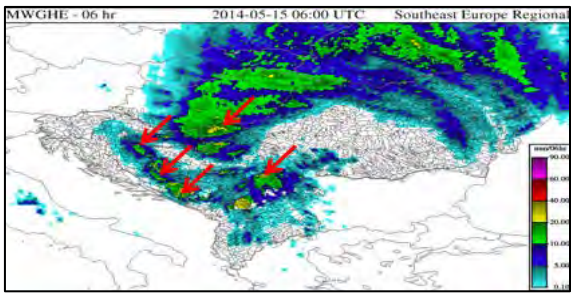

Figure 152. 6-hr MWGHE, 15 May 2014, 06 UTC

It is evident that MWGHE precipitation temporal and spatial distributions were in line with the ECMWF QPF forecasts with varying precipitation intensity.

On 13 May 2014 at 06 UTC (Figure 153), 5-10 mm MAP (dark blue) existed over Croatia and 0-5 mm (light blue) MAP existed over Bosnia and Herzegovina and Albania and southeast Romania. On the other hand, on 13 May 2014 at 18 UTC (Figure 154), the precipitation pattern moved to the east and spatial distribution was extended over central SEE having maximum values of 10-20 mm over Serbia (green).

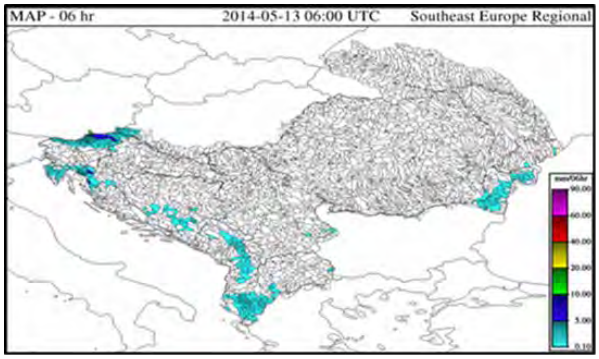

Figure 153. 6-hr MAP, 13 May 2014 at 06 UTC

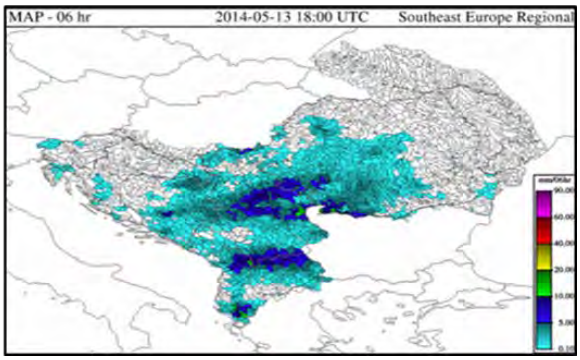

Figure 154. 6-hr MAP, 13 May 2014 at 18 UTC

On 15 May 2014 at 00 UTC (Figure 155), 20-40 mm MAP (yellow) existed over Bosnia and Herzegovina, Serbia and western Romania, while at 12 UTC (Figure 156), MAP remained over the same region except western Romania and had the same magnitude. On the other hand, on 16 May 2015 at 00 UTC (Figure 157), MAP diminished in Serbia and Romania and moved to Croatia and to the Adriatic coast of Bosnia and Herzegovina with maximum MAP values of 40-60 mm (red).

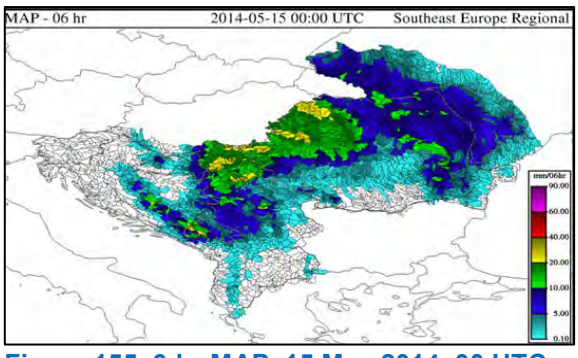

Figure 155. 6-hr MAP, 15 May 2014, 00 UTC

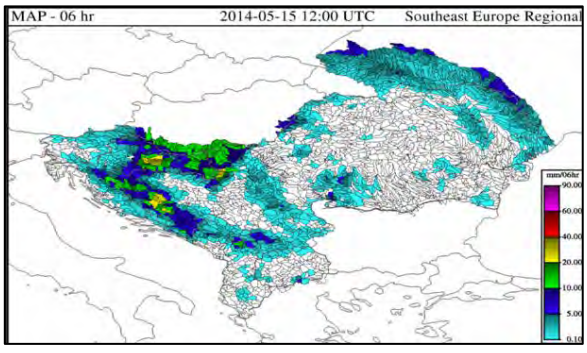

Figure 156. 6-hr MAP, 15 May 2014, 12 UTC

24.2. Flash Flood and Flood Event in the SEE Region, May 2014

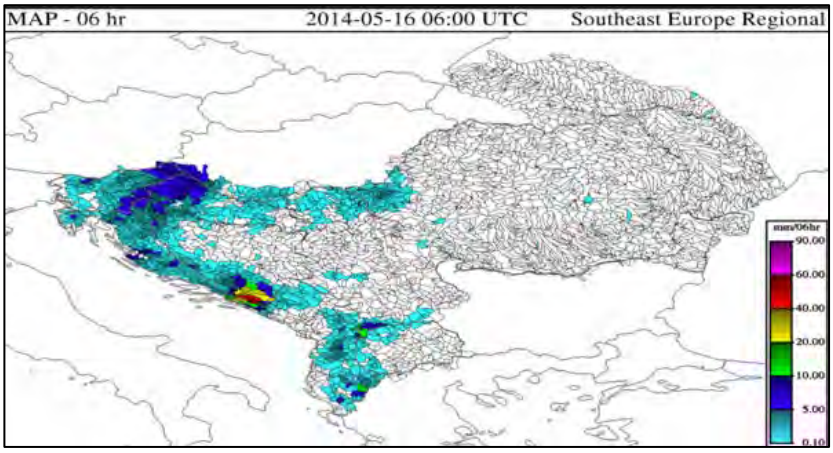

Figure 157. 6-hr MAP, 16 May 2014 at 06 UTC

The Average Soil Moisture (ASM) product shows soil water saturation fraction for the upper zone of soil for each of the sub-basins. Saturation of the upper zone is very important for flash floods because if rainfall continues, most of the rainfall will become surface runoff. Spatial and temporal distribution of 6-hour ASM are shown on 13 May 2014 at 00 UTC (Figure 158), 14 May 2014 at 12 UTC (Figure 159) and 18 UTC (Figure 160), indicating that upper soil was completely saturated (dark blue; value 1.00) rapidly in Bosnia and Herzegovina, Albania, Serbia and western Romania.

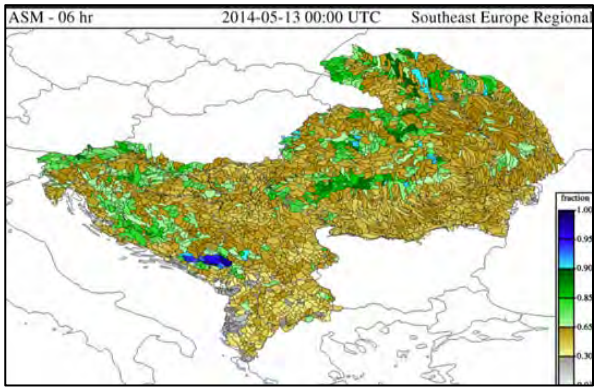

Figure 158. 6-hr ASM, 13 May 2014, 00 UTC

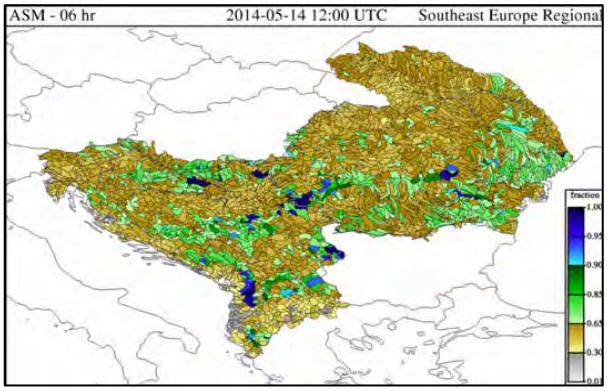

Figure 159. 6-hr ASM, 14 May 2014, 12 UTC

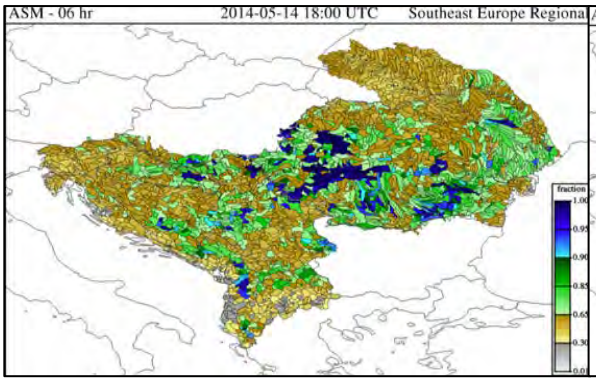

Figure 160. 6-hr ASM, 14 May 2014, 18 UTC

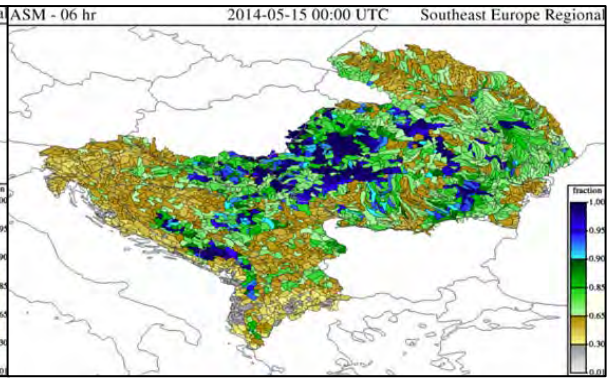

Figure 161. 6-hr ASM, 15 May 2014, 00 UTC

24.2. Flash Flood and Flood Event in the SEE Region, May 2014

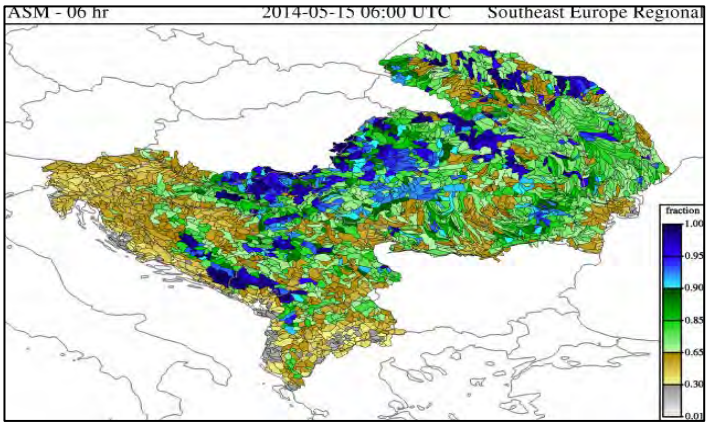

Figure 162. 6-hr ASM, 15 May 2014 at 06 UTC

There were also a lot of sub-basins with a soil moisture fraction higher than 0.65 (light green) so they must have been monitored for possible flash flood occurrences. On 15 May 2014 at 00 UTC (Figure 161) and 06 UTC (Figure 162), ASM images showed more sub-basin upper soil saturated associated with continued rainfall in the region. In particular, sub-basins in Bosnia and Herzegovina and northern Serbia remained saturated for up to 24 hours, making the region very vulnerable to flood and flash flood occurrences. Figure 163 shows the extent of the affected area in the SEE region, as well as a correlation between soil saturation showed at ASM products.

Figure 163. Flooded area in SEE, May 2014

The next step is to investigate how FFG values changed over time and what their magnitudes were. FFG is one of the key products for determining flash flood potential when using FFG system. The FFG is defined as the amount of actual rainfall of a given duration (e.g. 1, 3 or 6 hours) that is just enough to cause bankfull flow at the outlet of the catchment. Figure 164 shows that FFG values significantly decreased from 13 May 2014 at 00 UTC to 15 May 2014 at 00 UTC from predominantly 30-60 mm (yellow) to 0-15 mm (purple). Recall that the lower the FFG, the higher the possibility of flash flood occurrence. On 15 May 2014 at 12 UTC, 6-hour FFG values reached their minimums (Figure 165), with 0-15 mm (pink) over the northern Serbia, Bosnia and Herzegovina, eastern Croatia, and western Romania. Some sub-basins had a value of 0.01 mm/06 hr, which means that rain is not even necessary for the possibility of flash flooding –a

high possibility of occurring at that time. On the other hand, 6-hour FFG values increased significantly on 16 May 2014 at 12 UTC (Figure 166), indicating that precipitation reduced considerably in the SEE region.

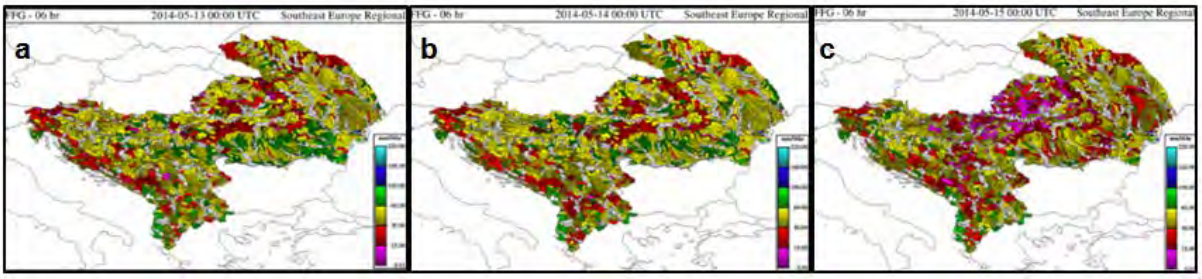

Figure 164. 6-hr FFG on a) 13 May 2014 at 00 UTC, b) 14 May 2014 at 00 UTC, c) 15 May 2014 at 00 UTC

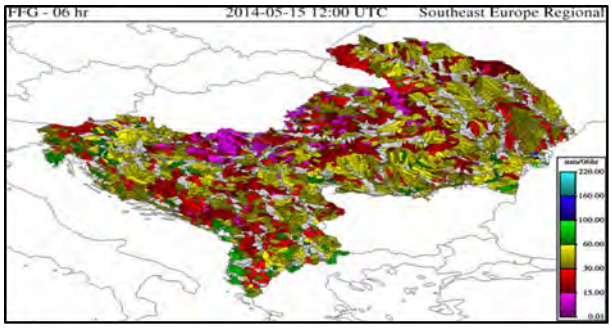

Figure 165. 6-hr FFG on 15 May 2014, 12 UTC

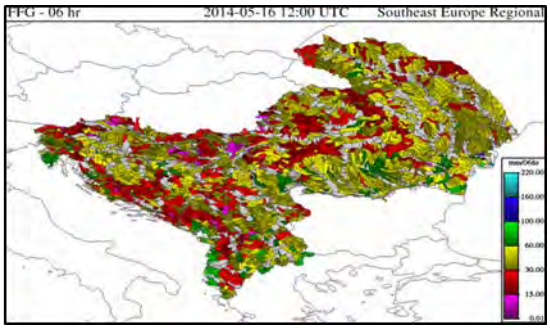

Figure 166. 6-hr FFG on 16 May 2014, 12 UTC

So, forecasters must monitor and compare spatial and temporal distribution and variation of FFG with mean areal distribution of rainfall e.g., merge MAP or forecast MAP which are generated from different QPF models like ALADIN or WRF to find out whether or not an excess amount of rainfall will occur in a particular sub-basin. Forecast Mean Areal Precipitation (FMAP) generated from ALADIN mesoscale precipitation forecasts are shown on Figure 167 to find out QPF spatial and temporal variations from 13 to 15May 2014.

On 13 May at 00 UTC (first column), FMAP shows that 24-hr precipitation accumulation was 35-50 mm (yellow). However, on 14 May at 00 UTC (second column), 6-hr FMAP values were 20-40 mm (yellow) and 24-hr FMAP values were 75-120 mm (purple) over Bosnia and Herzegovina, east Croatia and Serbia.

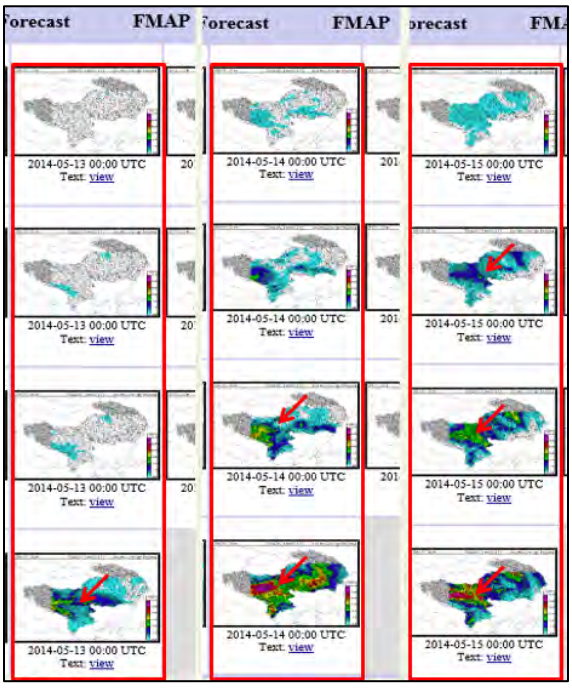

Figure 167. FMAP on 13, 14 and 15 May 2014

24.2. Flash Flood and Flood Event in the SEE Region, May 2014

A forecaster must be very careful when observing such situations. QPF shows that 24-precipitation accumulation will be 120 mm in the SEE region. Therefore, it may take the responsibility to issue flash flood watches. On 15 May 2014 at 00 UTC (third column), 6-hour FMAP values were 20-40 mm (yellow) and 24-hr FMAP values were again 75-120 mm (purple) over Bosnia and Herzegovina, east part of Croatia and Serbia. Thus, taking into account FFG, ASM, merged MAP, FMAP products and the forecaster's local forecasting experiences, one may conclude that occurrences of the flash floods in the region was very likely.

The FFG system has three flash flood threat products, which indicate the likelihood of occurrences of flash floods in a particular sub-basin for a given duration. The higher the FFT, the higher the possibility of flash floods occurring. If we recall the definitions of IFFT, PFFT and FFFT, that may guide us on how to interpret these products. IIFFT is the difference between the corresponding merged MAP and FFG for the same duration, indicating that a flash flood is happening now or is about to happen very soon. It should be noted that IFFT is estimated and updated using current precipitation. Thus, it represents a "nowcast" weather situation. PFFT assumes that precipitation at the time of FFG estimates will persist in the next 1, 3 or 6 hours. This product has two deficiencies: first, it assumes that the precipitation amount will not change in the next 1, 3, or 6 hours; second, it does not take into account the possibility of storm movement in different directions. Therefore, a forecaster should be very careful with this product, recognizing that threats are generated after the storm passes. FFFT is generated using mesoscale model precipitation forecast (ALADIN), and may have advantages over PFFT that may take precipitation as "stationary" rather than propagating in time and space. However, forecasters must ask themselves how well the concerned mesoscale precipitation forecast is reliable in a particular region.

Figure 168 shows 6-hour PFFT on 14 May at 06, 12 UTC and PFFT on 15 April at 00 UTC. PFFT existed over Bosnia and Herzegovina, and the eastern parts of Croatia and Serbia, and spatially extended and strengthened in the next 24 hours with maximum values of 0-10 mm (yellow) and 10-40 mm (orange).

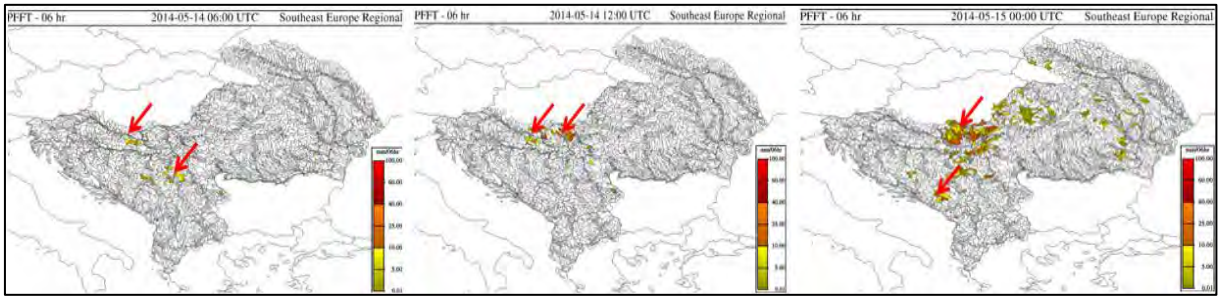

Figure 168. 6-hr Persistence Flash Flood Threat (PFFT) at 06 and 12 UTC on 14 May 2014 and at 00 UTC on 15 May 2015

FFFT provides the forecaster with an idea of which regions are forecasted to be of concern for flash flooding based on difference of the FMAP forecast of mean areal rainfall and the corresponding FFG. Figure 169 shows that 6-hour FFFT existed over Bosnia and Herzegovina on 14 May 2014 at 00 UTC, with maximum values of 10-40 mm (orange). On 14 May 2014 at 06 UTC, it propagated toward the east with the same maximum values and then moved to east Croatia and Serbia on 15 May 2014 at 00 UTC, expending its spatial coverage. Forecasters at

this time should already issue a warning and pay close attention for the catchments that are orange where flash flood occurrence is most likely.

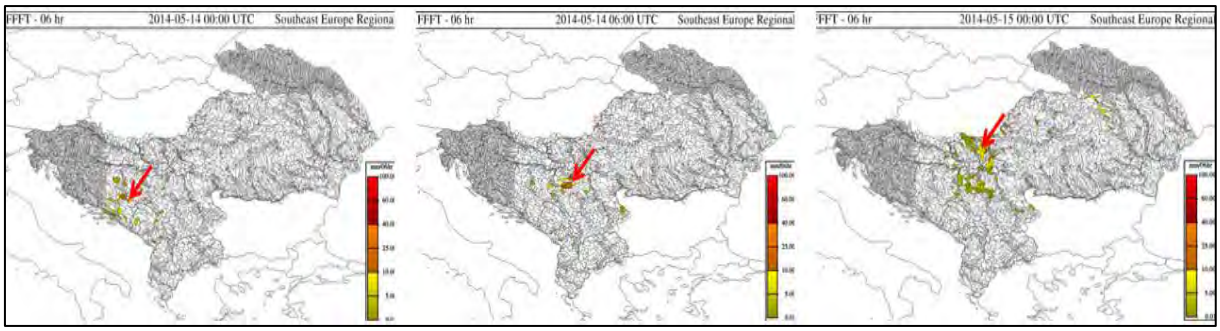

Figure 169. 6-hour Forecasted Flash Flood Threat (FFFT) at 00 and 06 UTC on 14 May 2014 and at 00 UTC on 15 May 2015

When PFFT and FFFT are compared, their location and intensities are different, for the reasons indicated earlier.

Hydrological conditions

The hydrologic response of the Sava tributaries to large precipitation amounts in mid-May was very quick due to high soil saturation. The torrential streams were the first to react, with very powerful, flash floods characterized by high flow velocities, enormous amounts of sediment and numerous landslides activated.

Figure 170. Torrential flow of Sava tributaries, May 2014

Figure 171. The consequences of flash floods in SEE region, May 2014

Huge flood waves occurred on the large right tributaries of Sava River in Bosnia and Herzegovina and Serbia; extremely high water levels of Vrbas River were recorded in the city of Banja Luka, where water level rose by 7 meters between 14 and 16 May. The return period of the flood peak on the Bosna River was 500 years, and 100 years on torrential tributaries. On

24.2. Flash Flood and Flood Event in the SEE Region, May 2014

hydrological station Doboj, water level rose by more than 6 meters in less than 24 hours, with disastrous consequences.

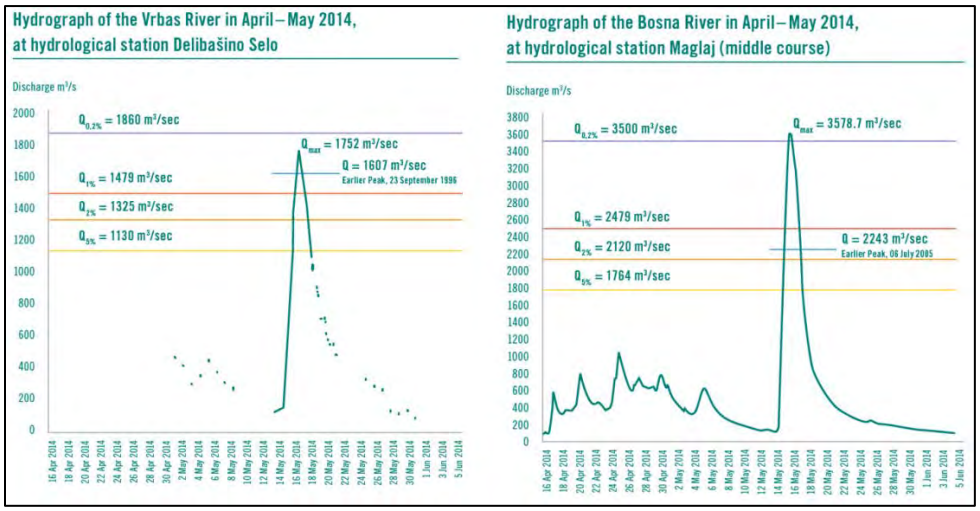

Figure 172. Hydrographs of the Vrbas and Bosna Rivers in Bosnia and Herzegovina, May 2014, ***Source: (ICPDR and ISRBC, 2015)***

The high levels of the Sava River (the largest tributary of the Danube River) prevented Bosna River from freely discharging and created a backwater effect that flooded Samac City. Drina River received flood water on its lower course from tributaries and flooded the municipality of Bijeljina. At the location of hydrological station Beli Brod, Kolubara River in Serbia rose for 7 meters in 24 hours, with simultaneous flood waves on all tributaries. The result was disastrous flooding, including in an open-pit mine, which received about 190 million m^3 of water and mud, and in Obrenovac City. Serbian main electrical power production facility – TPP Nikola Tesla was also endangered.

24.2. Flash Flood and Flood Event in the SEE Region, May 2014

Figure 173. Flood in Obrenovac, Serbia

The May 2014 Sava flood wave had surprisingly quick rise for such a large river. Measured water levels, flow velocities and flow rates were higher than ever before. Croatian Meteorological and Hydrological Service measured 6,008 m^3/s at Slavonski Samac at water level of 889 cm. Based on hydrological analysis, it was concluded that this discharge had a return period of 1,000 years. Embankments along Sava River at these sections have or do not have a design freeboard of 1.2 meters above the theoretical 100-year flood level, and could not sustain the May 2014 flood which was a 1000-year event. An almost simultaneous breaching of embankments at two locations in Croatia occurred on 17 May, flooding the nearby lowland area, including parts of Serbia. Closing the embankment breach was not possible for a few days, due to inaccessibility and high flow force. In Bosnia and Herzegovina, on 17 and 18 May, embankments on the right bank of Sava River also breached at several locations, causing flooding of large areas.

Figure 174. Embankment breach in Croatia

Figure 175. Embankments breaches in BiH

24.2. Flash Flood and Flood Event in the SEE Region, May 2014

The Moderate Resolution Imaging Spectroradiometer (MODIS) on NASA's Aqua satellite captured an image[2] of flooding in Croatia, Serbia, and Bosnia and Herzegovina on 19 May 2014. The second image shows the same area one year ago during a more typical spring.

Figure 176. MODIS image of the flooded areas 19 May 2014

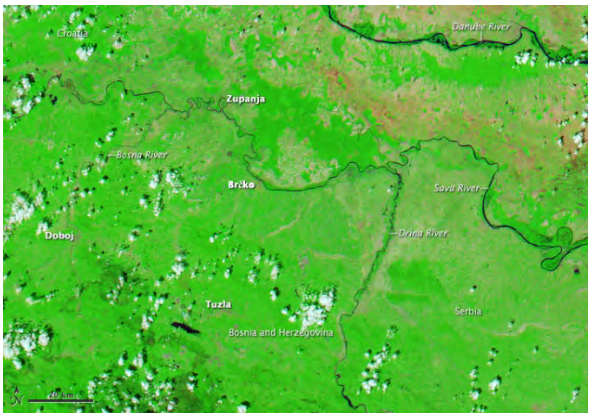

Figure 177. MODIS image of the same area on one year before the catastrophic flood event

The rough estimate based on satellite images revealed that the flooded areas were 266.3 km^2 in Bosnia and Herzegovina, 53.5 km^2 in Croatia, and 22.4 km^2 in Serbia (ICPDR and ISRBC, 2015).

The catastrophic floods, flash floods, and landslides that raged through parts of Bosnia and Herzegovina, Serbia and Croatia were unprecedented in the historical record of the region. Because floods know no borders, regional cooperation is vital in flood control, warnings and response. The effects could have been even worse, but the event was well forecasted by European and local meteorological agencies. During this event, the SEEFFG System was under development but it showed quite accurate forecasts. Now, after many experiences in operational work with the SEEFFG System, it proved to be valuable for disseminating warnings in this region, and highlighted a great opportunity for enhancing collaboration with response agencies in disaster risk reduction and raising community awareness.

Because time is the most critical factor, collaboration and involvement is necessary for an effective "end-to-end" flash flood and flood forecasting early warning system.

[2] The images are both composed with false colour, using a combination of infrared and visible light (MODIS bands 7-2-1). Flood water appears black; vegetation is bright green; and bare ground is brown. This band combination makes it easier to spot changes in river dimensions.

24.3. Flash Flood in Skopje, August 2016

On 6 August 2016, The former Yugoslav Republic of Macedonia faced one of the worst hydrometeorological disasters in their history. Several rainstorms hit the western and northwestern parts of the country, leaving at least 21 people dead and dozens injured or missing. National weather service reported that 93 litres per square metre fell in two hours on Skopje, which is equivalent to the average for the entire month of August. The water level in some affected areas reached a height of 1.5 metres, which was combed by Macedonia's police and army for survivors and other victims. Meteorologists reported that more than 800 lightning strikes were recorded in the first two hours of the storm, which went on for about five hours in total. Three villages to the northeast of the city were cut off due to landslides.

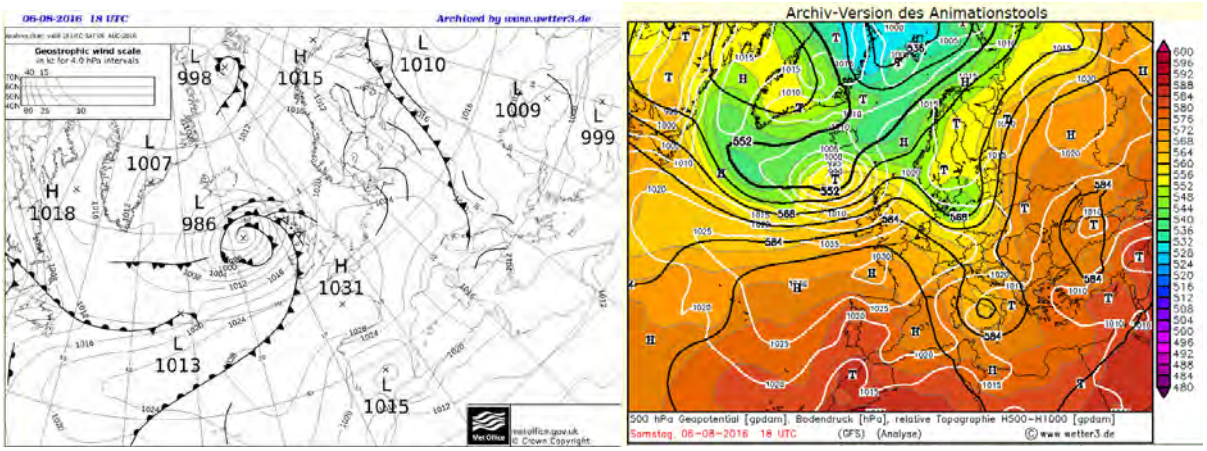

Figure 178. a) Synoptic Analysis over Europe on 6 August 2016 at 18UTC, and b) 500 hPa Geopotential on 6 August 2016 at 18UTC

Figure 178 a) shows the synoptic situation over Europe on 6 August 2016. The Genova cyclone formed over southern Italy together with a front situated over eastern Europe. On Figure 178 b) 500 hPa Geopotential chart reveals that southern Balkan region, including The former Yugoslav Republic of Macedonia, was under the influence of the southern flow at the front part of the cyclone. Cape values were relatively high (Figure 179). An area of instability was located over central and southern Adriatic Sea, indicating potential threat for convection.

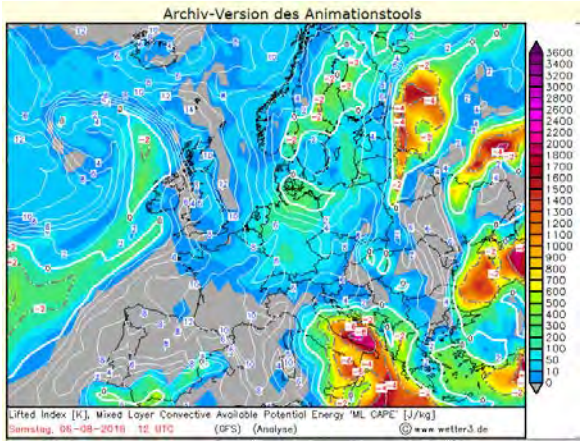

Figure 179. CAPE values over Europe on 6 August 2016 at 12 UTC

24.3. Flash Flood in Skopje, August 2016

6 August at 06 UTC

After analysing the weather situation in the region, it is imperative to analyse the SEEFFGS products very carefully. Average Soil Moisture values were fairly low throughout the country prior to the flash flood event. Forecasters should note that during the summer and when soil is dry, soil crusts can form, which can significantly reduce soil infiltration rate and subsequently water resources utilization, and increase surface runoff, especially during intense summer convective rainfall. 6-hour FFG values were 30mm/6-hr or higher over The former Yugoslav Republic of Macedonia.

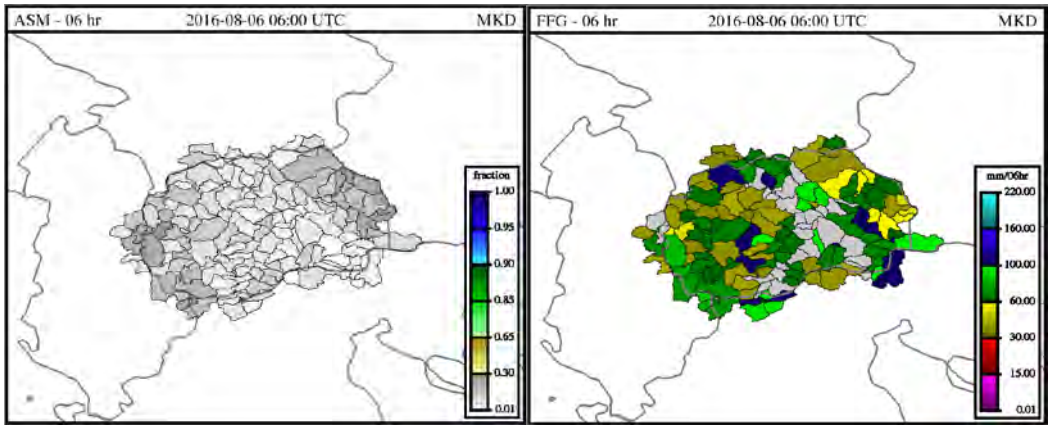

Figure 180. The former Yugoslav Republic of Macedonia; ASM and 6hr-FFG at 06 UTC

On the Figure 181, ALADIN QPF on 6 October 2016 at 06 UTC showed that system has maximum values of 120 mm/24-hr over northern Albania, northwestern The former Yugoslav Republic of Macedonia, southeastern Montenegro and Bosnia and Herzegovina.

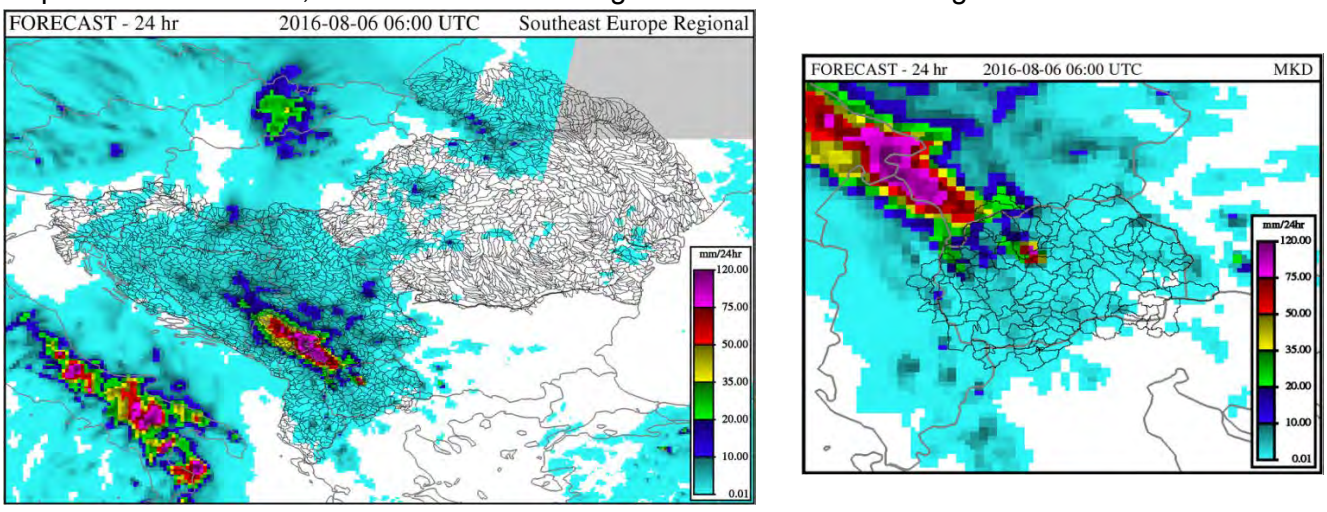

Figure 180. Forecast precipitation generated by ALADIN model; 24-hr forecast accumulation for SEEFFGS region on 6 August at 06 UTC (left), 24-hr forecast accumulation, The former Yugoslav Republic of Macedonia on 6 August at 06 UTC (right)

24.3. Flash Flood in Skopje, August 2016

As a result of above analysis, forecaster may decide to issue a flash flood “watch” for the region for the next 24 hours and analyse SEEFFG products at 12 UTC.

6 August at 12 UTC

The 6-hour MWGHE product on 6 August 2016 at 12 UTC showed that precipitation was very low over the northwestern The former Yugoslav Republic of Macedonia with values up to 5 mm (Figure 182 a). The 6-hour FFG varied over the northern Macedonia, from 30 to 100 mm/6-hour, indicating that 30-100 mm of rainfall over that area was needed to cause bankfull condition at the outlets of the catchments (Figure 182 b).

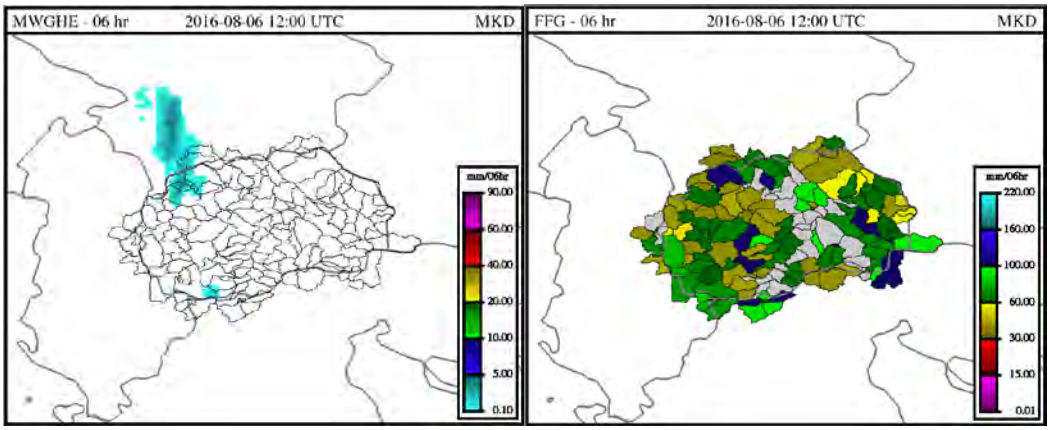

Figure 182. The former Yugoslav Republic of Macedonia; a) 6-hr MWGHE at 12 UTC, and b) 6-hr FFG at 12 UTC

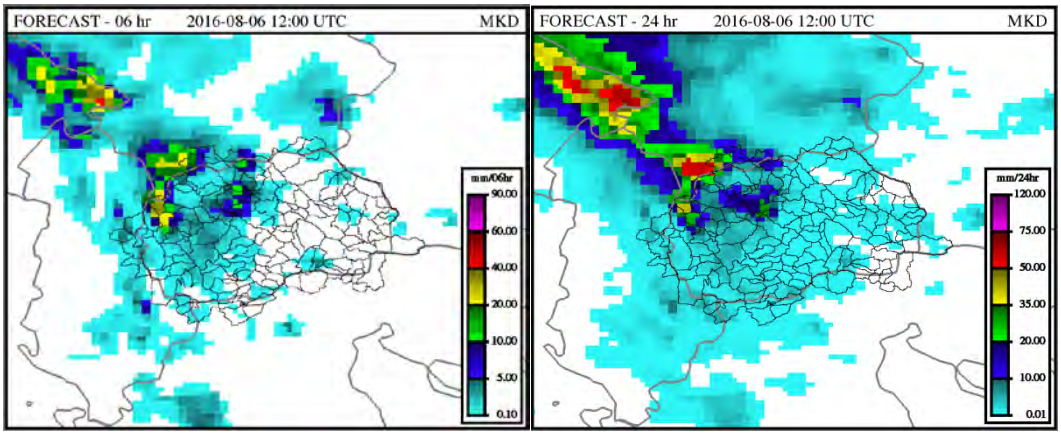

Figure 183. The former Yugoslav Republic of Macedonia; a) 6-hr ALADIN forecast at 12UTC, and b) 24-hr ALADIN forecast at 12 UTC

In Figure 183, ALADIN QPF on 6 October 2016 at 12 UTC showed that forecasted precipitation diminished, with maximum precipitation up to 40 mm/6-hr, and 75 mm/24-hr over the same areas as in the previous model run. After analysing past precipitation, it was necessary to compare the precipitation forecasts of several NWP models, paying attention to the regions where the maximum precipitation was forecasted. The signature of the image products indicated that precipitation formation was due to convective cells. Further development and propagation of the cells were to be monitored as a possible cause of flash floods.

24.3. Flash Flood in Skopje, August 2016

6 August at 18 UTC

The 6-hour MWGHE and Merged MAP products on 6 August 2016 at 18 UTC showed that Skopje region received up to 40 mm/6-hour of precipitation (Figure 184). As shown in figure 185 a) ASM values increased over the northwestern parts of the country where precipitation occurred, with soil moisture fraction up to 0.60.

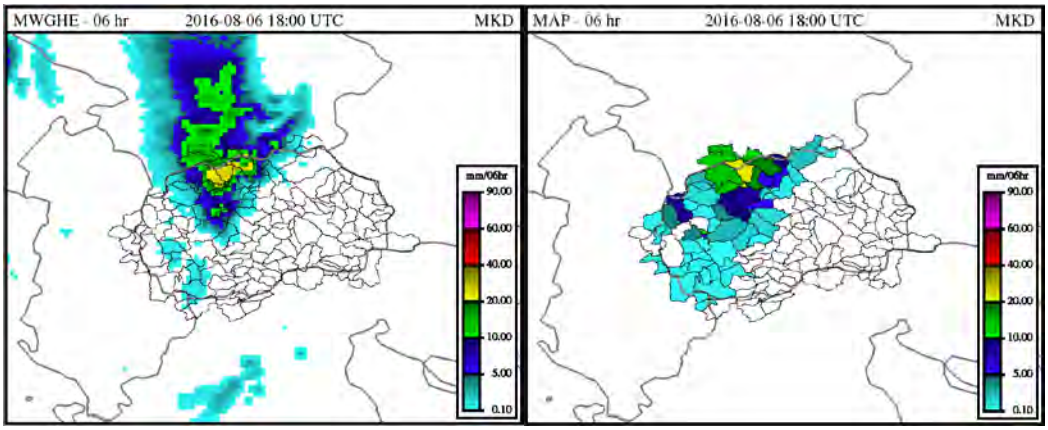

Figure 184. The former Yugoslav Republic of Macedonia; a) 6-hr MWGHE at 18UTC, and b) 6-hr MAP at 18UTC

Figures 185 b) and c) show FFG estimates at 18 UTC, indicating that FFG values decreased and varied quite a lot among the sub-basins, having 1-hour FFG values of 10 mm (red) over Skopje region, 25 mm (dark yellow), 40 mm (dark green) and 100 mm (blue); and 6-hour FFG values of 15 mm (red) over Skopje, 30 mm (dark yellow), 60 mm (green) and 100 mmm (blue). If the accumulated rainfall amount for the 1, 3, and 6-hour duration were higher than these FFG values, probability of the occurrences of flash floods was quite high, depending on the access amount of rainfall that determined the degree of flash flood threats.

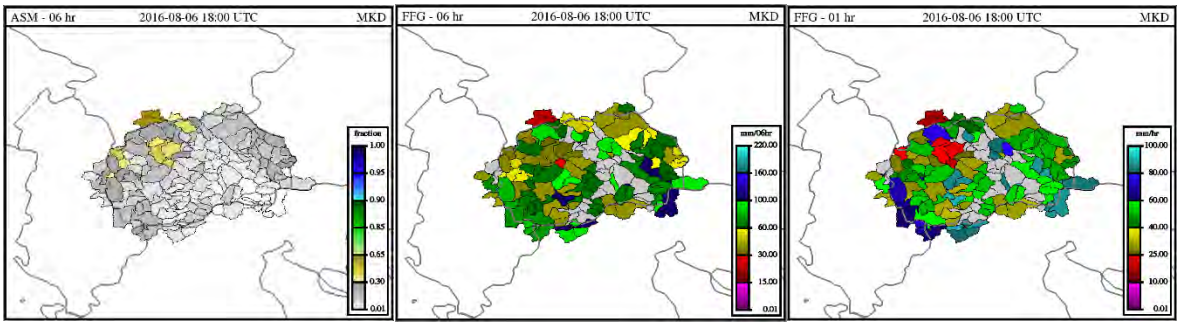

Figure 185. The former Yugoslav Republic of Macedonia; a) 6-hr ASM at 18 UTC, b) 6-hr FFG at 18 UTC, and c) 1-hr FFG at 18 UTC

24.3. Flash Flood in Skopje, August 2016

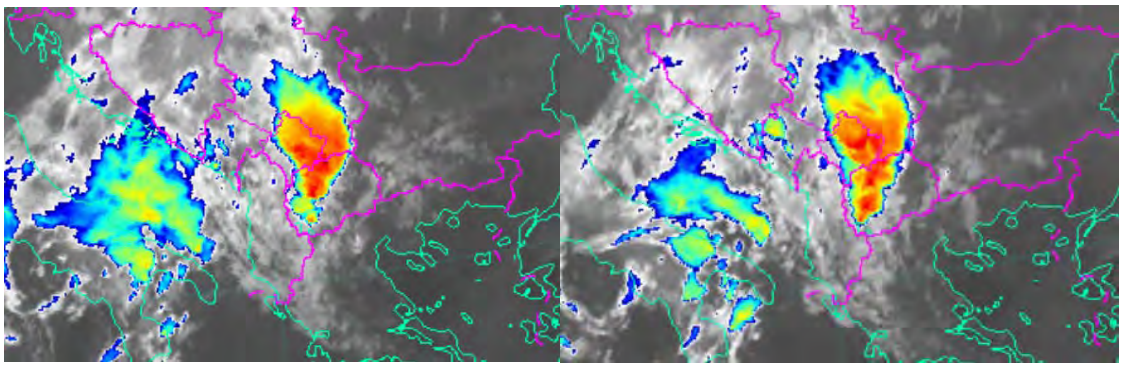

Figure 186. a) RGB satellite image at 18 UTC, and b) RGB satellite image at 19 UTC

Figure 186 shows satellite imagery of mesoscale convective complex (MCC) over The former Yugoslav Republic of Macedonia at 18 UTC (a) and 19 UTC (b) which produced locally heavy rainfall and caused severe flash flooding.

7 August at 00 UTC

The FFGS post event analysis showed that MAP on 7 August 2016 at 00 UTC had a maximum precipitation accumulation of 60 mm/6-hour over one sub-catchment on the north. The ASM product showed that upper soil in the Skopje region and over northern parts of the country were completely saturated. For the same areas, FFG values were very low, ranging from 0.01 to 30 mm/6-hour. 6-hour Persistent Flash Flood Threat (PFFT) with values up to 40 mm, and Imminent Flash Flood Threat (IFFT) existed over the northern The former Yugoslav Republic of Macedonia, indicating high probability of accordance of flash flood in the region. 6-hr ALADIN QPF had maximum values of 60 mm, located northwestern of The Former Yugoslav Republic of Macedonia.

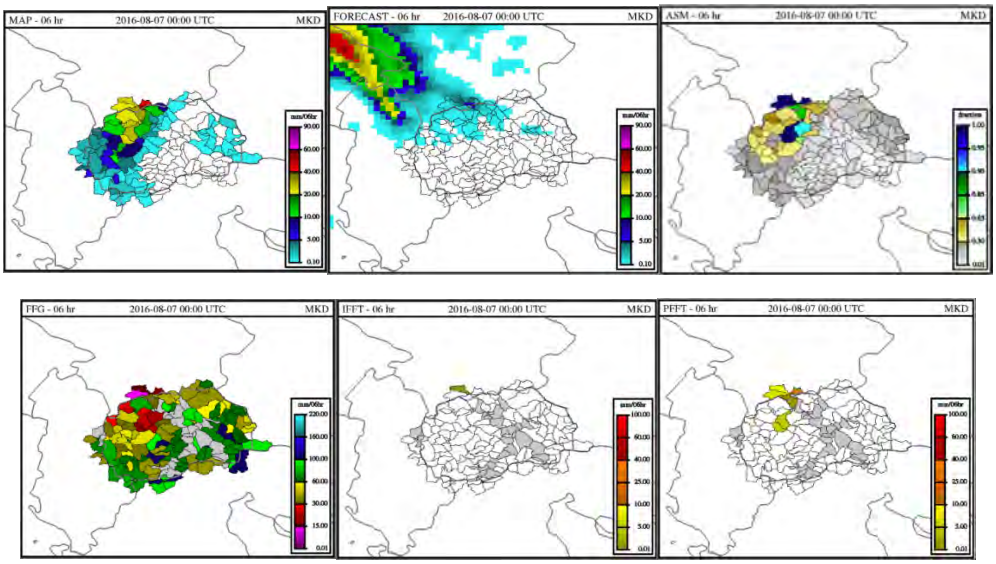

Figure 187. The former Yugoslav Republic of Macedonia: a) 06-hr MAP, b) 06-hr ALADIN precipitation, c) ASM, d) 06-hr FFG, e) 06-hr IFFT, and f) 06-hr PFFT; on 7 August 2016 at 00 UTC

24.3. Flash Flood in Skopje, August 2016

Observations

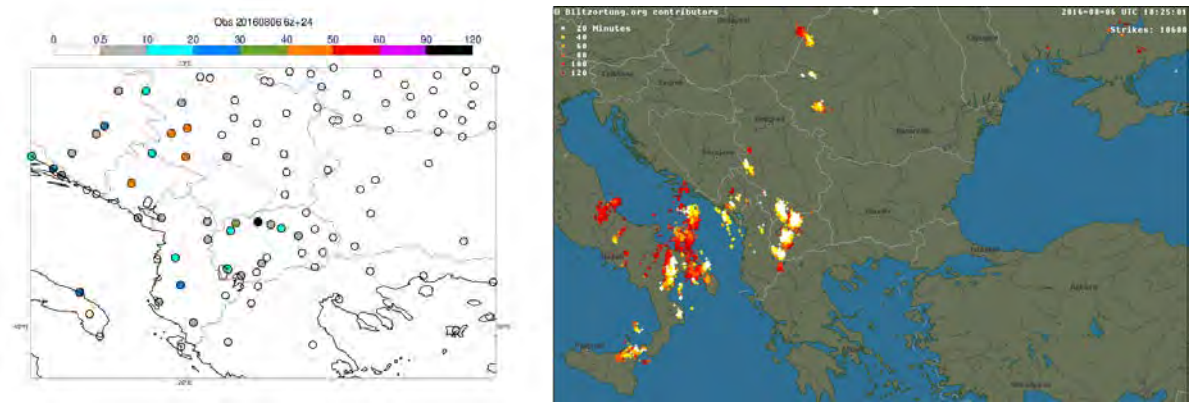

Figure 188. a) 24-hr observed precipitation on synoptic stations for the period 6th - 7th of August 2016., and b) observed lightning carried with convective system over The former Yugoslav Republic of Macedonia on 6 August 2016 at 18:25 UTC

Figure 188 a) presents 24-hr observed rainfall accumulations on 7 August 2016 at 06 UTC. The locality of an event was evident; Skopje station measured amount of rainfall between 90 and 120 mm (as mentioned before, precipitation intensity was 92 mm/-hr). Figure 188 b) shows observed lightening over southern Europe on 6 August at 18:25 UTC.

Conclusion

What we have learned from this case study are as follows:

1) Satellite precipitation retrievals are poor for frontal systems and other large scale circulations. Therefore, it is difficult for SEEFFG system to produce accurate products because the main input for the FFG system is precipitation, such that the better the precipitation estimation, the more accurate the FFG products generated.

2) In addition to SEEFFG products, forecasters must use additional tools and products e.g., weather Radar, high resolution satellite images (e.g., METEOSAT HRV), and instability analysis from sounding stations in the summer, autumn and spring months.

3) Knowledge of local micro climatological conditions are essential for preparing SEEFFG bulletins.

4) When forecasters combine all available tools and products, they will be able to prepare more realistic FFG bulletins.

5) As an alternative, precipitation source weather Radar precipitation products, depending on the availability, could be used if they were well calibrated and bias adjusted with ground gauge data.

25. VERIFICATION

Forecast verification studies are widely used to help understand the uncertainties and limitations in weather forecasting models, and the ways in which they can be improved (Sene, 2013).

The verification of flash floods is not an easy task but it is necessary for the evaluation of FFG system. The most difficult part of verification is to collect historical information and documentation about the actual flash flood events. In Croatia, the Meteorological and Hydrological Service collects information from the press and from the National Protection and Rescue Directorate, which delivers the GIS shape file with the locations of their interventions related to flash floods every few months.

The assessment of the quality of flash flood (FF) warnings based on FFG estimates is obtained using contingency tables. Contingency tables are highly flexible methods that can be used to estimate the quality of a deterministic forecast system and, in their simplest form, indicate its ability to anticipate correctly the occurrence or non-occurrence of predefined events. For verification with two categories, the 2x2 contingency table is commonly defined. It is for a yes/no configuration; for example, flash flood/no flash flood. For this simple yes/no table, the rows represent forecast categories and the columns represent categories for observations. In a flash flood/no flash flood categorization, "Yes" represents "Flash flood", either observed and/or forecast. "No" represents "no flash flood" either observed and/or forecast. The "a" box indicates the number of observed flash floods that were correctly forecast to be flash floods, or hits. The "b" box indicates the number of observed non-flash floods that had been incorrectly forecast to be flash floods, or false alarms. The "c" box indicates the number of observed flash floods that were forecast to be non-flash floods, or misses. The "d" box indicates the observed non-flash floods that were correctly forecast to be non-flash floods, or correct negatives. The "a+c" and "b+d" boxes are the total observed flash floods and non-flash floods. The "a+b" and "c+d" are the total forecasted flash floods and non-flash floods respectively.

a = Hits
b = False alarms
c = Misses
d = Correct negatives

		EVENT OBSERVED		
		Yes	No	Total
EVENT FORECASTED	Yes	a	b	a + b
	No	c	d	c + d
	Total	a + c	b + d	a + b + c + d = n

Figure 189. Contingency table

A “hit” is defined by the occurrence of at least one observation of FF event, anywhere in the forecast area, any time during the forecast valid time. Note that by this definition, more than one

report of FF event within the forecast valid area and time period does not add another event; only one hit is recorded.

A “false alarm” is recorded when FF is forecasted, but there is no observed event anywhere in the area for which the forecast is valid during the valid period.

A “missed event” is recorded when FF is reported outside the area and/or the time period for which the warning is valid, or whenever FF is reported and no warning is issued.

A “correct negative” or “correct non-event” is recorded for each day and each fixed forecast region for which no warning is issued and no FF event is reported.

A contingency table, illustrated in Figure 189, is then produced by totalling up the number of hits, misses, false alarms and correct negatives for a sufficiently large number of daily cases.

Based on contingency tables, the scores can be computed. The scores listed here are considered to be the most useful for verification of severe weather forecasts. Computation of these scores should be considered part of analysis and diagnosis functions that are routinely performed by forecasters. These scores all have specific interpretations, discussed below, which help the forecaster perform these diagnosis tasks. The scores provide the most meaningful information if they are computed from large enough samples of cases, say 100 or so. However, severe weather occurrences are rare events, thus the number of forecasts and observations of severe weather may be small (fortunately), which makes the task of verification not only more important but also more challenging (WMO-No. 1132).

Probability of detection (PoD) (hit rate (HR) or prefigurance):

$$P_0D = HR = \frac{a}{a+c}$$

The hit rate (HR) has a range of 0 to 1 with 1 representing a perfect forecast. As it uses only the observed events a and c in the contingency table, it is sensitive only to missed events and not false alarms. Therefore, the HR can generally be improved by systematically overforecasting the occurrence of the event. The HR is incomplete by itself and should be used in conjunction with either the false alarm ratio or the false alarm rate both explained below.

False alarm ratio (FAR):

$$FAR = \frac{b}{a+b}$$

The false alarm ratio (FAR) is the ratio of the total false alarms (b) to the total events forecast (a + b). Its range is 0 to 1 and a perfect score is 0. It does not include c and therefore is not sensitive to missed events. The FAR can be improved by systematically underforecasting rare events. It also is an incomplete score and should be used in connection with the HR.

25. VERIFICATION

Threat score (TS) (critical success index, CSI):

$$CSI = \frac{a}{a + b + c}$$

The threat score (TS), or critical success index (CSI), is frequently used as a standard verification measure (for example in USA). It has a range of 0 to 1 with a value of 1 indicating a perfect score. The CSI is more complete than the HR and FAR because it is sensitive to both missed events and false alarms.

The false alarm rate (FA):

$$FA = \frac{b}{b + d}$$

The false alarm rate (RA) is unfortunately often confused with the false alarm ratio. The false alarm rate is simply the fraction of observed non-events that are false alarms. By contrast, the false alarm ratio is referenced to the total number of forecasts; it is the fraction of forecasts that were false alarms. The best score for the FA is 0; that is, the wish is to have as few false alarms as possible. The FA is not often used by itself but rather is used in connection with the HR in a comparative sense. The HR is also referenced to the observations, specifically, the total number of observed events.

a = Hits
b = False alarms
c = Misses
d = Correct negatives

		EVENT OBSERVED		
		Yes	No	Total
EVENT FORECASTED	Yes	21 (a)	7 (b)	28
	No	1 (c)	113 (d)	114
	Total	22	120	142

Figure 190. Contingency table of flash flood warnings for Croatia in the period from 10 of October 2015 to 29 of February 2016

Hit Rate (POD): a/(a+c)	0.95
False Alarm Ratio (FAR): b/(a+b)	0.25
False Alarm Rate (POFD): b/(b+d)	0.058
Threat Score: a/(a+b+c)	0.72

Figure 191. The scores for flash flood warnings for Croatia in the period from 10 of October 2015 to 29 of February 2016

25. VERIFICATION

Figure 192 shows the location frequencies of flash flood events in Croatia from 10October 2015 to 29 February 2016 that were reported by press and/or the National Protection and Rescue Directorate. During this period, 28 flash flood events happened and spatial distribution reveals that majority of flash floods occurred along the Adriatic coast and in the hilly areas with torrents. Only one event was missed – a flash flood in the City of Rijeka.

Figure 192. Location frequencies of flash flood events in Croatia during the period from 10 October 2015 to 29 February 2016

Participating countries should be advised to collect flash flood events reports as much as possible and create maps and contingency table.

26. FLASH FLOOD EARLY WARNING SYSTEM

An effective flash flood early warning system is critical to disaster risk reduction. The development of early warning system is seen as part of the operational responsibility of NMHSs. In the WMO Guide to public weather services practices, it is acknowledged that warnings are only useful if they are received, understood, believed and acted upon by those at risk. To receive the warning information, users must be aware of the services available and be able to access them. To be understood, the messages must be clear, concise, and presented within the appropriate social and cultural context. To be believed, messages must be seen as coming from a credible authority. NMHSs must have a reputation for accuracy, reliability and timeliness. In essence, the need to improve flash flood warning understanding and response applies not only to the public but also to an NMHSs professional partners, in particular the media and water and emergency management.

There are three components to the Integrated Warning System, designed to reduce or eliminate the impact on people and property from flash flood:

- → Forecast, Detection and Warning
- → Dissemination and Communication
- → Response

The first component includes the scientific process of analysing SEEFFGS products, their adjustments, use of additional tools and data (e.g. weather radar images, high-resolution satellite images, instability analysis from sounding stations, local information on recent precipitation, flooding, flash flood prone areas, information about vulnerable communities), forecasting flash flood occurrence, and preparing flash flood watches and warnings.

Flash flood watches are issued when the expectation of a flash flood event has increased, but its occurrence, location and/or timing is still uncertain (Be prepared!). A flash flood watch should be valid from the time when the potential for flooding should start until the time when the potential for flooding should end, either as indicated in the headline or until the product is cancelled or has expired.

Flash flood watches help an NMHS meet its mission by providing notice and up-to-date information on the possibility of flooding. This allows users to begin monitoring hydrometeorological conditions more closely and elevate flood mitigation resources to a higher state of readiness, thus helping to protect life and property. Flash flood watches should be issued when one or more of the following conditions are met (Flash Flood Early Warning System Reference Guide):

- → The chance that meteorological, soil, and/or hydrologic conditions will lead to rapid-onset flooding within a 48-hour period is approximately 50 to 80%
- → The chance that meteorological, soil, and/or hydrologic conditions will lead to rapid-onset flooding more than 48 hours into the future is approximately 50 to 80%, and the forecaster determines that a flood watch is the best way to convey this possibility
- → The chance that meteorological, soil, hydrologic, and/or burn area conditions will lead to debris flows within a 48-hour period is approximately 50 to 80%
- → A dam or levee may fail and threaten lives or property, but the threat is not deemed to be imminent
- → The effective time of a previously issued flood watch changes
- → The geographic area covered by a previously issued flood watch increases

- → An update to a previously issued flood watch is required
- → A cancelation of all or part of a previously issued flood watch is required
- → The expiration of a previously issued flood watch is to be announced. When the flood threat has ended, an expiration or cancelation segment should be issued for the flood watch rather than allowing the product to expire on its own

Flash flood warnings are issued when flash flood is occurring, imminent, or likely. This reserved for those short-term events which require immediate action to protect life and property (Take action!). A flash flood warning will be valid from the time of issuance until the time when flooding (requiring immediate actions to protect life and property) is expected to end or until the product is cancelled. When determining the valid time or considering an appropriate time for warning cancelation, the end time for the flooding should be the determining factor rather than the end of heavy precipitation.

A flash flood warning should be issued in the following situations (Flash Flood Early Warning System Reference Guide):

- → Flash flooding is reported
- → A dam or levee failure is imminent or occurring
- → A sudden failure of a naturally-caused stream obstruction (including debris slide, avalanche, or ice jam) is imminent or occurring
- → Precipitation capable of causing flash flooding is indicated by radar, rain gauges, and/or satellite
- → Precipitation, as indicated by radar, rain gauges, satellite, and/or other guidance, is capable of causing debris flows, particularly (but not only) in burn areas
- → Local monitoring and prediction tools indicate flash flooding is likely
- → A hydrologic model indicates flash flooding for locations on small streams
- → A previously issued flash flood warning needs to be extended in time
- → Flash flooding is imminent or occurring in a geographical area currently not under a valid flash flood warning, e.g. expansion of an existing warning
- → Rapid rise in water level associated with an ice jam is expected to exceed flood stage

Effective warning message are short, concise, understandable, and actionable, answering the questions of “what?”, “where?”, “when?”, “why?” and “how to respond?”. The use of plain language in simple, short sentences or phrases enhances the user’s understanding of the warning. In addition, the most important in the warning should be presented first, followed by supporting information.

Forecasters at NMHSs must compress a great deal of information into standardized, concise and relatively brief messages for delivery to the public. The degree of detail in a warning can vary depending on its time span and the extent of the area to be warned. In greater detail, an effective flash flood warning should include: warning title, date/time of issue, issuing source/authority, validity period, threatened communities, headline, current intensity of precipitation, location of flash flood’s most likely impact(s) areas, expected consequences,

level of uncertainty, protective action statements, source(s) of further information and date/time at which or by which the next warning will be issued.

Flash flood warnings must be initiated, updated, corrected, cancelled and retired as soon as the need arises.

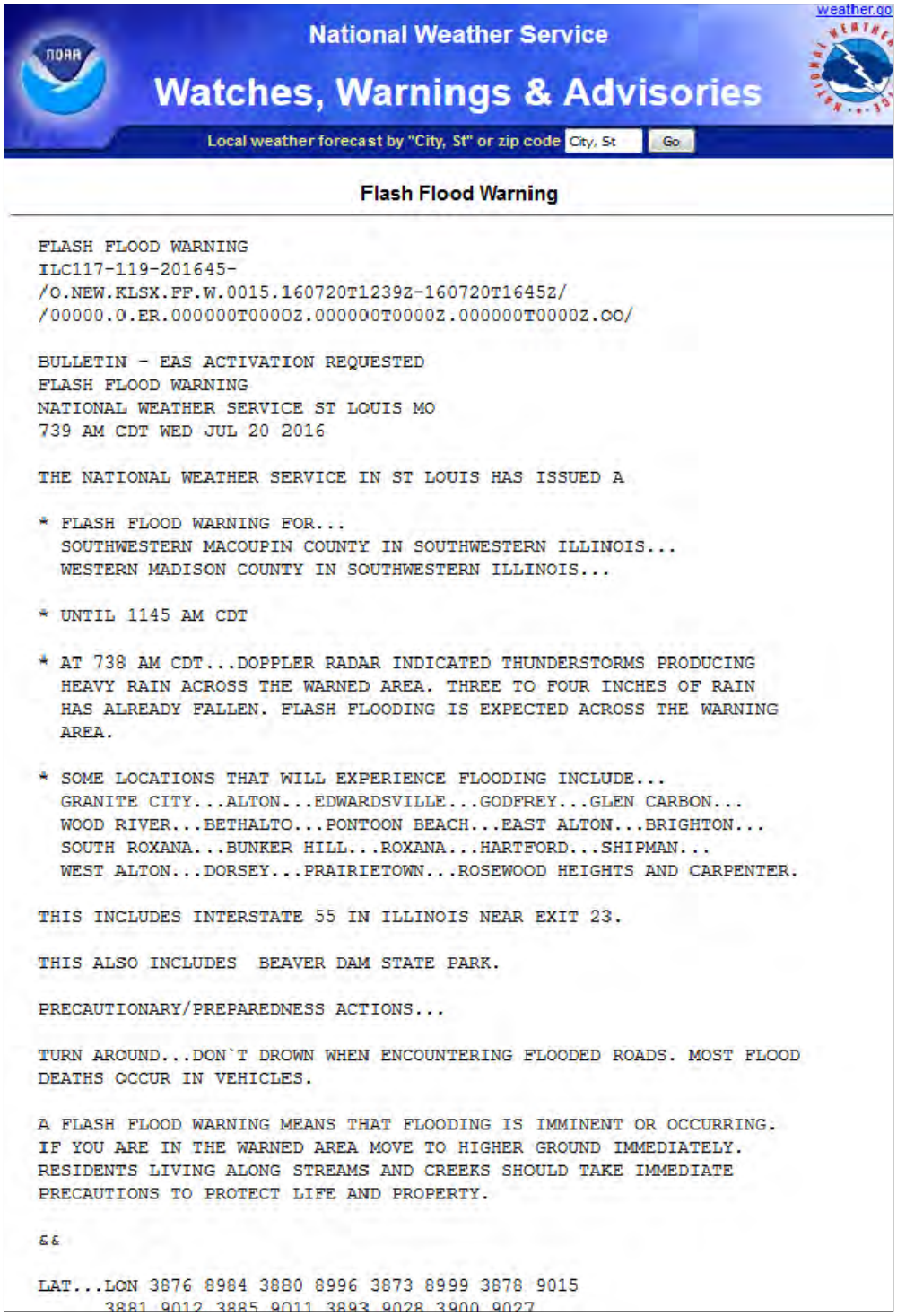

Figure 193. Example of flash flood warning text, NOAA, NWS

26. FLASH FLOOD EARLY WARNING SYSTEM

In many situations, there is insufficient information to forecast flash flood event. In such a situation, community confidence in the NMHS may increase by issuing an additional level of warning, such as a Precautionary Flash Flood Warning. Any delay in issuing a warning can result in catastrophic losses. There will be also occasions when adjustments to Flash Flood Guidance are needed when determining whether to issue a flash flood watch or warning. In evaluating and using products from SEEFFGS, the forecaster must always consider the impacts on FFG computations from items which can affect rainfall runoff: change in land use, change in deforestation areas, recent fires, seasonal changes in vegetation or forests, and existing soil moisture conditions. The SEEFFG system does not provide flash flood forecasts but can be used with other tools to develop forecasts of flash flood events and subsequently, watches and warnings.

As much as is practical, NMHSs should create standard forms for text and oral messages and store them for use during future events. There is increased demand from the public and media for graphical presentations of warnings. Keeping in mind that “a picture is worth a thousand words”, graphical or pictorial products are now being produced by many NMHSs to complement the textual warning. Graphical products may be delivered via both electronic and print media and should necessarily be clear, simple, easy to understand, in bold colours, and with significant well-known geographical landmarks and landscape features shown, source acknowledged, time and date of product labelled, and symbols, shades or intensity of colours explained in a key or legend.

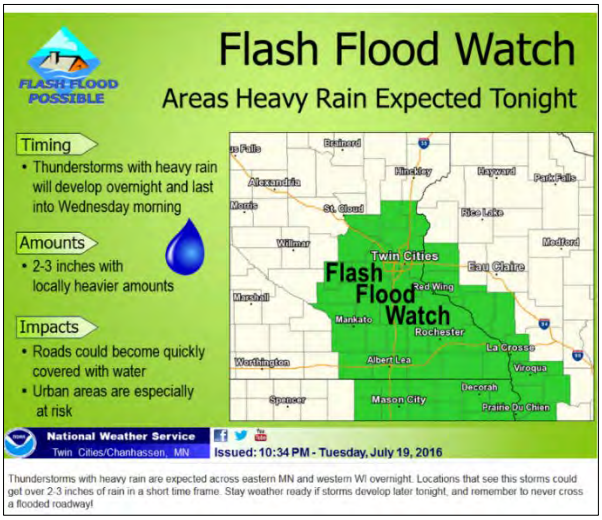

Figure 194. Example of graphical presentation of Flash flood watch

Dissemination refers to an NMHS physically delivering a message to its users. This is in contrast to *notification*, which is the understanding of the received message and, through prior outreach and education, users taking appropriate actions. Warnings for flash flood events are mostly up to 6-hours away need to be disseminated rapidly through special warning systems using messages that have been designed during calmer times. The dissemination process should be automated as much as possible to improve efficiency and decrease the time required to issue a warning. Whenever possible, NMHSs should use redundant communication paths to ensure dissemination of flash flood warnings and bulletins to its audiences. To enhance user response, it is vital that all sources disseminating the warning base their announcements on the same official information. To maximize chances that warnings will be received, NMHSs are strongly urged to disseminate flash flood warning

via multiple communication channels, because some communication channels may be more accessible or effective than others. Warning information should be disseminated in a wide variety of formats (text, graphical, audio) to enhance the capability of people with hearing and vision disabilities to receive and understand the information. Some NMHSs disseminate flash flood warnings directly to emergency services. This allows them to organize and/or mobilize necessary response personnel in advance of the public reacting to warnings.

Successful response to flash flood warnings is most likely to occur when the people receiving the warning messages have been educated about the particular characteristics of the flash floods, are familiar with the extent of possible damage that could result, and have personalized the risk. To ensure that the population has sufficient knowledge to understand the flash flood risk, public education campaigns should be conducted by NMHSs on regular and as-needs basis. Public awareness initiatives are generally more effective when they are carried out by an NMHS in partnership with emergency and management agencies. Best practice and effective flash flood awareness education campaigns will only be achieved within dynamic and diverse communities by applying a range of educational approaches. Public awareness initiatives may be introduced at any time, and should be ongoing. Flash flood awareness education should be delivered in a range of formats via a range of media, such as:

- → Brochures/Pamphlets
- → Television, Radio, Newspaper
- → Internet
- → Public meetings
- → Educational institutions
- → Shows/Exhibitions
- → Service representatives

Brochures and pamphlets are relatively cheap to produce and distribute widely. They should contain concise information that is simple and instructive. They are successful when produced jointly with partners such as emergency services. Brochures should look colourful and interesting. They must include statements indicating the source of information, the authorities responsible for their production and distribution, and resources for further information. Examples of flood/flash floods brochure are presented below with the hyperlinks for easy access:

FFG brochure NOAA FF and Flood Preparedness El Paso County FF brochure

Figure 195. Examples of brochures about flash floods

26. FLASH FLOOD EARLY WARNING SYSTEM

For television, short video clips focused on an upcoming flash flood event can be prepared ahead of time and televised as needed. Well-handled live-to-air interviews are an excellent means of both communicating hazard information and building community trust.

Public radio is widely accessed by the public in most countries and is usually the preferred media for receiving and/or confirming hazard-warning messages. This is probably due to a community perception that radio is more reactive and responsive to “update” messages.

Internet is becoming an increasingly effective way of delivering flash flood awareness education. Care must be taken over however, to ensure that the same quality of information that is made available on the Internet is also available via other sources so as not to disadvantage those without access to this technology. The MetEd website hosts a suite of free, informative materials related to natural hazards preparedness and education. The “Flash Flood Processes” module offers an introduction to the distinguishing features of flash floods, the underlying hydrologic influences and the use of FFG products.

The ability to quickly adapt to emerging communication technology is becoming a key requirement of NMHSs. People expect to be notified about dangerous conditions through a variety of new platforms (mobile phones, tablet mobile computers, etc.) and via social networks. The popularity of such platforms and social networks can change quickly, so NMHSs must be equally flexible in order to successfully reach as many people as possible.

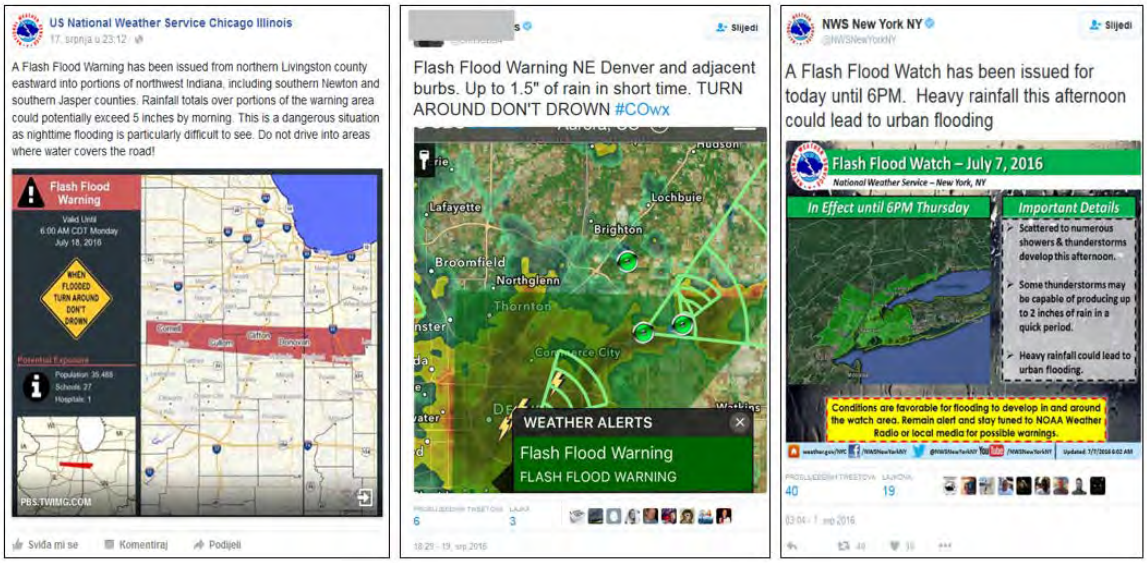

Figure 196. Examples of flash flood warnings and flash flood watch notifications on Facebook and Twitter

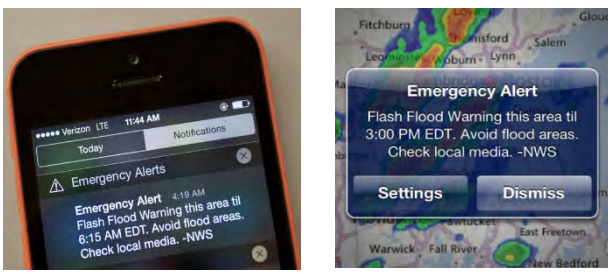

Figure 197. Wireless flash flood alerts

Most NMHSs present weather, flood and flash flood information to public and specialist user groups at public meetings and user forums on a regular and as-needed basis. These are generally more successful when carried out in partnership with other organization.

26. FLASH FLOOD EARLY WARNING SYSTEM

NMHSs can improve their public awareness activity through the effective use of their existing staff. Services can designate and develop a staff member as a public “focal point” or “Service representative” who is involved in the entire process of working with the users, to access their requirements, to develop products and services to meet their expectations, and to educate them on how to make the most out of information and services provided.

A good way for public education is via shows and exhibitions. Forecasters from NMHS should be available to answer public concerns and questions. Brochures and other printed materials should be available for interested members of public to take away with them. During the June 2015 at European Space Expo in Zagreb, forecasters from the Croatian Meteorological and Hydrological Service educated the public about FFGS satellite products and characteristics of flash floods and their risks. The exhibition was visited by more than 83 thousand people.

Figure 198. European Space Expo in Zagreb, Croatia, 2015 – Public education via exhibition

NMHSs can support school-based flash flood awareness education by contributing to the development and production of educational packages to be included in curriculum studies. Forecasters can also visit schools, deliver presentations and be available to answer questions.

To support an effective flash flood warning system, NMHSs should ensure that capacity building of their severe weather warning specialists is high on the national agenda. An integral part of implementing the global Flash Flood Guidance System is the training of hydrometeorologists; it is of critical importance in establishing sustainable local capabilities within the participating NMHSs. Trainees who have successfully completed and received the Hydrologic Research Center (HRC) eLearning Course Certification, with an additional HRC Certification after specialized training at HRC is completed, are awarded WMO certification as an FFGS trainer. WMO certified trainers would train forecasters from the participant countries, ensuring the continuous training of operational forecasters and enhancing flash flood forecasting and early warning capabilities. Training should not be limited to NMHS staff, but must also include specialized agencies that have defined responsibilities and public duties related to flash floods.

According to Jubach and Sezin Tokar (2016), close coordination must occur between all sectors and between national and local governments for the system to function properly, with clear lines of roles and responsibilities to avoid confusion and chaos during disasters. An important part of the process are the systems enabling user feedback to periodically improve and address the needs of decision makers. Because flash flood hazards do not recognize national boundaries, transboundary/regional programs and cooperation are essential to reduce the loss of lives and damage. The development and implementation of systems to provide early warnings for flash floods requires data and information sharing in real time, and coordination among the government agencies at all levels. It is of primary importance that early warning systems are truly end-to-end in nature. Each component in this process is critical to reduce the impacts of hydrometeorological extremes and provide essential lead

times to aid decisions. The failure of one component will lead to the failure of the entire system to save lives and livelihoods.

Weaknesses in monitoring and forecasting the hazards should be identified and research should be conducted to strengthen the technical capability. Publishing verification scores and post-event assessments can add to the credibility of NMHSs and, for stakeholders and partners, reinforce the perception of NMHSs as user-oriented and dedicated to the cause (WMO/TD No. 1559). An example of a large archive of National Weather Service's flash flood watches and warnings can be found at Iowa Environmental Mesonet where user can generate a custom GIS shapefile or Google Earth KML of NWS issued watches and warnings for a time period of his choice (even since 1986).

Even the most carefully designed warning system requires continual maintenance to ensure that it will be effective. The primary goal of flash flood early warning system is to prevent hazard to becoming disaster.

In the near future, we can expect the use of drones as an additional tool in flash flood warning system. This is already being tested in Saudi Arabia. This new drone system could give advance warnings of flash floods of between 30 minutes and 2 hours before a flood hits. The drones will help in predicting the precise path of the flooding so residents can know what to expect and when. Each drone will have a wireless sensor that can relay information to the central database where nearby cities and towns, or indeed anywhere where the population is vulnerable to flash flooding, can be informed of the details and whereabouts of the flash floods. The idea is a very simple one, albeit using high technology.

Figure 199. Drone - additional tool in flash flood warning system

27. REFERENCES

Allen, R.G., I.A. Walter, R. Elliott, T. Howell, D. Itenfisu, and M. Jensen, (Eds.) 2005: The ASCE standardized reference evapotranspiration equation. American Society of Civil Engineers, Reston, VA, 59 pp.

Anderson, E.A., 'National Weather Service River Forecast System - Snow Accumulation and Ablation Model', NOAA Technical Memorandum NWS HYDRO-17, 217 pp, November 1973.

Anderson, E.A., 2002. Calibration of conceptual hydrologic models for use in river forecasting. Office of Hydrologic Development, US National Weather Service, Silver Spring, MD.

Anderson, E. A. 2006. Snow Accumulation and Ablation Model – SNOW-17, http://www.nws.noaa.gov/oh/hrl/nwsrfs/users_manual/part2/_pdf/22snow17.pdf

Bras, R.L., 1990: Hydrology, Addison-Wesley, Reading, Mass.

Browning K. A., J. C. Fankhauser, J.-P. Chalon, P. J. Eccles, R. G. Strauch, F. H. Merrem, D. J. Musil, E. L. May, and W. R. Sand, 1976: Structure of an Evolving Hailstorm, Part V: Synthesis and Implications for Hail Growth and Hail Suppression; Mon. Wea. Rev., Vol. 104, p. 603 – 610

Bryndal, T., F. Pawel, R. Krocyak, W.Cabaj, A. Kolodzjej, 2017: The impact of extreme rainfall and flash floods on the flood risk management process and geomorphological changes in small Carpathian catchments: a case study of the Kasiniczanka river (Outer Carpathians, Poland). Natural Hazards, 88 (1), 95-120.

Burnash, R.J.C., 1995: The NWS River Forecast System - Catchment Modeling, Chapter 10, in Computer Models of Watershed Hydrology (Singh, V.P., ed.). Littleton, CO: Water Resources Publications.

Carpenter, T.M., J.A. Sperfslage, K.P. Georgakakos, T. Sweeney, D.L. Fread, 1999: National hreshold runoff estimation utilizing GIS in support of operational flash flood warning systems, Journal of Hydrology 224: 21-44.

Carpenter, T.M. and K.P. Georgakakos, 2004: Continuous streamflow simulation with the HRCDHM distributed hydrologic model. Journal of Hydrology 298: 61-79.

Carpenter, T.M., and K.P. Georgakakos, 2006: Intercomparison of lumped versus distributed hydrologic model ensemble simulations on operational forecast scale. Journal of Hydrology, 329 (1-2), 174-185.

Chappell, C. F., 1986: Quasi-stationary convective events. Mesoscale Meteorology and Forecasting, P. S. Ray, Ed., Amer. Meteor.Soc., 289 – 310.

Chow, V.T., D.R. Maidment and L.W. Mays, 1988. Applied Hydrology, McGraw-Hill, New York, 572 pp.

Doswell, C. A., III, H. E. Brooks, and R. A. Maddox, 1996: Flash flood forecasting: An ingredients-based methodology.Weather Forecasting,11,560–581.

Fritsch, J. M., R. J. Kane, and C. M. Chelius, 1986: The contribution of mesoscale convective weather to the warm-season precipitation in the United States. J. Climate Appl. Meteor., 25, 1333-1345.

Georgakakos, K.P., P.V. Unnikrishna, H.R. Bravo, J.A. Cramer, 1991: A national system for determining threshold runoff values for flash-flood prediction. Issue Paper, Department of

27. REFERENCES

Civil and Environmental Engineering and Iowa Institute of Hydraulic Research, The University of Iowa, Iowa City, IA.

Georgakakos, K.P., 2005: Modern Operational Flash Flood Warning Systems Based on Flash Flood Guidance Theory: Performance Evaluation. Proceedings, International Conference on Innovation, Advances and Implementation of Flood Forecasting Technology, 9-13 October 2005, Bergen - Tromsø, Norway, pp. 1-10.

Georgakakos, K.P., 2006: Analytical results for operational flash flood guidance. Journal of Hydrology 317: 81-103.

Georgakakos, K.P., R. Graham, R. Jubach, T.M. Modrick, E. Shamir, C. Spencer, J.A., Sperfslage 2013: Global Flash Flood Guidance System, Phase I. HRC Technical Report No. 7. Hydrologic Research Center, San Diego, CA.

Helfrich, S.R., D. McNamara, B.H. Ramsay, T. Baldwin, and T. Kasheta, 2007: Enhancements to, and forthcoming developments in the Interactive Multisensor Snow and Ice Mapping System (IMS). Hydrological Process 21: 1576-1586.

International Commission for the Protection of the Danube River and International Sava River Basin Commission, 2015: Floods in May 2014 in the Sava River Basin.

Jarrett, R.D., 1984: Hydraulics of high gradient streams. Journal of Hydraulic Engineering 110 (11), 1519–1539.

Jensen, M.E. and H.R. Haise, 1963. Estimating evapotranspiration from solar radiation. Journal of Irrigation and Drainage Division, Proceeding of the American Society of Civil Engineers 89: 15-471.

Johns, R. H., and C. A. Doswell III, 1992: Severe local storms forecasting. Weather Forecasting,7,588–612

Joyce, R.J., J.E. Janowiak, P.A. Arkin, P. Xie, 2004: CMORPH: A method that produces global precipitation estimates from passive microwave and infrared data at high spatial and temporal resolution. Journal of Hydrometeorology 5: 487–503.

Jubach, R., and A. Sezin Tokar, 2016: International Severe Weather and Flash Flood Hazard Early Warning Systems - Leveraging Coordination, Cooperation, and Partnerships through a Hydrometeorological Project in Southern Africa. Water 8(6), 258.

Koren, V., M. Smith, D. Wang, Z. Zhang, 2000: Use of soil properis datain the derivation of conceptual rainfall-runoff model parameters, American Meteorological Society 15th Conference on Hydrology, Long Beach, CA, pp. 103-106.

Maddox, R. A., C.F. Chappell and L.R. Hoxit, 1979: Synoptic And meso-α scale aspects of flash flood events. Bull. Amer.Meteor. Soc., 60, 375-389.

Maddox, R. A., 1980: MesoScale convective complexes. Bull. Amer. Meteorol.Soc., 61, 1374-1387.

Mogil, H.M., J.C. Monro, H.S. Groper, 1978: NWS's flash flood warning and disaster preparedness programs. Bulletin of the American Meteorological Society 59, 690–699.

Modrick, T.M., R. Graham, E. Shamir, R. Jubach, C.R. Spencer, J.A. Sperfslage, K.P. Georgakakos, 2014: Operational Flash Flood Warning Systems with Global Applicability. International Environmental Modelling and Software Society (iEMSs) 7th International Congress on Environmental Modelling and Software. San Diego, California, USA

27. REFERENCES

Mutic, P., and T. Jurlina, 2016: Flash Floods in Croatia – A Case Study of 14th October 2015. Flash Flood Guidance Gazette 1 (6). Hydrologic Research Center, San Diego, CA.

Mutic, P., T. Jurlina, T. Vujnovic, D. Oskorus, N. Strelec Mahovic, T. Renko, 2016: The first joint hydro-meteo warnings in Croatia during heavy rainfall period in October 2015. Perspectives on Atmospheric Sciences (Karacostas, T., Bais, A., Nastos, P., eds.). Springer (in press).

NOAA/COMET, 2010: Flash Flood Early Warning System Reference Guide, University Corporation for Atmospheric Research

Ntelekos, A.A., K.P. Georgakakos and W.F. Krajewski 2006: On the uncertainties of flash flood guidance: Towards probabilistic forecasting of flash floods, Journal of Hydrometeorology, 7(5), 896–915.

Rodriguez-Iturbe, I. and J.B. Valdes, 1979. The geomorphologic structure of hydrologic response. Water Resources Research 15 (6),1409–1419.

Rodiguez-Iturbe, I., M. Gonzalez-Sanabria and R.L. Bras, 1982. A geomorphoclimatic theory of the instantaneous unit hydrograph. Water Resources Research 18 (4), 886–887.

Scofield, R. A., and R. J. Kuligowski, 2003: Status and outlook of operational satellite precipitation algorithms for extreme-precipitation events. Monthly Weather Review 18: 1037-1051.

Sene K., 2013: Flash Flood Forecasting and Warning. Springer.

Shamir, E., B. Imam, H.V. Gupta, S. Sorooshian, 2005: Aplication of temporal streamflow descriptors in hydrologic model parameter estimation. Water Resources Research 41 (6).

Shamir, E. and K.P. Georgakakos, 2014: Hydrologic model development for the Dalia-Taninim watershed in Israel. HRC Technical Report No. 66. Hydrologic Research Center, San Diego, CA.

Snow Hydrology, Summary Report of the Snow Investigations, North Pacific Division, Corps of Engineers, Portland, Oregon, 437 pp, June 1956.

Strelec Mahovic, N., 2014: Floods in SE Europe, Lecture slides, HIW Event Week EUMETRAIN.

Strelec Mahovic, N., T. Renko, V. Tutis, T. Trosic, 2015: Synoptic analysis of the Catastrophic Floods in SE Europe, May 2014. The European Forecaster 43-47.

Sweeney, T.L., 1992: Modernized areal flash flood guidance. NOAA Technical Report NWS HYDRO 44, Hydrology Laboratory, National Weather Service, NOAA, Silver Spring, MD, 21 pp. and an appendix.

Szilagyi, J., 2006: Comment on ‘‘Using numerical modelling to evaluate the capillary fringe groundwater ridging hypothesis of streamflow generation’’ by H. L. Cloke, et al. [J. Hydrol. 316 (2006) 141–162]. Journal of Hydrology 329: 724-729.

Tsintikidis, D., K.P. Georgakakos, J.A. Sperfslage, D.E. Smith, M.T. Carpenter, 2002: Precipitation Uncertainty and Raingauge Network Design within Folsom Lake Watershed. Journal of Hydraulic Engineering 7(2), 175-184.

27. REFERENCES

Tudor M., S. Ivatek-Sahdan, A. Stanesic, K. Horvath, and A. Bajic. Forecasting weather in Croatia using ALADIN numerical weather prediction model. Climate Change and Regional/Local Responses., pages 59–88, 2013.

Turkish Meteorological Service, 2015: Black Sea and Middle East Flash Flood Guidance System User Guide.

United Nations, Office of the Resident coordinator 2014: Bosnia and Herzegovina – Flood Disaster Situation Report (No.3.).

World Meteorological Organization 1994: Guide to hydrologic practices (WMO-No. 168)., Geneva.

World Meteorological Organization, 1999: Guide to public Weather Services Practices (WMO-No. 834). Geneva.

World Meteorological Organization, 2002: Guide on improving public understanding of and response to warnings (WMO/TD-No. 1139). Geneva.

World Meteorological Organization, 2007: Prospectus, Implementation of a Flash Flood Guidance System with global coverage (CBS-MG-VII/Doc. 5(7)). Geneva

World Meteorological Organization, 2010: Guidelines on Early Warning Systems and Application on Nowcasting and Warning Operations (WMO/TD No. 1559). Geneva.

World Meteorological Organization, 2014: Forecast Verification for the African Severe Weather Forecasting Demonstration Projects (WMO-No. 1132). Geneva.

27.1. WEB RESOURCES

Advanced Spaceborne Thermal Emission and Reflection Radiometer Global Digital Elevation Model, NASA, http://asterweb.jpl.nasa.gov/gdem.asp

Bosnia and Herzegovina – Flood Disaster Situation Report, United Nations, http://reliefweb.int/sites/reliefweb.int/files/resources/Situation%20Report%2027May2014%20.pdf

CGIAR Consortium for Spatial Information, SRTM 90 m Digital Elevation Data http://srtm.csi.cgiar.org/

COMET MetEd, Flash Flood Case Studies, https://www.meted.ucar.edu/training_module.php?id=267#.V86AHzVWJSA

COMET MetEd, Flash Flood Processes, https://www.meted.ucar.edu/training_module.php?id=233#.V86AQzVWJSA

COMET MetEd, Introduction to Verification of Hydrologic Forecasts, https://www.meted.ucar.edu/training_module.php?id=486#.V85__TVWJSA

COMET MetEd, Precipitation Estimates, Part 1: Measurement, https://www.meted.ucar.edu/training_module.php?id=526#.V85_2DVWJSA

COMET MetEd, Runoff Processes, https://www.meted.ucar.edu/training_module.php?id=207#.V86AbDVWJSA

Copernicus Land Monitoring Services, EU-DEM v.1.1., http://land.copernicus.eu/pan-european/satellite-derived-products/eu-dem/eu-dem-v1.1

Diva GIS Data, http://www.diva-gis.org/gdata

El Paso County, Pikes Peak Region, Preparedness Guide, Flash Flood and Debris flow http://adm.elpasoco.com/emprep/Documents/El%20Paso%20County%20Flood%20Prep%20Brochure%20PDF.pdf

Eumetrain, Manual of Synoptic Satellite Meteorology, http://www.eumetrain.org/satmanu/

EuroGeographics, Euro Global Map, http://www.eurogeographics.org/products-and-services/euroglobalmap

European Environmental Agency, Corine Land Cover database, http://www.eea.europa.eu/data-and-maps/data#c17=&c11=&c5=all&c0=5&b_start=5&c12=corine

Cairo F. 2011: Atmospheric Thermodynamics, Thermodynamics - Interaction Studies - Solids, Liquids and Gases, Dr. Juan Carlos Moreno PirajÃin (Ed.), InTech, DOI: 10.5772/19429. Available from: http://www.intechopen.com/books/thermodynamics-interaction-studies-solids-liquids-and-gases/atmospheric-thermodynamics

International Steering Committee for Global Mapping, https://www.iscgm.org/gmd/

Iowa Environmental Mesonet, Archived NWS Watch/Warnings, https://mesonet.agron.iastate.edu/request/gis/watchwarn.phtml

Joint Research Centre, European Soil Database, http://esdac.jrc.ec.europa.eu/content/european-soil-database-v20-vector-and-attribute-data

Kuligowski B., Hydro-Estimator - Technique Description, http://www.star.nesdis.noaa.gov/smcd/emb/ff/HEtechnique.php

27.1. WEB RESOURCES

NASA, Aqua Earth-observing satellite mission, http://aqua.nasa.gov/

NASA, Moderate Resoultion Imaging Spectroradiometer (MODIS), http://modis.gsfc.nasa.gov/

National Oceanic and Atmospheric Organization, Flash floods and Floods, http://w4ehw.fiu.edu/flood%20guide%20noaa.pdf

National Weather Service, National Oceanic and Atmospheric Organization, Flash Flood Threat Within Fire Burn Scars, http://www.weather.gov/riw/burn_scar_flooding

National Weather Service River Forecast System (NWSRFS).,1999: User Manual. National Weather Service Office of Hydrologic Development, Hydrology Laboratory, Silver Springs, MD http://www.nws.noaa.gov/oh/hrl/nwsrfs/users_manual/htm/xrfsdocpdf.php

Natural Earth, http://www.naturalearthdata.com/

NOAA/COMET, 2010: Flash Flood Early Warning System Reference Guide, http://www.meted.ucar.edu/communities/hazwarnsys/ffewsrg/FF_EWS.pdf

Sayin, A., 2015: The worst flood events in South East Europe,13-15 May 2014 Case study http://www.wmo.int/pages/prog/hwrp/flood/ffgs/SAsiaFFG/documents/presentations/day3/SEEFFGCase-studyI-13-15052014-floods.pdf

Sayin,.A., 2015: Black Sea and Middle East Flash Flood Guidance System (BSMEFFGS) User Guide.
http:// http://www.wmo.int/pages/prog/hwrp/flood/ffgs/documents/BSMEFFG_UserGuide-opt.pdf

World Meteorological Organization, 1999: Guide to public Weather Services Practices, https://www.wmo.int/pages/prog/amp/pwsp/documents/834_Ed-1999_en.pdf

World Meteorological Organization, 2007: Prospectus, Implementation of a Flash Flood Guidance System with Global Coverage, https://www.google.hr/url?sa=t&rct=j&q=&esrc=s&source=web&cd=1&ved=0ahUKEwixw7Pu8J_OAhWpKsAKHSHcBMwQFggbMAA&url=https%3A%2F%2Fwww.wmo.int%2Fpages%2Fprog%2Fwww%2FCBS%2FMeetings%2FMG_7%2FDoc5(7)_CHy.doc&usg=AFQjCNF4AggNBDg3LUGx_UxnLap9icp3Zg&cad=rja

World Meteorological Organization, 2010: Guidelines on Early Warning Systems and Application on Nowcasting and Warning Operations, https://www.wmo.int/pages/prog/amp/pwsp/documents/PWS-21.pdf

World Meteorological Organization, 2016: Flash Flood Guidance System with global coverage Brochure, http://www.wmo.int/pages/prog/hwrp/flood/ffgs/documents/2016_ffgs-brochure_en.pdf